BEILSTEIN JOURNAL OF ORGANIC CHEMISTRY

Biosynthesis and function of secondary metabolites

Edited by Jeroen S. Dickschat

Imprint

Beilstein Journal of Organic Chemistry
www.bjoc.org
ISSN 1860-5397
Email: journals-support@beilstein-institut.de

The *Beilstein Journal of Organic Chemistry* is published by the Beilstein-Institut zur Förderung der Chemischen Wissenschaften.

Beilstein-Institut zur Förderung der Chemischen Wissenschaften
Trakehner Straße 7–9
60487 Frankfurt am Main
Germany
www.beilstein-institut.de

Beilstein Journal of Organic Chemistry

Biosynthesis and function of secondary metabolites

Jeroen S. Dickschat

Editorial

Open Access

Address:
Institut für Organische Chemie, Technische Universität Carolo-Wilhelmina zu Braunschweig, Hagenring 30, D-38106 Braunschweig, Germany

Email:
Jeroen S. Dickschat - j.dickschat@tu-bs.de

Beilstein J. Org. Chem. **2011,** *7,* 1620–1621.
doi:10.3762/bjoc.7.190

Received: 20 October 2011
Accepted: 25 October 2011
Published: 05 December 2011

This article is part of the Thematic Series "Biosynthesis and function of secondary metabolites".

Guest Editor: J. S. Dickschat

Natural products have long been used by humans owing to their beneficial effects. Indulgences such as coffee and tea, with their moderate stimulatory properties, have a long cultural tradition and are today some of the most important agricultural products worldwide. Other drugs have much stronger impacts on the central nervous system. For example, coca was originally used by the Inca civilisation because of its strong stimulatory effects, which result in feelings of happiness and euphoria. Opium was used by many ancient cultures as an efficient analgesic, but this also illustrates one of the first examples of drug abuse as it was used by warriors as an anxiolytic when girding their loins. Besides their pleasant traits these highly active drugs have adverse side effects, including most importantly an extremely high potential to cause addiction in combination with physical and mental prostration upon long-term abuse. Therefore, the production, importation, trading, and possession of these drugs are today under strict control by public authorities. Another historically interesting example of drug misuse is given by the death penalty imposed on Socrates in 399 B.C., carried out by the forced ingestion of the proverbial cup of hemlock.

These traditional and historical examples of the usage of bioactive natural products all originated in the ancient cultures, without any knowledge about the underlying chemistry. This situation started to change at the beginning of the 19th century, when Friedrich Wilhelm Adam Sertürner (1783–1841) first isolated morphine from opium, naming it after Morpheus, the Greek god of dreams and demonstrating its activity in self-tests, as was typical practice during these early times of chemistry. A likewise important discovery was made by Alexander Fleming (1881–1955), who isolated the antibiotic penicillin from the mould *Penicillium notatum* in a groundbreaking contribution, which was awarded the Nobel Prize in 1945.

The discovery of new bioactive natural products is still a fascinating field in organic chemistry as demonstrated by the recent paradigms of the anticancer drug epothilon, the immunosuppressant rapamycin, or the proteasome inhibitor salinosporamide, to name but a few of hundreds of possible examples. Finding new secondary metabolites is a prerequisite for the development of novel pharmaceuticals, and this is an especially urgent task in the case of antibiotics due to the rapid spreading of bacterial resistances and the emergence of multiresistant pathogenic strains, which poses severe clinical problems in the treatment of infectious diseases. This Thematic Series on the biosynthesis and function of secondary metabolites deals with the discovery of new biologically active compounds from all kinds of sources, including plants, bacteria, and fungi, and also

with their biogenesis. Biosynthetic aspects are closely related to functional investigations, because a deep understanding of metabolic pathways to natural products, not only on a chemical, but also on a genetic and enzymatic level, allows for the expression of whole biosynthetic gene clusters in heterologous hosts. This technique can make interesting, new secondary metabolites available from unculturable microorganisms, or may be used to optimise their availability by fermentation, for further research and also for production in the pharmaceutical industry. Especially fascinating is the intrinsic logic of the polyketide and nonribosomal peptide biosynthetic machineries, which is strongly correlated with the logic of fatty acid biosynthesis as part of the primary metabolism. Insights into the mechanisms of modular polyketide and nonribosomal peptide assembly lines open up the possibility for direct modifications, e.g., of oxidation states of the natural product's carbon backbone by simple domain knockouts within the responsible megasynthases, or the introduction of a variety of alternative biosynthetic starters by mutasynthesis approaches, thus leading to new variants of known metabolites, which may have improved properties for therapeutic use. Another interesting aspect is the usage of enzymes in chemical transformations, which can provide synthetic organic chemists with an efficient access route to typically chiral building blocks that may otherwise be difficult to obtain.

It is my great pleasure to thank all of the contributors to this Thematic Series, the staff of the Beilstein-Institut, and my esteemed colleague and teacher Prof. Henning Hopf (Braunschweig) for opening the opportunity to guest-edit the present issue. Enjoy reading it!

Jeroen S. Dickschat

Braunschweig, October 2011

Beilstein Journal of Organic Chemistry

Natural product biosyntheses in cyanobacteria: A treasure trove of unique enzymes

Jan-Christoph Kehr, Douglas Gatte Picchi and Elke Dittmann*

Review

Open Access

Address:
University of Potsdam, Institute for Biochemistry and Biology, Karl-Liebknecht-Str. 24/25, 14476 Potsdam-Golm, Germany

Email:
Jan-Christoph Kehr - jckehr@uni-potsdam.de; Douglas Gatte Picchi - dgpicchi@daad-alumni.de; Elke Dittmann* - editt@uni-potsdam.de

* Corresponding author

Keywords:
cyanobacteria; natural products; NRPS; PKS; ribosomal peptides

Beilstein J. Org. Chem. **2011,** *7,* 1622–1635.
doi:10.3762/bjoc.7.191

Received: 22 July 2011
Accepted: 19 September 2011
Published: 05 December 2011

This article is part of the Thematic Series "Biosynthesis and function of secondary metabolites".

Guest Editor: J. S. Dickschat

Abstract

Cyanobacteria are prolific producers of natural products. Investigations into the biochemistry responsible for the formation of these compounds have revealed fascinating mechanisms that are not, or only rarely, found in other microorganisms. In this article, we survey the biosynthetic pathways of cyanobacteria isolated from freshwater, marine and terrestrial habitats. We especially emphasize modular nonribosomal peptide synthetase (NRPS) and polyketide synthase (PKS) pathways and highlight the unique enzyme mechanisms that were elucidated or can be anticipated for the individual products. We further include ribosomal natural products and UV-absorbing pigments from cyanobacteria. Mechanistic insights obtained from the biochemical studies of cyanobacterial pathways can inspire the development of concepts for the design of bioactive compounds by synthetic-biology approaches in the future.

Introduction

The role of cyanobacteria in natural product research

Cyanobacteria flourish in diverse ecosystems and play an enormous role in the biogeochemical cycles on earth. They are found in marine, freshwater and terrestrial environments and even populate such extreme habitats as the Antarctic or hot springs [1]. Due to their capability to fix nitrogen from the atmosphere some species are attractive partners in symbioses [2] (Figure 1). Other cyanobacteria show a strong tendency for mass developments during summer months, so-called blooms [3] (Figure 1). Cyanobacteria do not belong to the established sources of natural products and are only incidentally screened by pharmaceutical industries. For a long time, natural product research on cyanobacteria was mostly focused on toxins, in par-

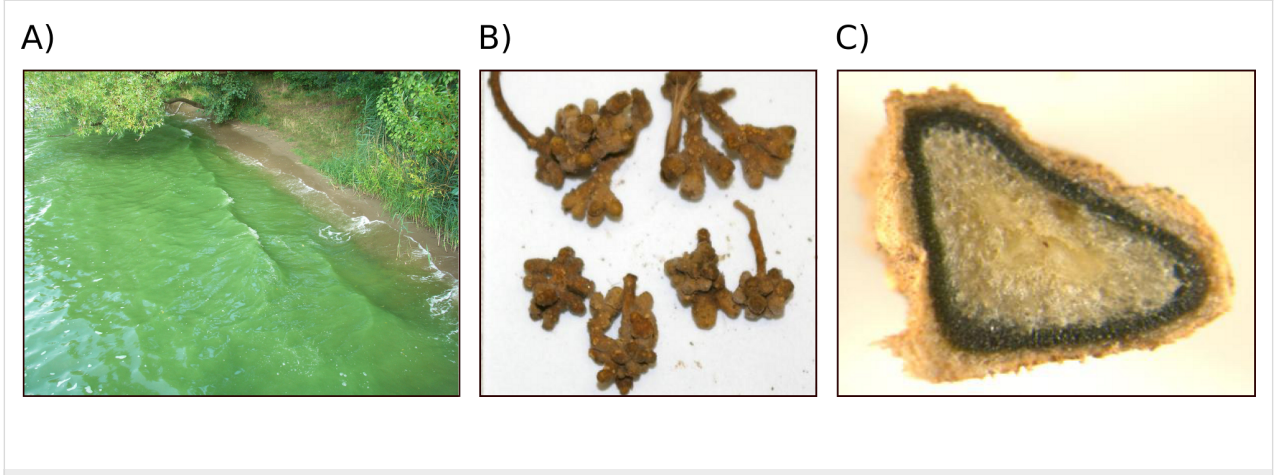

Figure 1: Cyanobacteria proliferate in diverse habitats. A) Bloom-forming freshwater cyanobacteria of the genus *Microcystis*. B) Roots of cyanobacterial symbiosis host *Cycas circinalis*. C) Terrestrial cyanobacteria living in corraloid roots of *Cycas circinalis*.

ticular on the widespread hepatotoxin microcystin **1** [4]. Starting in the eighties, however, a number of promising compounds was isolated by means of bioactivity-guided screening techniques towards cytotoxic, multidrug-resistance reversal, antiprotease, antifungal and antiviral activities [5]. Many bioactive metabolites possess a peptide or a macrolide structure, or a combination of both types [6-8]. Other metabolites belong to the alkaloid class of compounds. In the last two decades, biosynthesis gene clusters were assigned to an increasing number of these cyanobacterial natural products [7,9]. Part of the genetic analyses was assisted by biochemical studies of the enzymes. These studies revealed a truly fascinating variety of enzymatic features, including many that are not or only rarely seen in other microorganisms. The potential of cyanobacteria for natural product research thus goes far beyond the exploitation of the bioactivity of the products. Knowledge about the biochemistry of unique enzymes is particularly valuable for synthetic biology approaches towards libraries of new compounds or for rational biotransformation of existing leading compounds. This review gives an overview of the current trends in cyanobacterial natural-product research, with a special emphasis on the biosynthetic enzymes.

Review

Biosynthesis of peptides and polyketides in microorganisms

Microbial natural products of the peptide class are produced by two types of biosynthetic pathways: By giant multi-domain enzymes, the nonribosomal peptide synthetases (NRPS) or by ribosomal synthesis and subsequent post-translational modification and processing. NRPS consist of modules, each being responsible for the incorporation of a single amino acid. The order of these modules typically follows a colinearity rule, i.e., the succession of modules corresponds to the order of amino acids in the final product. A minimal module is composed of an amino acid-activating adenylation (A) domain, a peptidyl carrier (PCP) domain carrying the phosphopantetheine cofactor, and a condensation (C) domain (Figure 2) [10]. NRPS can accept about 300 proteinogenic and nonproteinogenic substrates and may contain further domains introducing tailoring modifications or epimerizing the amino acid substrates [11]. In contrast, ribosomal biosynthesis of peptides is limited to 20 proteinogenic amino acids. This group of peptides nevertheless displays a high diversity and a considerable biosynthetic and bioactive potential. The ribosomal prepeptides are typically composed of a leader peptide and a core peptide. Associated post-translational modification enzymes (PTMs) catalyze different types of macrocyclizations of the core peptide and side-chain modifications of amino acids. Peptide maturation further requires cleavage of the leader peptide by processing proteases (PP) frequently combined with transport across the plasma membrane [12] (Figure 2).

Macrolides in microorganisms are produced by modular type polyketide synthases (PKS) resembling NRPS with respect to their modular nature. In contrast to the peptide-synthesizing enzymes, different types of carboxylic acids are activated, assembled and optionally modified. The maximal set of domains of an individual PKS module is identical to animal fatty acid synthase (FAS) [13] and consists of ketosynthase (KS), acyltransferase (AT), ketoreductase (KR), dehydratase (DH), enoyl reductase (ER) and acyl carrier protein (ACP) domains [14]. Parts of the domains (KR, DH, ER) are optionally used leading to a different reduction state of the keto groups of polyketides. There are also alternative PKS assembly lines cooperating with AT domains encoded in trans of the multienzymes [15], or PKS types comprising single modules that work iteratively [16].

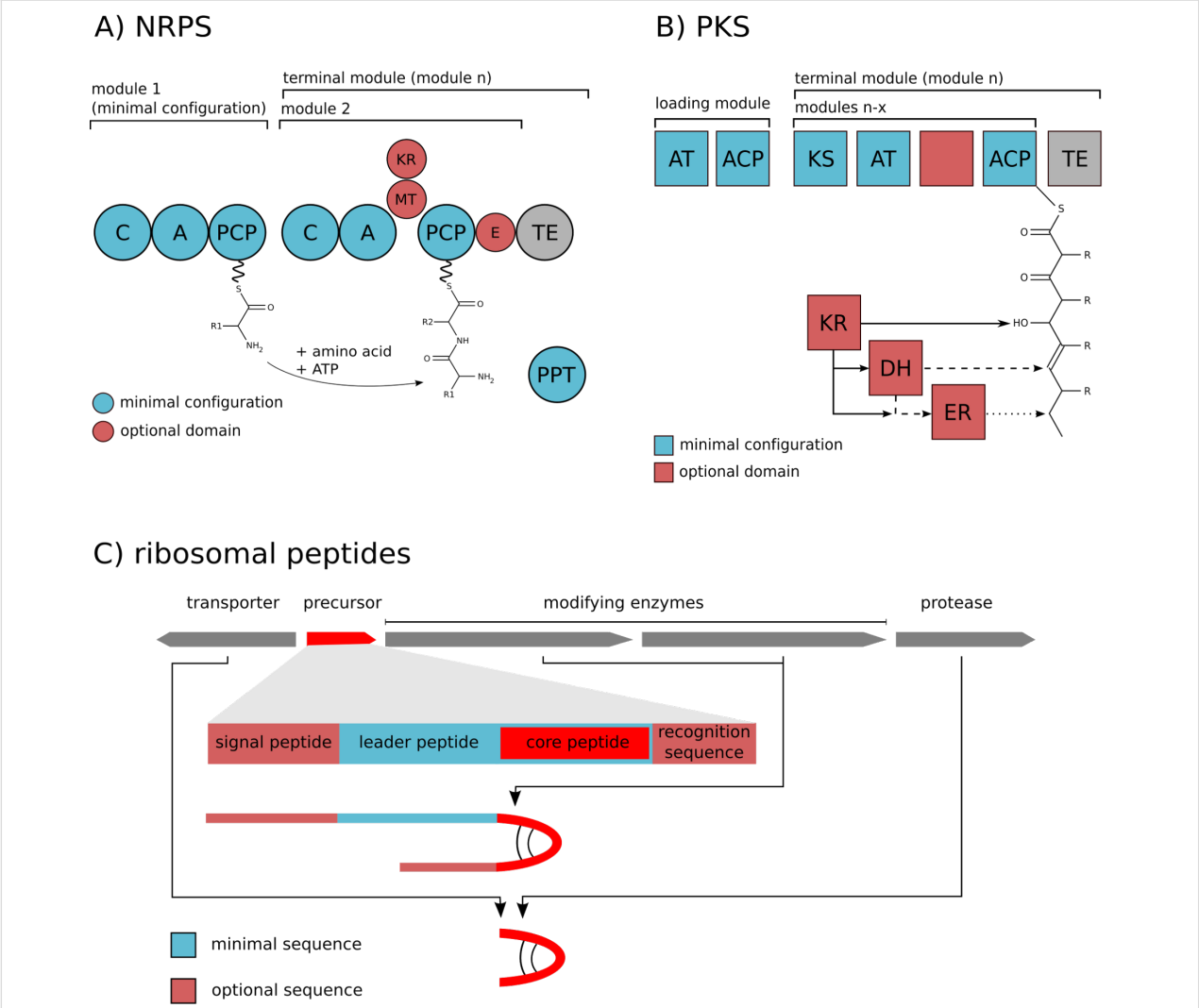

Figure 2: Schematic representation of enzymatic domains in A) nonribosomal peptide synthetases (NRPS); B) polyketide synthases (PKS) and C) the typical organisation of a ribosomal biosynthetic gene cluster. Abbreviations: C: Condensation domain; A: Adenylation domain; PCP: Peptidyl carrier protein; MT: Methyltransferase; E: Epimerase; AT: Acyltransferase; ACP: Acyl carrier protein; KS: Ketosynthase; KR: Ketoreductase; DH: Dehydratase; ER: Enoyl reductase; TE: Thioesterase.

Nonribosomal peptide, polyketide and hybrid biosyntheses in cyanobacteria

Research on NRPS and PKS gene clusters started almost in parallel in freshwater, marine and terrestrial cyanobacteria. A major trait of cyanobacterial pathways is their hybrid character, i.e., the frequent mixture of NRPS and PKS modules. Hereafter, we highlight the most interesting biochemical features of cyanobacterial assembly lines. Although we specifically refer to enzymes that were analyzed biochemically, the additional unusual characteristics of the compounds (the formations of which remain to be elucidated) will be mentioned. The list is divided into freshwater, marine and terrestrial biosyntheses and arranged chronologically according to the first description of the respective biosynthetic pathway. As cyanobacterial secondary metabolites frequently occur as classes of related molecules, only a single representative of each structural class will be discussed.

NRPS and PKS pathways in freshwater cyanobacteria

Microcystin

The first biosynthetic pathway identified and partially characterized for cyanobacteria was the mixed NRPS/PKS pathway catalyzing the formation of the hepatotoxin microcystin **1** (Figure 3) in the cyanobacterium *Microcystis aeruginosa* [17-19]. Microcystins are produced by different genera of freshwater cyanobacteria and inhibit eukaryotic protein phosphatases of types 1 and 2A. A signature of this heptapeptide family is the unusual β-amino acid Adda (3-amino-9-methoxy-2,6,8-trimethyl-10-phenyldeca-4,6-dienoic acid); more than 60

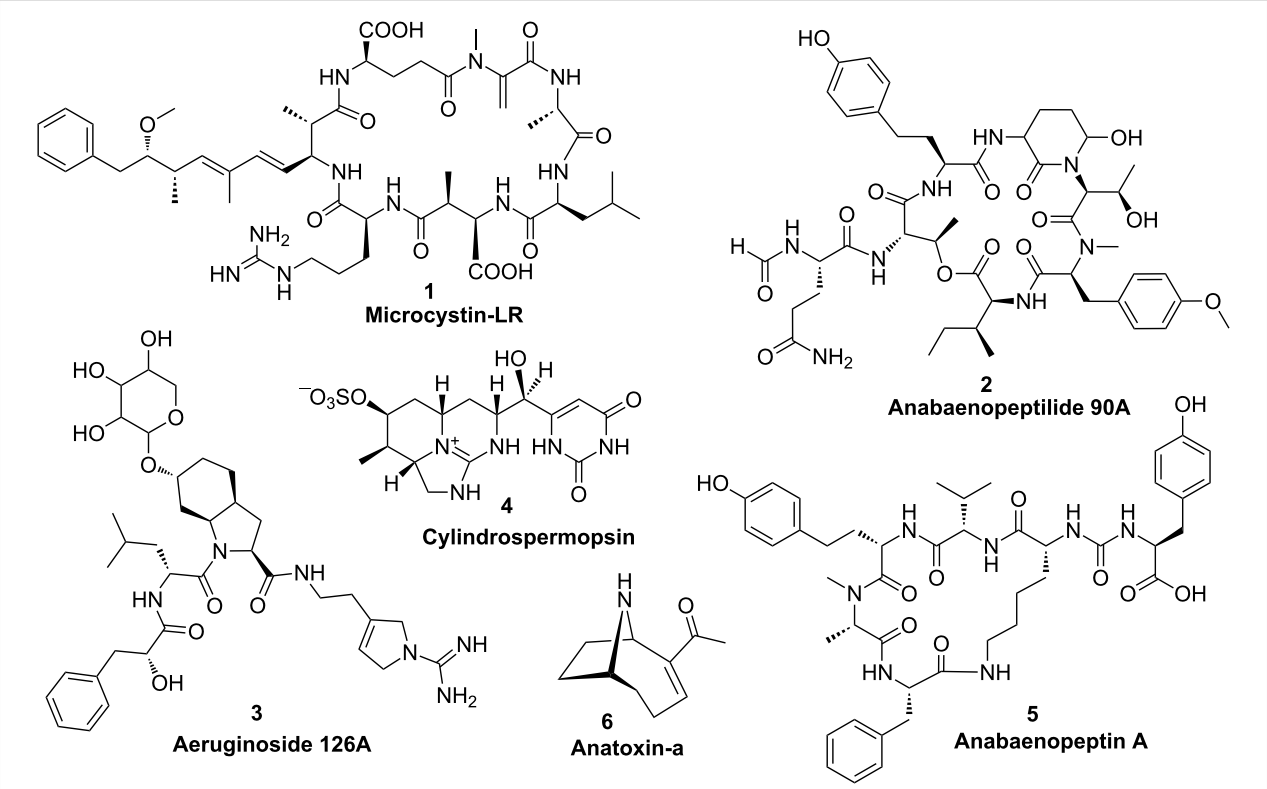

Figure 3: Structures of NRPS and PKS products in freshwater cyanobacteria.

isoforms of the peptide have been described. The pentapeptide nodularin is structurally closely related and shares a highly similar biosynthetic pathway [20]. The biosynthetic assembly line of microcystin was predicted to start with the activation of phenylacetate; however, in vitro studies showed that phenylpropanoic acids are preferentially activated and loaded onto the neighboring PCP carrier domain and disproved the activation of phenylacetate [21]. Nevertheless, in order to generate the expected polyketide chain one carbon must be excised following extension with malonyl-CoA. The mechanism by which this truncation occurs is currently unknown (Figure 4A). Further unique features of microcystin biosynthesis include the standalone aspartate racemase McyF [22], the *O*-methyltransferase McyJ [23] and the 2-hydroxy-acid dehydrogenase McyI [24]. In addition, microcystins contain two amino acids that are linked with their ω-carboxy group in the peptide chain, namely glutamate and aspartate. Although the mechanism by which these amino acids are activated is still unknown, the microcystin biosynthesis pathway exemplifies the high number of unique features in cyanobacterial modular biosyntheses.

Anabaenopeptilide

The anabaenopeptilide pathway in the strain *Anabaena* 90 was described soon after first reports about microcystin biosynthesis. Anabaenopeptilides **2** belong to the cyanopeptolin family of depsipeptides that were shown to inhibit different types of serine proteases [7]. Like microcystins, these peptides are frequently produced by bloom-forming freshwater cyanobacteria. The signature of this group is the unusual 3-amino-6-hydroxy-2-piperidone moiety (Ahp). The corresponding NRPS assembly line consists of seven modules [25]. Unique features include an integrated formyl transferase domain in the initiation module and NAD-dependent halogenase. The formation of Ahp remains to be analyzed.

Aeruginosin

Aeruginosins are specific inhibitors of serine type proteases and produced by different genera of freshwater cyanobacteria. The strain *Planktothrix agardhii* NIVA-CYA 126 was used to identify and partially characterize the corresponding biosynthetic pathway [26]. The strain produces glycosylated variants of the peptides, aeruginosides **3**, via a mixed NRPS/PKS pathway. The signature of this group is the 2-carboxy-6-hydroxyoctahydroindole (Choi) moiety. The loading module was predicted to activate phenylpyruvate which is reduced by an integrated KR domain to phenyllactate [26]. Mutational analyses have revealed that the Choi moiety is synthesized by the three enzymes AerD, AerE and AerF [26]. AerD has been shown to catalyze a prephenate decarboxylation step [27], the exact roles of AerE and AerF remain to be elucidated (Figure 4B). The

succeeding NRPS adenylation domain is then directly activating Choi as a substrate. The aeruginoside assembly line does not contain a thioesterase or reductase domain [26]. It is thus currently unclear how the final product is released from the enzyme complex.

Cylindrospermopsin

Cylindrospermopsin (**4**) is a hepatotoxin produced by different genera of freshwater cyanobacteria, including *Cylindrospermopsis raciborskii*, *Aphanizomenon ovalisporum* and *Aphanizomenon flos-aquae*. The polyketide-derived alkaloid inhibits glutathione and protein synthesis as well as cytochrome P450. Characteristic features of cylindrospermopsins include a guanidine moiety and a hydroxymethyluracil attached to the tricyclic carbon skeleton. According to feeding assays, the polyketide chain assembly starts with the activation of guanidinoacetate [28]. The precursor is formed via the activity of the unique L-arginine-glycine amidinotransferase CyrA (AoaA in *A. ovalisporum*) [29,30] (Figure 4C). The assembly line further comprises seven additional malonyl-CoA specific PKS modules [28]. It has been discussed that the three cyclization steps necessary for the formation of the characteristic tricyclic structure of cylindrospermopsins occur spontaneously by Michael addition during polyketide elongation rather than by enzymatic control [28]. Two enzymes, CyrG and CyrH with similarity to amidohydrolases/ureases/dihydroorotases are discussed to be responsible for uracil ring formation, although biochemical evidence is currently missing. The final hydroxylation step towards cylin-

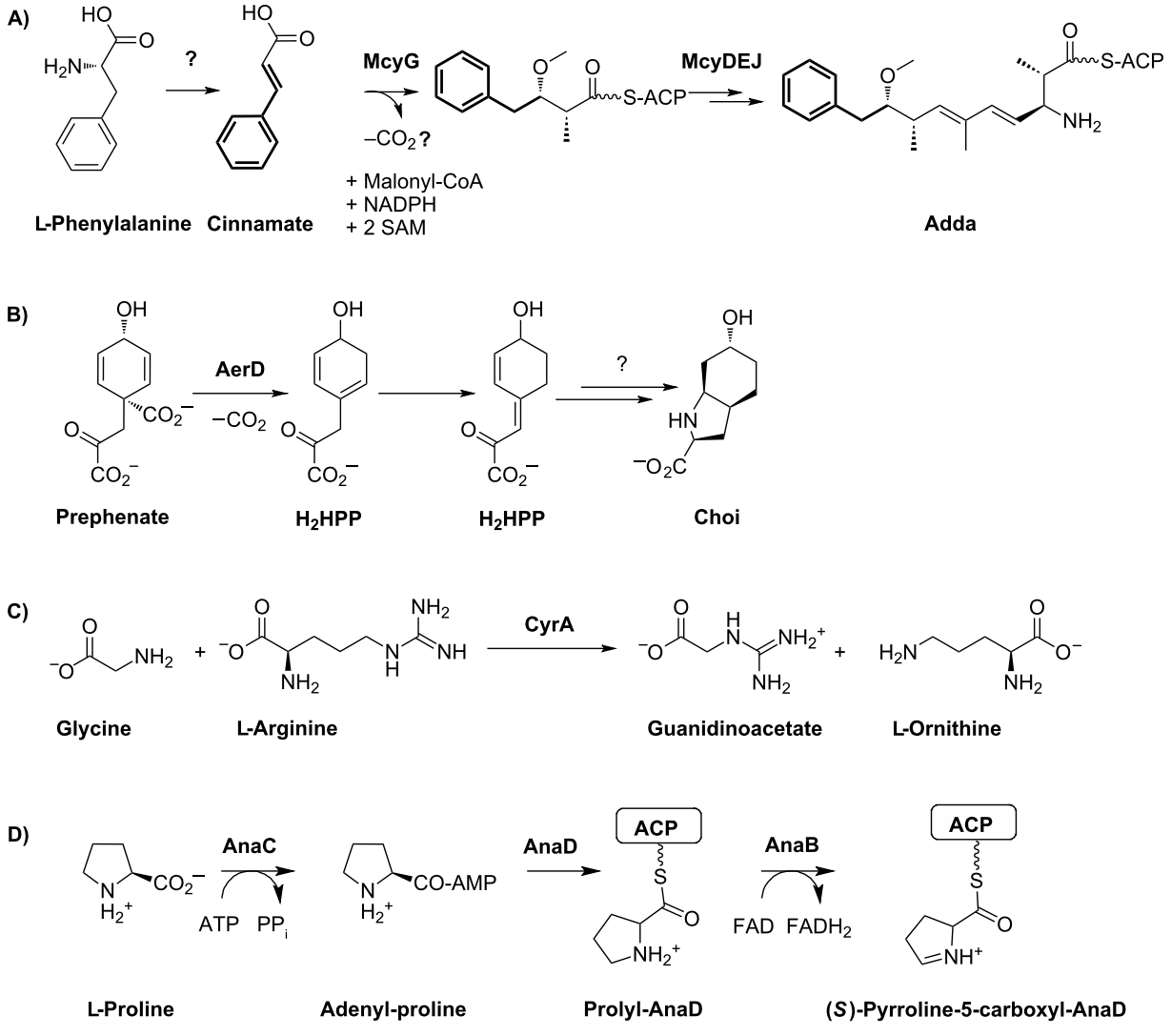

Figure 4: A) Synthesis of the Adda ((2*S*,3*S*,8*S*,9*S*)-3-amino-9-methoxy-2,6,8-trimethyl-10-phenyl-4,6-decadienoic acid) moiety of microcystin (**1**) starting with cinnamate. The mechanism of α-carbon decarboxylation has to be elucidated. B) Synthesis of the Choi moiety of the aeruginosin **3**. H_2HPP: Dihydro-4-hydroxyphenylpyruvate. C) Formation of the guanidinoacetate starter unit for the subsequent PKS assembly line of cylindrospermopsin (**4**). D) Formation of the (*S*)-pyrroline-5-carboxylate starter unit from proline in anatoxin-a (**6**) synthesis. ACP: Acyl carrier protein.

drospermopsin has been shown to be catalyzed by CyrI, a 2-oxoglutarate-dependent iron oxygenase [31]. Interestingly, two epimers were described for the corresponding hydroxyl group resulting in either 7-*epi*-cylindrospermopsin or cylindrospermopsin. The proportion of these two epimers varies in different cylindrospermopsin producing strains. It remains to be shown if the corresponding hydroxylase produces both stereoisomers or if a second unidentified hydroxylase is involved in the alternative epimer formation [32]. The CyrJ protein is the candidate protein for the sulfatation tailoring step.

Anabaenopeptin

Anabaenopeptins **5** are a highly diverse family of cyclic hexapeptides produced by various genera of freshwater cyanobacteria. Several members of the family potently inhibit proteases. A signature of the group is the conserved ureido linkage connecting the side-chain amino acid to D-lysine. The corresponding NRPS gene cluster was first analyzed in the strain *Anabaena* sp. 90 and revealed a new mechanism underlying production of diverse variants by the same strain: Two alternative NRPS starter modules [33]. Other cyanobacterial strains achieve diversity of anabaenopeptins by a different mode: Promiscuous A-domains [34]. The anabaenopeptin cluster contains five additional NRPS modules and an uncharacterized protein with similarity to pyruvate carboxyltransferases. The mechanism of ureido bond formation remains to be elucidated. Recently, ureido bond formation was characterized for the protease inhibitor syringolin A that is produced by *Pseudomonas syringiae* [35]. The responsible freestanding NRPS module contains a sequence stretch with similarity to acyltransferases between the condensation and adenylation domain. This sequence stretch does not show homology to any of the anabaenopeptin (Apt) biosynthesis proteins, suggesting a different mechanism of ureido bond formation for anabaenopeptins and syringolin [33].

Anatoxin

Anatoxin-a (**6**) and homoanatoxin-a are potent neurotoxins produced by cyanobacteria. A gene cluster for the alkaloid was first described for the strain *Oscillatoria* sp. PCC 6506 [36]. Analysis of the gene cluster and feeding studies suggested a biosynthetic scheme starting from L-proline and involving three polyketide synthases, with (*S*)-1-pyrolline-5-carboxylate proposed as the starter (Figure 4D) [37]. The first part of the biosynthesis could be reproduced with the acyl carrier protein AnaD, the Sfp-like phosphopantetheinyl transferase OsPPT, the A domain protein AnaC and the prolyl-AnaD dehydrogenase AnaB. The resulting (*S*)-pyrroline-5-carboxyl-AnaD is assumed to be the starter of polyketide chain assembly at the polyketide synthase AnaE [38]. The following polyketide extension step is predicted to be catalyzed by the polyketide synthase AnaF. The predicted protein ORF1 that is encoded in direct proximity of the *ana* cluster is expected to catalyze a Claisen-type cyclization step to form the characteristic bicyclic ring structure of anatoxin while the growing chain is tethered to the AnaF ACP domain. Experimental evidence for this suggestion is currently lacking. Finally, the bicyclic thioester is suggested to be transferred to the polyketide synthase AnaG for chain extension and is followed by chain release, which is expected to be catalyzed by the type II thioesterase AnaA. The reaction scheme as proposed would yield 11-carboxyanatoxin-a and 11-carboxyhomoanatoxin-a. Either a spontaneous or an enzymatically catalyzed decarboxylation step is thus necessary to finally yield anatoxin-a and homoanatoxin-a [38].

NRPS and PKS pathways in marine cyanobacteria

Barbamide

Several NRPS/PKS assembly lines were identified and partially characterized for the marine cyanobacterium *Lyngbya majuscula* [39]. These filamentous tropical cyanobacteria are important contributors to coral reef ecosystems and extremely rich in bioactive secondary metabolites. The first pathway described was the biosynthesis of barbamide (**7**) (Figure 5), a chlorinated lipopeptide with potent molluscidal activity. The lipopeptide contains a unique trichloroleucyl starter unit that is halogenated by unique biochemical mechanisms through the two non-heme iron(II)-dependent halogenases BarB1 and BarB2 (Figure 6A) [40]. Further extraordinary features of the pathway include one-carbon truncation during chain elongation, *E*-double bond formation and thiazole ring formation.

Jamaicamide

The second biosynthetic pathway identified in a strain of the tropical marine cyanobacterium *Lyngbya majuscula* was assigned to jamaicamides **8**. Jamaicamides are neurotoxins and show sodium-channel-blocking activity. The lipopeptide is highly functionalized and contains a bromo-alkynyl, a chlorovinylidene substituent, a beta-methoxy eneone system, and a pyrrolinone ring [41]. The incorporation of the chlorovinylidene group was partially elucidated and predicted to be highly similar to the cyclopropane ring formation of curacin A biosynthesis (Figure 6B) ([42], see below). The enzyme cassette comprises a PKS module containing an integrated halogenase and a tandem acyl carrier protein tridomain (ACP_3), a discrete ACP_{IV}, a discrete ketosynthase (KS), a 3-hydroxy-3-methylglutaryl CoA synthetase (HMGCS), a dehydratase (ECH_1)/decarboxylase (ECH_2) pair and an enoyl reductase (ER) domain. HMG-CoA synthetases were shown to introduce β-branching carboxyl units into a number of polyketide chains. Feeding studies for jamaicamides revealed the incorporation of an acetate unit at the corresponding position followed

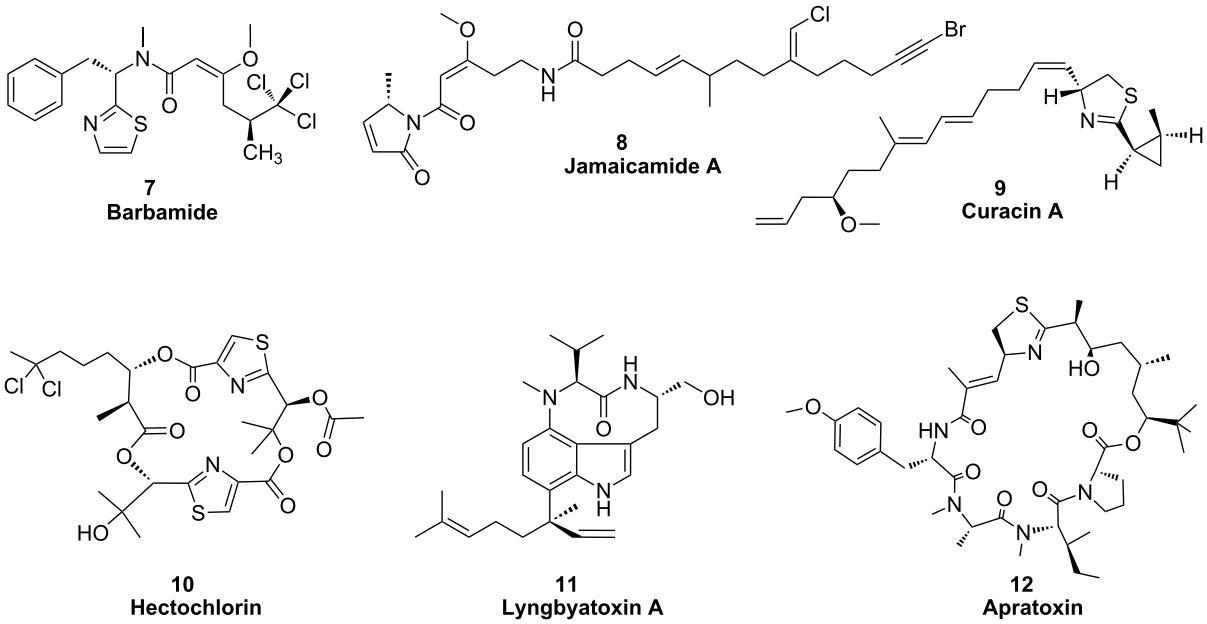

Figure 5: Structures of NRPS and PKS products in marine cyanobacteria.

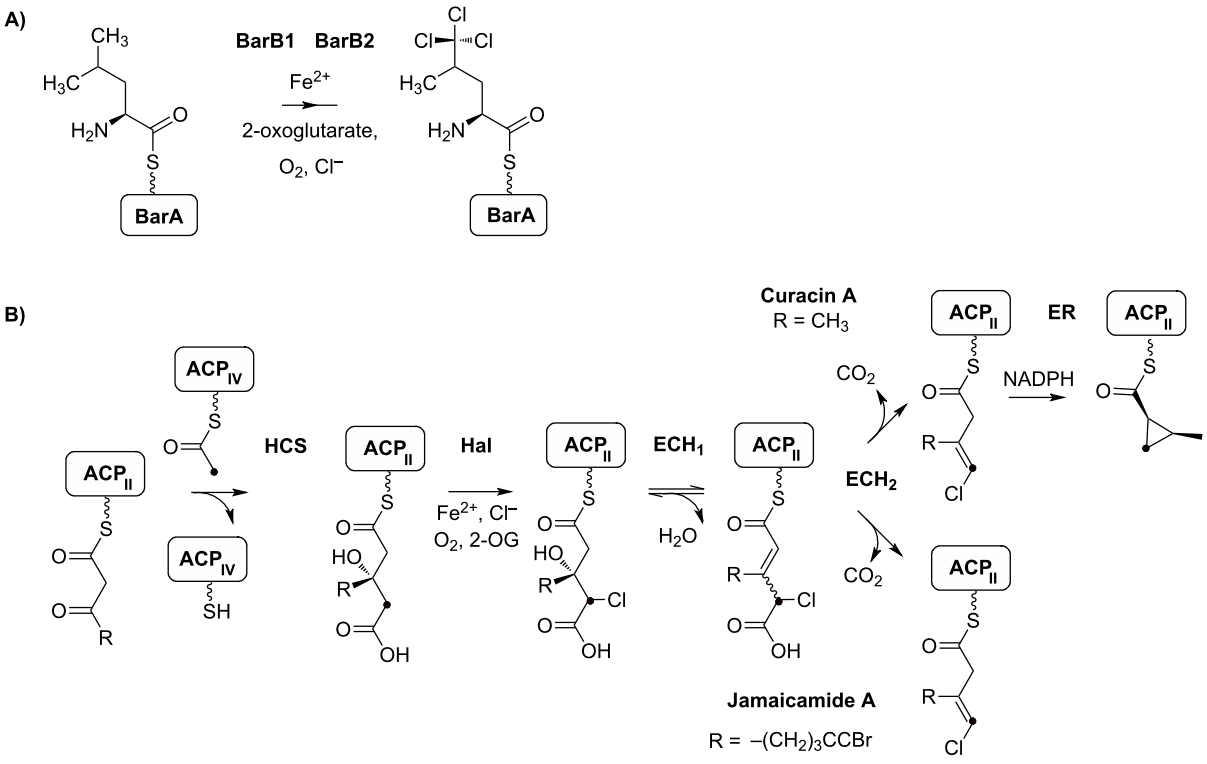

Figure 6: A) Formation of the trichloroleucyl starter unit of barbamide (**7**) synthesis through the non-heme iron(II)-dependent halogenases BarB1 and BarB2. B) Formation of cyclopropane and vinyl chloride functional groups in curacin A (**9**) and jamaicamide A (**8**) biosynthesis, respectively. The halogenated carbon is highlighted with a black dot. ACP: Acyl carrier protein; HCS: HMG-CoA synthase-like enzyme; Hal: Halogenase; ECH_1: Dehydratase; ECH_2: Decarboxylase; ER: Enoyl reductase.

by dehydratisation, decarboxylation and halogenation [41]. Further interesting features of jamaicamide biosynthesis include a six-carbon carboxylic acid unit as starter moiety. In vitro studies revealed the activation of either hexanoic, hexenoic or hexynoic acids at the JamA enzyme, whereas bromination clearly succeeded thioester formation [43].

Curacin A

Curacin A (**9**) was originally isolated from a *Lyngbya majuscula* strain found in Curacao, and it exhibits potent antiproliferative and cytotoxic activities [44]. This intriguing structure contains a thiazoline and a cyclopropyl ring. Interestingly, the pathway comprises a HMG-CoA synthase cassette, highly similar to the one of the jamaicamide assembly line, including the PKS module with the tandem acyl carrier protein tridomain (ACP_3) as well as the discrete ACP_{IV}, the discrete ketosynthase, the 3-hydroxy-3-methylglutaryl CoA synthetase (HMGCS), the dehydratase (ECH_1)/decarboxylase (ECH_2) pair and the ER domain [42,44]. Notably, the PKS module harbors a halogenation domain, although this could not be expected from the structure of curacin A. In vitro studies revealed that indeed cyclopropyl ring formation is preceded by a halogenation step (Figure 6B) [42]. The Cur ECH_2 was found to catalyze the formation of a α,β-enoyl thioester, which is in contrast to the related enzyme of the Jam pathway, which generates a β,γ-thioester of the 3-methyl-4-chloroglutaconyl decarboxylation intermediate product [42]. The jamaicamide and curacin pathways thus provide a nice example of how diversification of single enzymes can lead to very different functionalities in the product.

The initiation module of curacin biosynthesis contains a GCN5-related *N*-acetyltransferase (GNAT) domain. These enzymes typically catalyze acyl transfer to a primary amine. The curacin GNAT, however, was shown to be bifunctional and to exhibit decarboxylase/*S*-acetyltransferase activities [45]. The corresponding PKS module was found to activate malonyl-CoA, which is expected to be transferred to the thiol group of the adjacent ACP domain via the embedded GNAT domain. However, only an acetyl group could be detected on the ACP, supporting an additional decarboxylase activity for the GNAT domain [46].

Hectochlorin

Hectochlorin (**10**) was isolated from a Jamaican isolate of *Lyngbya majuscula* and exhibits antifungal activity. It also shows potent activity towards a number of cancer cell lines. HctA, an acyl-CoA synthetase homologue, is expected to activate free hexanoic acid and to provide the starter for hectochlorin synthesis. Chain elongation is performed by a monomodular PKS and two bimodular NRPS. Two of the NRPS modules are suggested to activate 2-oxo-isovaleric acid, which is reduced by an embedded KR domain to 2-hydroxyisovaleric acid and proposed to be further oxidized by one of two cytochrome-P450-type monooxygenases encoded by the cluster, HctG or HctH, to 2,3-dihydroxyisovaleric acid. Two other NRPS modules contain all the required domains for adenylation and heterocyclization of cysteine, and an FMN-dependent oxidase domain, which is likely involved in thiazole ring formation. The cluster further encodes a halogenase/ACP didomain protein that is suggested to be responsible for the gem-dichloro group in hectochlorin, HctB. The specifities of the NRPS adenylation domains have been confirmed in vitro [47].

Lyngbyatoxin

Lyngbyatoxins **11**, produced by *Lyngbya majuscula,* can cause skin irritations and are implicated in the so-called "swimmers itch". The compounds are also potent tumor promoters, which operate by competitively binding to protein kinase C (PKC). The characteristic indolactam ring of the toxin is synthesized by the bimodular NRPS LtxA [48]. The resulting dipeptide is tethered to a PCP domain and reductively released by the terminal NADPH-dependent reductase domain of LtxA [49]. The indolactam ring formation further requires the activity of the P450-dependent monooxygenase/cyclase LtxB [50]. Finally, the *ltx* cluster encodes the aromatic prenyltransferase LtxC, which was shown to catalyze geranyl pyrophosphate (GPP) addition to the indolactam ring in vitro [48].

Apratoxin

Apratoxin A (**12**) was isolated from a *Lyngbya bouillonii* strain isolated from a shallow-reef environment surrounding the island of Guam, Palau. Apratoxin A is a potent cytotoxin showing selective toxicity to cancer cells grown on solid agar as well as in the case of in vivo mouse models [51]. The corresponding hybrid PKS/NRPS pathway was identified through a single-cell genome-amplification approach and features a PKS-type loading module and nine extension modules (four PKS and five NRPS) [52]. Unique features of the cluster include a putative GCN_5-related transferase, which is suggested to transfer three methyl groups from *S*-adenosyl-methionine (SAM) to malonyl-CoA to yield the *tert*-butyl terminus of apratoxin. The cluster further encodes a series of proteins resembling an HCS-like gene cassette that is expected to be involved in β-branching of polyketides [52].

NRPS and PKS pathways in terrestrial cyanobacteria

Nostopeptolide

The nostopeptolide gene cluster was the first NRPS/PKS type gene cluster described for a terrestrial cyanobacterial strain, namely *Nostoc* sp. GSV 224 [53]. Nostopeptolides **13**

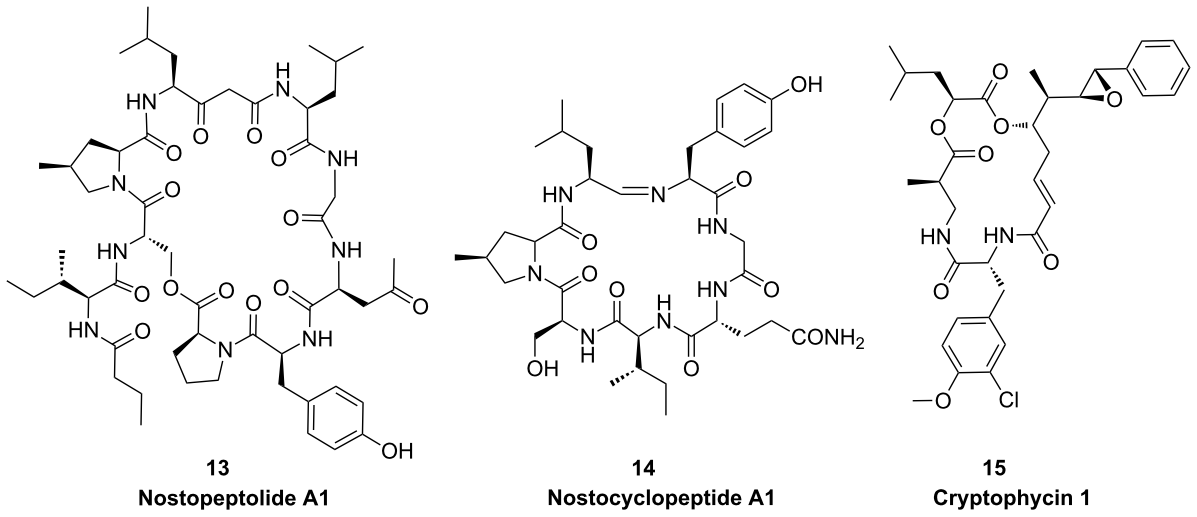

Figure 7: Structures of NRPS and PKS products in terrestrial cyanobacteria.

(Figure 7) are nonapeptides carrying a butyric acid and an internal acetate-derived unit. No cytotoxic, antifungal or protease-inhibition activities could be assigned to the compound. One of the unique components of the peptide backbone is the nonproteinogenic amino acid L-4-methylproline, which is synthesized from L-leucine by the zinc-dependent long-chain dehydrogenase NosE and the Δ^1-pyrroline-5-carboxylic acid reductase homologue NosF (Figure 8) [54].

Nostocyclopeptide

The nostocyclopeptide **14** pathway is one of the few pure NRPS assembly lines of cyanobacteria and has been described for the terrestrial cyanobacterium *Nostoc* sp. ATCC 53789 [55]. The cyclic heptapeptide shares the L-4-methylproline unit of nostopeptolides and is synthesized by two enzymes closely resembling NosE and NosF. A unique feature of nostocyclopeptide biosynthesis is the mechanism of macrocyclization through imino bond formation between the N-terminal and C-terminal amino acids. The responsible enzyme NcpB contains a C-terminal reductase domain that has been shown to catalyze the reductive release of the peptide from the synthetase as an aldehyde followed by spontaneous formation of the imino head-to-tail linkage [56].

Cryptophycin

Cryptophycins were shown to be produced by terrestrial strains of *Nostoc* that are either free living or associated with a lichen symbiont. Cryptophycin 1 (**15**) is the most potent tubulin-destabilizing compound ever discovered and serves as a leading product for the development of cancer therapeutics. The corresponding biosynthetic pathway comprises three PKS and two NRPS-type enzymes [57]. The chain-initiation module of the enzyme CrpA closely resembles the loading module of microcystin biosynthesis where phenylpropanoic acids are activated and finally phenylacetate is incorporated in the product [21]. Characteristic features of the pathway further include an adenylation/ketoreductase didomain for the generation of α-hydroxy acids following activation of leucine [57]. The pathway also features an FAD-dependent halogenase [57] and the CYP450 epoxidase CrpE [58].

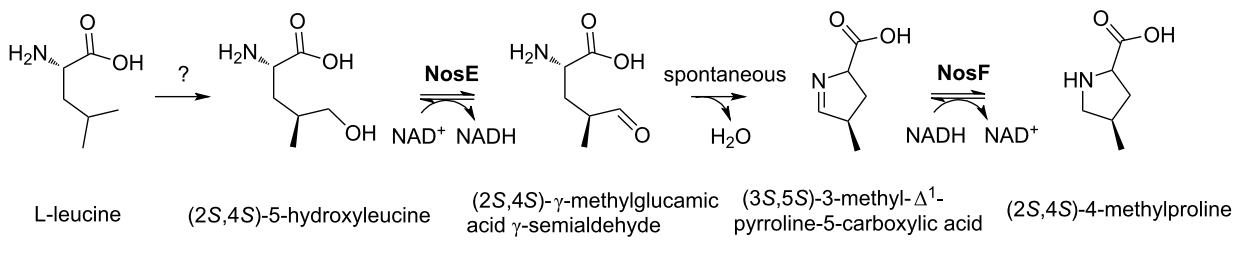

Figure 8: Synthesis of the (2*S*,4*S*)-4-methylproline moiety of nostopeptolides A (**13**).

Peptides ribosomally produced and post-translationally modified

Although the majority of cyanobacterial peptides are produced nonribosomally, for two peptide families, namely patellamides **16** and microviridins **17** (Figure 9), no NRPS pathway could be assigned, thus initiating research on ribosomal peptide pathways in cyanobacteria. Genome-scale analyses have unravelled further peptide families. Cyanobacteria can now be considered as one of the most prolific sources of ribosomally produced natural products. Hereafter, we give an overview of three major peptide families and their underlying biochemistry.

Cyanobactins

The first ribosomal pathway discovered was the biosynthesis of patellamides in the symbiotic cyanobacterium *Prochloron*. The cyclic octapeptides are pseudosymmetric and contain thiazole and oxazolin rings. Patellamides **16** are typically moderately cytotoxic, and some variants were further reported to reverse multidrug resistance [59]. The patellamide gene cluster consists of seven genes, expression of which in *E. coli* leads to the production of the peptides [59]. Heterocyclization of serine, cysteine and threonine, respectively is catalyzed by the heterocyclase PatD [60]. In contrast to other heterocyclases studied, PatD is a single ATP-dependent enzyme not requiring an additional oxidase enzyme [60]. The PatG protease encoded by the cluster was shown to macrocyclize diverse substrates by a mechanism closely resembling the thioesterase-catalyzed chemistry of most NRPS systems [61]. Several related pathways were later discovered in a variety of cyanobacterial strains. The PatG-type of macrocylization is the signature of this diverse group, which is now called the cyanobactin family [62,63]. The pathways optionally contain prenyltransferases: The substrate specificity and scope of which remain to be determined [62,63].

Microviridins

Microviridins **17** are a group of tricyclic depsipeptides predominantly detected in bloom-forming freshwater cyanobacteria. Several members of the family potently inhibit various serine-type proteases. The biosynthetic pathway of microviridins was described for the genera *Microcystis* and *Planktothrix* [64,65]. Post-translational modification of microviridins is achieved by the activity of two closely related ATP grasp ligases, MdnB and MdnC (MvdC and D in *Planktothrix*). The enzymes introduce

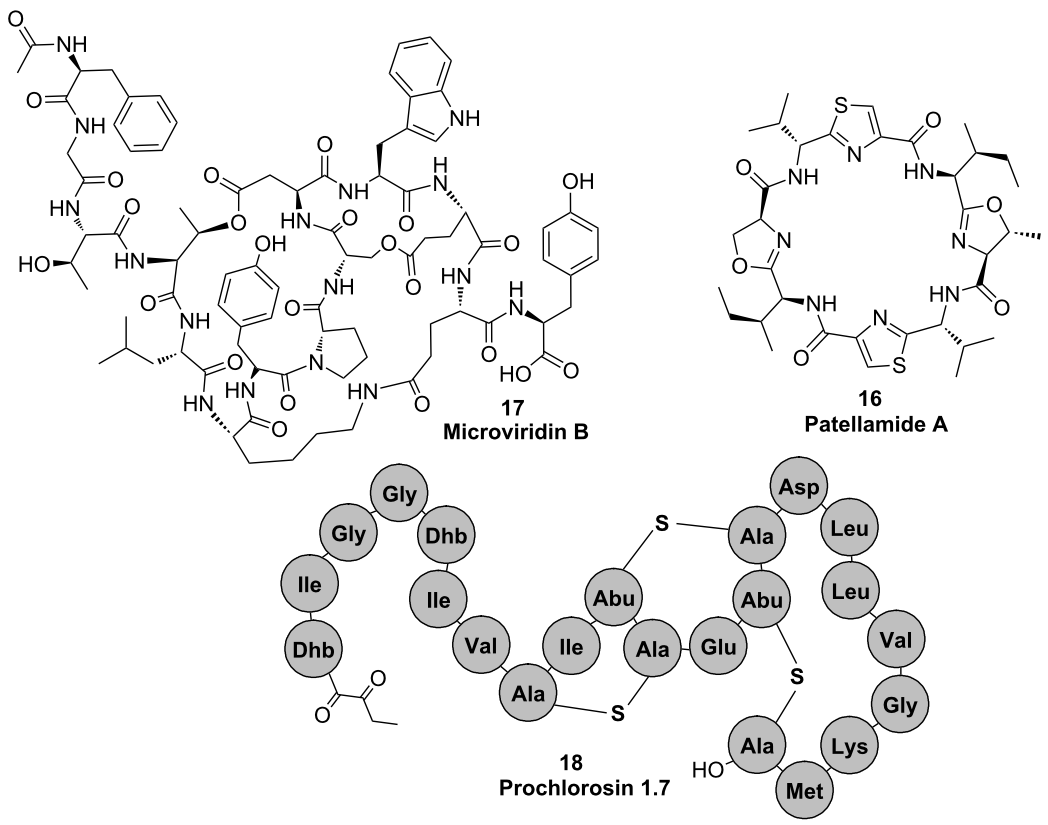

Figure 9: Structures of cyanobacterial peptides that are synthesized ribosomally and post-translationally modified.

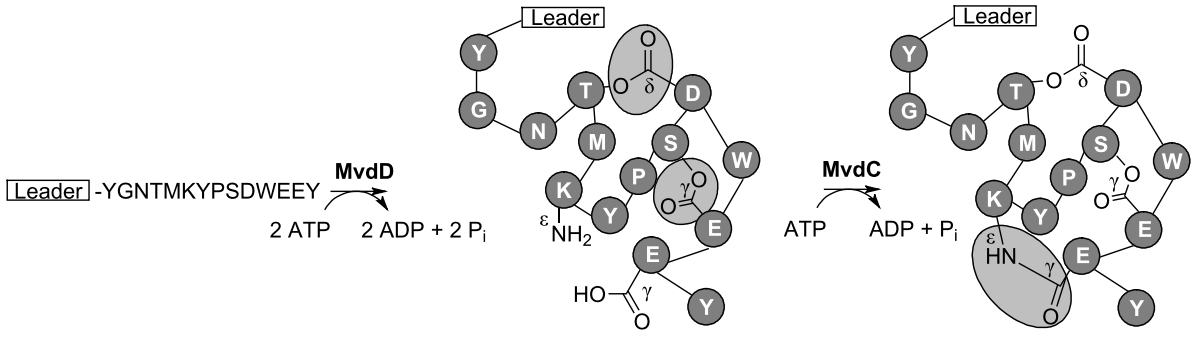

Figure 10: Formation of ester linkages and ω-amide linkage in microviridins **17** by the ATP grasp ligases MvdD and MvdC, respectively.

two ω-ester linkages between threonine and aspartate and serine and glutamate (MdnC/MvdD) and one ω-amide linkage between lysine and aspartate (MdnB/MvdC) (Figure 10) [64,65]. Microviridins can be heterologously produced in *E. coli* [65]. Cyclizations occur in a strictly defined order. Ring size and composition of the microviridin core peptide is invariant [66], whereas N-terminal and C-terminal amino acids are highly variant [67]. The enzyme system further contains a GNAT-type *N*-acetyltransferase and an ABC transporter. The mechanism, by which the leader peptide of microviridins is cleaved off, remains to be elucidated.

Lantipeptides

Lantipeptides are produced by various types of bacteria. The characteristic feature of the group is lanthionine bridges, which are formed by dehydration of serine or threonine followed by intramolecular addition of cysteine thiols to the resulting dehydro amino acids. Lantipeptides exhibit a variety of bioactivities, in particular antimicrobial activities (lantibiotics) [68]. Cyanobacteria were shown to frequently encode LanM type enzymes, i.e., bifunctional enzymes catalyzing both dehydration and cyclization reactions [68]. An interesting phenomenon was observed for the strain *Prochlorococcus* MIT9313, which is a single-celled planktonic marine cyanobacterium [69]. A single LanM-type enzyme, ProcM, was found to cooperate with 29 different precursor peptides in vitro and in vivo. The enzyme thus showed a remarkable catalytic promiscuity. The precursor peptides were encoded either *cis* or *trans* to the ProcM enzyme, and the resulting family of lantipeptides was designated prochlorosins **18** [69].

UV-absorbing pigments

Photosynthetic cyanobacteria depend on light for energy production. At the same time they are exposed to damaging solar UV radiation. Microorganisms have evolved different strategies to cope with UV light: UV avoidance/protection, and UV-absorption compounds. Cyanobacteria produce two types of sunscreen compounds, induced under UV irradiation: Scytonemin (**19**) and mycosporine-like amino acids **20** (Figure 11). Biosynthesis of the two groups of compounds has recently been elucidated, providing further examples for the fascinating natural product biochemistry of cyanobacteria.

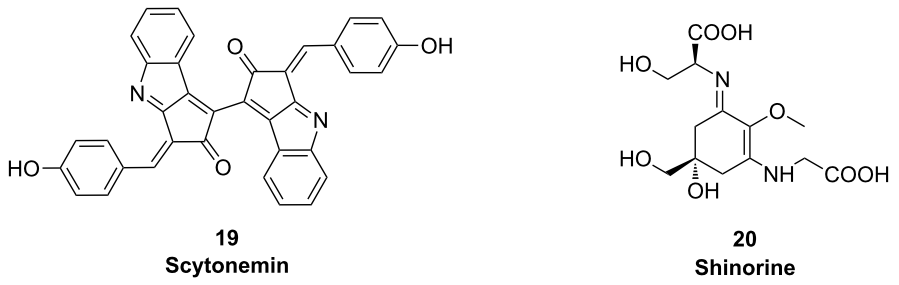

Figure 11: Structures of cyanobacterial sunscreen compounds.

Scytonemin

A gene cluster responsible for scytonemin (**19**) biosynthesis was initially discovered by random mutagenesis in the terrestrial symbiotic cyanobacterium *Nostoc punctiforme* [70]. The gene cluster contains a number of genes related to aromatic amino acid biosynthesis [70]. The biosynthetic route was proposed to start with tryptophan and tyrosine. Two of the initial steps of the sunscreen synthesis were reproduced in vitro [71]. The ORF NpR1275 was confirmed to act as a tryptophan dehydrogenase, whereas *p*-hydroxyphenylpyruvic acid was proposed to be generated by the putative prephenate dehydrogenase NpR1269. Both substrates are then further transformed by the thiamin diphosphate (ThDP)-dependent enzyme NpR1276 to isomeric acyloins representing one-half of the carbon framework of scytonemin [71]. The enzyme showed a remarkable selectivity for the specific C-C bond reaction that is unprecedented in natural systems. Further enzymatic transformations of the scytonemin pathway remain to be elucidated [71].

Mycosporine-like amino acids (MAAs)

Mycosporines were initially discovered in fungi and found to trigger light-induced fungal sporulation. Beside microsporines that consist of a single amino acid linked to cyclohexenone, cyanobacteria and other algae produce mycosporine-like amino acids (MAAs, **20**), which contain two substituents linked to the central ring by imine linkages. Four enzymes are involved in the synthesis of the specific MAA shinorine in *Anabaena variabilis* ATCC 29413: A dehydroquinase synthase homologue (DHQS), an *O*-methyl-transferase (O-MT), an ATP grasp ligase and an NRPS-like enzyme. Cloning of the entire gene cluster in *E. coli* led to the production of shinorine. The production of the intermediate 4-deoxygadusol by DHQS and O-MT could be reproduced in vitro. Unexpectedly, the DHQS homologue accepted sedoheptulose 7-phosphate as a substrate. The ATP grasp ligase and the NRPS-like enzyme could be related to the amino acid attachment to the cyclohexenone core by two unique enzyme strategies for imine formation.

Conclusion

Genome sequencing projects of cyanobacteria have revealed a far greater potential of cyanobacteria to produce natural products than expected. It can thus be anticipated that genomic mining techniques that start with the theoretical prediction of structures from genomic data will be of increasing importance for the discovery of natural products in the future. In order to identify products of cryptic cyanobacterial pathways, several research groups have used heterologous expression approaches, e.g., for the discovery of cyanobactins, microviridins and prochlorosins. The expansion of the existing genomic mining toolbox to access the genomic resources and to discover hidden treasures remains a challenge for the future.

Cyanobacterial biosynthetic enzymes have revealed great potential for synthetic biology approaches for rational modifications of existing leading compounds and for the generation of libraries of new compounds. Enzymes catalyzing macrocyclization of cyanobactins, as an example, are highly promiscuous and have been successfully used for the cyclization of diverse peptides. Future studies will have to show how many of the fascinating biochemical features of cyanobacterial biosynthetic enzymes can be utilized for the design of novel compounds and their optimization toward medical targets.

Acknowledgements

E.D. was supported by a grant of the German Research Foundation (DFG, Di 910/4-1). D.G.P. was supported by the National Council for Scientific and Technological Development (CNPq), an agency linked to the Brazilian Ministry of Science and Technology (MCT) and the German Academic Exchange Service (DAAD). We thank Holger Jenke-Kodama for critical reading of an earlier version of the manuscript. We thank Katrin Hinrichs for providing cycad photographs.

References

1. Rippka, R. *Methods Enzymol.* **1988,** *167,* 3–27. doi:10.1016/0076-6879(88)67004-2
2. Rai, A. N.; Söderbäck, E.; Bergman, B. *New Phytol.* **2000,** *147,* 449–481. doi:10.1046/j.1469-8137.2000.00720.x
3. Paerl, H. W.; Fulton, R. S., III; Moisander, P. H.; Dyble, J. *TheScientificWorldJOURNAL* **2001,** *1,* 76–113. doi:10.1100/tsw.2001.16
4. Dittmann, E.; Wiegand, C. *Mol. Nutr. Food Res.* **2006,** *50,* 7–17. doi:10.1002/mnfr.200500162
5. Patterson, G. M. L.; Larsen, L. K.; Moore, R. E. J. *Appl. Phycol.* **1994,** *6,* 151–157. doi:10.1007/BF02186069
6. Dittmann, E.; Neilan, B.; Börner, T. *Appl. Microbiol. Biotechnol.* **2001,** *57,* 467–473. doi:10.1007/s002530100810
7. Welker, M.; von Döhren, H. *FEMS Microbiol. Rev.* **2006,** *30,* 530–563. doi:10.1111/j.1574-6976.2006.00022.x
8. Gerwick, W. H.; Tan, L. T.; Sitachitta, N. In *Alkaloids: Chemistry and Biology;* Cordell, G. A., Ed.; Academic Press: San Diego, CA, 2001; Vol. 57, pp 75–184.
9. Jones, A. C.; Gu, L.; Sorrels, C. M.; Sherman, D. H.; Gerwick, W. H. *Curr. Opin. Chem. Biol.* **2009,** *13,* 216–223. doi:10.1016/j.cbpa.2009.02.019
10. Koglin, A.; Walsh, C. T. *Nat. Prod. Rep.* **2009,** *26,* 987–1000. doi:10.1039/b904543k
11. Grünewald, J.; Marahiel, M. A. *Microbiol. Mol. Biol. Rev.* **2006,** *70,* 121–146. doi:10.1128/MMBR.70.1.121-146.2006
12. Oman, T. J.; van der Donk, W. A. *Nat. Chem. Biol.* **2010,** *6,* 9–18. doi:10.1038/nchembio.286
13. Jenke-Kodama, H.; Sandmann, A.; Müller, R.; Dittmann, E. *Mol. Biol. Evol.* **2005,** *22,* 2027–2039. doi:10.1093/molbev/msi193
14. Staunton, J.; Weissman, K. J. *Nat. Prod. Rep.* **2001,** *18,* 380–416. doi:10.1039/a909079g
15. Piel, J. *Nat. Prod. Rep.* **2010,** *27,* 996–1047. doi:10.1039/B816430B
16. Campbell, C. D.; Vederas, J. C. *Biopolymers* **2010,** *93,* 755–763. doi:10.1002/bip.21428

17. Nishizawa, T.; Asayama, M.; Fujii, K.; Harada, K.-i.; Shirai, M. *J. Biochem.* **1999,** *126,* 520–529.
18. Nishizawa, T.; Ueda, A.; Asayama, M.; Fujii, K.; Harada, K.-i.; Ochi, K.; Shirai, M. *J. Biochem.* **2000,** *127,* 779–789.
19. Tillett, D.; Dittmann, E.; Erhard, M.; von Döhren, H.; Börner, T.; Neilan, B. A. *Chem. Biol.* **2000,** *7,* 753–764. doi:10.1016/S1074-5521(00)00021-1
20. Moffitt, M. C.; Neilan, B. A. *Appl. Environ. Microbiol.* **2004,** *70,* 6353–6362. doi:10.1128/AEM.70.11.6353-6362.2004
21. Hicks, L. M.; Moffitt, M. C.; Beer, L. L.; Moore, B. S.; Kelleher, N. L. *ACS Chem. Biol.* **2006,** *1,* 93–102. doi:10.1021/cb500007v
22. Sielaff, H.; Dittmann, E.; Tandeau De Marsac, N.; Bouchier, C.; Von Döhren, H.; Börner, T.; Schwecke, T. *Biochem. J.* **2003,** *373,* 909–916. doi:10.1042/BJ20030396
23. Christiansen, G.; Fastner, J.; Erhard, M.; Börner, T.; Dittmann, E. *J. Bacteriol.* **2003,** *185,* 564–572. doi:10.1128/JB.185.2.564-572.2003
24. Pearson, L. A.; Barrow, K. D.; Neilan, B. A. *J. Biol. Chem.* **2007,** *282,* 4681–4692. doi:10.1074/jbc.M606986200
25. Rouhiainen, L.; Paulin, L.; Suomalainen, S.; Hyytiainen, H.; Buikema, W.; Haselkorn, R.; Sivonen, K. *Mol. Microbiol.* **2000,** *37,* 156–167. doi:10.1046/j.1365-2958.2000.01982.x
26. Ishida, K.; Christiansen, G.; Yoshida, W. Y.; Kurmayer, R.; Welker, M.; Valls, N.; Bonjoch, J.; Hertweck, C.; Börner, T.; Hemscheidt, T.; Dittmann, E. *Chem. Biol.* **2007,** *14,* 565–576. doi:10.1016/j.chembiol.2007.04.006
27. Mahlstedt, S.; Fielding, E. N.; Moore, B. S.; Walsh, C. T. *Biochemistry* **2010,** *49,* 9021–9023. doi:10.1021/bi101457h
28. Mihali, T. K.; Kellmann, R.; Muenchhoff, J.; Barrow, K. D.; Neilan, B. A. *Appl. Environ. Microbiol.* **2008,** *74,* 716–722. doi:10.1128/AEM.01988-07
29. Muenchhoff, J.; Siddiqui, K. S.; Poljak, A.; Raftery, M. J.; Barrow, K. D.; Neilan, B. A. *FEBS J.* **2010,** *277,* 3844–3860. doi:10.1111/j.1742-4658.2010.07788.x
30. Shalev-Alon, G.; Sukenik, A.; Livnah, O.; Schwarz, R.; Kaplan, A. *FEMS Microbiol. Lett.* **2002,** *209,* 87–91. doi:10.1111/j.1574-6968.2002.tb11114.x
31. Mazmouz, R.; Chapuis-Hugon, F.; Pichon, V.; Méjean, A.; Ploux, O. *ChemBioChem* **2011,** *12,* 858–862. doi:10.1002/cbic.201000726
32. Mazmouz, R.; Chapuis-Hugon, F.; Mann, S.; Pichon, V.; Méjean, A.; Ploux, O. *Appl. Environ. Microbiol.* **2010,** *76,* 4943–4949. doi:10.1128/AEM.00717-10
33. Rouhiainen, L.; Jokela, J.; Fewer, D. P.; Urmann, M.; Sivonen, K. *Chem. Biol.* **2010,** *17,* 265–273. doi:10.1016/j.chembiol.2010.01.017
34. Christiansen, G.; Philmus, B.; Hemscheidt, T.; Kurmayer, R. *J. Bacteriol.* **2011,** *193,* 3822–3831. doi:10.1128/JB.00360-11
35. Imker, H. J.; Walsh, C. T.; Wuest, W. M. *J. Am. Chem. Soc.* **2009,** *131,* 18263–18265. doi:10.1021/ja909170u
36. Cadel-Six, S.; Iteman, I.; Peyraud-Thomas, C.; Mann, S.; Ploux, O.; Méjean, A. *Appl. Environ. Microbiol.* **2009,** *75,* 4909–4912. doi:10.1128/AEM.02478-08
37. Méjean, A.; Mann, S.; Maldiney, T.; Vassiliadis, G.; Lequin, O.; Ploux, O. *J. Am. Chem. Soc.* **2009,** *131,* 7512–7513. doi:10.1021/ja9024353
38. Méjean, A.; Mann, S.; Vassiliadis, G.; Lombard, B.; Loew, D.; Ploux, O. *Biochemistry* **2010,** *49,* 103–113. doi:10.1021/bi9018785
39. Chang, Z.; Flatt, P.; Gerwick, W. H.; Nguyen, V.-A.; Willis, C. L.; Sherman, D. H. *Gene* **2002,** *296,* 235–247. doi:10.1016/S0378-1119(02)00860-0
40. Galonić, D. P.; Vaillancourt, F. H.; Walsh, C. T. *J. Am. Chem. Soc.* **2006,** *128,* 3900–3901. doi:10.1021/ja060151n
41. Edwards, D. J.; Marquez, B. L.; Nogle, L. M.; McPhail, K.; Goeger, D. E.; Roberts, M. A.; Gerwick, W. H. *Chem. Biol.* **2004,** *11,* 817–833. doi:10.1016/j.chembiol.2004.03.030
42. Gu, L.; Wang, B.; Kulkarni, A.; Geders, T. W.; Grindberg, R. V.; Gerwick, L.; Håkansson, K.; Wipf, P.; Smith, J. L.; Gerwick, W. H.; Sherman, D. H. *Nature* **2009,** *459,* 731–735. doi:10.1038/nature07870
43. Dorrestein, P. C.; Blackhall, J.; Straight, P. D.; Fischbach, M. A.; Garneau-Tsodikova, S.; Edwards, D. J.; McLaughlin, S.; Lin, M.; Gerwick, W. H.; Kolter, R.; Walsh, C. T.; Kelleher, N. L. *Biochemistry* **2006,** *45,* 1537–1546. doi:10.1021/bi052333k
44. Chang, Z.; Sitachitta, N.; Rossi, J. V.; Roberts, M. A.; Flatt, P. M.; Jia, J.; Sherman, D. H.; Gerwick, W. H. *J. Nat. Prod.* **2004,** *67,* 1356–1367. doi:10.1021/np0499261
45. Gu, L.; Geders, T. W.; Wang, B.; Gerwick, W. H.; Håkansson, K.; Smith, J. L.; Sherman, D. H. *Science* **2007,** *318,* 970–974. doi:10.1126/science.1148790
46. Gu, L.; Wang, B.; Kulkarni, A.; Gehret, J. J.; Lloyd, K. R.; Gerwick, L.; Gerwick, W. H.; Wipf, P.; Håkansson, K.; Smith, J. L.; Sherman, D. H. *J. Am. Chem. Soc.* **2009,** *131,* 16033–16035. doi:10.1021/ja9071578
47. Ramaswamy, A. V.; Sorrels, C. M.; Gerwick, W. H. *J. Nat. Prod.* **2007,** *70,* 1977–1986. doi:10.1021/np0704250
48. Edwards, D. J.; Gerwick, W. H. *J. Am. Chem. Soc.* **2004,** *126,* 11432–11433. doi:10.1021/ja047876g
49. Read, J. A.; Walsh, C. T. *J. Am. Chem. Soc.* **2007,** *129,* 15762–15763. doi:10.1021/ja077374d
50. Huynh, M. U.; Elston, M. C.; Hernandez, N. M.; Ball, D. B.; Kajiyama, S.-i.; Irie, K.; Gerwick, W. H.; Edwards, D. J. *J. Nat. Prod.* **2010,** *73,* 71–74. doi:10.1021/np900481a
51. Tidgewell, K.; Engene, N.; Byrum, T.; Media, J.; Doi, T.; Valeriote, F. A.; Gerwick, W. H. *ChemBioChem* **2010,** *11,* 1458–1466. doi:10.1002/cbic.201000070
52. Grindberg, R. V.; Ishoey, T.; Brinza, D.; Esquenazi, E.; Coates, R. C.; Liu, W.-t.; Gerwick, L.; Dorrestein, P. C.; Pevzner, P.; Lasken, R.; Gerwick, W. H. *PLoS One* **2011,** *6,* e18565. doi:10.1371/journal.pone.0018565
53. Hoffmann, D.; Hevel, J. M.; Moore, R. E.; Moore, B. S. *Gene* **2003,** *311,* 171–180. doi:10.1016/S0378-1119(03)00587-0
54. Luesch, H.; Hoffmann, D.; Hevel, J. M.; Becker, J. E.; Golakoti, T.; Moore, R. E. *J. Org. Chem.* **2003,** *68,* 83–91. doi:10.1021/jo026479q
55. Becker, J. E.; Moore, R. E.; Moore, B. S. *Gene* **2004,** *325,* 35–42. doi:10.1016/j.gene.2003.09.034
56. Kopp, F.; Mahlert, C.; Grünewald, J.; Marahiel, M. A. *J. Am. Chem. Soc.* **2006,** *128,* 16478–16479. doi:10.1021/ja0667458
57. Magarvey, N. A.; Beck, Z. Q.; Golakoti, T.; Ding, Y.; Huber, U.; Hemscheidt, T. K.; Abelson, D.; Moore, R. E.; Sherman, D. H. *ACS Chem. Biol.* **2006,** *1,* 766–779. doi:10.1021/cb6004307
58. Ding, Y.; Seufert, W. H.; Beck, Z. Q.; Sherman, D. H. *J. Am. Chem. Soc.* **2008,** *130,* 5492–5498. doi:10.1021/ja710520q
59. Schmidt, E. W.; Nelson, J. T.; Rasko, D. A.; Sudek, S.; Eisen, J. A.; Haygood, M. G.; Ravel, J. *Proc. Natl. Acad. Sci. U. S. A.* **2005,** *102,* 7315–7320. doi:10.1073/pnas.0501424102
60. McIntosh, J. A.; Donia, M. S.; Schmidt, E. W. *J. Am. Chem. Soc.* **2010,** *132,* 4089–4091. doi:10.1021/ja9107116
61. Lee, J.; McIntosh, J.; Hathaway, B. J.; Schmidt, E. W. *J. Am. Chem. Soc.* **2009,** *131,* 2122–2124. doi:10.1021/ja8092168
62. Donia, M. S.; Ravel, J.; Schmidt, E. W. *Nat. Chem. Biol.* **2008,** *4,* 341–343. doi:10.1038/nchembio.84
63. Leikoski, N.; Fewer, D. P.; Jokela, J.; Wahlsten, M.; Rouhiainen, L.; Sivonen, K. *Appl. Environ. Microbiol.* **2010,** *76,* 701–709. doi:10.1128/AEM.01061-09

64. Philmus, B.; Christiansen, G.; Yoshida, W. Y.; Hemscheidt, T. K. *ChemBioChem* **2008,** *9,* 3066–3073. doi:10.1002/cbic.200800560
65. Ziemert, N.; Ishida, K.; Liaimer, A.; Hertweck, C.; Dittmann, E. *Angew. Chem., Int. Ed. Engl.* **2008,** *47,* 7756–7759. doi:10.1002/anie.200802730
66. Philmus, B.; Guerrette, J. P.; Hemscheidt, T. K. *ACS Chem. Biol.* **2009,** *4,* 429–434. doi:10.1021/cb900088r
67. Ziemert, N.; Ishida, K.; Weiz, A.; Hertweck, C.; Dittmann, E. *Appl. Environ. Microbiol.* **2010,** *76,* 3568–3574. doi:10.1128/AEM.02858-09
68. Goto, Y.; Li, B.; Claesen, J.; Shi, Y.; Bibb, M. J.; van der Donk, W. A. *PLoS Biol.* **2010,** *8,* e1000339. doi:10.1371/journal.pbio.1000339
69. Li, B.; Sher, D.; Kelly, L.; Shi, Y.; Huang, K.; Knerr, P. J.; Joewono, I.; Rusch, D.; Chisholm, S. W.; van der Donk, W. A. *Proc. Natl. Acad. Sci. U. S. A.* **2010,** *107,* 10430–10435. doi:10.1073/pnas.0913677107
70. Soule, T.; Stout, V.; Swingley, W. D.; Meeks, J. C.; Garcia-Pichel, F. *J. Bacteriol.* **2007,** *189,* 4465–4472. doi:10.1128/JB.01816-06
71. Balskus, E. P.; Walsh, C. T. *J. Am. Chem. Soc.* **2008,** *130,* 15260–15261. doi:10.1021/ja807192u

License and Terms

Beilstein Journal of Organic Chemistry

Marilones A–C, phthalides from the sponge-derived fungus *Stachylidium* sp.

Celso Almeida[1], Stefan Kehraus[1], Miguel Prudêncio[2] and Gabriele M. König[*1]

Letter

Open Access

Address:
[1]Institute for Pharmaceutical Biology, University of Bonn, Nussallee 6, D-53115 Bonn, Germany and [2]Instituto de Medicina Molecular, Malaria Unit, Faculdade de Medicina, Universidade de Lisboa, Av. Prof. Egas Moniz, 1649-028 Lisboa, Portugal

Email:
Gabriele M. König[*] - g.koenig@uni-bonn.de

* Corresponding author

Keywords:
marine fungi; natural products; phthalides; polyketides

Beilstein J. Org. Chem. **2011,** *7,* 1636–1642.
doi:10.3762/bjoc.7.192

Received: 23 May 2011
Accepted: 02 September 2011
Published: 05 December 2011

This article is part of the Thematic Series "Biosynthesis and function of secondary metabolites".

Guest Editor: J. S. Dickschat

Abstract

The marine-derived fungus *Stachylidium* sp. was isolated from the sponge *Callyspongia* sp. cf. *C. flammea.* Culture on a biomalt medium supplemented with sea salt led to the isolation of three new phthalide derivatives, i.e., marilones A–C (**1**–**3**), and the known compound silvaticol (**4**). The skeleton of marilones A and B is most unusual, and its biosynthesis is suggested to require unique biochemical reactions considering fungal secondary metabolism. Marilone A (**1**) was found to have antiplasmodial activity against *Plasmodium berghei* liver stages with an IC_{50} of 12.1 μM. Marilone B (**2**) showed selective antagonistic activity towards the serotonin receptor 5-HT_{2B} with a K_i value of 7.7 μM.

Introduction

Phthalides are a class of structurally very diverse secondary metabolites with more than 180 naturally occurring compounds described [1]. They are produced by a wide range of organisms, i.e., by marine and terrestrial fungi belonging to genera such as *Ascochyta* [2], *Aspergillus* [3-5], *Alternaria* [6], *Penicillium* [7], *Hericium* [8] or *Talaromyces* [9], but also by plants and liverworts [1].

Phthalides exhibit an equally broad spectrum of bioactivity, including modulation of the central nervous system, protection against brain eschemia, modulation of platelet aggregation and cardiac function, inhibition of smooth muscle cell proliferation, anti-angina activity, and smooth muscle relaxation, as well as antibacterial, antifungal, antiviral and phytotoxic activity [1]. The medically most important member of this family of natural

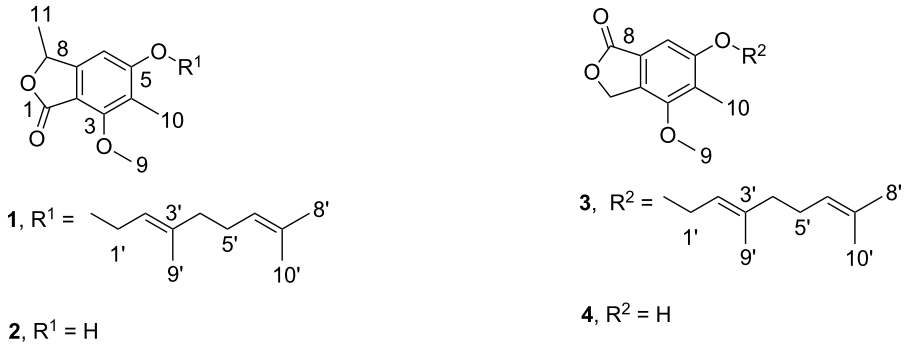

Scheme 1: Secondary metabolites **1**–**4** isolated from *Stachylidium* sp.

products is mycophenolic acid, initially isolated from *Penicillium brevicompactum*, and used in the form of its derivative mycophenolate mofetil as an immunosuppressant drug [10].

During our search for new natural products produced from the marine-derived fungus *Stachylidium* sp., several phthalide derivatives, i.e., marilones A–C, were isolated from a culture on agar-BMS media supplemented with artificial sea salt (Scheme 1). Albeit phthalide-like structures are not rare, the structural skeleton of marilones A and B is most unusual, and its biosynthesis is suggested to require unique reactions in fungal secondary metabolism. Marilone A (**1**) exhibited antiplasmodial activity against *Plasmodium berghei* with an IC_{50} of 12.1 µM. Marilone B (**2**) showed a specific antagonistic effect on the serotonin receptor 5-HT_{2B} with a K_i value of 7.7 µM.

Results and Discussion

The molecular formula of **1** was deduced by accurate mass measurement (HRMS–EI) to be $C_{21}H_{28}O_4$, requiring eight degrees of unsaturation. The ^{13}C NMR and DEPT135 spectra contained 21 carbon resonances, including six resulting from methyl groups, three from sp^2 methines, and one from an sp^3 methine, whereas a further three signals resulted from methylene groups, and eight resonances were assigned to quaternary carbons (Table 1, Table 2 and Supporting Information File 1). The ^1H NMR spectrum of **1** displayed a singlet resonance for the aromatic methine (6-CH) at δ 6.95 indicating, together with UV and ^{13}C NMR data, the presence of a penta-substituted benzene ring. The methyl group 10-CH_3 (δ_C 8.8) was linked to C-4 of the aromatic ring due to heteronuclear long range correlations of the methyl protons with C-3, C-4 and C-5. The methoxy group 9-OCH_3 (δ_H 3.98) had a heteronuclear long range correlation to C-3 of the aromatic ring, thus, clearly delineating its position. Besides the aromatic proton 6-H, the ^1H NMR spectrum showed two further resonance signals in the downfield shifted region (δ_H 5.52 and 5.09) indicating, together with ^{13}C NMR and $^1H/^{13}C$ HMBC data, the presence of a geranyl substituent. The C-1' to C-10' part of the molecule was deduced from two proton coupling spin systems observed in the $^1H/^1H$ COSY spectrum, namely 1'-H_2 to 2'-H (J = 6.6 Hz) and 4'-H_2 to 6'-H through 5'-H_2. $^1H/^{13}C$ HMBC data showed correlations from 9'-H_3 to C-2', C-3' and C-4', and from methyl protons 8'-H_3 and 10'-H_3 to C-6'and C-7', disclosing a geranyl fragment. Based on literature comparisons we established the configuration of $\Delta^{2'/3'}$ as *E* [11]. The aromatic quaternary carbon C-5 (δ_C 164.2) had a carbon resonance that indicated a connection to an oxygen atom. The monoterpenyl substituent was established to be connected to C-5 through an oxygen atom, based on the heteronuclear long range correlations of 1'-H_2 (δ_H 4.69, 4.74) to C-5.

The $^1H/^{13}C$ HMBC spectrum exhibited a correlation from 6-H to C-8. Furthermore, the ^{13}C NMR resonance of C-8 at δ 77.0 was found to be characteristic for a carbon bound to an oxygen atom. The $^1H/^1H$ COSY spectrum showed a coupling of 8-H with 11-H_3 (J = 6.6 Hz), and the $^1H/^{13}C$ HMBC spectrum contained correlations from 8-H to C-6, C-7 and C-2 of the penta-substituted aromatic ring, as well as to the carbonyl carbon C-1. Ring double bond equivalents required a second ring within compound **1**, and together with heteronuclear correlations of 8-H to C-1 and the carbon resonance of C-1 at δ_C 168.2 indicating the presence of a carbonyl group, this gave evidence for a C-8-methylated phthalide skeleton, i.e., the C-1 to C-11 part of the structure. Since the resonance signal for 6-H did not show heteronuclear long range correlations to that of the carbonyl C-1, but instead correlated with the sp^3 methine C-8, the carbonyl group was assigned at C-1. In this way, a phthalide-nucleus identical to that of the known natural product nidulol was formed [6]. To further prove that the carbonyl group is positioned at C-1 and not at C-8 of **1**, ^1H NMR spectra of **1** were compared with those of nidulol and silvaticol (**4**) (and

Table 1: ^{13}C NMR spectroscopic data for compounds **1**, **2**, and **3**.

	1	2	3
pos.	δ_C, mult.[a, b]	δ_C, mult.[a, b]	δ_C, mult.[a, b]
1	168.2, qC	168.2, qC	68.9, CH_2
2	110.0, qC	109.1, qC	128.4, qC
3	158.0, qC	158.9, qC	153.9, qC
4	120.4, qC	118.8, qC	124.8, qC
5	164.2, qC	163.2, qC	159.7, qC
6	100.8, CH	103.6, CH	102.0, CH
7	154.2, qC	153.9, qC	125.8, qC
8	77.0, CH	76.6, CH	171.1, qC
9	62.1, CH_3	62.0, CH_3	59.3, CH_3
10	8.8, CH_3	8.6, CH_3	9.8, CH_3
11	20.9, CH_3	21.0, CH_3	–
1'	66.5, CH_2	–	66.4, CH_2
2'	120.1, CH	–	120.5, CH
3'	142.1, qC	–	141.6, qC
4'	40.1, CH_2	–	40.1, CH_2
5'	26.9, CH_2	–	26.9, CH_2
6'	124.6, CH	–	124.6, CH
7'	132.1, qC	–	132.1, qC
8'	25.8, CH_3	–	25.8, CH_3
9'	16.7, CH_3	–	16.7, CH_3
10'	17.7, CH_3	–	17.7, CH_3

[a]Acetone-d_6, 75.5 MHz. [b]Implied multiplicities determined by DEPT.

Table 2: ^1H NMR spectroscopic data for compounds **1**, **2**, and **3**.

	1	2	3
pos.	δ_H[a, b] (J in Hz)	δ_H[a, b] (J in Hz)	δ_H[a, b] (J in Hz)
1	–	–	5.50, s
2	–	–	–
3	–	–	–
4	–	–	–
5	–	–	–
6	6.95, s	6.75, s	7.03, s
7	–	–	–
8	5.43, q (6.6)	5.37, q (6.6)	–
9	3.98, s	3.98, s	3.96, s
10	2.09, s	2.10, s	2.15, s
11	1.54, d (6.6)	1.48, d (6.6)	–
1'	a: 4.69, dd (6.6, 12.1) b: 4.74, dd (6.6, 12.1)	–	4.71, d (6.6)
2'	5.52, t (6.6)	–	5.51, t (6.6)
3'	–	–	–
4'	2.10, m	–	2.10, m
5'	2.13, m	–	2.14, m
6'	5.09, m	–	5.10, m
7'	–	–	–
8'	1.63, br s	–	1.63, br s
9'	1.76, br s	–	1.78, br s
10'	1.58, br s	–	1.58, br s

[a]Acetone-d_6, 300 MHz. [b]Assignments are based on extensive 1D and 2D NMR experiments (HMBC, HSQC, COSY).

derivatives, see Supporting Information File 1). The latter are known regioisomeric phthalides with the carbonyl group at C-1 and C-8, respectively. Differences in ^1H NMR resonances can be discerned especially for 6-H, resonating at δ_H 6.59 ($CDCl_3$) for nidulol and δ_H 7.04 ($CDCl_3$) for silvaticol [6]. The ^1H NMR spectrum of **1** (δ_H 6.54 in $CDCl_3$) was shown to be similar to that of nidulol and the nidulol derivative 5-(3',3'-dimethylallyloxy)-7-methoxy-6-methylphthalide with 6-H resonating at δ_H 6.62 (see Supporting Information File 1) [5]. For compound **1** the trivial name marilone A is suggested.

The molecular formula of **2** was deduced by accurate mass measurement (HRMS–EI) to be $C_{11}H_{12}O_4$, requiring six sites of unsaturation. The NMR spectral data (see Table 1, Table 2 and Supporting Information File 1) indicated that compound **2** is identical to **1**, except for the missing geranyl moiety attached to the hydroxy group at C-5. We propose the trivial name marilone B for compound **2**.

The molecular formula of **3**, was deduced by accurate mass measurement (HRMS–EI) to be $C_{20}H_{26}O_4$, requiring eight degrees of unsaturation. The spectroscopic data of **3** revealed that the compound is also very similar to **1** (Table 1, Table 2 and Supporting Information File 1). In contrast to compound **1**, however, resonance signals for a methylene group, i.e., 1-CH_2 (δ_C 68.9) were found in the NMR spectra, instead of those for a methine (8-CH) and methyl group (11-CH_3) as in **1**. The resonance signal for 6-H did not have a heteronuclear long range correlation to C-1, but correlated with the carbonyl carbon C-8. Hence, the location of carbonyl group in **3** was assigned to C-8, thus, forming a phthalide-nucleus as present in silvaticol (**4**). For compound **3** the name marilone C is suggested.

Spectroscopic data of **4** were determined to be identical to those of silvaticol (Supporting Information File 1) [6].

Compounds **1** and **2** possess a single chiral center at C-8. The measurement of the specific optical rotation for these compounds yielded values close to zero, and furthermore, the CD measurements showed hardly any CD effect for the referred compounds. This was expected at around 260 nm due to the proximity of the chiral center to the chromophoric penta-substituted benzene ring. We thus assumed the presence of racemic mixtures for these chiral compounds. Extensive trials to sepa-

rate the enantiomers, employing three different HPLC chiral stationary phases, were unsuccessful. However, the presence of racemic mixtures was proven for the analogous, nitrogen-containing compounds, i.e., phthalimidine derivatives isolated from the same fungus (Almeida et al., unpublished data).

Marilones A, B and C (**1**–**3**) were tested for antiplasmodial activity, and marilone A exhibited an IC_{50} of 12.1 μM against the liver stage of *Plasmodium berghei* (see Supporting Information File 1). Interestingly, marilone C (**3**) showed no activity at 25 μM concentration, indicating that the methyl group 11-CH_3 and/or the position of the ketone functionality is essential for this bioactivity.

Marilones A, B, and C (**1**–**3**) were also tested for cytotoxic activity towards three cancer cell lines (NCI-H460, MCF7 and SF268). Marilone A and C (**1**, **3**) showed weak antiproliferative activity with an average GI_{50} of 36.7 and 26.6 μM, respectively (see Supporting Information File 1).

Marilone B (**2**) was assayed in a panel of 44 psychoactive receptors, including 11 serotonin receptors, and marilone B showed a specific antagonistic effect on the serotonin receptor 5-HT_{2B} with a K_i value of 7.7 μM.

Compounds **1**–**4** were further evaluated for antiviral activity, for inhibition of protein kinases and proteases, for growth inhibition of antibiotic-resistant *Mycobacterium tuberculosis* as well as further microbial pathogens, for activity in an antidiabetic activity assay panel, in a 3T3-L1 murine adipocyte assay, and in a NF-κB protein complex assay, but they exhibited no activity (see detailed description in Supporting Information File 1).

Phthalide derivatives are compounds of the polyketide metabolism, which are common in nature [1]. Secondary metabolites **1** and **2** discovered in the marine-derived *Stachylidium* sp. were found to be derivatives of the natural product nidulol, whilst compound **3** was a derivative of silvaticol (**4**) (see Supporting Information File 1), formerly described from the fungus *Aspergillus silvaticus* [6]. Nidulol and silvaticol (**4**) are regioisomeric compounds and differ in terms of the position of the carbonyl group, which is either placed *peri* to the aromatic hydrogen, as in **3** and **4**, or it is positioned *peri* to the aromatic methoxy moiety, e.g., in **1** and **2**. The *Stachylidium* species investigated here is thus able to produce both types of phthalides, which are suspected to differ significantly in terms of their biosynthesis (Supporting Information File 1; Figure S15).

Whereas compound **3** is simply the O-prenylated form of silvaticol (**4**), the nidulol derivatives **1** and **2** are distinguished by an additional methyl substituent (11-CH_3) at C-8. In terms of biosynthesis, i.e., polyketide metabolism, this substitution is most unusual for phthalides and, to the best of our knowledge, it was only found once in dimethoxydimethylphthalide (DDP) [12].

Biosynthetic studies focusing on phthalide structures, e.g., for mycophenolic acid [13], nidulol and silvaticol [9], were previously performed by means of feeding experiments with labeled precursors, evidencing the tetraketide nature of the phthalide nucleus (Supporting Information File 1; Figure S15). Compounds **1**–**4**, possess a basic skeleton which is related to that of the well-known tetraketide 3-methyl-orsellinic acid [14]. Closing of the lactone ring would for compounds **1** and **2** require the oxidation of C-8 to obtain a hydroxy group, which could subsequently form a lactone with the C-1 carboxy group (Supporting Information File 1; Figure S15A). In contrast to that for **3** and **4**, a reduction of the C-1 carboxy group to an alcoholic function and an oxidation of C-8 to a carboxylic function would be required (Supporting Information File 1; Figure S15 B).

Most intriguing, however, is that in compounds **1** and **2** the acetate-derived methyl group 8-CH_3 in the methyl-orsellinic acid precursor would be replaced by an ethyl group. Thus, the biosynthesis seems to require either a propionate starter unit (see C in Figure S15; Supporting Information File 1) or a methylation (e.g., via a SAM-dependent methyl-transferase) at C-8 (see D in Figure S15; Supporting Information File 1). A third possibility would be the loss of a carbon atom from a pentaketide intermediate. To our knowledge, to date propionate as a starter unit was only described for pseurotin A and austrocorticinic acid in fungal polyketide metabolism [15,16]. Feeding experiments are under way in order to determine the building blocks for these molecules.

It is worthwhile to mention that marilones were produced solely on solid biomalt medium (BMS) supplemented with sea salt, whereas in other media such as Czapek or YPM no phthalides were formed.

Experimental

General experimental procedures. Optical rotations were measured on a Jasco DIP 140 polarimeter. UV and IR spectra were obtained with a Perkin-Elmer Spectrum BX instrument. All NMR spectra were recorded in MeOD or $(CD_3)_2CO$ on a Bruker Avance 300 DPX spectrometer. Spectra were referenced to residual solvent signals with resonances at $\delta_{H/C}$ 3.35/49.0 for MeOD and $\delta_{H/C}$ 2.04/29.8 for $(CD_3)_2CO$. HRMS–EI were recorded on a Finnigan MAT 95 spectrometer. HRMS–ESI were recorded on a Bruker Daltonik micrOTOF-Q

time-of-flight mass spectrometer with ESI source. HPLC was carried out on a system composed of a Waters 515 pump together with a Knauer K-2300 differential refractometer. HPLC columns were from Knauer (250 × 8 mm, Eurospher-100 Si and 250 × 8 mm, Eurospher-100, C18, 5 µm; flow 2 mL/min) and Macherey-Nagel (Nucleodur C18 EC Isis 250 × 4.6 mm, 5 µm, flow: 1 mL/min). Merck silica gel 60 (0.040–0.063 mm, 70–230 mesh) was used for vacuum liquid chromatography (VLC). Columns were wet-packed under vacuum with petroleum ether (PE). Before applying the sample solution, the columns were equilibrated with the first designated eluent. Standard columns for crude extract fractionation had dimensions of 13 × 4 cm.

Fungal material. The marine-derived fungus *Stachylidium* sp. was isolated from the sponge *Callyspongia* sp. cf. *C. flammea* (collected at Bear Island, Sydney, Australia) and identified by P. Massart and C. Decock, BCCM/MUCL, Catholic University of Louvain, Belgium. A specimen is deposited at the Institute for Pharmaceutical Biology, University of Bonn, isolation number "293K04", culture collection number "220".

Cultivation, extraction and isolation. Compounds **1**–**4** were isolated from a 60 days culture (12 L) of *Stachylidium* sp. on an agar–biomalt medium supplemented with sea salt (BMS). An extraction with 5 L EtOAc yielded 5.9 g of extract, which was subjected to a VLC fractionation in an open column with silica as solid phase and a gradient solvent system with petroleum ether/acetone of 10:1, 5:1, 2:1, 1:1, 100% acetone and 100% MeOH, resulting in six VLC fractions. Compounds **1** and **3** were isolated from VLC fraction 1. VLC fraction 1 was again fractionated using petroleum ether/acetone 90:1 and 10:1 in order to eliminate fatty acid content of the sample. The VLC fraction 10:1 was subjected to NP-HPLC fractionation using petroleum ether/acetone 30:1 to yield a mixture of both compounds (subfraction 4 of 7). Further fractionation using MeOH/H_2O 8:2 (RP-HPLC, Isis column) yielded compound **1** (subfraction 1 of 2; 19 mg, t_R 13 min) and compound **3** (subfraction 2 of 2; 14.2 mg, t_R 15 min).

Compounds **2** and **4** were isolated from VLC fraction 2, followed by NP-HPLC fractionation using PE/acetone 11:1 to yield a mixture of both compounds (fraction 6 of 7). Further fractionation using MeOH/H_2O 4:6 (RP-HPLC, Isis column) yielded compound **2** (fraction 1 of 2; 5.2 mg, t_R 35 min) and the known compound **4**, silvaticol (fraction 2 of 2; 5.6 mg, t_R 38 min).

Marilone A (1): transparent oil (1.6 mg/L, 0.32%); UV (MeOH) λ_{max}, nm (log ε): 219 (4.38), 261 (2.95); IR (ATR) ν_{max}: 2964, 1745, 1603 cm^{-1}; ^1H NMR and ^{13}C NMR (Table 1 and Table 2); LRMS–EI (*m/z*): 344.2 $[M]^+$; HRMS–EI (*m/z*): $[M]^+$ calcd for $C_{21}H_{28}O_4$, 344.1988; found, 344.1996.

Marilone B (2): white amorphous solid (0.4 mg/L, 0.09%); UV (MeOH) λ_{max}, nm (log ε): 215 (4.09), 260 (2.83); IR (ATR) ν_{max}: 3238 (br), 2931, 1708, 1601 cm^{-1}; ^1H NMR and ^{13}C NMR (Table 1 and Table 2); LRMS–EI (*m/z*): 208.1 $[M]^+$; HRMS–EI (*m/z*): $[M]^+$calcd for $C_{11}H_{12}O_4$, 208.0736; found, 208.0737.

Marilone C (3): transparent oil (1.3 mg/L, 0.27%); UV (MeOH) λ_{max}, nm (log ε): 223 (4.10), 255 (2.80); IR (ATR) ν_{max}: 2921, 1760, 1619 cm^{-1}; ^1H NMR and ^{13}C NMR (Table 1 and Table 2); LRMS–EI (*m/z*): 330.2 $(M)^+$; HRMS–EI (*m/z*): $[M]^+$ calcd for $C_{20}H_{26}O_4$, 330.1831; found, 330.1833.

Methodology for the performed biological assays

The referred compounds were tested in antibacterial (*Escherichia coli*, *Bacillus megaterium*), antifungal (*Mycotypha microspora*, *Eurotium rubrum*, and *Microbotryum violaceum*), and antialgal (*Chlorella fusca*) assays as described before [17,18]. The inhibition of the following panel of proteases inhibition assays (chymotrypsin, trypsin, the protease elastase HLE, papain, porcine cease and acetylcholine esterase) were performed according to Neumann et al. [19]. Compounds were tested for protein kinase inhibition assays (DYRK1A and CDK5) according to Bettayeb et al. [20]. The triglyceride accumulation inhibition in the 3T3-L1 murine adipocytes assay was performed as described by Shimokawa et al. [21]. Cytotoxic activity assay against a panel of three cancer cell lines, NCI-H460, MCF7 and SF268 at the 100 µM level was performed according to Saroglou et al. [22] and Monks et al. [23]. Compounds were tested for antiplasmodial activity against *Plasmodium berghei* liver stages as described by Ploemen et al. [24]. Inhibition of the viral HIV-1- and HIV-2-induced cytopathogenic effect in MT-4 cells assays was performed according to Pannecouque et al. [25] and Zhan et al. [26]. Severe Acute Respiratory Syndrome coronavirus (SARS) assays were performed according to Kumaki et al. [27], the Herpes Simplex Virus-2 (HSV-2) activity assays according to Harden et al. [28], the Respiratory Syncytial virus (RSV) activity assays according to Barnard et al. [29,30], the Influenza viruses A and B (Flu A and B) activity assays as described by Sidwell and Smee [31], and the Hepatitis B virus was performed according to Sells et al. [32] and Korba and Gerin [33]. The activity assays against two strains of antibiotic resistant *Mycobacterium tuberculosis* were performed according to Bauer et al. [34]. The methodology for the inhibition of the NF-κB protein complex is described by Schumacher et al. [35]. The compounds were tested against a panel of antidiabetic

activity assays as described by Marrapodi and Chiang [36], Dey et al. [37] and Seale et al. [38]. The binding assays against a panel of 44 psychoactive receptors (activity considered with at least 50% inhibition at the 10 μM level against 5-HT_{1A}, 5-HT_{1B}, 5-HT_{1D}, 5-HT_{1E}, 5-HT_{2A}, 5-HT_{2B}, 5-HT_{2C}, 5-HT_3, 5-HT_{5A}, 5-HT_6, 5-HT_7, α_{1A}, α_{1B}, α_{1D}, α_{2A}, α_{2B}, α_{2C}, β_1, β_2, β_3, BZP Rat Brain Site, D_1, D_2, D_3, D_4, D_5, DAT, δ, κ, μ, $GABA_A$, H_1, H_2, H_3, H_4, M_1, M_2, M_3, M_4, M_5, NET, SERT, σ_1, σ_2) are fully described [39].

Supporting Information

Supporting Information File 1

Spectroscopic data and other relevant information for compounds **1**–**4**.
[http://www.beilstein-journals.org/bjoc/content/supplementary/1860-5397-7-192-S1.pdf]

Acknowledgements

We thank the efforts of Dr. K. Dimas (Biomedical Research Foundation of Academy of Athens, Athens, Greece) for the cytotoxicity assays, Prof. Dr. M. Gütschow (Institute for Pharmaceutical Chemistry, University of Bonn, Germany) for performing the panel of proteases inhibition assays, Dr. L. Meijer (Protein Phosphorylation & Disease, CNRS, Roscoff, France) for performing the protein kinases assays and Dr. C. Pannecouque (Rega Institute for Medical Research, Leuven, Belgium) for performing the HIV-1 and HIV-2 antiviral assays; we also kindly thank Indra Bergval (KIT Biomedical Research, Royal Tropical Institute, Amsterdam, Netherlands) for performing the *M. tuberculosis* activity assays, Dr. Marc Diederich (Fondation Recherche sur le Cancer et les Maladies du Sang Laboratoire de Biologie Moleculaire et Cellulaire du Cancer (LBMCC), Luxembourg) for performing the NF-κB activity assays and Dr. Steinar Paulsen (University of Tromsø, MabCent, Tromsø, Norway); the K_i determinations and antagonist functional data that was generously provided by the National Institute of Mental Health's Psychoactive Drug Screening Program, Contract # HHSN-271-2008-00025-C (NIMH PDSP). The NIMH PDSP is directed by Bryan L. Roth MD, PhD at the University of North Carolina at Chapel Hill and Project Officer Jamie Driscol at NIMH, Bethesda MD, USA; we kindly thank also the remaining antiviral bioactivity tests performed by the U.S. National Institute of Health drug discovery program, which were supported by contracts NO1-A1-30048 (Institute for Antiviral Research, IAR) and NO1-AI-15435 (IAR) from Virology Branch, National Institute of Allergic and Infectious Diseases, NIAID; we also kindly thank the financial support from FCT (Science and Technology Foundation, Portugal), and BMBF (project No. 03F0415A).

References

1. Lin, G.; Chan, S.-K.; Chung, H.-S.; Li, S.-L. In *Studies in Natural Products Chemistry;* Rahman, A., Ed.; Elsevier: Amsterdam, Netherlands, 2005; pp 611–669.
2. Seibert, S. F.; Eguereva, E.; Krick, A.; Kehraus, S.; Voloshina, E.; Raabe, G.; Fleischhauer, J.; Leistner, E.; Wiese, M.; Prinz, H.; Alexandrov, K.; Janning, P.; Waldmann, H.; König, G. M. *Org. Biomol. Chem.* **2006,** *4,* 2233–2240. doi:10.1039/b601386d
3. Fujita, M.; Yamada, M.; Nakajima, S.; Kawai, K.; Nagai, M. *Chem. Pharm. Bull.* **1984,** *32,* 2622–2627.
4. Achenbach, H.; Mühlenfeld, A.; Brillinger, G. U. *Liebigs Ann. Chem.* **1985,** 1596–1628. doi:10.1002/jlac.198519850808
5. Kawahara, N.; Nozawa, K.; Nakajima, S.; Udagawa, S.; Kawai, K. *Chem. Pharm. Bull.* **1988,** *36,* 398–400.
6. Suemitsu, R.; Ohnishi, K.; Morikawa, Y.; Nagamoto, S. *Phytochemistry* **1995,** *38,* 495–497. doi:10.1016/0031-9422(94)00546-6
7. Makino, M.; Endoh, T.; Ogawa, Y.; Watanabe, K.; Fujimoto, Y. *Heterocycles* **1998,** *48,* 1931–1934. doi:10.3987/COM-98-8253
8. Kawagishi, H.; Ando, M.; Mizuno, T. *Tetrahedron Lett.* **1990,** *31,* 373–376. doi:10.1016/S0040-4039(00)94558-1
9. Ayer, W. A.; Racok, J. S. *Can. J. Chem.* **1990,** *68,* 2095–2101. doi:10.1139/v90-319
10. Dewick, P. M. *Medicinal Natural Products: A biossynthetic approach,* 3rd ed.; John Wiley & Sons, Ltd.: Chichester, U.K., 2009.
11. Tanaka, Y.; Sato, H.; Kageyu, A.; Tomita, T. *J. Chromatogr.* **1985,** *347,* 275–283. doi:10.1016/S0021-9673(01)95493-7
12. Bradamante, S.; Barenghi, L.; Beretta, G.; Bonfa', M.; Rollini, M.; Manzoni, M. *Biotechnol. Bioeng.* **2002,** *80,* 589–593. doi:10.1002/bit.10418
13. Bedford, C. T.; Knittel, P.; Money, T.; Phillips, G. T.; Salisbury, P. *Can. J. Chem.* **1973,** *51,* 694–697. doi:10.1139/v73-105
14. Geris, R.; Simpson, T. J. *Nat. Prod. Rep.* **2009,** *26,* 1063–1094. doi:10.1039/b820413f
15. Mohr, P.; Tamm, C. *Tetrahedron* **1981,** *37,* 201–212. doi:10.1016/0040-4020(81)85056-9
16. Gill, M.; Giménez, A. *J. Chem. Soc., Chem. Commun.* **1988,** 1360–1362. doi:10.1039/C39880001360
17. Schulz, B.; Sucker, J.; Aust, H. J.; Krohn, K.; Ludewig, K.; Jones, P. G.; Döring, D. *Mycol. Res.* **1995,** *99,* 1007–1015. doi:10.1016/S0953-7562(09)80766-1
18. Schulz, B.; Boyle, C.; Draeger, S.; Römmert, A.-K.; Krohn, K. *Mycol. Res.* **2002,** *106,* 996–1004. doi:10.1017/S0953756202006342
19. Neumann, K.; Kehraus, S.; Gütschow, M.; König, G. M. *Nat. Prod. Commun.* **2009,** *4,* 347–354.
20. Bettayeb, K.; Oumata, N.; Echalier, A.; Ferandin, Y.; Endicott, J. A.; Galons, H.; Meijer, L. *Oncogene* **2008,** *27,* 5797–5807. doi:10.1038/onc.2008.191
21. Shimokawa, K.; Iwase, Y.; Miwa, R.; Yamada, K.; Uemura, D. *J. Med. Chem.* **2008,** *51,* 5912–5914. doi:10.1021/jm800741n
22. Saroglou, V.; Karioti, A.; Demetzos, C.; Dimas, K.; Skaltsa, H. *J. Nat. Prod.* **2005,** *68,* 1404–1407. doi:10.1021/np058042u
23. Monks, A.; Scudiero, D.; Skehan, P.; Shomaker, R.; Paull, K.; Vistica, D.; Hose, C. *J. Natl. Cancer Inst.* **1991,** *83,* 661–757.
24. Ploemen, I. H. J.; Prudêncio, M.; Douradinha, B. G.; Ramesar, J.; Fonager, J.; van Gemert, G.-J.; Luty, A. J. F.; Hermsen, C. C.; Sauerwein, R. W.; Baptista, F. G.; Mota, M. M.; Waters, A. P.; Que, I.; Lowik, C. W. G. M.; Khan, S. M.; Janse, C. J.; Franke-Fayard, B. M. D. *PLoS One* **2009,** *4,* e7881. doi:10.1371/journal.pone.0007881
25. Pannecouque, C.; Daelemans, D.; De Clercq, E. *Nat. Protoc.* **2008,** *3,* 427–434. doi:10.1038/nprot.2007.517

26. Zhan, P.; Liu, X.; Fang, Z.; Pannecouque, C.; De Clercq, E. *Bioorg. Med. Chem.* **2009,** *17,* 6374–6379. doi:10.1016/j.bmc.2009.07.027
27. Kumaki, Y.; Day, C. W.; Wandersee, M. K.; Schow, B. P.; Madsen, J. S.; Grant, D.; Roth, J. P.; Smee, D. F.; Blatt, L. M.; Barnard, D. L. *Biochem. Biophys. Res. Commun.* **2008,** *371,* 110–113. doi:10.1016/j.bbrc.2008.04.006
28. Harden, E. A.; Falshaw, R.; Carnachan, S. M.; Kern, E. R.; Prichard, M. N. *Antiviral Res.* **2009,** *83,* 282–289. doi:10.1016/j.antiviral.2009.06.007
29. Barnard, D. L.; Huffman, J. H.; Meyerson, L. R.; Sidwell, R. W. *Chemotherapy* **1993,** *39,* 212–217. doi:10.1159/000239128
30. Barnard, D. L.; Hill, C. L.; Gage, T.; Matheson, J. E.; Huffman, J. H.; Sidwell, R. W.; Otto, M. I.; Schinazi, R. F. *Antiviral Res.* **1997,** *34,* 27–37. doi:10.1016/S0166-3542(96)01019-4
31. Sidwell, R. W.; Smee, D. F. *Antiviral Res.* **2000,** *48,* 1–16. doi:10.1016/S0166-3542(00)00125-X
32. Sells, M. A.; Zelent, A. Z.; Shvartsman, M.; Acs, G. *J. Virol.* **1988,** *62,* 2836–2844.
33. Korba, B. E.; Gerin, J. L. *Antiviral Res.* **1992,** *19,* 55–70. doi:10.1016/0166-3542(92)90056-B
34. Bauer, A. W.; Kirby, W. M.; Sherris, J. C.; Turck, M. *Am. J. Clin. Pathol.* **1966,** *45,* 493–496.
35. Schumacher, M.; Cerella, C.; Eifes, S.; Chateauvieux, S.; Morceau, F.; Jaspars, M.; Dicato, M.; Diederich, M. *Biochem. Pharmacol.* **2010,** *79,* 610–622. doi:10.1016/j.bcp.2009.09.027
36. Marrapodi, M.; Chiang, J. Y. L. *J. Lipid Res.* **2000,** *41,* 514–520.
37. Dey, D.; Pal, B. C.; Biswas, T.; Roy, S. S.; Bandyopadhyay, A.; Mandal, S. K.; Giri, B. B.; Bhattacharya, S. *Mol. Cell. Biochem.* **2007,** *300,* 149–157. doi:10.1007/s11010-006-9378-1
38. Seale, A. P.; de Jesus, L. A.; Kim, S.-Y.; Choi, Y.-H.; Lim, H. B.; Hwang, C.-S.; Kim, Y.-S. *Biotechnol. Lett.* **2005,** *27,* 221–225. doi:10.1007/s10529-004-7855-8
39. University of North Carolina At Chapel Hill, National Institute of Mental Health, Psychoactive Drug Screening Program, Assay Protocol Book. http://pdsp.med.unc.edu/UNC-CH%20Protocol%20Book.pdf.

License and Terms

Beilstein Journal of Organic Chemistry

Tertiary alcohol preferred: Hydroxylation of *trans*-3-methyl-L-proline with proline hydroxylases

Christian Klein and Wolfgang Hüttel*

Letter

Open Access

Address:
Institute of Pharmaceutical Sciences, Department of Pharmaceutical and Medicinal Chemistry, Albert-Ludwigs-Universität Freiburg, Albertstr. 25, 79104 Freiburg, Germany

Email:
Wolfgang Hüttel* - wolfgang.huettel@pharmazie.uni-freiburg.de

* Corresponding author

Keywords:
asymmetric catalysis; enzyme catalysis; hydroxyproline; α-ketoglutarate dependent iron(II) oxygenases; regioselectivity; stereoselectivity

Beilstein J. Org. Chem. **2011,** *7,* 1643–1647.
doi:10.3762/bjoc.7.193

Received: 09 September 2011
Accepted: 14 November 2011
Published: 05 December 2011

This article is part of the Thematic Series "Biosynthesis and function of secondary metabolites".

Guest Editor: J. S. Dickschat

Abstract

The enzymatic synthesis of tertiary alcohols by the stereospecific oxidation of tertiary alkyl centers is a most-straightforward but challenging approach, since these positions are sterically hindered. In contrast to P450-monooxygenases, there is little known about the potential of non-heme iron(II) oxygenases to catalyze such reactions. We have studied the hydroxylation of *trans*-3-methyl-L-proline with the α-ketoglutarate (α-KG) dependent oxygenases, *cis*-3-proline hydroxylase type II and *cis*-4-proline hydroxylase (*cis*-P3H_II and *cis*-P4H). With *cis*-P3H_II, the tertiary alcohol product (3*R*)-3-hydroxy-3-methyl-L-proline was obtained exclusively but in reduced yield (~7%) compared to the native substrate L-proline. For *cis*-P4H, a complete shift in regioselectivity from C-4 to C-3 was observed so that the same product as with *cis*-P3H_II was obtained. Moreover, the yields were at least as good as in control reactions with L-proline (~110% relative yield). This result demonstrates a remarkable potential of non-heme iron(II) oxygenases to oxidize substrates selectively at sterically hindered positions.

Findings

Enantiomerically pure tertiary alcohols are valuable building blocks for the synthesis of natural products, biologically active compounds, and pharmaceuticals. However, their stereoselective synthesis is often challenging, as the reaction centers are sterically hindered or electronically disfavored. In addition to numerous approaches for the synthesis of tertiary alcohols with classical organic chemistry [1-5], enzyme-catalyzed approaches have also been successfully established, and especially, hydrolases, i.e., lipases and esterases, are used for the kinetic resolution of tertiary alcohols [6-9]. Other less common approaches include stereospecific enzyme-catalyzed hydrolyses of epoxides, stereoselective additions to ketones with hydroxynitrile lyases or carboligases, and the application of enzymes involved in terpene biosynthesis, such as dehydratases, cyclases or transferases [6,8]. An approach whose potential has not yet been fully exploited is the stereospecific hydroxylation of tertiary

alkyl moieties with oxygenases. Most oxidations to tertiary alcohols described so far were observed during degradation of steroids and other terpenoid bioactive compounds by microbial whole cells [10-12]. Hydroxylations to tertiary alcohols with isolated or heterologously expressed enzymes have mostly exploited P450-monooxygenases. The application of these enzymes for chemical synthesis has been recently reviewed in several articles [13-16].

In contrast, little is known about the ability of non-heme iron(II) enzymes to oxidize tertiary carbon centers. To our knowledge, the formation of tertiary alcohols with α-ketoglutarate (α-KG) dependent iron(II) oxygenases has not been previously reported. These enzymes typically catalyze CH-activation reactions in primary and secondary metabolism [17-21]. For the catalytic cycle, one α-KG and one oxygen molecule are required, besides the main substrate. The ketoacid is decarboxylated oxidatively by one oxygen atom from O_2, whereas the other is used for substrate oxidation (Scheme 1).

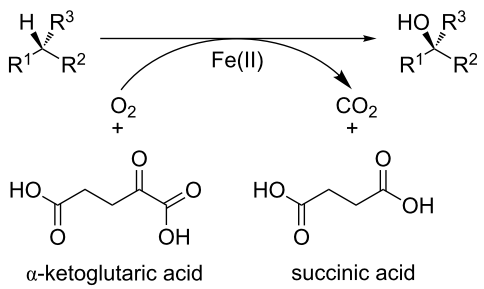

Scheme 1: Catalytic cycle of α-KG dependent oxygenases.

Here, we describe a regio- and stereospecific hydroxylation of *trans*-3-methyl-L-proline to (3*R*)-3-hydroxy-3-methyl-L-proline with two different proline hydroxylases.

In contrast to the mechanistically related and more common prolyl hydroxylases, which accept peptide bound proline as a substrate and play a key role in collagen biosynthesis, proline hydroxylases exclusively hydroxylate the free L-amino acid and are limited to some bacteria and filamentous fungi. As far as it is known, they are involved in secondary metabolism, for example, in the biosynthesis of the non-ribosomal peptide antibiotics etamycin, telomycin and pneumocandin [22-24]. So far, five bacterial proline hydroxylases have been cloned and overexpressed in *E. coli*: A *trans*-4-proline hydroxylase (*trans*-P4H) from *Dactylosporangium* sp. [25] two *cis*-3-proline hydroxylase isoenzymes from *Streptomyces* sp. strain TH1 (*cis*-P3H_I and *cis*-P3H_II) [26,27] and two *cis*-4-proline hydroxylases (*cis*-P4H) from *Sinorhizobium meliloti* and *Mesorhizobium loti* [28]. Since hydroxyprolines are important chiral building blocks for chemical synthesis [29,30], a procedure for the large-scale production of *cis*-3- and *trans*-4-hydroxyproline was established in which a recombinant *E. coli* strain expresses the corresponding proline hydroxylase [31-33]. Recently, we presented an analogous approach for synthesis on a laboratory scale in combination with a significantly simplified method for product purification [34]. This allows the production not only of hydroxyprolines, but also of hydroxylated proline derivatives on a preparative scale. This system provides an ideal platform for further studies on proline hydroxylase activities with new substrates or enzyme variants. Previous testing showed that the substrate specificity of the enzymes is strict towards the secondary amino acid moiety, but "relaxed" towards changes in the carbohydrate backbone of L-proline [35]. We therefore incubated the commercially available *trans*-3-methyl-L-proline for 16 h with purified *cis*-P3H_II and *cis*-P4H (*Sinorhizobium meliloti)*, which hydroxylate the natural substrate L-proline to *cis*-3- and *cis*-4-hydroxyproline, respectively (Scheme 2).

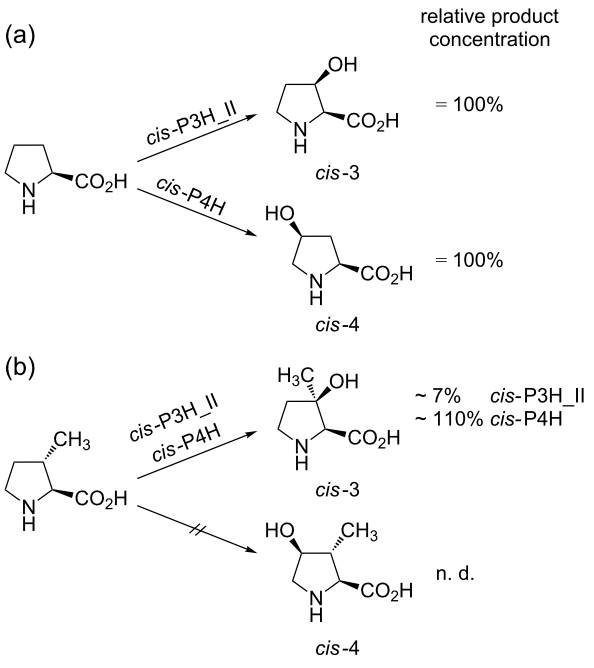

Scheme 2: Selectivities and relative yields in conversions of (a) L-proline (defined as 100% yield) and (b) *trans*-3-methyl-L-proline with *cis*-P3H_II and *cis*-P4H.

For reference, L-proline was converted in parallel with an identical amount of the enzyme preparation. The samples were then analyzed by HPLC by using a fluorescence assay [34]. Since the fluorescence activity of the Fmoc-derivatized proline and derivatives that we have investigated is virtually identical (data not shown), and the measured emissions were in a linear range,

the peak areas were used for an approximate quantification of the compound concentrations (Figure 1). In case of *cis*-P3H_II, a new compound was found, but product concentrations were only approx. 7% compared to those obtained in conversions of L-proline. Based on the *cis*-3-selectivity of the enzyme we assumed that the tertiary alcohol was formed. Surprisingly, the conversion with *cis*-P4H gave a product with the same retention time as the product of *cis*-P3H_II, but in much better relative yield (~110% compared to the L-proline control) (Figure 1a).

To determine their structure, the products were produced on a semi-preparative scale; 26 mg *trans*-3-methyl-L-proline was converted in vivo in 100 mL *E. coli* cultures, overexpressing the corresponding enzyme [34]. After full conversion, the supernatants were purified by ion-exchange chromatography and the products were analyzed by one- and two-dimensional NMR techniques (see NMR and MS spectra in Supporting Information File 1). It was found that both enzymes indeed yielded the same compound, which was identified unambiguously as the C-3 hydroxylated product.

Since the substrate has L-configuration and the enzyme is strictly *cis*-diastereoselective, it can be assumed that (3*R*)-3-hydroxy-3-methyl-L-proline is the product. 1D- and 2D-NOESY NMR-spectra clearly show a correlation between the methyl group and the proton at C-2, suggesting a *cis* position for these substituents and, consequently, a *cis*-configuration for the tertiary alcohol (Supporting Information File 1). Whereas the reactivity of *cis*-P3H_II could be expected, the shift in regioselectivity and the high activity of *cis*-P4H is remarkable. A certain degree of flexibility in the regioselectivity of this enzyme was already found in conversions with the 6-ring-analogue of L-proline, i.e., L-pipecolic acid. In that case

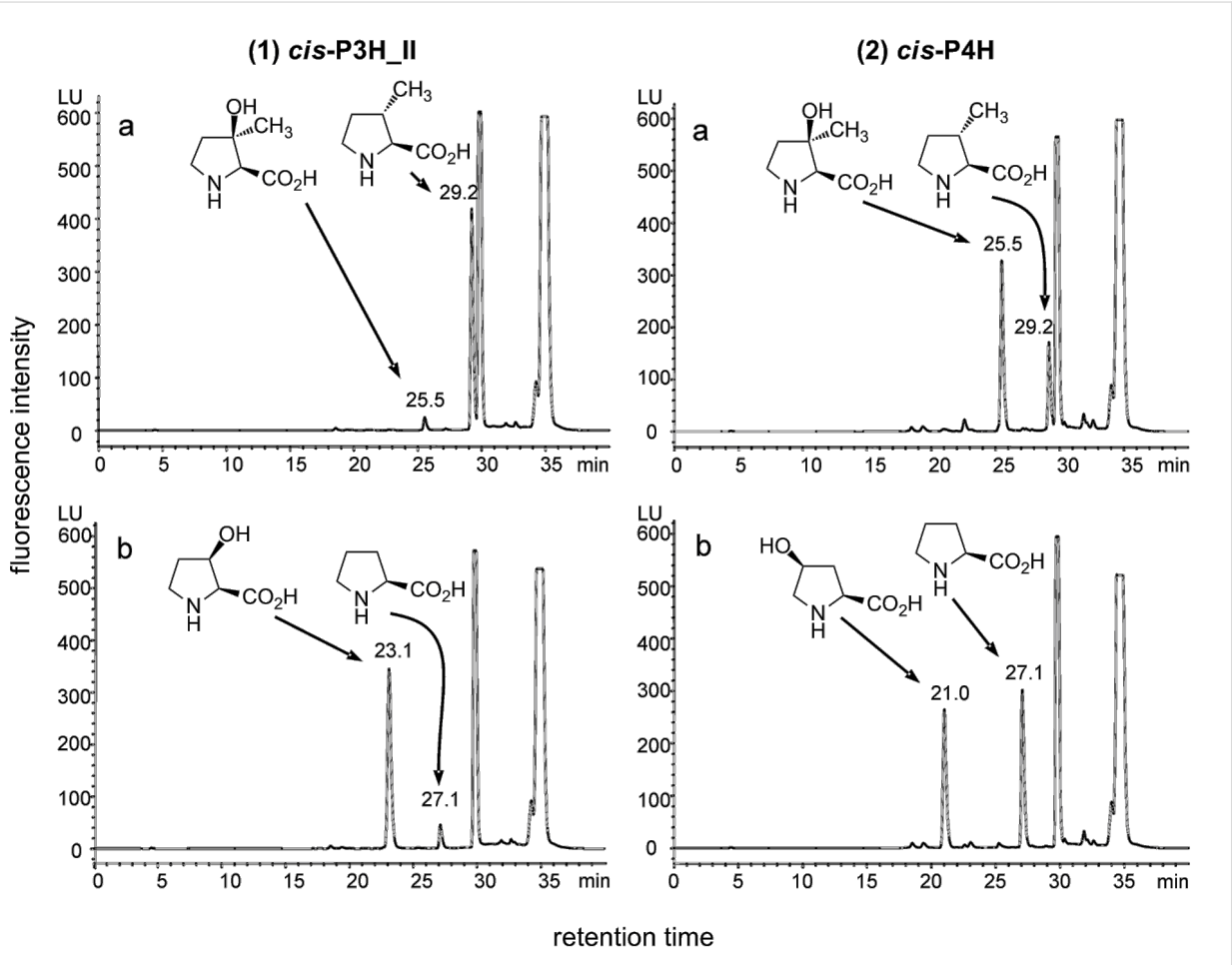

Figure 1: Typical HPLC-chromatograms of the conversions of (a) *trans*-3-methyl-L-proline and (b) L-proline under identical conditions with (1) *cis*-P3H_II and (2) *cis*-P4H. Yields are dependent on the amount of enzyme used. In this example the quantities are: (1)(a): 6.4% (0.25 mM); (1)(b): 90% (3.6 mM); (2)(a): 67% (2.7 mM); (2)(b): 50% (2.0 mM). The more significant relative yields in comparison to a reference reaction with L-proline are discussed in the text. Peaks at retention times >30 min are due to Fmoc-adducts formed during the derivatization reaction. Fluorescence assay wavelengths: Excitation = 254 nm, emission = 316 nm.

an approx. 1:1 mixture of the expected *cis*-5-hydroxypipecolic acid and its *cis*-3-isomer, which is also the product of *cis*-P3H_II, was obtained [34]. In general, it can be assumed that the shift of reactivity in the reaction with *trans*-3-methyl-L-proline is due to the increased stability of the tertiary radical intermediate at C-3 compared to the secondary at one C-4. However, this putative effect does not increase the reactivity of *cis*-P3H_II. So it is most likely that the complex interplay between kinetic and steric factors determines the reactivity of these enzymes. Further spectroscopic and structural data are required in order to provide an insight into the functionality of these enzymes. Nevertheless, our results show that α-KG dependent oxygenases have high potential for the production of tertiary alcohols. Both enzymes investigated afford only a single product selectively and, in the case of *cis*-P4H, the activity was comparable to that with the native substrate. Moreover, proline hydroxylases can be applied for whole cell biotransformations on a preparative scale. Even though the activity of the enzymes is still difficult to predict for conversions with unnatural substrates, highly efficient catalytic systems may be accessible from other α-KG dependent oxygenases.

Supporting Information

Supporting Information File 1

Experimental section, analytical data (NMR and MS).
[http://www.beilstein-journals.org/bjoc/content/supplementary/1860-5397-7-193-S1.pdf]

Acknowledgements

We thank Prof. Michael Müller for his generous support. The skillful technical assistance of Olga Fuchs and Alexandra Walter is gratefully acknowledged. We also thank Volker Brecht for measuring the NMR spectra. This work was financially supported by the Deutsche Bundesstiftung Umwelt (DBU, ChemBioTec: AZ13234-32).

References

1. Cozzi, P. G.; Hilgraf, R.; Zimmermann, N. *Eur. J. Org. Chem.* **2007,** 5969–5994. doi:10.1002/ejoc.200700318
2. Stymiest, J. L.; Bagutski, V.; French, R. M.; Aggarwal, V. K. *Nature* **2008,** *456,* 778–782. doi:10.1038/nature07592
3. Garcia, C.; Martin, V. S. *Curr. Org. Chem.* **2006,** *10,* 1849–1889. doi:10.2174/138527206778249847
4. Hatano, M.; Ishihara, K. *Synthesis* **2008,** 1647–1675. doi:10.1055/s-2008-1067046
5. Shibasaki, M.; Kanai, M. *Chem. Rev.* **2008,** *108,* 2853–2873. doi:10.1021/cr078340r
6. Kourist, R.; Bornscheuer, U. T. *Appl. Microbiol. Biotechnol.* **2011,** *91,* 505–517. doi:10.1007/s00253-011-3418-9
7. Herter, S.; Nguyen, G.-S.; Thompson, M. L.; Steffen-Munsberg, F.; Schauer, F.; Bornscheuer, U. T.; Kourist, R. *Appl. Microbiol. Biotechnol.* **2011,** *90,* 929–939. doi:10.1007/s00253-011-3124-7
8. Kourist, R.; Domínguez de María, P.; Bornscheuer, U. T. *ChemBioChem* **2008,** *9,* 491–498. doi:10.1002/cbic.200700688
9. Christoffers, J.; Baro, A. *Quaternary Stereocenters: Challenges and Solutions for Organic Synthesis;* Wiley-VCH: Weinheim, Germany, 2006.
10. Liu, J.-H.; Yu, B.-Y. *Curr. Org. Chem.* **2010,** *14,* 1400–1406. doi:10.2174/138527210791616786
11. Simeo, Y.; Sinisterra, J. V. *Mini-Rev. Org. Chem.* **2009,** *6,* 128–134. doi:10.2174/157019309788167710
12. Fernandes, P.; Cruz, A.; Angelova, B.; Pinheiro, H. M.; Cabral, J. M. S. *Enzyme Microb. Technol.* **2003,** *32,* 688–705. doi:10.1016/S0141-0229(03)00029-2
13. O'Reilly, E.; Köhler, V.; Flitsch, S. L.; Turner, N. J. *Chem. Commun.* **2011,** *47,* 2490–2501. doi:10.1039/C0CC03165H
14. Schroer, K.; Kittelmann, M.; Lütz, S. *Biotechnol. Bioeng.* **2010,** *106,* 699–706. doi:10.1002/bit.22775
15. Zehentgruber, D.; Hannemann, F.; Bleif, S.; Bernhardt, R.; Lütz, S. *ChemBioChem* **2010,** *11,* 713–721. doi:10.1002/cbic.200900706
16. Chefson, A.; Auclair, K. *Mol. BioSyst.* **2006,** *2,* 462–469. doi:10.1039/b607001a
17. Abu-Omar, M. M.; Loaiza, A.; Hontzeas, N. *Chem. Rev.* **2005,** *105,* 2227–2252. doi:10.1021/cr040653o
18. Bruijnincx, P. C. A.; van Koten, G.; Klein Gebbink, R. J. M. *Chem. Soc. Rev.* **2008,** *37,* 2716–2744. doi:10.1039/b707179p
19. Hausinger, R. P. *Crit. Rev. Biochem. Mol. Biol.* **2004,** *39,* 21–68. doi:10.1080/10409230490440541
20. Kovaleva, E. G.; Lipscomb, J. D. *Nat. Chem. Biol.* **2008,** *4,* 186–193. doi:10.1038/nchembio.71
21. Purpero, V.; Moran, G. R. *JBIC, J. Biol. Inorg. Chem.* **2007,** *12,* 587–601. doi:10.1007/s00775-007-0231-0
22. Petersen, L.; Olewinski, R.; Salmon, P.; Connors, N. *Appl. Microbiol. Biotechnol.* **2003,** *62,* 263–267. doi:10.1007/s00253-003-1264-0
23. Lawrence, C. C.; Sobey, W. J.; Field, R. A.; Baldwin, J. E.; Schofield, C. J. *Biochem. J.* **1996,** *313,* 185–191.
24. Mori, H.; Shibasaki, T.; Uozaki, Y.; Ochiai, K.; Ozaki, A. *Appl. Environ. Microbiol.* **1996,** *62,* 1903–1907.
25. Shibasaki, T.; Mori, H.; Chiba, S.; Ozaki, A. *Appl. Environ. Microbiol.* **1999,** *65,* 4028–4031.
26. Mori, H.; Shibasaki, T.; Yano, K.; Ozaki, A. *J. Bacteriol.* **1997,** *179,* 5677–5683.
27. Shibasaki, T.; Mori, H.; Ozaki, A. *Biotechnol. Lett.* **2000,** *22,* 1967–1973. doi:10.1023/A:1026792430742
28. Hara, R.; Kino, K. *Biochem. Biophys. Res. Commun.* **2009,** *379,* 882–886. doi:10.1016/j.bbrc.2008.12.158
29. Johnston, R. M.; Chu, L. N.; Liu, M.; Goldberg, S. L.; Goswami, A.; Patel, R. N. *Enzyme Microb. Technol.* **2009,** *45,* 484–490. doi:10.1016/j.enzmictec.2009.08.006
30. Remuzon, P. *Tetrahedron* **1996,** *52,* 13803–13835. doi:10.1016/0040-4020(96)00822-8
31. Shibasaki, T.; Mori, H.; Ozaki, A. *Biosci., Biotechnol., Biochem.* **2000,** *64,* 746–750. doi:10.1271/bbb.64.746
32. Shibasaki, T.; Ozaki, A.; Mori, H.; Chiba, S.; Ando, K. Process for producing *trans*-4-hydroxy-l-proline. U.S. Patent 5,854,040, Dec 29, 1998.

33. Ando, K.; Chiba, S.; Mori, H.; Ochiai, K.; Ozaki, A.; Shibasaki, T.; Uosaki, Y. Process for producing *cis*-3-hydroxy-L-proline. U.S. Patent 6,413,748, July 2, 2002.
34. Klein, C.; Hüttel, W. *Adv. Synth. Catal.* **2011,** *353,* 1375–1383. doi:10.1002/adsc.201000863
35. Shibasaki, T.; Sakurai, W.; Hasegawa, A.; Uosaki, Y.; Mori, H.; Yoshida, M.; Ozaki, A. *Tetrahedron Lett.* **1999,** *40,* 5227–5230. doi:10.1016/S0040-4039(99)00944-2

License and Terms

Beilstein Journal of Organic Chemistry

Novel fatty acid methyl esters from the actinomycete *Micromonospora aurantiaca*

Jeroen S. Dickschat*, Hilke Bruns and Ramona Riclea

Full Research Paper

Open Access

Address:
Institut für Organische Chemie, Technische Universität Braunschweig, Hagenring 30, 38106 Braunschweig, Germany

Email:
Jeroen S. Dickschat* - j.dickschat@tu-braunschweig.de

* Corresponding author

Keywords:
actinomycetes; FAMEs; fatty acid biosynthesis; GC–MS; volatiles

Beilstein J. Org. Chem. **2011,** *7,* 1697–1712.
doi:10.3762/bjoc.7.200

Received: 20 August 2011
Accepted: 28 November 2011
Published: 20 December 2011

This article is part of the Thematic Series "Biosynthesis and function of secondary metabolites".

Associate Editor: S. Flitsch

Abstract

The volatiles released by *Micromonospora aurantiaca* were collected by means of a closed-loop stripping apparatus (CLSA) and analysed by GC–MS. The headspace extracts contained more than 90 compounds from different classes. Fatty acid methyl esters (FAMEs) comprised the major compound class including saturated unbranched, monomethyl and dimethyl branched FAMEs in diverse structural variants: Unbranched, α-branched, γ-branched, (ω−1)-branched, (ω−2)-branched, α- and (ω−1)-branched, γ- and (ω−1)-branched, γ- and (ω−2)-branched, and γ- and (ω−3)-branched FAMEs. FAMEs of the last three types have not been described from natural sources before. The structures for all FAMEs have been suggested based on their mass spectra and on a retention index increment system and verified by the synthesis of key reference compounds. In addition, the structures of two FAMEs, methyl 4,8-dimethyldodecanoate and the ethyl-branched compound methyl 8-ethyl-4-methyldodecanoate were deduced from their mass spectra. Feeding experiments with isotopically labelled [$^2H_{10}$]leucine, [$^2H_{10}$]isoleucine, [$^2H_8$]valine, [$^2H_5$]sodium propionate, and [*methyl*-$^2H_3$]methionine demonstrated that the responsible fatty acid synthase (FAS) can use different branched and unbranched starter units and is able to incorporate methylmalonyl-CoA elongation units for internal methyl branches in various chain positions, while the methyl ester function is derived from *S*-adenosyl methionine (SAM).

Introduction

Lipids in general, and particularly fatty acids (FAs), belong to the most important building blocks of biological systems. They fulfill various physiological functions, such as cell-membrane assembly or, as highly reduced carbon compounds, energy storage, and are therefore found in every single living cell on earth. In bacteria the cell membranes are mainly formed from phospholipids such as phosphatidylcholines that contain a FA diglyceride, a phosphate, and a phophate-bound choline. The simplest type of phospholipid is made up from unbranched saturated FAs with typical chain lengths of 16 or 18 carbon atoms,

but sometimes also shorter or longer FAs can be found. The fluidity of bacterial cell membranes can be tuned, e.g., by the introduction of methyl branches or olefinic double bonds [1].

The biosynthesis of FAs is a repetitive chain elongation process catalysed in animals and fungi by multifunctional megasynthases, and in plants or bacteria by a set of discrete enzymes with equal functions to the individual and respective megasynthase domains. In both cases a starter unit, usually acetyl-CoA, is selected by the acetyl transferase (AT) and loaded onto an acyl-carrier-protein (ACP), or, more precisely, onto the thiol end of a phosphopantetheinyl linker that is attached to a highly conserved serine residue of the ACP (Scheme 1A). The acetyl moiety is then taken over by a conserved cystein residue of the

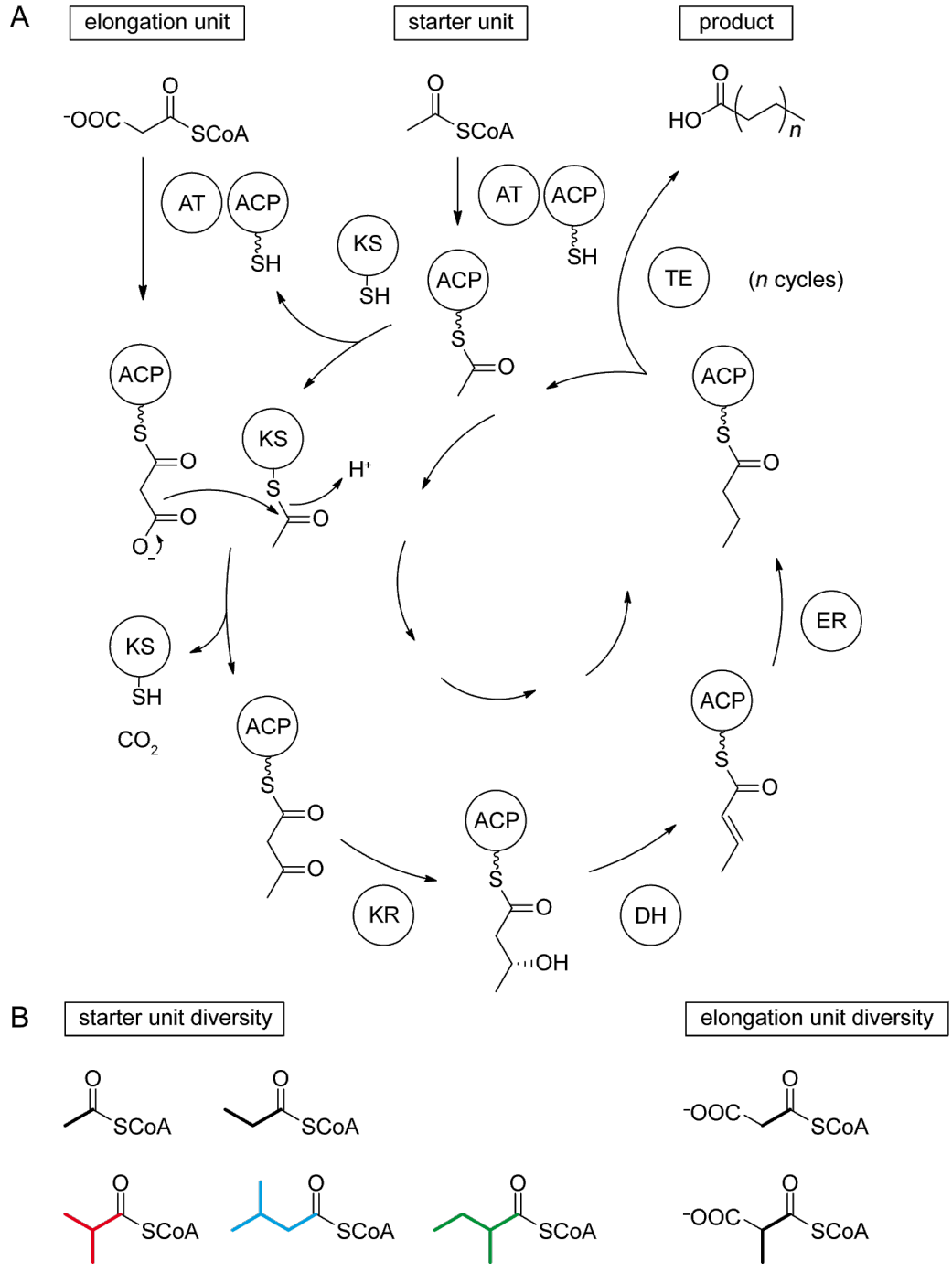

Scheme 1: Fatty acid biosynthesis.

ketosynthase (KS) making the ACP in turn available for the uptake of an elongation unit, in most cases malonyl-CoA, which is again selected and transferred by the AT. The reaction between the ACP-bound malonyl and the KS-bound acetyl group under decarboxylation conditions results in the formation of acetoacetyl-S~ACP by release of the KS. A three-step reductive process involving the subsequent actions of a ketoreductase (KR), a dehydratase (DH), and an enoyl reductase (ER) yields butyryl-S~ACP via (*R*)-3-hydroxybutyryl-S~ACP and crotyl-S~ACP. In summary of these transformations, the starter unit is elongated by two fully reduced carbon atoms, and *n* iterations of this elongation procedure yield a fatty acyl-S~ACP product with a chain length of (2*n* + 2) carbon atoms, with the final chain length being solely dependent on the size of the acting FAS's active site (although FA biosynthesis is catalysed by several discrete enzymes in bacteria, the term FAS, strictly speaking short for fatty acid synthase and thereby implying the action of only one single enzyme, will be used here for the complete bacterial FA biosynthetic machinery for reasons of brevity and simplicity). Product release from the ACP is achieved by action of a thioesterase (TE) to provide the unbound FA. The combination of an acetyl-CoA starter and malonyl-CoA elongators always leads to unbranched FAs with an even number of carbon atoms (even FAs). Structural variations are possible through the use of alternative starters, such as propionyl-CoA, for the synthesis of odd FAs (Scheme 1B). The branched amino acids valine and leucine provide, by transamination and oxidative decarboxylation, the *iso*-branched starters isobutyryl-CoA (red) for *iso*-even FAs and isovaleryl-CoA (blue) for *iso*-odd FAs, whereas the same reactions from isoleucine yield (*S*)-2-methylbutyryl-CoA (green) for *anteiso*-odd FA biosynthesis. Internal methyl branches can be introduced through the use of methylmalonyl-CoA elongation units, and occur due to the logic of FA biosynthesis in even-numbered positions of the FA carbon chain. An alternative mechanism leading to the same methyl branching pattern is well-known from polyketide biosynthesis and involves the incorporation of a malonyl-CoA unit followed by SAM-dependent methylation of the new α-carbon. Further alternative starters are known [2-4], but these cases are rare. In contrast, the usage of alternative elongation units such as ethylmalonyl-CoA [5], propylmalonyl-CoA [6], isobutylmalonyl-CoA [7], or methoxymalonyl-ACP [8] remains almost limited to polyketide synthesis and is only found in very exceptional cases of fatty acid biosynthesis [9].

Due to their ability to participate in hydrogen bonds and to form stabilised dimers, carboxylic acids have relatively low vapour pressures and, therefore, high boiling points. The volatility of carboxylic acids can be increased by their transformation into methyl esters, e.g., compare the boiling points of acetic acid (bp 118 °C) and methyl acetate (bp 57 °C). Some bacteria can methylate FAs to yield the corresponding methyl esters, resulting not only in an increased volatility, but making them at the same time unavailable for other biosynthetic transformations. Such fatty acid methyl esters (FAMEs) have previously been reported as headspace constituents of diverse bacteria [10]. The saturated compounds methyl butanoate (**1**), methyl isobutyrate (**2**), methyl 2-methylbutyrate (**3**), methyl isovalerate (**4**), methyl 2-methylpentanoate (**5**), methyl isocaproate (**6**), and methyl 3-methylpentanoate (**7**) were found in actinomycetes [11,12]. Methyl 9-methyldecanoate (**8**) is released by the myxobacterium *Stigmatella aurantiaca* DW4/3-1 [13]. A complex mixture of several methyl 2-methylalkanoates (**9**–**26**) was recently reported from the gliding bacterium *Chitinophaga* Fx7914 [14]. Some α,β-unsaturated FAMEs have also been described, such as methyl 4-methylpent-2-enoate (**27**), methyl tiglate (**28**), and methyl 3-methylcrotonate (**29**) from actinomycetes [12], and various methyl 2-methylalk-2-enoates (**30**–**43**) from *Chitinophaga* [14]. The proposed building blocks for the biosynthesis of these methyl esters are highlighted in bold and by use of a colour code in Figure 1. For the methyl 2-methylalkanoates and -alk-2-enoates from *Chitinophaga*, the origin of the methyl group from *S*-adenosyl methionine (SAM, purple) and of the 2-methyl groups from methylmalonyl-CoA was determined by feeding experiments [14].

During our ongoing analysis of the volatiles released by different bacteria and fungi with high potential for secondary metabolism, the actinomycete *Micromonospora aurantiaca* ATCC 27029 came to our attention. This gram-positive, sporulating bacterial genus includes producers of important antibiotics such as the aminoglycoside gentamycin [15] and the antitumor antibiotics lomaiviticins A and B (*Micromonospora lomaivitiensis*) [16]. Here the results of the headspace analyses of *M. aurantiaca* are described. Besides compounds from other classes, several methyl esters were identified. The identification of these esters from their mass spectra and retention indices, as well as the verification of the proposed structures by synthesis of representative reference compounds is presented.

Besides several other compounds, such as terpenes, pyrazines, aromatic compounds and methyl ketones, more than half of the components identified are unbranched and mono- and dimethyl-branched FAMEs, many of this last group having not been reported before.

Results and Discussion

Volatiles from *Micromonospora aurantiaca*

The volatiles released by agar plate cultures of the actinomycete *M. aurantiaca* ATCC 27029 were collected by use of a closed-loop stripping apparatus (CLSA), as described previ-

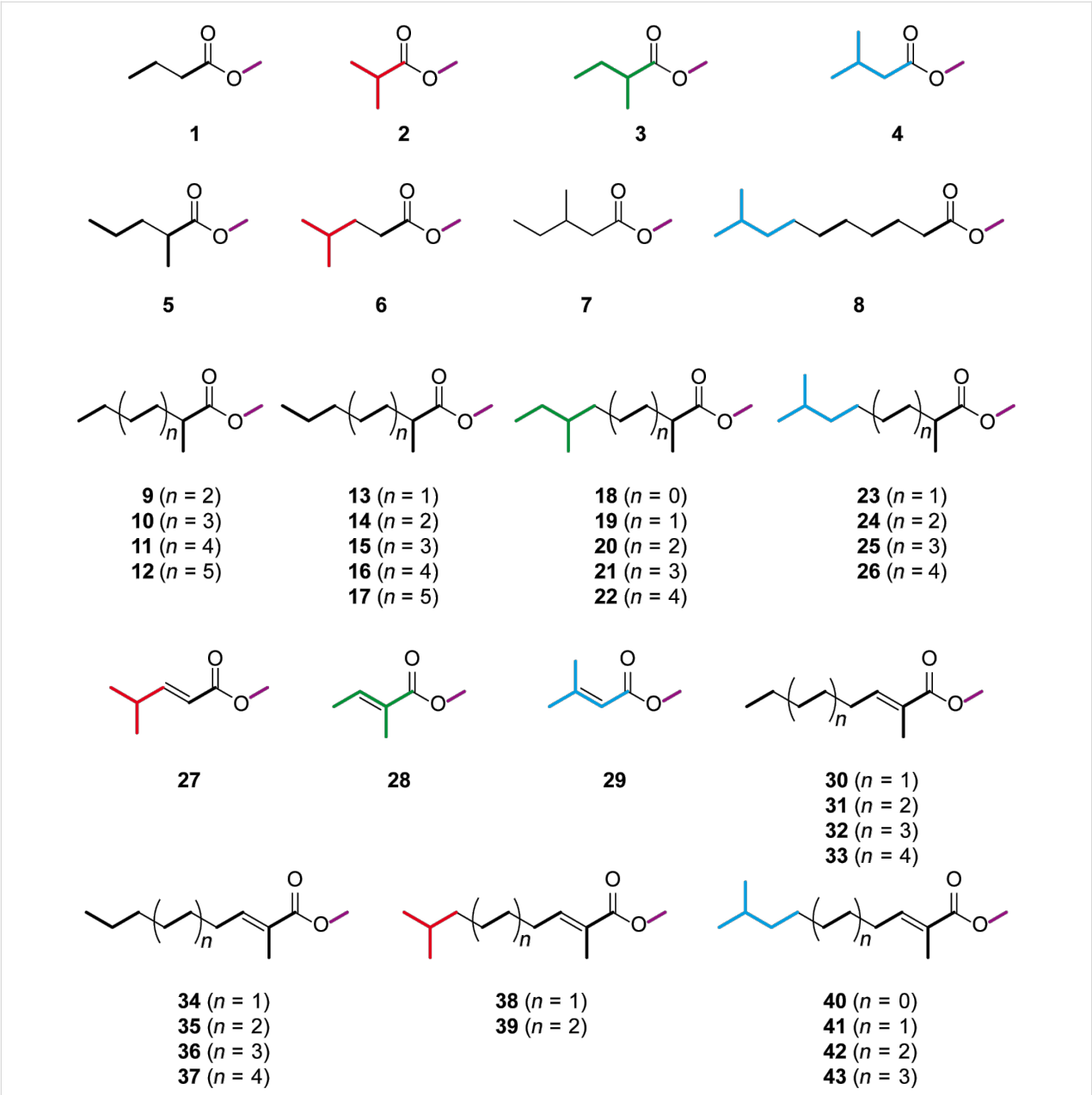

Figure 1: Volatile methyl esters from bacteria.

ously [17,18], and the obtained headspace extracts were analysed by GC–MS. The structures of the identified compounds (apart from FAMEs, which will be discussed below) are shown in Figure 2, the chromatogram of a representative sample is presented in Figure 3A, and the full results from two extracts are summarised in Table S1 of Supporting Information File 1. *M. aurantiaca* released more than 90 compounds from different compound classes including carboxylic acids, FAMEs, lactones, alcohols, aldehydes, acyloins, nitrogen and oxygen heterocycles, aromatic compounds, and terpenoids. Carboxylic acids were dominating, and this class was composed of the branched isobutyric acid (**49**), isovaleric acid (**50**), and 2-methylbutyric acid (**51**) as the main compounds, with minor amounts of 5-methylhexanoic acid (**55**) and 4-methylhexanoic acid (**56**), the α,β-unsaturated 3-methylbut-2-enoic acid (**53**) and 2-methylbut-2-enoic acid (**54**), a homologous series of unbranched saturated compounds from butyric acid to decanoic acid (**57**–**63**), and the unusual 2,2-dimethylpropanoic acid (**52**). Compound **51** was accompanied by minor amounts of its methyl ester **3**. The acids **49**–**51** can arise from the amino acids valine, leucine, and isoleucine, respectively, by transamination and oxidative decarboxylation, whereas **52** is equally available from the unusual

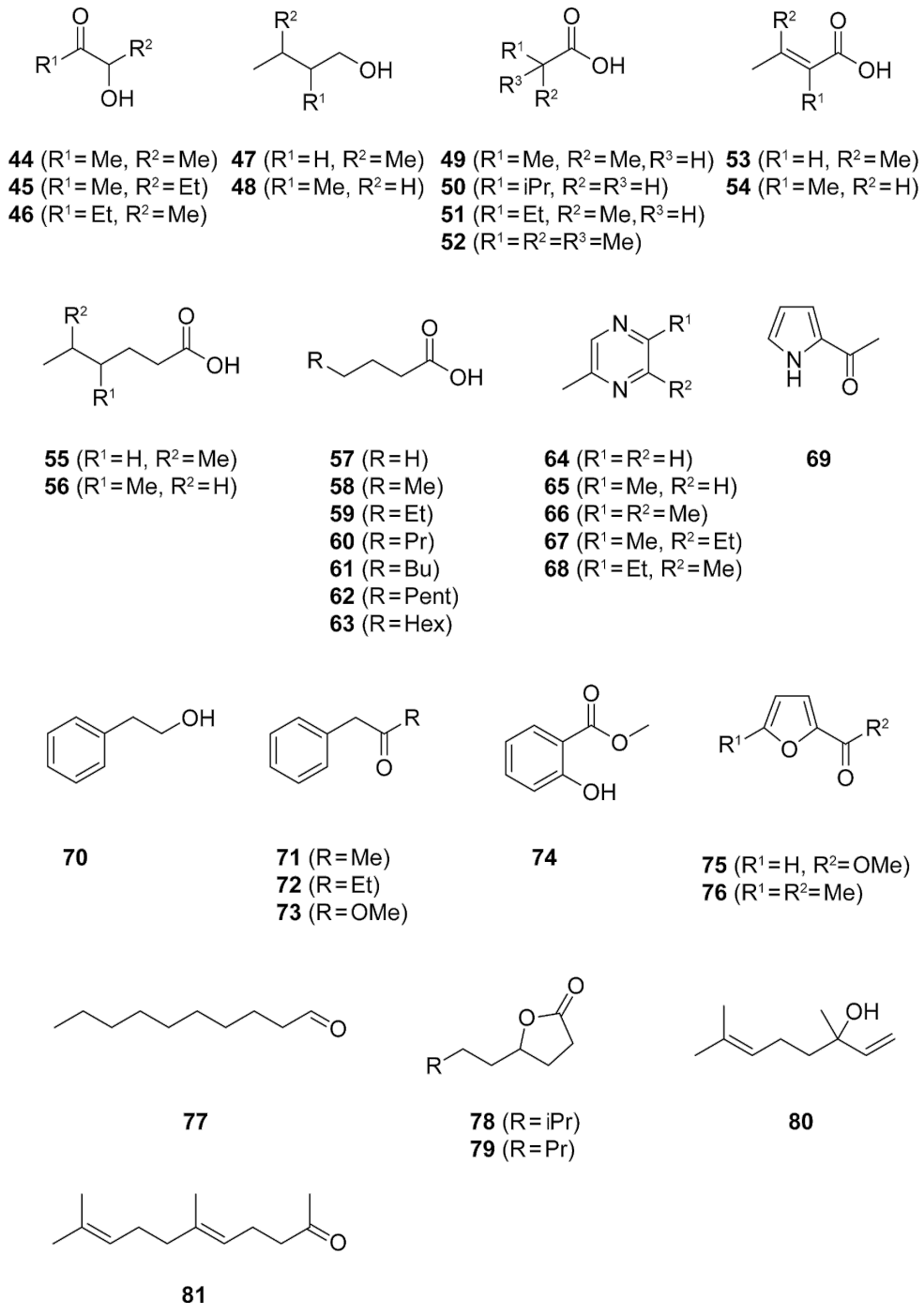

Figure 2: Compounds found in the headspace extracts of *M. aurantiaca*.

tert-leucine. The acids **53** and **54** can arise from their saturated counterparts **50** and **51** by dehydrogenation. A two-carbon elongation of **50** and **51** by means of the fatty acid biosynthetic pathway can generate **55** and **56**, while their reduction to the respective alcohols provides **47** and **48**. Acetoin (**44**) was also found as a major compound, together with its derivatives 3-hydroxypentan-2-one (**45**) and 2-hydroxypentan-3-one (**46**). Acyloins were recently identified as precursors for pyrazines from *Corynebacterium glutamicum* in our laboratory [19]. The *M. aurantiaca* headspace extracts contained methylpyrazine (**64**), 2,5-dimethylpyrazine (**65**), trimethylpyrazine (**66**), 2-ethyl-3,6-dimethylpyrazine (**67**), and 2-ethyl-3,5-dimethylpyrazine (**68**), which may also arise from acyloins. Further identified compounds were 2-acetylpyrrole (**69**),

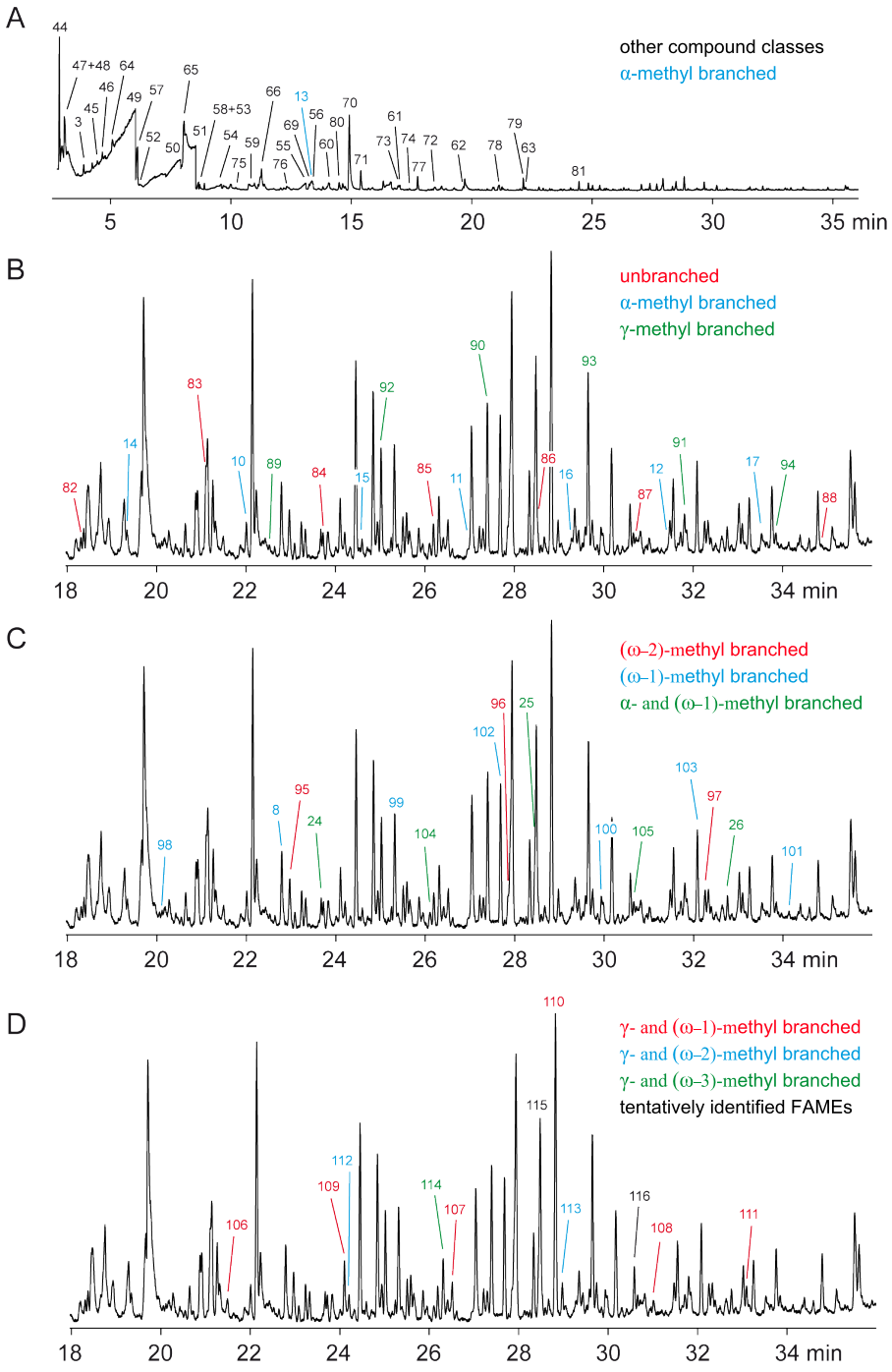

Figure 3: Total ion chromatograms of the headspace extract from *M. aurantiaca* (A), and expansions of the total ion chromatogram (18–36 min) showing the relevant peaks of the FAMEs (B–D, for clarity the same expansion is shown in three replicates for FAMEs from different series). The colour code used for these series of FAMEs is given in the respective figures.

2-phenylethanol (**70**), phenylacetone (**71**), 1-phenylbutan-2-one (**72**), methyl phenylacetate (**73**), methyl salicylate (**74**), methyl furan-2-carboxylate (**75**), 2-acetyl-5-methylfuran (**76**), decanal (**77**), 7-methyloctan-4-olide (**78**), nonan-4-olide (**79**), and the terpenoids linalool (**80**) and geranyl acetone (**81**).

Besides the compounds mentioned above, several saturated FAMEs were present in the headspace extracts (Figure 4). All the identified FAMEs were divided into groups according to their pattern of methyl branchings. Unbranched FAMEs (Figure 3B, red) included all even and odd members of the

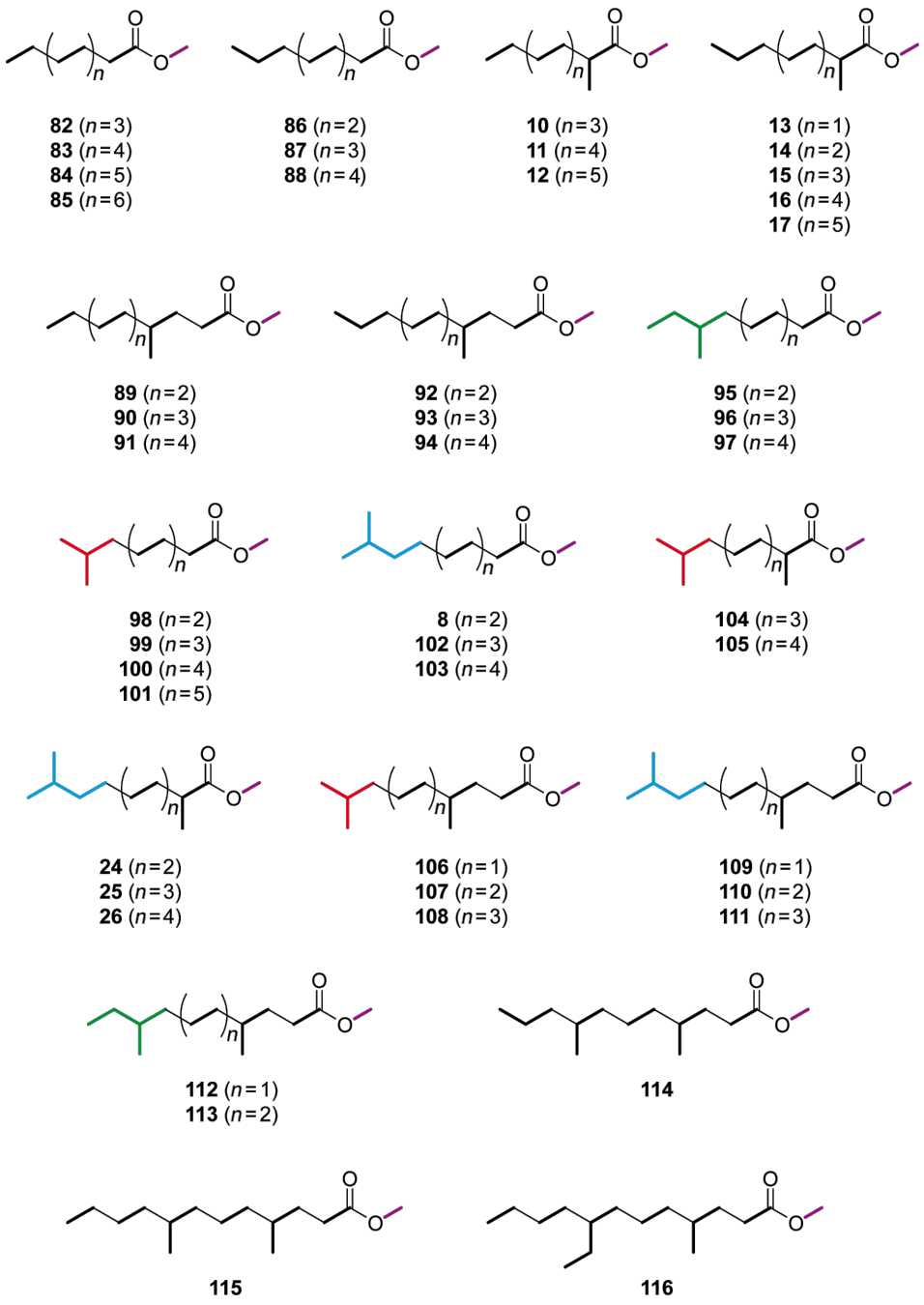

Figure 4: FAMEs identified in the headspace extracts from *M. aurantiaca*.

homologous series from methyl nonanoate to methyl tetradecanoate, in addition to methyl hexadecanoate. These compounds were readily identified from their mass spectra by comparison to library spectra and subsequent GC–MS analysis of synthetic standards. Mass spectra of unbranched FAMEs (for mass spectrum of methyl dodecanoate see Figure 5A) are characterised by fragment ions at m/z = 74 (McLafferty rearrangement, Scheme 2), m/z = 87 (β-cleavage), and $[M - 31]^+$ (loss of OMe). Further fragment ions $[M - C_nH_{2n+1}]^+$ arise from cleavage of the saturated unbranched alkyl chain.

All other FAMEs were isomers of these unbranched compounds and were assumed to be methyl branched FAMEs due to biosynthetic considerations as outlined above. The structures of these branched compounds have been suggested based on careful analysis of their mass spectra and on a modified reten-

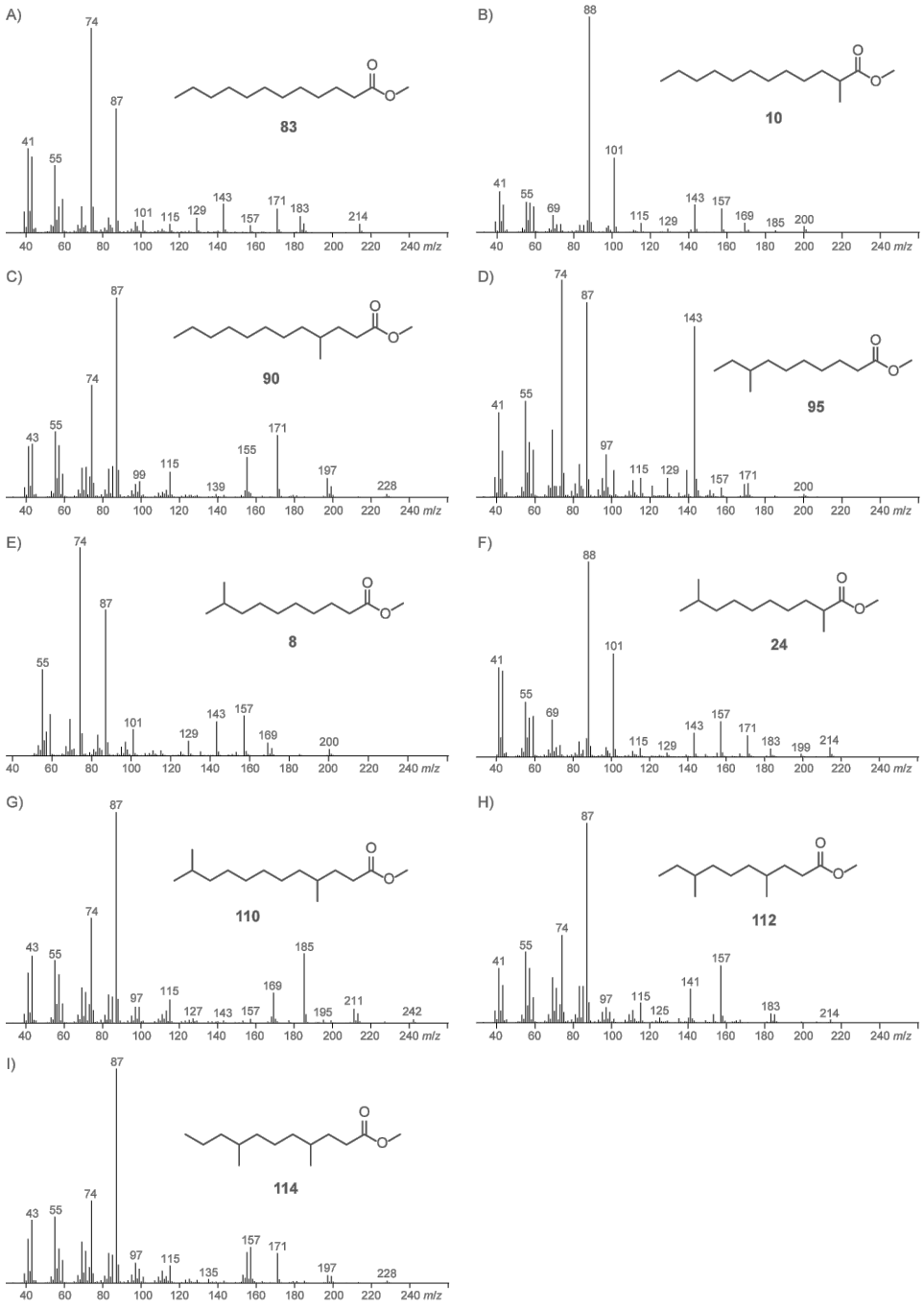

Figure 5: Mass spectra of (A) methyl dodecanoate (**83**), (B) methyl 2-methyldodecanoate (**10**), (C) methyl 4-methyldodecanoate (**90**), (D) methyl 8-methyldecanoate (**95**), (E) methyl 9-methyldecanoate (**8**), (F) methyl 2,9-dimethyldecanoate (**24**), (G) methyl 4,11-dimethyldodecanoate (**110**), (H) methyl 4,8-dimethyldecanoate (**112**), and (I) methyl 4,8-dimethylundecanoate (**114**).

tion-index increment system [20]. Following this system, the retention index $I_{calc.}$ of a methyl branched compound can be calculated (Equation 1) by

$$I_{calc.}(n) = N(n) + FG + \sum Me_i \ . \qquad (1)$$

The increment $N(n)$ depends on the number of carbon atoms n in the longest alkyl chain and is $N(n) = 100\ n$, FG is an increment for the functional group, and the increments Me_i have to be considered for methyl branches depending on the positions i of branching. The increments FG and Me_i have to be determined for each type of GC column. In a first approximation,

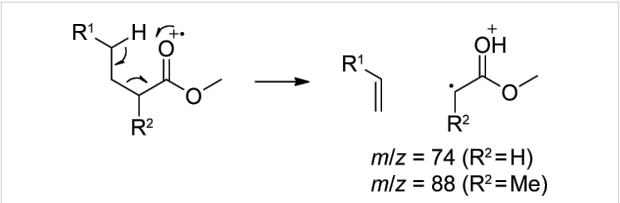

Scheme 2: McLafferty fragmentation of FAMEs.

these increments can be assumed to be constants, but as will be discussed below both $FG(n)$ and $Me_i(n)$ are slightly dependent on the length of the alkyl chain, giving better results for the calculated retention indices if this dependency is considered. For all of the following analyses the functional group increment for FAMEs on a HP-5 MS column ($FG(n)_{\text{FAME, HP-5 MS}}$) was determined from the homologous series of unbranched FAMEs (Table S2 and Figure S1 of Supporting Information File 1). By linear regression (Figure 6) the functional group increment (Equation 2) was

$$FG(n)_{\text{FAME, HP-5 MS}} = 327 - 0.54\,n\ , \qquad (2)$$

resulting in a modified Equation 1

$$I_{\text{calc.}}(n) = 99.46\,n + 327 + \sum Me_i\ . \qquad (3)$$

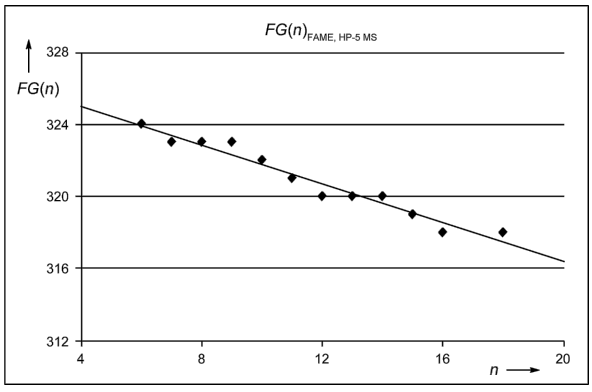

Figure 6: The functional group increment $FG(n)_{\text{FAME, HP-5 MS}}$.

A series of compounds (Figure 3A and Figure 3B, blue) exhibited mass spectra with two significant fragment ions at m/z = 88 as the base peak and at m/z = 101, indicating a methyl branching in a α-position (Scheme 2, cf. Figure 5B for mass spectrum of methyl 2-methyldecanoate). For the determination of the increment Me_α the reference compound methyl 2-methyldecanoate (**10**) was synthesised by α-alkylation of **82** (Scheme 3). The mass spectrum and retention index (I = 1357) of the product were identical to those of the natural compound. By using Equation 3 the increment for a methyl branching in a α-position was determined as Me_α = 35, resulting in the calculated retention indices for the α-methyl branched FAMEs as listed in Table S3 of Supporting Information File 1, column 4. The calculated retention indices fitted perfectly for compounds with a chain length of around 10 carbon atoms, which is not surprising since Me_α was determined from **10**, but the indices deviated slightly from the measured values for shorter (n = 7: $I_{\text{nat.}} - I_{\text{calc.}} = 4$) or longer ($n$ = 15: $I_{\text{nat.}} - I_{\text{calc.}} = -2$) FAMEs. In other words, Me_α was dependent on the chain length. A linear regression analysis gave

$$Me_\alpha(n) = 43 - 0.72\,n\ . \qquad (4)$$

Recalculation of the retention indices of the α-methyl branched FAMEs, taking into account the dependency of Me_α on the chain length, resulted in the values listed in Table S3 of Supporting Information File 1, column 5, which perfectly fitted the measured retention indices.

The next class of compounds (Figure 3B, green) showed characteristic fragment ions at m/z = 87 and m/z = 74 similar to the unbranched FAMEs, but in contrast the β-cleavage was more important than the McLafferty fragmentation (cf. Figure 5C for mass spectrum of methyl 4-methyldodecanoate). This, together with an almost completely missing fragment ion at m/z = 101, accounting for a γ-cleavage in unbranched FAMEs, suggested the presence of a methyl group in a γ-position, which leads to a γ-fragmentation with m/z = 115. A synthesis of methyl 4-methyldodecanoate (**90**) was performed starting from **10** (Scheme 3). Reduction to the aldehyde **123d** and subsequent Horner–Wadsworth–Emmons reaction gave the α,β-unsaturated ester **124d**, which upon catalytic hydrogenation yielded **90**. The synthetic compound was identical to the natural FAME as judged by mass spectrum and retention index (I = 1572). The retention index of this reference compound was used for to determine that Me_γ = 51, resulting in the calculated retention indices for all γ-methyl branched FAMEs as summarised in Table S4 of Supporting Information File 1. Correction of the increment Me_γ by linear regression gave

$$Me_\gamma(n) = 58 - 0.54\,n\ . \qquad (5)$$

The corrected calculated retention indices, taking Equation 5 into consideration, were in good agreement with the measured retention indices.

Another group of FAMEs (Figure 3C, red) showed mass spectra with significant fragment ions at m/z = 74 and m/z = 87, like the unbranched compounds (for mass spectrum of methyl

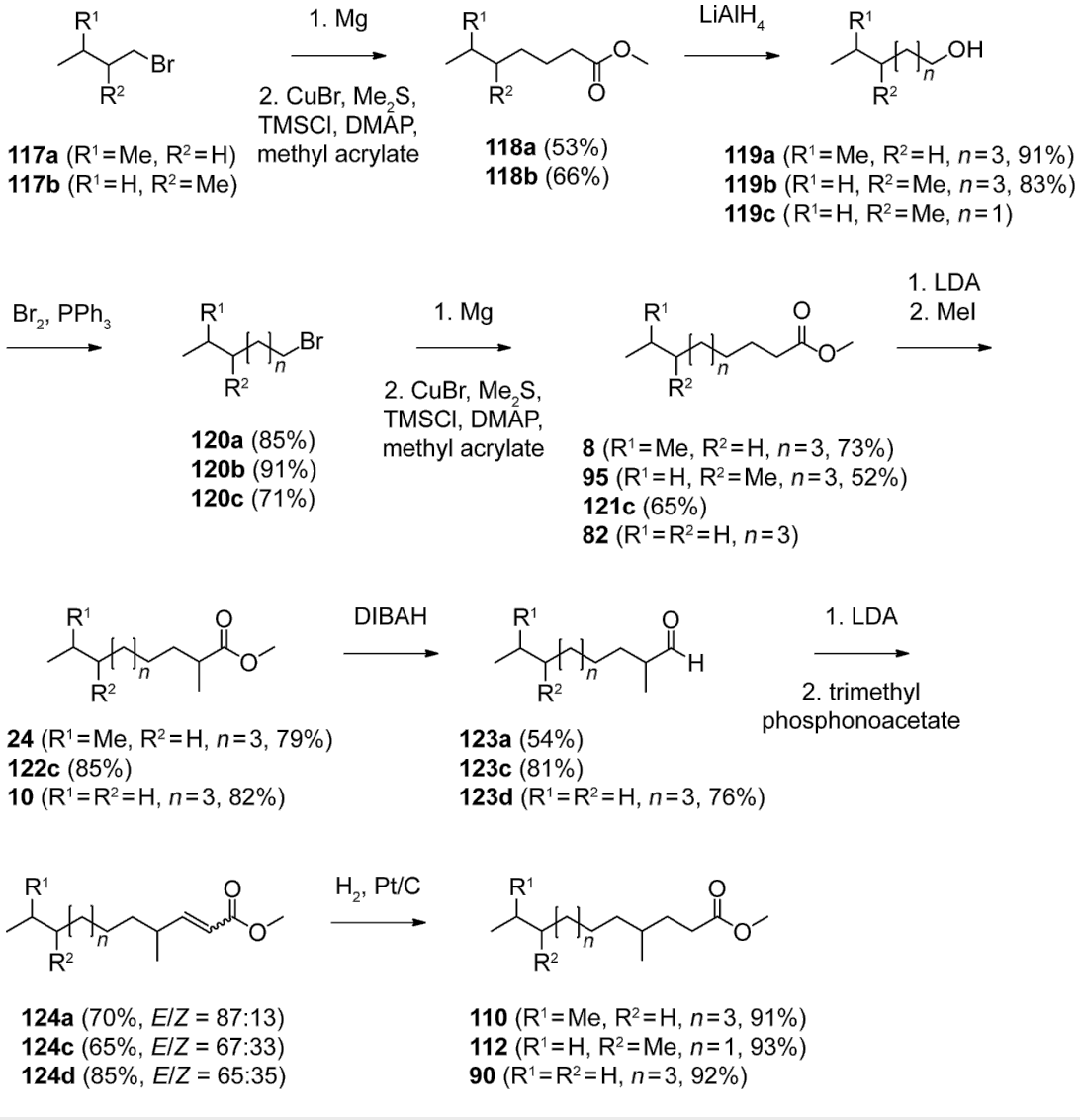

Scheme 3: Synthesis of FAMEs identified from *M. aurantiaca*.

8-methyldecanoate cf. Figure 5D), and were assumed to be branched towards the Me terminus, i.e., these FAMEs are suggested to originate from a branched amino acid starter. Within this group only the FAMEs derived from the odd FAs were found, pointing to an isoleucine-derived starter and a methyl branching in the (ω−2)-position. Furthermore, this suggestion was supported by the intensity of the $[M - 57]^+$ ion, which is typical for *anteiso*-FAMEs. The synthesis of methyl 8-methyldecanoate (**95**) as a reference compound was started from 1-bromo-2-methylbutane (**117b**, Scheme 3). Copper-catalysed 1,4-addition of the respective Grignard reagent to methyl acrylate in the presence of trimethylchlorosilane, dimethyl sulfide, and 4-dimethylaminopyridine gave methyl 5-methylheptanoate (**118b**). A sequence of $LiAlH_4$ reduction to the alcohol **119b**, conversion into the bromide **120b**, and Cu-mediated 1,4-addition of the Grignard reagent to methyl acrylate furnished the desired FAME **95**. Its mass spectrum and retention index (I = 1392) were in good agreement with those of the natural product. The increment $Me_{\omega-2}$ = 70 was determined from the retention index of compound **95**. In contrast to the increments Me_α and Me_γ the increment $Me_{\omega-2}$ proved to be largely independent of the chain lengths of the FAMEs and gave good results for the calculated retention indices over a wide range of n, including all other natural FAMEs of this type from *M. aurantiaca* and the compounds **118b** and **121c**, which were obtained in the syntheses of **95** and methyl 4,8-dimethyldecanoate (**112**) as described below (Table S5 of Supporting Information File 1). Furthermore, the value of $Me_{\omega-2}$ was in good agreement with a previously published value determined on a BPX-5 column ($Me_{\omega-2}$ = 73) [20].

The next series of FAMEs (Figure 3C, blue) also had very similar mass spectra compared to the unbranched and (ω−2)-methyl branched compounds dominated by the fragments at m/z = 74 and m/z = 87 (the mass spectrum of methyl 9-methyldecanoate is shown in Figure 5E). Within this series both even and odd FAMEs were detected, and therefore, these compounds were suggested to be (ω−1)-methyl branched and derived from leucine or valine starters, respectively. As typical for (ω−1)-methyl branched compounds, these FAMEs eluted slightly earlier than their (ω−2)-methyl branched counterparts. Additional support for this suggestion was given by the occurrence of relatively intense fragments at $[M - 43]^+$, as can be expected for *iso*-FAMEs. In direct analogy to the synthesis of **95**, methyl 9-methyldecanoate (**8**) was synthesised from 1-bromo-3-methylbutane (**117a**, Scheme 3) and was identical to the volatile from *M. aurantiaca* in terms of mass spectrum and retention index (I = 1385), according to an increment of $Me_{\omega-1}$ = 63. The retention indices of all other volatiles from *M. aurantiaca* and of the intermediate **118a** in the synthesis of **8** were calculated from this constant increment and were in good agreement with the measured values (Table S6 of Supporting Information File 1).

In addition to these mono-methyl branched FAMEs, several classes of multiply methyl branched compounds were identified. The first group of compounds (Figure 3C, green) exhibited mass spectra that were very similar to those of the α-branched FAMEs described above, with dominating fragment ions at m/z = 88 and m/z = 101 (the mass spectrum of methyl 2,9-dimethyldecanoate is depicted in Figure 5F), but compounds of this class eluted significantly earlier than their mono-branched isomers, pointing to a second methyl branch within the alkyl chain, likely towards the methyl terminus. Since both even and odd compounds of this series were present, the structures of α- and (ω−1)-methyl branched FAMEs derived from leucine and valine starters, respectively, were suggested (Table S7 of Supporting Information File 1). The increments $FG(n)_{\text{FAME, HP-5 MS}}$, $Me_{\alpha}(n)$, and $Me_{\omega-1}$ as determined above were used for the calculation of retention indices. The calculated values were in perfect agreement with the measured values, thus corroborating the suggested structures. For unambiguous proof, an exemplary reference compound of this series was synthesised (Scheme 3). α-Methylation of **8** yielded methyl 2,9-dimethyldecanoate (**24**), which was identical to the respective FAME from *M. aurantiaca*.

A second series of dimethyl branched FAMEs (Figure 3D, red) exhibited very similar mass spectra to the γ-methyl branched esters (for mass spectrum of methyl 4,11-dimethyldodecanoate cf. Figure 5G). Within this class again both even and odd FAMEs were found, suggesting that they were derived from valine or leucine starters and therefore γ- and (ω−1)-methyl branched. Calculations of the retention indices for the suggested structures were in good agreement with the measured data (Table S8 of Supporting Information File 1), thus providing further evidence for the suggested structures. Final verification was obtained by synthesis of methyl 4,11-dimethyldodecanoate (**110**) from **24** by its reduction to the aldehyde **123a**, Horner–Wadsworth–Emmons olefination to **124a**, and catalytic hydrogenation (Scheme 3). The synthetic material was identical to the natural compound **110**.

A related group of compounds (Figure 3D, blue) proved to have very similar mass spectra, thus indicating a methyl group in a γ-position (Figure 5H shows the mass spectrum of methyl 4,8-dimethyldecanoate). The relatively high intensity of the $[M - 57]^+$ fragment ion suggested the structures of *anteiso*-FAMEs, and accordingly, only the isoleucine-derived methyl esters of even-numbered FAs were found. Retention-index calculations (Table S9 of Supporting Information File 1) showed full agreement of the calculated retention indices with the experimental data. A synthesis of methyl 4,8-dimethyldecanoate (**112**) as a reference compound was carried out starting from 3-methylpentan-1-ol (**119c**), by similar methods as described above (Scheme 3). The alcohol **119c** was transformed into the bromide **120c**. The copper-catalysed Michael addition of the respective Grignard reagent to methyl acrylate yielded methyl 6-methyloctanoate (**121c**), which was α-methylated to **122c**. Reduction with DIBAH to the aldehyde **123c**, Horner–Wadsworth–Emmons olefination to **124c**, and final catalytic hydrogenation afforded **112**. The product exhibited the same mass spectrum and retention index (I = 1441) as the natural FAME. The slight deviations between the calculated and measured retention indices for compounds **106** (ΔI = 2) and **112** (ΔI = 3) may be attributed to the fairly close proximity of the two methyl branches, which are only three methylene units apart.

The FAME **114** (Figure 3D, green) was also suggested to be γ-methyl branched based on its mass spectrum (the mass spectrum of methyl 4,8-dimethylundecanoate is presented in Figure 5I). This compound was an isomer of methyl 4-methyldodecanoate (**90**) and methyl 4,10-dimethylundecanoate (**107**), but eluted slightly earlier than **107**, resulting in a suggested structure of methyl 4,8-dimethylundecanoate. A synthesis of this compound was performed starting with bromination of 2-methylpentan-1-ol (**125**) and subsequent Cu-catalysed 1,4-addition of the respective Grignard reagent to methyl acrylate, resulting in methyl 5-methyloctanoate (**127**, Scheme 4). Reduction to the aldehyde **129** via the alcohol **128**, addition of methylmagnesium bromide, and bromination resulted in the secondary bromide **131**. Michael addition of its Grignard reagent to methyl

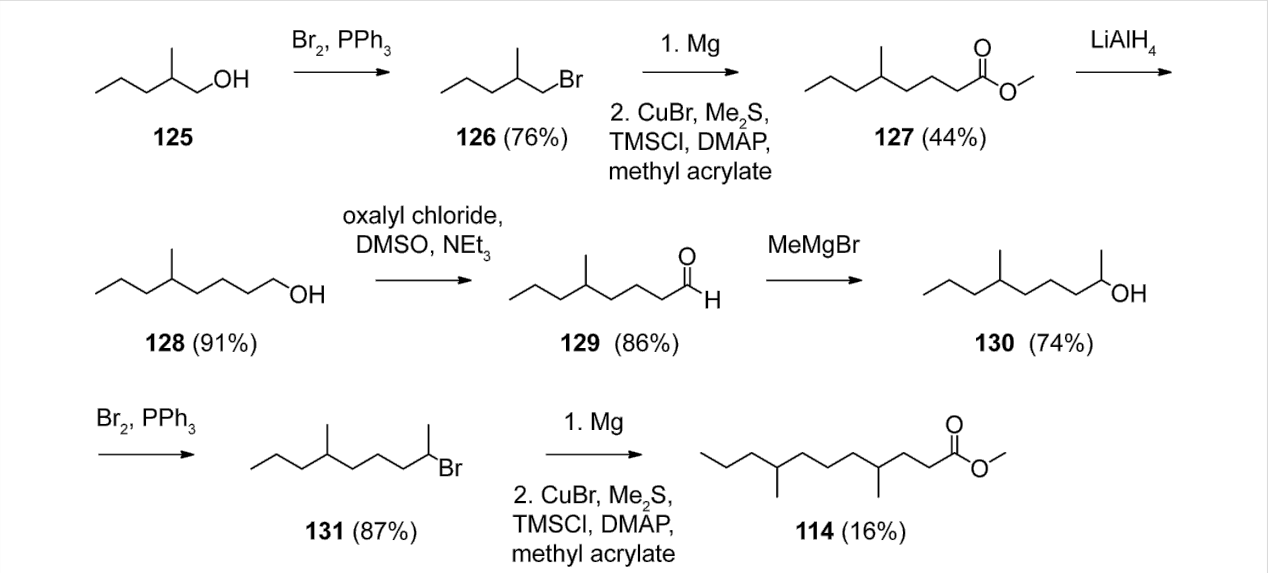

Scheme 4: Synthesis of the γ- and (ω−3)-methyl branched FAME **114**.

acrylate was less efficient than for primary bromides, but gave the desired product **114** in low yield. The identity to the natural product was confirmed by comparison of GC–MS data.

The structures of two additional FAMEs were suggested based on their mass spectra, but these were not verified by synthesis and therefore only tentatively identified (Figure 7). Both compounds were suggested to be γ-methyl branched due to the relative intensities of the fragment ions at *m*/*z* = 87 and *m*/*z* = 74. The first compound (Figure 7A) showed a molecular ion at *m*/*z* = 242 and further fragment ions at *m*/*z* = 157 and *m*/*z* = 185 resulting from the loss of C_4H_9 or C_6H_{13}, whereas no fragment ion accounting for the loss of C_5H_{11} (*m*/*z* = 171) was observed. This pattern is in accordance with the structure of methyl 4,8-dimethyldodecanoate (**115**). The second compound (Figure 7B) exhibited a molecular ion at *m*/*z* = 256 and fragment ions at *m*/*z* = 157 and *m*/*z* = 199 according to the loss of C_4H_9 and C_7H_{15}, but not at *m*/*z* = 171 and *m*/*z* = 185 (loss of C_5H_{11} and C_6H_{13}, respectively). This pattern suggested an ethyl branch in the 8-position corresponding to the structure of methyl 8-ethyl-4-methyldodecanoate (**116**). This compound is interesting in terms of its biosynthesis, because it may be formed by incorporation of an ethylmalonyl-CoA elongation unit. However, since no further compounds with ethyl branches were found, another biosynthetic option seems more likely. The compound 2-ethylhexanol is a widespread pollutant originating from plasticisers, and this compound could have been oxidised to 2-ethylhexanoic acid, transformed into its CoA derivative, and used as an unusual starter unit by the FAS to make **116**.

Several of the FAMEs emitted by *M. aurantiaca* are chiral, including, e.g., the α-, γ-, and (ω−2)-methyl branched FAMEs. In addition, compounds such as the γ- and (ω−2)-methyl branched FAMEs exist in two different diastereomers. However, these diastereomers, which were both contained in the synthetic material, e.g., of compounds **112** and **114**, were

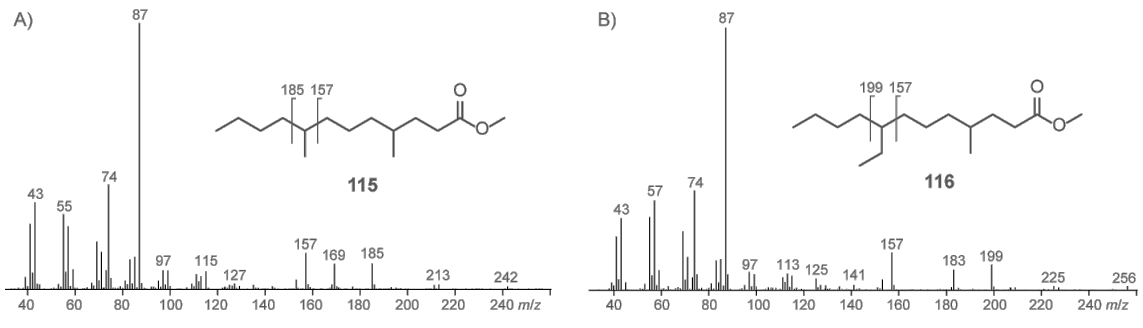

Figure 7: Mass spectra of tentatively identified methyl 4,8-dimethyldodecanoate (**115**) and methyl 8-ethyl-4-methyldodecanoate (**116**).

not separated on the HP5-MS column used for GC–MS analyses, and therefore the elucidation of the relative configurations was not possible, at least not by our GC approach. The only very small differences in the physical properties of these compounds were also reflected by the occurrence of only one set of signals in the NMR spectra of these mixtures of diastereomers. The separation of enantiomers of the chiral compounds described here on chiral GC columns is also a very hard task, especially for internally methyl branched FAMEs, and was beyond the scope of our work.

Feeding experiments

To investigate the biosynthetic origin of the FAMEs, several feeding experiments with deuterated precursors were performed. These were directly added to the agar plate cultures and the headspace extracts were prepared by CLSA after ca. 2–3 days of growth. The CLSA extracts were then analysed by GC–MS. Incorporation of deuterated precursors was observable through the increased molecular masses and *m*/*z* ratios of certain fragment ions that could be used to localise the deuterium incorporation. One advantage of using deuterated precursors is that deuterium incorporation results in a decrease in the retention time of the analyte with respect to its unlabelled counterpart, i.e., the deuterated isotopomers are separated and their mass spectra can easily be interpreted [21].

Feeding of [$^2H_{10}$]isoleucine

One possible pathway to (ω−2)-methyl branched FAMEs is through the use of 2-methylbutyryl-CoA as a starting unit, which is available from isoleucine by transamination and oxidative decarboxylation. The alternative would be to use an acetyl-CoA starter followed by incorporation of a methylmalonyl-CoA elongation unit. The question as to which of these two alternatives is operative in *M. aurantiaca* was addressed by feeding of [$^2H_{10}$]isoleucine. In this feeding experiment *M. aurantiaca* produced large amounts of [$^2H_9$]-2-methylbutyric acid ([$^2H_9$]-**51**) and its respective methyl ester [$^2H_9$]methyl 2-methylbutyrate ([$^2H_9$]-**3**), both with incorporation rates >70%. The transamination of [$^2H_{10}$]isoleucine to 2-oxo-3-methylpentanoic acid proceeds with the loss of one deuterium, and accordingly, nine deuterium atoms were incorporated into **3**, as indicative by a shift of the molecular ion of **3** from *m*/*z* = 116 to *m*/*z* = 125 (compare Figures S2A and S2B of Supporting Information File 1). The fragment ion at *m*/*z* = 101, arising through the loss of a methyl group, shifted to *m*/*z* = 107, whereas no signal was detected at *m*/*z* = 110 in the mass spectrum of [$^2H_9$]-**3**. Therefore, the respective fragment ion only arises by methyl cleavage from the acyl moiety, and not by loss of the methyl group from the ester function. Further diagnostic fragment ions formed by α-cleavage (*m*/*z* = 57) and McLafferty rearrangement (*m*/*z* = 88) shifted to *m*/*z* = 66 and *m*/*z* = 93, in full agreement with the structure of [$^2H_9$]-**3**. For the respective free acid **51** no molecular ion is visible, but the fragment ion at *m*/*z* = 101, formed by loss of one hydrogen from the carboxylic acid function, was detected at *m*/*z* = 110 for [$^2H_9$]-**51**, indicating the incorporation of nine deuteriums (Figures S2C and S2D of Supporting Information File 1). Further fragment ions were observed at *m*/*z* = 66 (α-cleavage, + 9 amu), *m*/*z* = 79 (McLafferty rearrangement, + 5 amu), and *m*/*z* = 101 (loss of methyl group, + 6 amu), clearly establishing the identity of [$^2H_9$]-**51**. The uptake of isoleucine in the (ω−2)-methyl branched FAMEs was also observed with high incorporation rates (>90%) for methyl 12-methyltetradecanoate (**97**, Figures S2E and S2F of Supporting Information File 1), methyl 10-methyldodecanoate (**96**), and methyl 14-methylhexadecanoate (not shown). The mass spectrum of [$^2H_9$]-**97** is characterised by a molecular ion at *m*/*z* = 265 showing the incorporation of nine deuteriums, whereas the fragment ions at *m*/*z* = 74 and *m*/*z* = 87 indicative of the structure of a methyl ester are not shifted relative to the unlabelled material. The compound methyl 14-methylhexadecanoate was not found under the original experimental conditions without feeding of [$^2H_9$]isoleucine, demonstrating that the production of (ω−2)-methyl branched FAMEs by *M. aurantiaca* can be activated by isoleucine supply. Unfortunately, the γ- and (ω−2)-methyl branched compounds **112** and **113** were not produced under the conditions of isoleucine feeding, and therefore, their biosynthetic origin remained elusive.

Feeding of [$^2H_{10}$]leucine

Feeding of [$^2H_{10}$]leucine was performed to investigate the biosynthetic origin of the (ω−1)-methyl branched FAMEs. Incorporation was observed for a series of (ω−1)-methyl branched FAs including isovaleric acid, 5-methylhexanoic acid, 7-methyloctanoic acid, 9-methyldecanoic acid (Figures S3A and S3B of Supporting Information File 1), and 11-methyldodecanoic acid, all with high incorporation rates (>70%). The uptake of deuterated leucine for the last compound was observable by a shift of the molecular ion from *m*/*z* = 186 to *m*/*z* = 195. The fragment ions of the McLafferty rearrangement (*m*/*z* = 60) and the β-cleavage (*m*/*z* = 73) remained unchanged, whereas fragment ions arising from cleavage of the terminal isopropyl group (*m*/*z* = 43 and *m*/*z* =143) shifted to *m*/*z* = 50 and *m*/*z* = 145 in agreement with the deuterium labelling of this portion of the molecule.

The labelling was also introduced into the *iso*-odd FAMEs **102** and **103** (Figures S3C to S3F of Supporting Information File 1) and the higher homologue methyl 15-methylhexadecanoate (not shown). Methyl 15-methylhexadecanoate was only found during feeding of [$^2H_{10}$]leucine, similar to the formation of methyl 14-methylhexadecanoate found only during feeding of [$^2H_{10}$]isoleucine.

Feeding of [$^2H_8$]valine

Feeding of [$^2H_8$]valine resulted in the incorporation of the isotopic labelling into its transamination-oxidative decarboxylation product isobutyric acid (**49**) and the *iso*-even FAMEs methyl 12-methyltridecanoate (**100**) and methyl 14-methylpentadecanoate (**101**) with high incorporation rates (>50%), as indicated by the increase of the molecular ions by 7 amu in combination with the overall expected fragmentation pattern (Figure S4 of Supporting Information File 1). The transamination product of valine, 2-oxoisovaleric acid, can be used by most organisms for the biosynthesis of the leucine precursor 2-oxoisocaproic acid. The enzymes for catalysis of this pathway are encoded in the genome of *M. aurantiaca*, but the pathway seemed not to be active under the experimental conditions, judged by the fact that no incorporation of [$^2H_8$]valine into the *iso*-odd FAMEs was observed. Furthermore, no uptake of labelling from [$^2H_{10}$]leucine into the *iso*-even FAMEs was found, which also rules out a similar formation of the higher homologue 2-oxo-5-methylcaproic acid from 2-oxoisocaproic acid. These results also demonstrate that the FAs in *M. aurantiaca* are not subject to α-oxidation, a process in which FAs are oxidatively degraded by one carbon.

Feeding of [$^2H_5$]sodium propionate

To investigate the biosynthetic origin of the α- and γ-methyl branches, a feeding experiment with [$^2H_5$]sodium propionate was performed. This compound was expected to be carboxylated to yield methylmalonyl-CoA, which would serve as an elongation unit for the introduction of methyl branches. Alternative mechanisms could include the chain elongation with malonyl-CoA, followed by methylation with SAM by catalysis of a *C*-methyltransferase. Indeed the incorporation of isotopic labelling into the α- and γ-methyl branched FAMEs was observed with high incorporation rates (>90%, Figure S5 of Supporting Information File 1). Incorporation into methyl 2,11-dimethyldodecanoate (**25**) and its higher homologue **26** was observable by an increase of the molecular ion by 3 amu, while the fragment ions at m/z = 88 and m/z = 101, indicative of an α-methyl branch, shifted to m/z = 91 and m/z = 104. The incorporation of only three deuterium atoms from [$^2H_5$]sodium propionate is in agreement with the biosynthesis of FAs (Scheme 1): One deuterium is lost during carboxylation of propionyl-CoA to yield methylmalonyl-CoA, the second is possibly exchanged with water due to the C,H-acidity of malonyl-CoA derivatives, but it is lost, at the latest, in the dehydration of the 3-hydroxy-2-methylacyl-S~ACP to the respective 2-methyl-2-enoyl-S~ACP intermediate. The incorporation of [$^2H_5$]sodium propionate was also observed for the γ-methyl branched compounds represented by methyl 4,11-dimethyldodecanoate (**110**). The uptake of deuterium was in the first instance visible by an increase of the molecular ion from m/z = 242 to m/z = 245, whereas the McLafferty rearrangement and β-cleavage fragment ions were detected at m/z = 74 and m/z = 87, as for the unlabelled compound. The deuterium labelling of the γ-methyl group was indicated by a shift of the fragment ion at m/z = 115 (γ-cleavage) to m/z = 118. No incorporation was observed into the (ω−2)-methyl branches of the respective FAMEs, ruling out their alternative formation from an acetate starter in combination with an initial methylmalonyl-CoA elongation unit, instead of from isoleucine.

Feeding of [*methyl*-$^2H_3$]methionine

Feeding of [*methyl*-$^2H_3$]methionine was performed, first as a control experiment with respect to the biosynthetic origin of the α- and γ-methyl branches, and second, to investigate the biosynthetic origin of the methyl ester moiety of the FAMEs. The feeding experiment resulted in the incorporation into **103** (Figure S6 of Supporting Information File 1) and **97** (not shown), as indicated by a shift of the molecular ion from m/z = 256 to m/z = 259, of the McLafferty ion from m/z = 74 to m/z = 77, and of the β-cleavage fragment ion from m/z = 87 to m/z = 90. Further FAMEs were not produced during the course of this experiment. The results clearly demonstrate the formation of FAMEs from methionine via SAM as the methyl donor for the methylation of FAs.

Conclusion

In summary, the headspace extracts from *M. aurantiaca* contain unbranched even and odd FAMEs that are made from an acetyl-CoA or propionyl-CoA starter. In particular the even FAMEs are very widespread in nature. Several α-methyl branched FAMEs were also present that were previously described from *Chitinophaga* [14]. These compounds can be synthesised by incorporation of a final methylmalonyl-CoA elongation unit. When methylmalonyl-CoA is used as the penultimate building block followed by malonyl-CoA, the synthesis results in the formation of γ-methyl branched FAs that upon *O*-methylation yield the respective FAMEs. Only one such compound has previously been found in nature represented by methyl 4-methyloctanoate, and this is a constituent of the pheromone blend of the date palm fruit stalk borer *Oryctes elegans* [22], whereas the related FAMEs **89**–**94** emitted by *M. aurantiaca* are all new natural products. The use of alternative starter units from branched amino acids for the biosynthesis of FAMEs was demonstrated in feeding experiments. Although the respective FAs are widespread in nature, only a few reports of these FAMEs exist, e.g., the isoleucine-derived compounds **95** and **96** occur in the volatile fraction from *Medicago sativa* [23], the valine-derived FAME **99** is known from *Capsicum annuum* [24], and the leucine-derived compound **8** was previously found in *Stigmatella aurantiaca* [13], whereas the compounds **102** and **103** (from leucine), and **98** (from valine) have not been

described before. The same is true for all FAMEs described here that are derived from a branched amino acid and that are in addition α- or γ-methyl-branched, and there is only one report on such unusual FAs with a similar methyl branching pattern from *Bacillus* [25]. The biosynthesis of these compounds was established in feeding experiments with [$^2H_5$]sodium propionate and [*methyl*-$^2H_3$]methionine, which allowed us to distinguish between two possible pathways, i.e., the incorporation of methylmalonyl-CoA elongation units, or the alternative incorporation of malonyl-CoA elongations units followed by methylation with SAM. The experiments clearly demonstrated the usage of methylmalonyl-CoA building blocks, whereas the feeding experiment with [*methyl*-$^2H_3$]methionine gave proof for the origin of the methyl ester functions by SAM-dependent methylation of the respective FAs.

Supporting Information

Supporting Information contains experimental details for the syntheses and analytical data of all synthesized compounds, the tabulated full results of the headspace analyses, and mass spectra of labelled FAMEs obtained during feeding experiments together with the mass spectra of the unlabelled compounds for comparison.

Supporting Information File 1

Experimental details and analytical data.
[http://www.beilstein-journals.org/bjoc/content/supplementary/1860-5397-7-200-S1.pdf]

Acknowledgements

This work was supported by the Deutsche Forschungsgemeinschaft with an Emmy Noether fellowship (to J. S. D., DI1536/1-1).

References

1. Kaneda, T. *Microbiol. Rev.* **1991,** *55,* 288–302.
2. Wang, J.-F.; Dai, H.-Q.; Wei, Y.-L.; Zhu, H.-J.; Yan, Y.-M.; Wang, Y.-H.; Long, C.-L.; Zhong, H.-M.; Zhang, L.-X.; Cheng, Y.-X. *Chem. Biodiversity* **2010,** *7,* 2046–2053. doi:10.1002/cbdv.201000072
3. Hamilton, J. T. G.; Harper, D. B. *Phytochemistry* **1997,** *44,* 1129–1132. doi:10.1016/S0031-9422(96)00697-8
4. Cropp, T. A.; Wilson, D. J.; Reynolds, K. A. *Nat. Biotechnol.* **2000,** *18,* 980–983. doi:10.1038/79479
5. Hutchinson, C. R.; Sherman, M. M.; McInnes, A. G.; Walter, J. A.; Vederas, J. C. *J. Am. Chem. Soc.* **1981,** *103,* 5956–5959. doi:10.1021/ja00409a076
6. Liu, Y.; Hazzard, C.; Eustaquio, A. S.; Reynolds, K. A.; Moore, B. S. *J. Am. Chem. Soc.* **2009,** *131,* 10376–10377. doi:10.1021/ja9042824
7. Xu, Z.; Ding, L.; Hertweck, C. *Angew. Chem., Int. Ed.* **2011,** *50,* 4667–4670. doi:10.1002/anie.201008265
8. Carroll, B. J.; Moss, S. J.; Bai, L.; Kato, Y.; Tölzer, S.; Yu, T.-W.; Floss, H. G. *J. Am. Chem. Soc.* **2002,** *124,* 4176–4177. doi:10.1021/ja0124764
9. Smith, A.; Calder, A. G. *Biomed. Mass Spectrom.* **1979,** *6,* 347–349. doi:10.1002/bms.1200060808
10. Schulz, S.; Dickschat, J. S. *Nat. Prod. Rep.* **2007,** *24,* 814–842. doi:10.1039/b507392h
11. Schöller, C. E. G.; Gürtler, H.; Pedersen, R.; Molin, S.; Wilkins, K. *J. Agric. Food Chem.* **2002,** *50,* 2615–2621. doi:10.1021/jf0116754
12. Wilkins, K.; Schöller, C. *Actinomycetologica* **2009,** *23,* 27–33. doi:10.3209/saj.SAJ230202
13. Dickschat, J. S.; Bode, H. B.; Wenzel, S. C.; Müller, R.; Schulz, S. *ChemBioChem* **2005,** *6,* 2023–2033. doi:10.1002/cbic.200500174
14. Nawrath, T.; Gerth, K.; Müller, R.; Schulz, S. *Chem. Biodiversity* **2010,** *7,* 2228–2253. doi:10.1002/cbdv.201000190
15. Weinstein, M. J.; Luedemann, G. M.; Oden, E. M.; Wagman, G. H.; Rosselet, J. P.; Marquez, J. A.; Coniglio, C. T.; Charney, W.; Herzog, H. L.; Black, J. *J. Med. Chem.* **1963,** *6,* 463–464. doi:10.1021/jm00340a034
16. He, H.; Ding, W. D.; Bernan, V. S.; Richardson, A. D.; Ireland, C. M.; Greenstein, M.; Ellestad, G. A.; Carter, G. T. *J. Am. Chem. Soc.* **2001,** *123,* 5362–5363. doi:10.1021/ja010129o
17. Dickschat, J. S.; Wenzel, S. C.; Bode, H. B.; Müller, R.; Schulz, S. *ChemBioChem* **2004,** *5,* 778–787. doi:10.1002/cbic.200300813
18. Dickschat, J. S.; Zell, C.; Brock, N. L. *ChemBioChem* **2010,** *11,* 417–425. doi:10.1002/cbic.200900668
19. Dickschat, J. S.; Wickel, S.; Bolten, C. J.; Nawrath, T.; Schulz, S.; Wittmann, C. *Eur. J. Org. Chem.* **2010,** 2687–2695. doi:10.1002/ejoc.201000155
20. Schulz, S.; Toft, S. *Tetrahedron* **1993,** *49,* 6805–6820. doi:10.1016/S0040-4020(01)80424-5
21. Dickschat, J. S.; Citron, C. A.; Brock, N. L.; Riclea, R.; Kuhz, H. *Eur. J. Org. Chem.* **2011,** 3339–3346. doi:10.1002/ejoc.201100188
22. Rochat, D.; Mohammadpoor, K.; Malosse, C.; Avand-Faghih, A.; Lettere, M.; Beauhaire, J.; Morin, J.-P.; Pezier, A.; Renou, M.; Abdollahi, G. A. *J. Chem. Ecol.* **2004,** *30,* 387–407. doi:10.1023/B:JOEC.0000017984.26917.52
23. Core, R. J.; Henning, J. A.; Gardea-Torresdey, J. *J. Agric. Food Chem.* **1994,** *42,* 2932–2936. doi:10.1021/jf00048a054
24. Guadayol, J. M.; Caixach, J.; Ribé, J.; Cabañas, J.; Rivera, J. *J. Agric. Food Chem.* **1997,** *45,* 1868–1872. doi:10.1021/jf960266i
25. Carballeira, N. M.; Miranda, C.; Lozano, C. M.; Nechev, J. T.; Ivanova, A.; Ilieva, M.; Tzvetkova, I.; Stefanov, K. *J. Nat. Prod.* **2001,** *64,* 256–259. doi:10.1021/np000494d

Beilstein Journal of Organic Chemistry

Conserved and species-specific oxylipin pathways in the wound-activated chemical defense of the noninvasive red alga *Gracilaria chilensis* and the invasive *Gracilaria vermiculophylla*

Martin Rempt[1], Florian Weinberger[2], Katharina Grosser[1] and Georg Pohnert[*1]

Full Research Paper

Open Access

Address:
[1]Institute for Inorganic and Analytical Chemistry, Lessingstr. 8, Friedrich-Schiller-University, D-07743 Jena, Germany, Tel: +493641948171; Fax +493641948172 and [2]Leibniz-Institut für Meereswissenschaften, IFM-GEOMAR, Düsternbrooker Weg 20, D-24105 Kiel, Germany

Email:
Georg Pohnert[*] - Georg.Pohnert@uni-jena.de

* Corresponding author

Keywords:
activated chemical defense; invasive species; oxylipins; prostaglandins; red algae; regulation

Beilstein J. Org. Chem. **2012,** *8,* 283–289.
doi:10.3762/bjoc.8.30

Received: 25 November 2011
Accepted: 03 February 2012
Published: 21 February 2012

This article is part of the Thematic Series "Biosynthesis and function of secondary metabolites".

Guest Editor: J. S. Dickschat

Abstract

Chemical defense of the invasive red alga *Gracilaria vermiculophylla* has been studied and compared to that of the noninvasive but related *Gracilaria chilensis*. Both species rely on a wound-activated chemical defense that makes them less attractive to the herbivorous sea snail *Echinolittorina peruviana*. The chemical stress response of both species was monitored by LC–ESIMS-based metabolic profiling and revealed commonalities and differences. Both algae rely on a rapid lipoxygenase mediated transformation of arachidonic acid to known and novel oxylipins. Common products are 7,8-dihydroxyeicosatetraenoic acid and a novel eicosanoid with an unusual γ-lactone moiety. Several prostaglandins were predominantly formed by the invasive species. The role of some of these metabolites was investigated by surveying the attachment of *E. peruviana* on artificial food containing the respective oxylipins. Both algae species are defended against this general herbivore by 7,8-dihydroxyeicosatetraenoic acid, whereas the prostaglandins and the novel oxylipins were inactive at naturally occurring concentrations. The role of different oxylipins in the invasive potential of *Gracilaria spp.* is discussed.

Introduction

The red alga *Gracilaria chilensis* is native along the Chilean coast and is commercially farmed for the production of agar hydrocolloids [1]. Since the alga can be easily planted and harvested, this crop is exploited by the local population widely along the Chilean coast. However, no uncontrolled invasion has been reported to date. In contrast, the related *Gracilaria*

vermiculophylla, which is native to the Northwest Pacific, is an invasive species in the north Atlantic and represents a potential threat to the native flora and fauna [2]. The species is spreading in habitats that are dominated by generalist herbivores and suffers only minor losses due to grazing. It has been hypothesized that introduced species are most likely to be successful in the presence of generalist herbivores if they are well defended. Here we address the chemical defenses of the two related algae, which are both particularly rich in oxylipins that are predominantly produced after physical wounding [3,4]. For *G. chilensis*, the role of specific oxylipins in the chemical defense against epiphytism has been demonstrated. This alga has two major lines of defense, including a rapid wound-activated production of oxylipins and a slower induced defense involving the up regulation of phospholipases and lipoxygenases and subsequent fatty-acid transformation [3,5]. Among the up-regulated metabolites, arachidonic acid derived hydroxylated and dihydroxylated fatty acids are most prominent, with 7,8-dihydroxyeicosatetraenoic acid (7,8-di-HETE (**3**)) being the most active metabolite in the chemical defense against epiphytism. Recent work indicates that the invasive *G. vermiculophylla* also relies on wound-activated transformations of arachidonic acid for its chemical defense. Bioassays with the generalist isopod grazer *Idotea baltica,* which is found in the areas in which *G. vermiculophylla* is invasive, revealed that among all the detected oxylipins a minor prostaglandin is responsible for the chemical defense [6]. Both *Gracilaria* form common (hydroxylated and dihydroxylated fatty acids **3** and **4**) and unique (prostaglandins **1** and **2** in *G. vermiculophylla*) arachidonic acid derived oxylipins. Using a novel chemometric evaluation of metabolic profiles, we followed arachidonic acid metabolism in both species and identified known and novel oxylipins [6]. We asked ourselves whether the species-specific oxylipin profiles may explain a different chemical defense and may thus be a prospective cause for the invasive potential of *G. vermiculophylla*. We selected the sea snail *Echinolittorina peruviana* as a model herbivore to monitor the role of the oxylipins in the chemical defence of the algae. This snail is highly abundant on Chilean and Peruvian coasts where *G. chilensis* is native and can reach population densities of up to 2000 individuals/m^2 [7]. *E. peruviana* is known to graze on biofilms as well as on macroalgae and can thus be employed in the monitoring of ecologically relevant interactions.

Results and Discussion

As reported previously, wounding of *G. chilensis* triggers the pronounced formation of arachidonic acid derived oxylipins, including the most dominant 7,8-di-HETE (**3**) and 8-hydroxyeicosatetraenoic acid (8-HETE (**4**)) [3]. This was verified by comparative LC–ESIMS and LC–ESIMS/MS analysis of algae that were wounded by grinding in a mortar, incubated at room temperature for five minutes, and extracted (wounded), versus algae that were boiled before grinding and extraction (Figure 1). Boiling prevents enzymatic reactions during work-up and results in the extraction of metabolites found in the intact algae (hereafter termed "intact"). Only trace levels of prostaglandins were detected in the wounded algae. The boiling of samples leads to a suppression of enzyme activity that would occur during wounding and thus allows profiling of the secondary metabolites in the intact cells. Independent experiments showed that the oxylipins in question are stable and survive the brief boiling without detectable degradation. Previously we were able to verify that the feeding activity of herbivores triggers metabolic responses similar to the introduced wounding procedure in *G. vermiculophylla*, thereby justifying this treatment as appropriate for the monitoring of wound-activated defences [6].

By using a precursor-directed search for novel arachidonic acid derived oxylipins [6], we detected an additional signal of an arachidonic acid derived metabolite with a characteristic UV spectrum of a conjugated tetraene. Purification yielded about 2.3 mg of an unstable metabolite, which was submitted to MS, 1D and 2D-NMR analysis. The molecular formula $C_{20}H_{28}O_2$ was determined by HRMS–ESI ($[M + Na]^+$ calcd for 323.1986; found, 323.1982). ^1H–^1H COSY allowed us to follow the entire spin system of the metabolite, including 10 olefinic protons, 7 CH_2, 1 CH_3 and 1 CH groups (Scheme 1, spectra are shown in Supporting Information File 1).

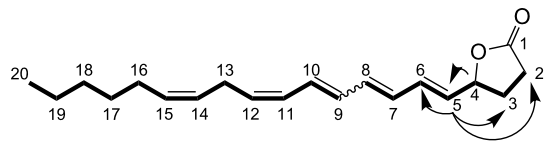

Scheme 1: 5-((1*E*,3,5*E*,7*Z*,10*Z*)-hexadeca-1,3,5,7,10-pentaenyl)dihydrofuran-2(3*H*)-one (**5**) with ^1H–^1H COSY (bold bonds) and relevant HMBC (arrows) correlations.

In combination with HMBC data all hydrogen and carbon signals were assigned, but the stereochemistry of the double bond C7/C8 remained open. The signal at 5.0 ppm in the proton range (proton at C4) and the resonance at 80.45 ppm (^{13}C, HMBC, C4) as well as HMBC and ^1H–^1H COSY signals led to the assignment of a γ-lactone ring (Scheme 1). HMBC correlations from the carbon C4 to H2, H3, H5 and H6 clarified the location of the lactone. Two protons on an isolated *Z*-configured double bond were observed at 5.44–5.31 ppm. The stereochemistry of the remaining conjugated tetraene system was assigned by analysis of the coupling constants according to [8]. The hydrogen at position-5 couples to H6 with a coupling constant of 15.6 Hz, which is indicative of an *E*-double bond.

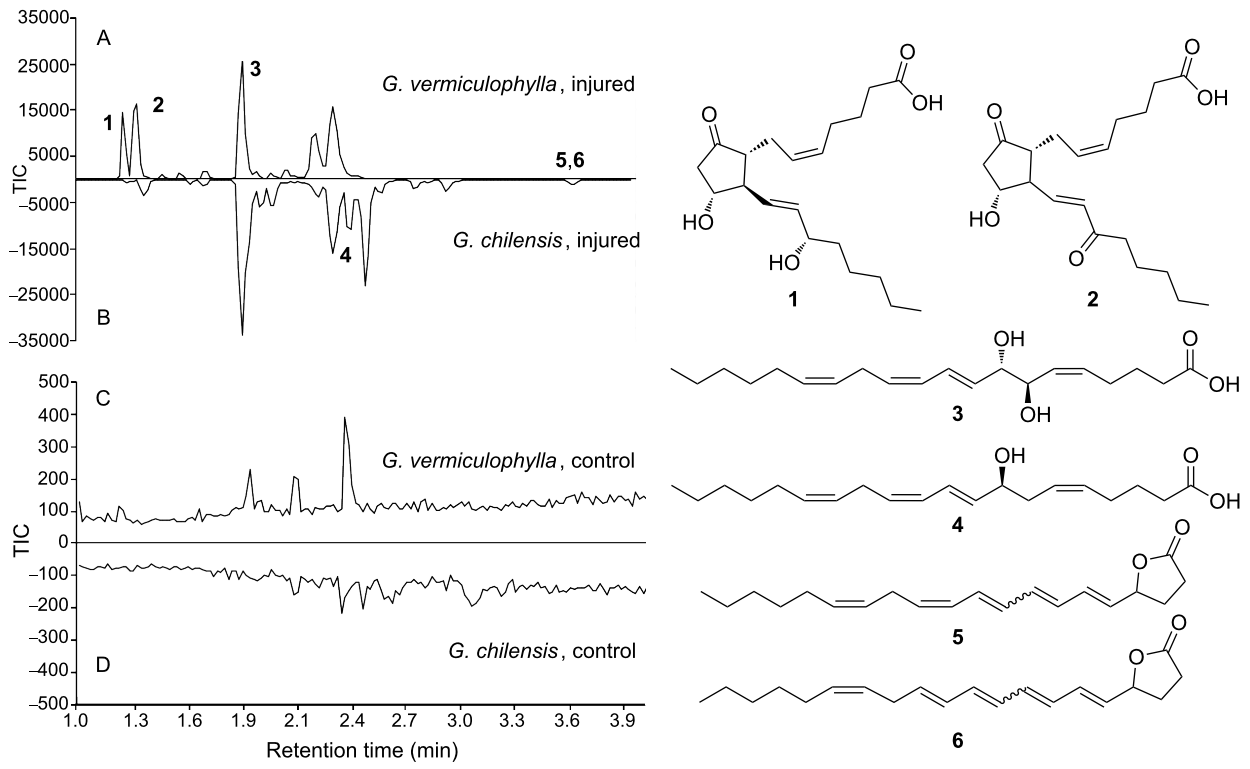

Figure 1: UPLC–ESIMS-based metabolic profiles of *Gracilaria vermiculophylla* (A) and *Gracilaria chilensis* (B) induced by grinding and incubation for 5 min at rt. In comparison, control runs with intact algal material that was boiled to prevent enzyme activity before extraction are given in (C) and (D). Total-ion-count (TIC) traces (ESI-negative mode) are shown; note: TIC normalized to 35000 counts in the wounded and to 500 counts in the chromatographic profiles of the control. The structures of the major metabolites are given, and the retention times of **5** and **6** are indicated; these metabolites do not show up in the ESI negative mode.

The H9 to H10 coupling constant of 14.6 Hz indicates an *E*-configuration as well, while the H11 to H12 coupling of 11.45 Hz indicated a *Z*-configuration. The double-bond configuration between H7 and H8 could not be resolved due to the substantial overlap of the signals. An isomer of **5** bearing also a conjugated tetraene unit was isolated and tentatively assigned to a stereoisomer with an *E*-configured double bond between C11 and C12 and open stereochemistry of the C7/C8 bond. Despite the stereocenter at C4, **5** and **6** were optically inactive and exhibited no signal in circular dichroism measurements. Both isomers **5** and **6** were already detected in the crude extracts, but also after work-up and during storage in $CDCl_3$ further isomerization was observed. The biosynthetic origin of **5** and **6** from arachidonic acid was proven by applying the stable isotope-labeled precursor [$^2H_2$]-arachidonic acid [6] to the frozen powder before incubation and extraction. Analysis of the resulting mass spectra showed incorporation rates of 56% and confirmed an efficient transformation to **5** and **6**. The racemic nature of **5** and **6** indicates the involvement of a nonenzymatic step during their formation. A possible biosynthetic pathway to **5** and **6** (Scheme 2) could involve an oxidation at C4. This oxidation could proceed in a similar way to that required for the introduction of the 7-OH group in 7,8-di-HETE (**3**). A lipoxygenase-mediated transformation of arachidonic acid to an 8-hydroperoxide, followed by reduction and elimination of

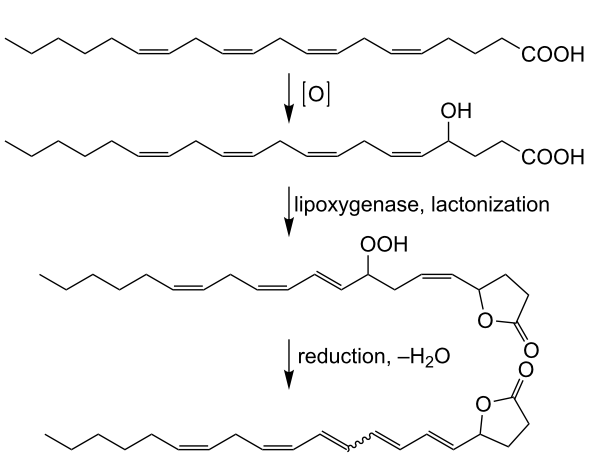

Scheme 2: Suggested pathway for the biosynthesis of **5**.

water along with isomerization of the double bonds, could then provide the substrate for lactonization. Since **5** and **6** were configurationally unstable during purification, subsequent isomerizations may lead to the observed products. Other mechanisms, involving the formation of an extended conjugated double-bond system and the attack of the carboxylic acid on an intermediate double bond at C4 can, however, not be excluded.

Wounding of *G. vermiculophylla* also led to pronounced changes in the metabolic profile (Figure 1, [6]). As in *G. chilensis* the major up-regulated metabolite was 7,8-di-HETE (**3**), which was detected in very similar concentrations in both species. 8-HETE (**4**) was only present in trace amounts. In contrast to *G. chilensis*, the wound-activated production of the prostaglandins **1** and **2** is a lot more pronounced. It can be estimated that these metabolites can account for more than 50% of the total oxylipins, if integrals of the corresponding signals from the oxylipins are evaluated while neglecting possibly differences in the response factors in ESIMS. The novel lactones **5** and **6** were also detected in this species.

Quantification of the oxylipins bears some uncertainty, since the absolute and relative amounts detected after wounding vary strongly. This can be attributed to a certain phenotypic plasticity, but since multiple samples from the same individual also exhibited fluctuations, it is more likely that the wounding procedure triggers a highly uncontrolled action of lipases, lipoxygenases, oxidases [3], and cyclooxygenases [9], which results in the observed varying amounts of oxylipins. In all experiments the quantities of prostaglandins were high in *G. vermiculophylla*, while only traces were detected in *G. chilensis* (Figure 1). To determine the amount of potential defense metabolites to be used in bioassays, the mean concentrations of the metabolites were determined in triplicates from batches that were also used for bioassays. The mean values of the determined amounts of prostaglandins from *G. vermiculophylla* were used for the bioassays. Since the amounts of 7,8-di-HETE (**3**), **5**, and **6** were similar in *G. vermiculophylla* and *G. chilensis*, the mean concentrations of these metabolites in both species were employed. We thus tested 15-keto-PGE_2 **2** as a 2 µg/g treatment in agar, PGE_2 **1** (2.6 µg/g agar), 7,8-di-HETE **3** (1.7 µg/g agar), and a 1/1 mixture of **5** and **6** (total 8.2 µg/g agar).

To evaluate the response of the sea snail *E. peruviana* towards the algal compounds, we developed a new bioassay based on the avoidance reaction of the snail. When the snails were put on a Petri dish that was partially filled with agar prepared with seawater, the snails attached to this layer of jellified seawater. When the plate was turned upside down after seven minutes, the snails stayed attached to the surface (control). In contrast, when the agar contained extracts or active chemicals, the snails retracted and fell down directly after the Petri dish was turned. After counting the attached and fallen individuals, we could determine the risk of attachment from the odds ratio {(snails on extract, attached)/(snails on extract, unattached)}/{(snails on solvent control, attached)/(snails on solvent control, unattached)}, as described in [10]. A risk of 1 would indicate that the same amount of snails remained on the agar in the treatment compared to the solvent control; values smaller than 1 indicate that snails avoided the surface with the treatment, which in nature would also result in cessation of feeding. When the agar was treated with methanolic extracts of intact *G. chilensis* and *G. vermiculophylla* no reduced attachment was observed. In contrast, when extracts from wounded algae of both species were incorporated, a significantly reduced proportion of snails remained attached to the agar compared to the control (Figure 2). In these experiments we selected the concentration of the embedded algal extract to be equivalent to that in the fresh (wet weight) algae. The intensity of this response was clearly dose-dependent. For example, the extract of wounded *G. chilensis* caused reduced snail retraction at a 0.1-fold dilution, and only an insignificant reduction was observed when the extract was applied in a 0.01-fold natural concentration (data not shown). Both species seem thus to be defended against the generalist herbivore, exploiting a strategy based on the formation of active metabolites after wounding.

To identify the compounds responsible for the observed activated defense, we undertook a large-scale (2 kg) extraction of

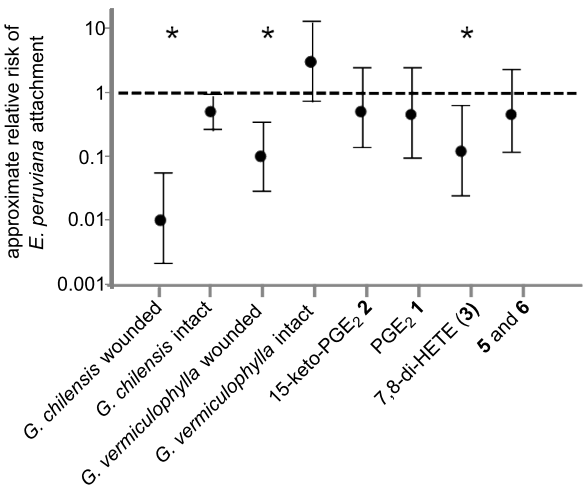

Figure 2: Relative risk (mean ± 95% confidence interval) of *Echinolittorina peruviana* attachment on surfaces treated with *Gracilaria chilensis* and *Gracilaria vermiculophylla* extracts obtained before and after wounding. In addition, the relative risk of attachment to pure compounds in natural concentrations is given. Asterisks indicate significant effects when examined with the χ^2-test, as described in Fisher and van Belle [10].

G. vermiculophylla and purified the up-regulated metabolites using silica chromatography and preparative reversed-phase HPLC. The purified compounds (**1**, **2**, **3** and a ca. 1:1 mixture of **5** and **6**) were incorporated into agar matrices in natural concentrations and the response of the snails was tested by using the attachment bioassay, as described above. Of the tested metabolites only 7,8-di-HETE (**3**) was active when applied at concentrations corresponding to those detected in wounded *G. vermiculophylla*. The isolated prostaglandins and the new lactones (**5** and **6**) did not exhibit any activity at natural concentrations (Figure 1) or 10-fold higher amounts (data not shown). Interestingly, 7,8-di-HETE (**3**), a compound that also proved to be the most-active metabolite in the chemical defense of *G. chilensis* against epiphytes [3], can explain the entire activity of the *G. vermiculophylla* and *G. chilensis* crude extracts against *E. peruviana*. This metabolite thus protects the invasive and the native species from herbivory by the snails. Apparently the higher diversity of oxylipins from *G. vermiculophylla* cannot explain its success as an invasive species if only grazing by the generalist *E. peruviana* is concerned. Nevertheless, prostaglandins play important roles in the chemical defense against the generalist herbivorous isopod *Idotea baltica* [6]. While *E. peruviana* is a herbivore that co-occurs with *G. chilensis*, *I. baltica* is a generalist that is often encountered in regions in which *G. vermiculophylla* spreads in an invasive manner. Thus our observation would explain that the algae are defended against herbivores that are co-occurring, by a conserved defense mechanism (this study), while the invasive potential of *G. vermiculophylla* can be explained by prostaglandins that are only detected in this species [6].

Conclusion

The chemical defense of *Gracilaria spp*. against *E. peruviana* is stimulated by tissue disruption and proceeds via the release of arachidonic acid derived oxylipins. We demonstrate that the structurally diverse oxylipins detected in *Gracilaria spp*. play individual roles in the chemical defense against different herbivores. The dihydroxylated fatty acid 7,8-di-HETE is generally active against co-evolved herbivores, while prostaglandins support an invasive success of the algae.

Experimental

General. NMR spectra were recorded on Bruker Avance 400 MHz or 600 MHz spectrometers, and chemical shifts are given in ppm relative to the chemical shift of the solvent signal of $CDCl_3$. HRMS were recorded on a MAT 95 XL (Thermo Finnigan, Bremen, Germany) equipped with an ESI probe. LC–MS measurements were performed on an UPLC–MS system equipped with a 2996 PDA detector and a Q-tof micro ESIMS (Waters, Manchester, UK). For separation of the analytes, a BEH C18 column (2.1 × 50 mm, particle size 1.7 µm) was used. LC on a semipreparative column was carried out by using a LC-8A liquid chromatography system from Shimadzu (Duisburg, Germany) equipped with a SPD-10AV UV–vis detector. A Licro Chart® 250-10 Purosphere® RP-18 endcapped column (particle size 5µm) supplied by Merck (Darmstadt, Germany) was used for separation. HPLC separation on an analytical scale was performed on the same LC system equipped with a Synergi MAX-RP 250 × 4.6 mm column (particle size 4 µm) from Phenomenex (Macclesfield, UK). Optical rotations were measured on a Jasco (Groß-Umstadt, Germany) 1030 polarimeter at 589 nm. Circular-dichroism spectra were recorded on a Jasco P810 instrument. Analytical thin-layer chromatography was carried out by using silica gel 60 F_{254} plates. Compounds were detected by ceric ammonium molybdate (CAM) staining. Solvents and reagents were purchased from Sigma Aldrich (Deisenhofen, Germany).

Biological material. Laboratory strains of *Gracilaria vermiculophylla* (originating from El Jedidah, Morocco, available from the culture collection of algae and protozoa, Oban, Scotland) and *Gracilaria chilensis* (strain CR14, originating from Caldera, Chile) were cultivated as described in Weinberger et al. [5]. The strains were used in order to generate extracts for the quantification of oxylipins, UPLC profiling, and bioassays. For large-scale purification *G. vermiculophylla* was collected at Norderhafen, Germany. The snail *Echinolittorina peruviana* was collected at Las Cruces, Chile, transferred to the lab and maintained in seawater at 10 °C on a diet of *Ulva sp*.

Extraction and bioassays. Herbivory was mechanically simulated by grinding of algae (10 g) in a mortar and subsequent incubation for 5 min at rt before extraction with MeOH (2 mL). After filtration through cellulose, the extracts were mixed in a glass Petri dish with hot (60 °C) seawater (10 mL) containing 1.5% agar (Sigma Aldrich, Deisenhofen, Germany) and immediately cooled to 10 °C, resulting in a layer of jellified seawater agar that contained the extract at natural concentrations, assuming a 100% extraction success; in reality these concentrations will be slightly below the natural concentrations. For the investigation of intact algae, algae (10 g) were boiled for 1 min in seawater to denature the enzymes. The algae were subsequently shock frozen in liquid nitrogen and treated as described above. Independent treatments showed that the oxylipins, besides **5** and **6**, are stable under these conditions (data not shown). Solvent controls were prepared in the same way with pure MeOH. To test for deterrence, 20 individuals of *E. peruviana* were placed upon agar containing either algal extracts or solvent only. After 7 min the Petri dishes with agar and snails were turned upside down, and the individuals that remained attached under these conditions were counted. The approximate relative risk of snail attachment to the agar-containing extract

was calculated as described above. To test specific metabolites, pure compounds (15-keto-PGE_2 **2**: 2 µg/g agar; PGE_2 **1**: 2.6 µg/g algae; 7,8-di-HETE (**3**): 1.7 µg/g algae; **5** and **6** as 1/1 mixture: 8.2 µg/g agar) were dissolved in acetonitrile and incorporated into the agar as described above for the extracts. Solvent controls were run with corresponding concentrations of acetonitrile.

Metabolic profiling. Methanolic extracts for metabolic profiling were prepared as described above and investigated with UPLC–MS. UPLC solvent A (water-acidified with 0.1% formic acid (v/v) and 1% acetonitrile (v/v)); solvent B (acetonitrile). Gradient: 0 min at 0% B; 0.5 min 50% B; 5 min 100% B; 5.5 min 100% B; 6 min 0% B. Total ion counts are shown in Figure 1.

Large-scale extraction. About 2 kg of *G. vermiculophylla* (wet weight) with minor impurities were harvested at Nordhafen, Germany. The biomass was frozen in liquid nitrogen and crushed in the cold state to a fine powder by using a household blender. The biomass was allowed to come to rt before 5 L of ethylacetate were added. Extraction was performed for 10 h under permanent shaking in brown glass bottles at 10 °C. Subsequently, the solvent was filtered and a second 5 h extraction with 5 L of ethylacetate was carried out. The pooled organic extracts were dried over Na_2SO_4 and the solvent was removed under reduced pressure. The residue was then immediately prepurified by flash column chromatography on silica gel (solvent system: chloroform/isopropanol/acetone 80:20:15 (v/v/v)). The oxylipin-rich fraction (verified by UPLC–MS) was then evaporated and portions of the residue (300 mg) were separated by semipreparative HPLC (solvent A: water acidified with 0.1% formic acid (v/v) and solvent B: methanol. Gradient: 0 min at 25% B; 18 min 60% B; 22 min to 80% B; 24 min to 100% B; 29 min at 100% B; 32 min 25% B). Further purification of metabolites **5** and **6** was performed by analytical HPLC (solvent A: water acidified with 0.1% formic acid (v/v) and 1% acetonitrile (v/v); solvent B: acetonitrile. Gradient: 0 min at 65% B; 11 min 100% B; 14 min at 100% B; 14.1 min to 65% B; 17 min 65% B).

Incorporation of labeled arachidonic acid. 2-[$^2H_2$]-arachidonic acid [6] (2 mg) was suspended in water (15 µL) in a 1.5 mL Eppendorf cap by using a laboratory vortexer. Frozen, powdered algae (5 mg; see above) were added. The mixture was vortexed and allowed to warm to rt. The mixture was maintained at rt for 5 min and subsequently MeOH/water (300 µL; 2:1 v/v) was added. After vortexing and centrifugation, the supernatant was directly used for UPLC–MS analysis. As a control, the same procedure was followed in the absence of the labeled fatty acid.

Quantitative analysis. The extracted or commercially available compounds were used to create three calibration standards for each analyte, covering the concentration range detected in the extract from wounded algae. A calibration curve was recorded on the LC–MS system by repeated (3 ×) injection of each standard. Analyte peaks were displayed by their pseudomolecular-ion trace, and the peak areas were used for quantification.

Structure elucidation of known metabolites. The identification of compounds **1**–**4** was achieved by comparison of the obtained NMR and MS spectra by co-injection with authentic standards [3]. Stereochemistry of PGE_2 was verified with CD spectroscopy in comparison with an authentic standard.

Spectroscopic data of 5. 5-((1*E*,3*E*,5*E*,7*Z*,10*Z*)-hexadeca-1,3,5,7,10-pentaenyl)dihydrofuran-2(3*H*)-one (**5**) was obtained as light-yellow oil. The molecular formula $C_{20}H_{28}O_2$ was determined by HRMS–ESI, $[M + Na]^+$ calcd for 323.1986; found, 323.1982. The UV–vis absorption maxima at 293 nm, 306 nm and 321 nm can be explained by a conjugated tetraene-structure. ^1H NMR (600 MHz, $CDCl_3$) δ (the numbering of atoms refers to Scheme 1) 0.89 (t, *J* = 6.8 Hz, 3H, H20), 1.40–1.24 (m, 6H, H17, H18, H19), 2.10–1.97 (m, 3H, H3, H16), 2.45–2.33 (m, 1H, H3), 2.60–2.51 (m, 2H, H2), 2.95 (dd, *J* = 6.9, 7.1 Hz, 2H, H13), 5.00 (dt, *J* = 7.1, 15.0 Hz, 1H, H4), 5.37 (dtd, *J* = 12.4, 6.9, 1.8 Hz, 1H, H14), 5.46 (dtd, *J* = 12.6, 7.3, 1.4 Hz, 1H, H15), 5.46 (dt, *J* = 7.8, 10.5 Hz, 1H, H12), 5.68 (dd, *J* = 6.62, 15.64 Hz, 1H, H5), 6.08–6.03 (dd, *J* = 11.1, 14.7 Hz, 1H, H11), 6.26–6.16 (m, 2H, H7, H9), 6.36–6.33 (m, 2H, H6, H8), 6.57 (m, 1H, H10); ^{13}C NMR (150 MHz, $CDCl_3$) δ 176.75 (C1), 135.25 (C6), 133.21 (C8), 132.24 (C9), 131.84 (C12), 131.01 (C7), 130.73 (C15), 129.60 (C10), 129.41 (C5), 128.50 (C11), 126.87 (C14), 80.45 (C4), 31.51 (C18), 29.27 (C19), 28.87 (C3), 28.54 (C2), 27.25 (C16), 26.31 (C13), 22.55 (C17), 14.04 (C20).

Supporting Information

Supporting Information File 1

Spectra for metabolites **5** and **6**.
[http://www.beilstein-journals.org/bjoc/content/supplementary/1860-5397-8-30-S1.pdf]

Acknowledgements

We thank the German Research Foundation (PO 628/6-1) for funding. Financial support by the Volkswagen Foundation in the framework of a Lichtenberg Professorship is acknowledged. Dr. Stefan Bartram is acknowledged for assisting with measurements of CD spectra.

References

1. Buschmann, A. H.; Correa, J. A.; Westermeier, R.; Hernández-González, M. d. C.; Norambuena, R. *Aquaculture* **2001,** *194,* 203–220. doi:10.1016/S0044-8486(00)00518-4
2. Nyberg, C. D.; Thomsen, M. S.; Wallentinus, I. *Eur. J. Phycol.* **2009,** *44,* 395–403. doi:10.1080/09670260802592808
3. Lion, U.; Wiesemeier, T.; Weinberger, F.; Beltrán, J.; Flores, V.; Faugeron, S.; Correa, J.; Pohnert, G. *ChemBioChem* **2006,** *7,* 457–462. doi:10.1002/cbic.200500365
4. Sajiki, J.; Kakimi, H. *J. Chromatogr., A* **1998,** *795,* 227–237. doi:10.1016/S0021-9673(97)00943-6
5. Weinberger, F.; Lion, U.; Delage, L.; Kloareg, B.; Potin, P.; Beltrán, J.; Flores, V.; Faugeron, S.; Correa, J.; Pohnert, G. *J. Chem. Ecol.* **2011,** *37,* 677–686. doi:10.1007/s10886-011-9981-9
6. Rempt, M.; Pohnert, G. *Angew. Chem., Int. Ed.* **2010,** *49,* 4755–4758. doi:10.1002/anie.201000825
7. Hidalgo, F. J.; Firstater, F. N.; Fanjul, E.; Bazterrica, M. C.; Lomovasky, B. J.; Tarazona, J.; Iribarne, O. O. *Helgoland Marine Research* **2008,** *62,* S73–S83. doi:10.1007/s10152-007-0086-3
8. Boland, W.; Schroer, N.; Sieler, C.; Feigel, M. *Helv. Chim. Acta* **1987,** *70,* 1025–1040. doi:10.1002/hlca.19870700415
9. Kanamoto, H.; Takemura, M.; Ohyama, K. *Appl. Microbiol. Biotechnol.* **2011,** *91,* 1121–1129. doi:10.1007/s00253-011-3349-5
10. van Belle, G.; Fisher, L. D.; Heagerty, P. J.; Lumley, T. *Biostatistics: A Methodology for the Health Sciences,* 2nd ed.; John Wiley & Sons: Hoboken, USA, 2004.

License and Terms

Beilstein Journal of Organic Chemistry

The volatiles of pathogenic and nonpathogenic mycobacteria and related bacteria

Thorben Nawrath[1], Georgies F. Mgode[2,3], Bart Weetjens[4], Stefan H. E. Kaufmann[2] and Stefan Schulz[*1]

Full Research Paper

Open Access

Address:
[1]Institut für Organische Chemie, Technische Universität Braunschweig, Hagenring 30, 38106 Braunschweig, Germany, [2]Department of Immunology, Max Planck Institute for Infection Biology, Charitéplatz 1, 10117 Berlin, Germany, [3]Pest Management Centre, Sokoine University of Agriculture, PO Box 3110, Chuo Kikuu, Morogoro, Tanzania and [4]Anti-Persoonmijnen Ontmijnende Product Ontwikelling (APOPO vzw), Groenenborgerlaan 171, 2020 Antwerpen, Belgium

Email:
Stefan Schulz[*] - stefan.schulz@tu-bs.de

* Corresponding author

Keywords:
aromatic compounds; CLSA; terpenes; tuberculosis; volatile profile

Beilstein J. Org. Chem. **2012,** *8,* 290–299.
doi:10.3762/bjoc.8.31

Received: 08 December 2011
Accepted: 30 January 2012
Published: 22 February 2012

This article is part of the Thematic Series "Biosynthesis and function of secondary metabolites".

Guest Editor: J. S. Dickschat

Abstract

Volatiles released by pathogenic and nonpathogenic mycobacteria, as well as by mycobacteria-related *Nocardia* spp., were analyzed. Bacteria were cultivated on solid and in liquid media, and headspace samples were collected at various times during the bacterial lifecycle to elucidate the conditions giving optimal volatile emission. Emitted volatiles were collected by using closed-loop stripping analysis (CLSA) and were analyzed by gas-chromatography–mass-spectrometry. A wide range of compounds was produced, although the absolute amount was small. Nevertheless, characteristic bouquets of compounds could be identified. Predominantly aromatic compounds and fatty-acid derivatives were released by pathogenic/nonpathogenic mycobacteria, while the two *Nocardia* spp. (*N. asteroides* and *N. africana*) emitted the sesquiterpene aciphyllene. Pathogenic *Mycobacterium tuberculosis* strains grown on agar plates produced a distinct bouquet with different volatiles, while liquid cultures produce less compounds but sometimes an earlier onset of volatile production because of their steeper growth curves under this conditions. This behavior differentiates *M. tuberculosis* from other mycobacteria, which generally produced fewer compounds in seemingly lower amounts. Knowledge of the production of volatiles by *M. tuberculosis* can facilitate the rational design of alternative and faster diagnostic measures for tuberculosis.

Introduction

Tuberculosis (TB) remains one of the most threatening diseases on earth. In 2008, up to 2 million people died as a result of TB infection [1]. The causative agent, *M. tuberculosis,* has a highly flexible physiology and metabolism that allows it to adapt to changes in the environment during the course of an infection [2]. Other pathogenic mycobacteria cause diseases such as

leprosy, evoked by *M. leprae*, or buruli ulcer, due to infection by *M. ulcerans* [3,4]. In addition, numerous nonpathogenic and facultative pathogenic mycobacteria exist.

Although several diagnostic measures have been developed for TB diagnosis [5,6], most of these techniques are expensive, e.g., immunological tests using antigens, DNA analysis, or specific culturing conditions, especially for developing countries with the highest burden of TB [7-9]. Thus, the analyses of species-specific volatiles obtained from breath samples of potentially infected individuals, or from the bacteria themselves, have recently been proposed for rapid diagnosis of TB [8-11]. The feasibility of these methods is supported by reports that trained *Cricetomys* rats can distinguish between sputum samples from TB-infected and noninfected persons [12,13].

While the first studies based on electronic sensors or fuzzy-logic experiments gave promising results [8,10], recent studies have focused on the characteristic compounds released by pathogenic *M. bovis* and *M. tuberculosis* strains [9,11]. Compounds from these species were also expected to occur in breath samples from TB patients [8,10]. In these studies, volatiles were collected by using solid-phase micro-extraction (SPME). Methyl phenylacetate (**1**), methyl *p*-anisate (**2**), methyl nicotinate (**3**), and *o*-phenylanisole (**4**) were emitted by pathogenic *M. bovis* and *M. tuberculosis* (Figure 1), while nontuberculous mycobacteria did not produce these four compounds [9]. Due to a central role in mycobacterial metabolism [14], nicotinic acid, closely related to (**3**), was used in these studies as a reference compound from the breath of TB-positive patients [11]. Infected individuals also released nicotinic acid (excluding smoking patients in this study), proving the utility of this approach [11].

Nevertheless, a broad analysis of the volatiles produced by *M. tuberculosis*, nontuberculous mycobacteria and mycobacteria-related species has not been performed. This knowledge is of utmost importance in the identification of potential compounds for use in pattern-recognition methods, such as electronic noses and trained *Cricetomys* rats. We report here on the identification of volatiles produced by different strains of *M. tuberculosis*, as well as of *M. smegmatis*, *M. aurum*, *M. neoaurum*, *M. aichiense*, *M. scrofulaceum*, *M. avium* spp. *avium*, *M. vaccae*, *Nocardia africana*, and *N. asteroides*, using closed-loop stripping analysis (CLSA) for the collection of volatile compounds [15,16]. This method allows sampling for longer periods than SPME, and usually results in a lower detection limit. Compounds not detectable by SPME can thus be detected. SPME preferentially favors less volatile compounds [17]. Furthermore, SPME may have a discriminative effect, and our experience has shown that minor components are often not detected when large amounts of a major component are present.

The investigated mycobacteria were in different stages of their lifecycles and grown on various different media. The volatiles released under these conditions were identified and their formation under different conditions is discussed.

Results and Discussion

Volatiles released from different mycobacteria and *Nocardia* spp. grown on solid or in liquid media were collected by using CLSA as described previously [15,16]. The headspace extracts were analyzed by gas-chromatography–mass-spectrometry (GC–MS). Compound identification was performed by comparison of mass spectra and gas-chromatographic retention indices with those of authentic reference compounds and mass-spectra libraries [18].

Analysis of bacteria grown on a solid medium

Different strains of *M. tuberculosis* grown on a 7H11 solid medium were analyzed after different incubation periods (days). The detection of bacteria-specific compounds was assured by the analysis of headspace samples from a sterile medium incubated in parallel with bacterial strains. Although many compounds were released from the medium, bacteria-specific compounds were distinguishable. A typical gas chromatogram is shown in Figure 2, revealing that many compounds are formed from the nutrient medium that is necessary to grow the bacteria. The identified compounds are listed in Table 1.

In addition to previously reported compounds **1**–**4** [9], several new volatiles were identified, predominantly aromatic compounds, such as 4-methylanisole (**5**), methyl salicylate (**6**), methyl 2-aminobenzoate (**7**), and methyl and ethyl benzoate (**8**

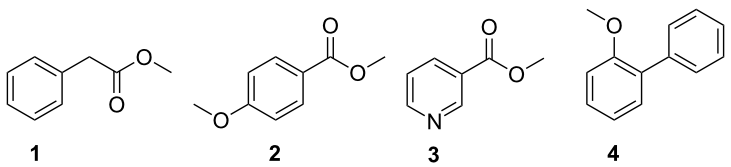

Figure 1: Volatile compounds released by *Mycobacterium tuberculosis* and *M. bovis* identified in previous studies [9].

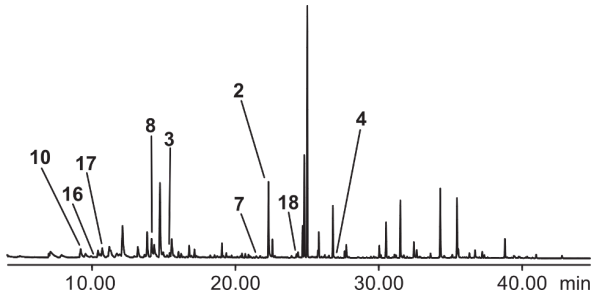

Figure 2: Total ion chromatogram of a headspace extract of a culture of *Mycobacterium tuberculosis* strain 2, grown on a 7H11 solid medium. Nonlabeled peaks originate from the nutrient medium.

and **9**), as well as fatty-acid derivatives, for example, 4-pentanolide (**10**) (Figure 3). Many of the compounds listed in Table 1 are known volatiles from other bacteria [19].

As shown in Table 1, early cultures produced few compounds; only those older than 18 days produced a bouquet of compounds. This is probably due to the slow growth of many mycobacteria [7,20]. Increased production of volatile compounds occurred in the stationary phase (i.e., starting after three weeks of growth), a phenomenon that corroborates the recent findings that *M. tuberculosis* culture is detected by trained rats mostly at this growth stage [20]. A full description of the growth stages used in this report has recently been published [20]. The analyses of cultures of *M. smegmatis*, *M. aurum*, *M. neoaurum*, *M. aichiense*, *M. scrofulaceum*, *M. avium* ssp. *avium*, and *M. vaccae* revealed that these diverse nontuberculous mycobacteria did not produce as many different compounds as *M. tuberculosis* (Table 2), and what they did produced was often in lower quantities. The exceptions are *M. scrofulaceum* and *M. avium* ssp. *avium*, which cause cervical lymphadenitis in children and avian TB, as well as opportunistic infections in immunocompromised humans [21,22].

Although certain volatile, aromatic compounds, such as **1**, **6**, **8**, and **9**, were produced in some cases, many compounds from extracts of *M. tuberculosis* were absent in the other mycobacteria. The low emission rate of volatile compounds was not a result of the early stage at which the mycobacteria were analyzed, since all strains were fast-growing [20,21,23-28]. Interestingly, some of the bacteria emitted sulfur-containing compounds, such as dimethyl disulfide (**11**), dimethyl trisulfide

Table 1: Volatiles released by *Mycobacterium tuberculosis* grown on a 7H11 solid medium.[a]

Compound	*I*	strain 1	strain 2	strain 5	strain 6	H37Ra
4-Hydroxy-4-methylpentan-2-one (**14**)	847	– – –[b]	– – – + [c]	– + – – – – –[d]	– – –[e]	–[f]
4-Pentanolide (**10**)	950	+ + +	+ + + +	– – + + + + +	+ + +	+
Methyl 2-furoate (**15**)	978	– – –	+ + – +	– – + + – – –	+ + –	+
3-Methyl-4-pentanolide (**16**)[g]	984	– + +	+ + + +	– – – – – – –	– – –	–
Unknown	1006	– – +	+ – + –	– – + + + + +	– – +	–
Unknown	1021	+ + –	+ + – +	– – – – – – –	– – –	–
4-Methylanisol (**5**)	1021	– – +	– – + –	– – + + + + +	– – +	–
Unknown	1084	– + +	+ + + –	– – + + + + +	– + +	–
Methyl benzoate (**8**)	1093	+ + +	+ + + +	+ + + + + + +	+ + +	+
2-Phenylethanol[h]	1113	+ + +	+ + + +	– + + + + + +	+ + +	–
4-Methyl-5-hexanolide (**17**)[g]	1133	– – –	– + + –	– – – – – – –	– – –	–
Methyl nicotinate[c] (**3**)	1136	+ + +	+ + + +	– + + + + + +	+ + +	–
Ethyl benzoate (**9**)	1169	– – –	– – – –	– – – + + + +	– – –	+
Methyl phenylacetate (**1**)	1177	+ + –	– + + +	– – – + + + +	+ + +	–
Methyl salicylate (**6**)	1193	+ – –	– – – –	– – + – – – +	– + –	+
Benzothiazole	1222	– – –	– – – +	– – – + – – –	– – –	–
Methyl 2-aminobenzoate (**7**)	1341	– – –	+ + – –	– – – + – – –	– – –	–
Methyl *p*-anisate (**2**)	1376	+ + +	+ + + +	– + + + + + +	+ + +	–
Ethyl *p*-anisate (**18**)	1450	– + –	+ + – –	– + + + – + +	+ + –	–
2-Phenylanisol (**4**)	1559	+ + +	+ + + +	– + + + + + +	+ + +	–

[a]*I*: gas-chromatographic retention index on DB-5; +: compound detected in sample; –: compound not detected in sample. [b]The results of three analyses are shown for each experiment performed on differently aged cultures: 25 days (d), 26 d, 32 d. [c]The results of four analyses are shown for each experiment performed on differently aged cultures: 20 d, 22 d, 30 d, 33 d. [d]The results of seven analyses are shown for each experiment performed on differently aged cultures: 4 d, 9 d, 18 d, 21 d, 28 d, 29 d, 48 d. [e]The results of three analyses are shown for each experiment performed on differently aged cultures: 19 d, 23 d, 31 d. [f]The results of an analysis on a 14 d old culture are shown. [g]Mixture of both diastereomers; *I* of first eluting isomer is shown. [h]Traces present in the medium.

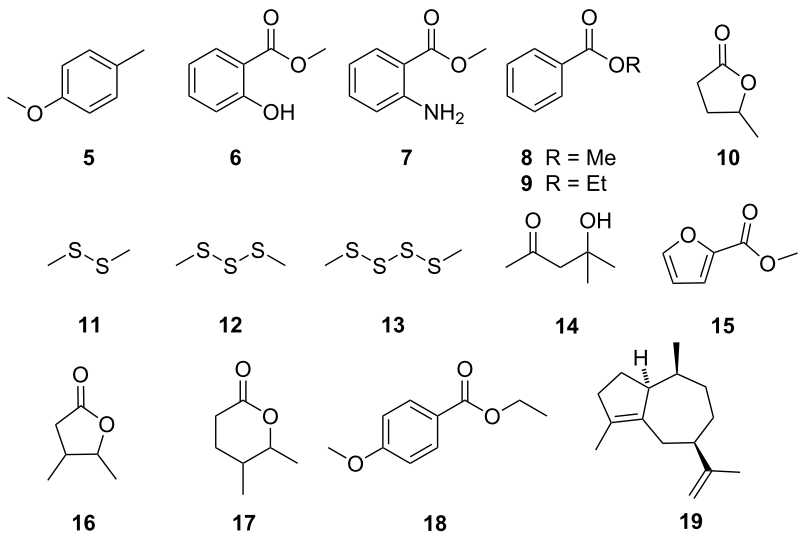

Figure 3: Volatiles released by mycobacteria and *Nocardia* spp. grown on a 7H11 solid medium.

Table 2: Volatiles released by diverse nontuberculous mycobacteria grown on a 7H11 solid medium.[a]

Compound	*I*	Msm	Mau	Mn	Mai	Msc	Maa	Mv
Dimethyl disulfide (**11**)		– – –[b]	+ + –[c]	+ + +[d]	– – –[e]	– –[f]	– –[g]	– –[h]
4-Pentanolide (**10**)	950	+ + +	+ + +	+ + +	+ + +	+ +	+ +	– –
Dimethyl trisulfide (**12**)	969	– + –	+ + –	+ + +	– – –	– –	– –	– –
Methyl 2-furoate (**15**)	978	– – –	– – –	– – –	– – –	+ +	– –	– –
3-Methyl-4-pentanolide (**16**)[i]	984	– – –	– – –	– – –	– – –	– –	– +	– –
6-Methylhept-5-en-2-one	988	– – –	– – –	– – –	– – –	– –	+ +	– –
Unknown	1006	– – –	– – –	– – –	– – –	+ +	– +	– –
Methyl benzoate (**8**)	1093	– – –	– – –	– – –	– – –	+ +	– –	– –
2-Phenylethanol[j]	1111	+ + –	– – –	– —	– – –	+ +	+ +	– –
Ethyl benzoate (**9**)	1169	– – –	– – –	– – –	– – –	+ +	– –	– –
Methyl phenylacetate (**1**)	1177	– – –	– – –	– – –	– – –	+ +	+ –	– –
Methyl salicylate (**6**)	1193	– – –	– – –	– – –	– – –	+ +	–+	– –
Dimethyl tetrasulfide (**13**)	1206	– – –	– – –	+ + +	– – –	– –	– –	– –
Ethyl salicylate	1270	– – –	– – –	– – –	– – –	+ +	– –	– –
Methyl methylsalicylate	1315	– – –	– – –	– – –	– —	– –	+ +	+ +
Unknown sesquiterpenes		– – –	– – +	– – –	+ + +	– –	– –	+ +

[a]*I*: gas-chromatographic retention index on DB-5; +: compound detected in sample; –: compound not detected in sample. Msm: *M. smegmatis,* Mau: *M. aurum*, Mn: *M. neoaurum,* Mai: *M. aichiense,* Msc: *M. scrofulaceum,* Maa: *M. avium* ssp. *avium,* Mv: *M. vaccae*. [b]The results of three analyses are shown for each experiment performed on differently aged cultures: 2 d, 3 d, 4 d. [c]The results of three analyses are shown for each experiment performed on differently aged cultures: 4 d, 5 d, 11 d. [d]The results of three analyses are shown for each experiment performed on differently aged cultures: 5 d, 6 d, 13 d. [e]The results of three analyses are shown for each experiment performed on differently aged cultures: 3 d, 8 d, 9 d. [f]The results of two analysis are shown for each experiment performed on differently aged cultures: 6 d, 11 d. [g]The results of two analysis are shown for each experiment performed on differently aged cultures: 5 d, 11 d. [h]The results of two analysis are shown for each experiment performed on differently aged cultures: 4 d, 7 d. [i]*I* of first eluting isomer is shown. [j]Traces present in the medium.

(**12**), and dimethyl tetrasulfide (**13**), which are known bacterial volatiles [19]; these compounds were not emitted from *M. tuberculosis*.

While the mycobacteria grown on the 7H11 solid medium emitted a wide variety of volatiles, *Nocardia asteroides* produced, even in different ages, only 4-pentanolide (**10**) (Table 3). Additionally, *N. africana* also released only one compound, the sesquiterpene aciphyllene (**19**), which is a known volatile from several plants [29], and the endophytic fungus *Muscodor albus* [30]. The structure of **19** has recently been revised [29]. This compound may act as marker for norcardiae,

Table 3: Compounds released by *Nocardia* spp. grown on a 7H11 solid medium.[a]

Compound	*I*	*N. asteroides*			*N. africana*		
		5 d	16 d	18 d	3 d	6 d	10 d
4-Pentanolide (**10**)	950	+	+	+	–	–	–
Aciphyllene (**19**)	1499	–	–	–	+	+	+

[a]*I*: gas-chromatographic retention index on DB-5; +: compound detected in sample; –: compound not detected in sample; d: days.

as it was produced as a single compound by *Nocardia* spp. grown on a 7H11 medium and has so far not been reported for other bacteria [19].

Analysis of bacteria grown in diverse liquid media

In these experiments, two different media were used for culturing bacteria. *Nocardia* spp. were only cultured on the 7H9 broth medium, and all mycobacteria were grown on the 7H9 broth and the Sauton liquid media. The results of the analyses of different strains of *M. tuberculosis* grown on the 7H9 broth medium are shown in Figure 4 and Table 4.

A 33-day-old culture of *M. tuberculosis* strain 2, and a 6-day-old culture of strain 5 produced the largest variety of compounds. Again, aromatic compounds including the previously observed volatiles **1**, **5**, **7**, and **8**, as well as the fatty acid derivative **10**, were present in the headspace extracts.

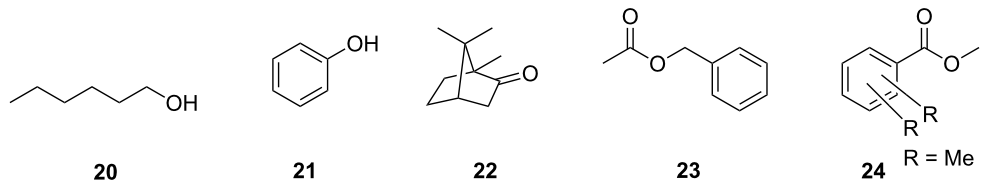

20 **21** **22** **23** **24**

Figure 4: Volatiles released by *M. tuberculosis* grown in a 7H9 broth liquid medium.

Table 4: Volatiles released by *Mycobacterium tuberculosis* grown in a 7H9 broth medium.[a]

Compound	*I*	Strain 2		Strain 5				Strain 6	
		12 d	33 d	3 d	6 d	10 d	13 d	14 d	15 d
1-Hexanol (**20**)	890	–	–	+	–	–	–	–	–
4-Pentanolide (**10**)	950	+	+	–	+	+	–	+	–
Methyl butenolide	979	–	+	–	+	–	–	–	–
Phenol (**21**)	984	–	+	–		–	–	–	–
Unknown	1021	–	+	+	+	–	–	–	–
4-Methylanisol (**5**)	1021	–	+	–	+	–	–	–	–
Methyl benzoate (**8**)	1093	–	+	–	+	–	+	+	+
2-Phenylethanol[b]	1113	+	–	–	+	+	+	+	+
Methyl nicotinate (**3**)[b]	1136	–	–	–	+	–	–	–	+
Camphor (**22**)	1143	–	–	+	+	–	–	–	+
Benzyl acetate (**23**)	1164	–	+	–		–	–	–	–
Methyl phenylacetate (**1**)	1177	–	–	–	+	–	–	+	+
Benzothiazole	1222	–	+	–	–	–	–	–	–
Methyl 2-aminobenzoate (**7**)	1341	–	+	–	–	–	–	–	–
Methyl dimethylbenzoate (**24**)	1348	–	+	–	–	–	–	+	–

[a]*I*: gas-chromatographic retention index on DB-5; +: compound detected in sample; –: compound not detected in sample; d: days. [b]Traces present in the medium.

Frequently, mycobacteria are observed to grow faster in liquid medium than on solid medium [31,32]. Consistent with this, *M. tuberculosis* strain 5 produced the most volatiles after six days of growth, unlike cultures of the same age grown on solid medium. Heavy inoculation of a fresh medium with a liquid culture of *M. tuberculosis* at the exponential growth phase may also generate a high yield of volatiles. Several volatiles released in the solid-medium experiments were not observed in liquid culture, and vice versa. On a solid medium, compounds **14**–**18** were formed but were not emitted in liquid cultures. In contrast, liquid cultures of *M. tuberculosis* released 1-hexanol (**20**), phenol (**21**), camphor (**22**), benzyl acetate (**23**), methyl dimethylbenzoate (**24**), and a methyl butenolide, all of which were absent in strains cultured on a solid medium.

The headspace extracts of the nontuberculous mycobacteria cultured in the 7H9 broth medium were investigated and the results (Table 5) revealed that most of the nontuberculous mycobacteria produced only a few volatiles, with the exception of *M. scrofulaceum* and *M. avium* ssp. *avium*, which produced a larger variety of compounds, including various aromatic volatiles also emitted by *M. tuberculosis*.

The analyses of the *Nocardia* strains revealed interesting differences between the two media types. Although aciphyllene (**19**) was again produced by *N. africana*, it was also present in the bouquet of an early culture of *N. asteroides* (Table 6). Additionally, both bacteria produced several unknown diterpenoids. Such relatively large compounds have rarely been reported as bacterial volatiles [33,34].

In additional experiments, a Sauton liquid medium was used to culture *M. tuberculosis* (Table 7). The two strains of *M. tuberculosis* produced fewer volatiles compared to cultures on

Table 5: Volatiles released by diverse nontuberculous mycobacteria grown in the 7H9 broth medium.[a]

Compound	*I*	Msm	Mau	Mn		Mai		Msc	Maa	Mv
		8 d	6 d	7 d	13 d	5 d	14 d	9 d	10 d	8 d
2-Methylbutanol		–	–	–	–	–	–	+	–	–
Methyl isovalerate		–	–	–	–	–	–	+	–	–
1-Hexanol (**20**)	890	+	–	–	–	–	–	–	–	–
Isobutyl isobutyrate	919	–	–	–	–	–	–	+	–	–
4-Pentanolide (**10**)	950	+	–	–	–	–	–	–	+	+
Methyl butenolide	979		+	+	+	+	+	–	–	–
3-Methyl-4-pentanolide (**16**)[b]	984	–	–	–	–	–	–	–	–	+
Methyl benzoate (**8**)	1093	–	–	–	–	–	–	+	+	–
2-Phenylethanol[c]	1111	+	–	–	–	–	–	+	+	+
Camphor (**22**)	1143	–	–	–	–	–	–	–	–	+
Methyl phenylacetate (**1**)	1177	–	–	–	–	–	–	+	+	–
Methyl salicylate (**6**)	1193	–	–	–	–	–	–	+	+	+
Indole	1289	–	–	–	–	+	+	–	–	–
2-Aminoacetophenone	1299	+	–	–	–	–	–	–	–	–
Methyl dimethylbenzoate (**24**)	1348	–	–	–	–	–	–	+	+	–

[a]*I*: gas-chromatographic retention index on DB-5; +: compound detected in sample; –: compound not detected in sample; d: days; Msm: *M. smegmatis*, Mau: *M. aurum*, Mn: *M. neoaurum*, Mai: *M. aichiense*, Msc: *M. scrofulaceum*, Maa: *M. avium* ssp. *avium*, Mv: *M. vaccae*. [b]Mixture of both diastereomers. [c]Traces present in the medium.

Table 6: Volatiles released by *Nocardia asteroides* and *N. africana* grown in the 7H9 broth medium.[a]

Compound	*I*	*N. asteroides*		*N. africana*		
		4 d	14 d	2 d	5 d	11 d
Aciphyllene (**19**)	1499	+	–	+	+	+
Unknown diterpenoids		+	–	+	–	+

[a]*I*: gas-chromatographic retention index on DB-5; +: compound detected in sample; –: compound not detected in sample; d: days.

Table 7: Volatiles released by *Mycobacterium tuberculosis* grown in a Sauton liquid medium.[a]

Compound	*I*	Strain 5			Strain 6
		24 d	26 d	46 d	25 d
2-Hydroxypentan-3-one		–	–	–	+
Trimethyloxazole		–	+	+	+
Unknown	947	–	–	+	+
Benzylalcohol	1035	–	+	–	+
Phenylacetaldehyde	1041	–	–	–	+
Methyl benzoate (**8**)	1093	–	–	+	–
2-Phenylethanol[b]	1113	+	+	+	+
Methyl phenylacetate (**1**)	1177	–	–	+	–
Methyl *p*-anisate (**2**)	1376	–	–	+	–
Methyl dimethylbenzoate (**24**)	1348	–	–	+	–

[a]*I*: gas-chromatographic retention index on DB-5; +: compound detected in sample; –: compound not detected in sample; d: days. [b]Traces present in the medium.

the solid medium of the same age. The growth of *M. tuberculosis* in the Sauton liquid medium was slower than in other liquid media. Thus, the type of medium used influenced the production of volatiles. Few volatiles were produced, including predominantly aromatic compounds, such as **1**, **2**, **8**, and **24**, especially in the 46-day-old culture of *M. tuberculosis* strain 5.

Analyses of the headspace extracts from nontuberculous mycobacteria grown in the Sauton medium (*M. smegmatis*, *M. aurum*, *M. neoaurum*, *M. aichiense*, and *M. avium* ssp. *avium*) showed that fewer compounds were produced by these species in this medium (Table 8).

As observed for the 7H9 medium, only *M. avium* ssp. *avium* emitted a diverse array of volatiles, while the other mycobacteria produced a few compounds only. The results of different analyses showed that *M. tuberculosis* produces more compounds than the previously described volatiles **1**–**4**, especially on the solid medium.

Apart from the production of specific compounds such as **3** and **4**, *M. tuberculosis* was characterized by a more pronounced production of volatiles compared to other mycobacteria and associated *Nocardia* bacteria. While many of these compounds, such as 2-phenylethanol, **1**, or **8**, are commonly found in some, but not all, bacteria [19], the individual components contribute to a specific bouquet of volatiles. This bouquet probably enables olfactory detection of *M. tuberculosis* by trained *Cricetomys* rats [13], or could enable potential detection by electronic noses. Only *M. scrofulaceum* and *M. avium* ssp. *avium*

Table 8: Volatiles released by diverse nontuberculous mycobacteria grown in a Sauton liquid medium.[a]

Compound		Msm	Mau	Mn	Mai	Maa
2-Hydroxypentan-3-one		– – –[b]	– – – –[c]	– – – –[d]	– – –[e]	+[f]
Benzylalcohol	1035	+ + –	– – – –	+ + – –	– – +	+
Methyl benzoate (**8**)	1093	– – –	– – – –	– – – –	– – –	+
Linalool	1099	– – –	– – – –	+ – – –	+ – –	+
2-Phenylethanol[g]	1113	+ + +	– – – –	+ + – –	– – –	+
Methyl phenylacetate (**1**)	1177	– – –	– – – –	– – – –	– – –	+
Methyl dimethylbenzoate (**24**)	1348	– – –	– – – –	– – – –	– – –	+
Unknown sesquiterpenes		+ + –	– – – –	– – – –	– – –	+

[a]*I*: gas-chromatographic retention index on DB-5; +: compound detected in sample; –: compound not detected in sample. Msm: *M. smegmatis,* Mau: *M. aurum*, Mn: *M. neoaurum,* Mai: *M. aichiense,* Maa: *M. avium* ssp. *avium.* [b]The results of three analyses are shown for each experiment performed on differently aged cultures: 7 d, 8 d, 9 d. [c]The results of four analyses are shown for each experiment performed on differently aged cultures: 1 d, 7 d, 11 d, 12 d. [d]The results of four analyses are shown for each experiment performed on differently aged cultures: 5 d, 6 d, 10 d, 20 d. [e]The results of three analyses are shown for each experiment performed on differently aged cultures: 8 d, 9 d, 10 d. [f]The results of an analysis on day 10 is shown. [g]Traces present in the medium.

were found to produce a nutrient mixture of volatiles while other strains did not. The volatiles identified belonged predominantly to the biosynthetic class of aromatic compounds, while metabolites of the fatty-acid-biosynthesis pathway were also present.

Since *M. tuberculosis* grown in the Sauton liquid medium produced only a few volatiles after more than 25 days, these experimental conditions are suboptimal. *M. tuberculosis* cultivated in the 7H9 broth medium emitted after a shorter incubation time more volatiles in comparison to cultures grown in solid medium. However, the number of volatiles produced compared to nontuberculous mycobacteria was much lower than for mycobacteria grown on solid medium. The compounds emitted by *M. tuberculosis* grown on the 7H9 broth medium are known, except for **3**, but are also released from other bacteria, thus diminishing their diagnostic potential [19,35,36]. Compound **19** may play a role as a marker for different *Nocardia* strains, depending on growth conditions. Further studies should focus on enhancing the production of volatiles in liquid medium, which support the rapid growth of bacteria. Currently the identified volatile compounds produced by *M. tuberculosis* are tested for tuberculosis detection by using *Cricetomys* rats.

Conclusion

In conclusion, profound qualitative and quantitative differences (number of compounds as well as probably higher emission rates) in the bouquet of volatiles from *M. tuberculosis*, nontuberculous mycobacteria and other bacteria grown on different media were found. *M. tuberculosis* produces a distinctive bouquet of compounds, consisting of compounds known to be produced by other bacteria, but also including relatively specific compounds such as methyl nicotinate (**3**). Variations occurred within individual analyses and also between different media. Therefore, it seems unlikely that GC–MS analyses of individual cultures can be used as a diagnostic tool. Nevertheless, a system able to detect mixtures within a given compositional tolerance seems more promising. In this sense, trained *Cricetomys* rats seem to be well suited for detection [20]. In a more technical variant, experiments with electronic noses, able to discriminate between different odor profiles, seem to be more promising for the detection of *Mtb*-specific odor profiles and, thus, could be potentially used for TB diagnosis.

Experimental

Media and growth conditions

Bacterial colonies from a 7H11 solid medium (Becton, Dickinson & Co., Sparks, USA, see Supporting Information File 1) or bacteria culture (100 µL) from a 7H9 liquid medium (Becton, Dickinson & Co., Sparks, USA, see Supporting Information File 1) were inoculated on a 7H11 solid medium and were spread out with sterile disposable loops to cover the entire plate/medium surface. Plates were wrapped in parafilm and aerobically incubated at 28–37 °C.

For bacteria grown in the 7H9 liquid medium, the inoculum (500 µL) was aseptically transferred from actively growing cultures and inoculated into fresh medium (15–20 mL). Cultures were incubated at 28–37 °C under aerobic conditions.

Bacterial cultures for inoculation into Sauton medium (without glycerol) were washed in order to remove traces of ingredients from the stock-culture medium (7H9). Washing was done three times by mixing the culture (3 mL) with phosphate-buffered saline (PBS; 10 mL) and centrifuging at 4000 rpm for 10 min. Supernatants were decanted and PBS (10 mL) was added to the pellet, which was dissolved by careful pipetting. The suspension was centrifuged again at 4000 rpm for 10 min. The final pellet was suspended in sterile PBS (4 mL), mixed thoroughly and 500 µL of the suspension was subcultured into fresh Sauton medium (30 mL). The Sauton medium consisted of the following ingredients in 1000 mL of distilled water: asparagine (4 g), $MgSO_4$ (0.5 g), K_2PO_4 (0.5 g), citric acid (1.83 g), ferric ammonium citrate (0.05 g), D-(+)-glucose monohydrate (4.82 g), and sodium pyruvate (4.82 g). The pH was adjusted to 6.8 and the medium was filter-sterilized by using a 0.22 µm membrane filter (Millipore Corp., USA). Cultures were incubated at 37 °C aerobically.

Sampling of volatiles

Volatile organic compounds emitted by cell cultures of the different mycobacteria were collected by using the CLSA technique [14,15]. The volatiles were adsorbed on charcoal (Chromtech; Precision Charcoal Filter, 5 mg) for 24 h, and then eluted with 30 µL of CH_2Cl_2. The obtained extracts were immediately analyzed by GC–MS, and stored at –30 °C.

GC–EIMS analysis

GC–EIMS analyses of the samples were carried out on a HP-6890 GC system connected to a HP-5973 mass-selective detector fitted with a BPX5 fused-silica capillary column (25 m, 0.22 mm i.d., 0.25 µm film; SGE, Australia), or on an Agilent 7890A connected with an Agilent 5975C inert mass detector fitted with a HP-5MS fused silica capillary column (30 m, 0.25 mm i.d., 0.25 µm film; J&W Scientific, USA). Conditions for the HP-6890/HP-5973 system were as follows: Inlet pressure: 77.1 kPa, 23.3 mL He min^{-1}; injection volume: 1 µL; transfer line: 300 °C; electron energy: 70 eV. The GC was programmed as follows: 5 min at 50 °C, increasing at 5 °C min^{-1} to 320 °C, operating in splitless mode (60 s valve time). Conditions for the Agilent 7890A/Agilent 5975C system were as follows: Inlet pressure: 77.1 kPa, He 23.3 mL min^{-1}; injec-

tion volume: 1 µL; transfer line: 300 °C; electron energy: 70 eV. The GC was programmed as follows: 5 min at 50 °C, increasing at 5 °C min^{-1} to 320 °C, operated in splitless mode (60 s valve time); He carrier gas at 1 mL min^{-1} (HP-6890) or 1.2 mL min^{-1} (Agilent 7890A).

Retention indices (*I*) were determined from a homologous series of *n*-alkanes (C8–C35) [19]. Identification of compounds was performed by comparison of mass spectra to the Wiley-6 Library, NIST 07, and the Essential Oils Library (Massfinder) and gas chromatographic retention indices, as well as by comparison with synthetic samples. Details can be found in the supporting information. The relative emission of volatiles was roughly estimated from peak areas, although overlapping peaks from the medium and the known difficulty in using CLSA for quantification allowed for only a rough approximation.

Supporting Information

Supporting Information File 1

Identification of compounds.
[http://www.beilstein-journals.org/bjoc/content/supplementary/1860-5397-8-31-S1.pdf]

Acknowledgements

We thank the Fonds der Chemischen Industrie for financial support to S.S. Funding by the UBS Optimus Foundation (UBS) to S.H.E.K. and B.J.W. is gratefully acknowledged.

References

1. WHO, Global tuberculosis control – a short update to the 2009 report; WHO Press, 2009.
2. Cook, G. M.; Berney, M.; Gebhard, S.; Heinemann, M.; Cox, R. A.; Danilchanka, O.; Niederweis, M. Physiology of Mycobacteria. In *Advances in Microbial Physiology;* Poole, R. K., Ed.; Elsevier: Amsterdam, The Netherlands, 2009; Vol. 55, pp 81–318.
3. Sangari, F. J.; Bermudez, L. E. In *Cytokines in Pulmonary Disease – Infection and Inflammation;* Nelson, S.; Martin, T. R., Eds.; Marcel Dekker, Inc.: New York, U. S. A., 2000; pp 213 ff.
4. Madigan, M. T.; Martinko, J. M.; Parker, J. *Biology of Microorganisms;* Prentice-Hall: New Jersey, 1997.
5. Wallis, R. S.; Doherty, T. M.; Onyebujoh, P.; Vahedi, M.; Laang, H.; Olesen, O.; Parida, S.; Zumla, A. *Lancet Infect. Dis.* **2009,** *9,* 162–172. doi:10.1016/S1473-3099(09)70042-8
6. Boehme, C. C.; Nabeta, P.; Hillemann, D.; Nicol, M. P.; Shenai, S.; Krapp, F.; Allen, J.; Tahirli, R.; Blakemore, R.; Rustomjee, R.; Milovic, A.; Jones, M.; O'Brien, S. M.; Persing, D. H.; Ruesch-Gerdes, S.; Gotuzzo, E.; Rodrigues, C.; Alland, D.; Perkins, M. D. *N. Engl. J. Med.* **2010,** *363,* 1005–1015. doi:10.1056/NEJMoa0907847
7. Knechel, N. A. *Crit. Care Nurse* **2009,** *29,* 34–43. doi:10.4037/ccn2009968
8. Phillips, M.; Cataneo, R. N.; Condos, R.; Ring Erickson, G. A.; Greenberg, J.; La Bombardi, V.; Munawar, M. I.; Tietje, O. *Tuberculosis* **2007,** *87,* 44–52. doi:10.1016/j.tube.2006.03.004
9. Syhre, M.; Chambers, S. T. *Tuberculosis* **2008,** *88,* 317–323. doi:10.1016/j.tube.2008.01.002
10. Pavlou, A. K.; Magan, N.; Jones, J. M.; Brown, J.; Klatser, P.; Turner, A. P. F. *Biosens. Bioelectron.* **2004,** *20,* 538–544. doi:10.1016/j.bios.2004.03.002
11. Syhre, M.; Manning, L.; Phuanukoonnon, S.; Harino, P.; Chambers, S. T. *Tuberculosis* **2009,** *89,* 263–266. doi:10.1016/j.tube.2009.04.003
12. Weetjens, B. J.; Mgode, G. F.; Machang'u, R. S.; Kazwala, R.; Mfinanga, G.; Lwilla, F.; Cox, C.; Jubitana, M.; Kanyagha, H.; Mtandu, R.; Kahwa, A.; Mwessongo, J.; Makingi, G.; Mfaume, S.; van Steenberge, J.; Beyene, N. W.; Billet, M.; Verhagen, R. *Int. J. Tuberc. Lung Dis.* **2009,** *13,* 737–743.
13. Mgode, G. F.; Weetjens, B. J.; Nawrath, T.; Cox, C.; Jubitana, M.; Machang'u, R. S.; Cohen-Bacrie, S.; Bedotto, M.; Drancourt, M.; Schulz, S.; Kaufmann, S. H. E. *J. Clin. Microbiol.* **2012,** *50,* 274–280. doi:10.1128/JCM.01199-11
14. Konno, K. *Science* **1956,** *124,* 985–986. doi:10.1126/science.124.3229.985
15. Boland, W.; Ney, P.; Jaenicke, L.; Gassmann, G. A. "closed-loop-stripping" technique as a versatile tool for metabolic studies of volatiles. In *Analysis of volatiles;* Schreier, P., Ed.; de Gruyter: Berlin, Germany, 1984; pp 371–380.
16. Dickschat, J. S.; Martens, T.; Brinkhoff, T.; Simon, M.; Schulz, S. *Chem. Biodiversity* **2005,** *2,* 837–865. doi:10.1002/cbdv.200590062
17. Bartelt, R. J. *Anal. Chem.* **1997,** *69,* 364–372. doi:10.1021/ac960820n
18. van den Dool, H.; Kratz, P. D. *J. Chromatogr.* **1963,** *11,* 463–471. doi:10.1016/S0021-9673(01)80947-X
19. Schulz, S.; Dickschat, J. S. *Nat. Prod. Rep.* **2007,** *24,* 814–842. doi:10.1039/b507392h
20. Mgode, G. F.; Weetjens, B. J.; Cox, C.; Jubitana, M.; Machang'u, R. S.; Lazar, D.; Weiner, J.; van Geertruyden, J.-P.; Kaufmann, S. H. E. *Tuberculosis*, in press. doi:10.1016/j.tube.2011.11.008
21. Prissick, F. H.; Masson, A. M. *Can. Med. Assoc. J.* **1956,** *75,* 798–803.
22. Zur Lage, S.; Goethe, R.; Darji, A.; Valentin-Weigand, P.; Weiss, S. *Immunology* **2003,** *108,* 62–69. doi:10.1046/j.1365-2567.2003.01564.x
23. Vindal, V.; Suma, K.; Ranjan, A. *BMC Genomics* **2007,** *8,* No. 289. doi:10.1186/1471-2164-8-289
24. Gupta, A.; Bhakta, S.; Kundu, S.; Gupta, M.; Srivastava, B. S.; Srivastava, R. *J. Antimicrob. Chemother.* **2009,** *64,* 774–781. doi:10.1093/jac/dkp279
25. Woo, P. C. Y.; Tsoi, H.-W.; Leung, K.-W.; Lum, P. N. L.; Leung, A. S. P.; Ma, C.-H.; Kam, K.-M.; Yuen, K.-Y. *J. Clin. Microbiol.* **2000,** *38,* 3515–3517.
26. Griffith, D. E.; Aksamit, T.; Brown-Elliott, B. A.; Catanzaro, A.; Daley, C.; Gordin, F.; Holland, S. M.; Horsburgh, R.; Huitt, G.; Iademarco, M. F.; Iseman, M.; Olivier, K.; Ruoss, S.; von Reyn, C. F.; Wallace, R. J., Jr.; Winthrop, K.; on behalf of the ATSMycobacterial Diseases Subcommittee. *Am. J. Respir. Crit. Care Med* **2007,** *175,* 367–416. doi:10.1164/rccm.200604-571ST
27. Thorel, M.-F.; Krichevsky, M.; Vincent Lévy-Frébault, V. *Int. J. Syst. Bacteriol.* **1990,** *40,* 254–260. doi:10.1099/00207713-40-3-254

28. O'Brien, M. E. R.; Saini, A.; Smith, I. E.; Webb, A.; Gregory, K.; Mendes, R.; Ryan, C.; Priest, K.; Bromelow, K. V.; Palmer, R. D.; Tuckwell, N.; Kennard, D. A.; Souberbielle, B. E. *Br. J. Cancer* **2000,** *83,* 853–857. doi:10.1054/bjoc.2000.1401
29. Blay, G.; Garcia, B.; Molina, E.; Pedro, J. R. *Tetrahedron* **2007,** *63,* 9621–9626. doi:10.1016/j.tet.2007.07.039
30. Atmosukarto, I.; Castillo, U.; Hess, W. M.; Sears, J.; Strobel, G. *Plant Sci.* **2005,** *169,* 854–861. doi:10.1016/j.plantsci.2005.06.002
31. James, B. W.; Williams, A.; Marsh, P. D. *J. Appl. Microbiol.* **2000,** *88,* 669–677. doi:10.1046/j.1365-2672.2000.01020.x
32. Sorlozano, A.; Soria, I.; Roman, J.; Huertas, P.; Soto, M. J.; Piedrola, G.; Gutierrez, J. *J. Microbiol. Biotechnol.* **2009,** *19,* 1259–1264.
33. Nawrath, T.; Gerth, K.; Müller, R.; Schulz, S. *ChemBioChem* **2010,** *11,* 1914–1919. doi:10.1002/cbic.201000296
34. Nawrath, T.; Gerth, K.; Müller, R.; Schulz, S. *Chem. Biodiversity* **2010,** *7,* 2228–2253. doi:10.1002/cbdv.201000190
35. Hayaloglu, A. A.; Cakmakci, S.; Brechany, E. Y.; Deegan, K. C.; McSweeney, P. L. H. *J. Dairy Sci.* **2007,** *90,* 1102–1121. doi:10.3168/jds.S0022-0302(07)71597-7
36. Callejón, R. M.; Tesfaye, W.; Torija, M. J.; Mas, A.; Troncoso, A. M.; Morales, M. L. *Food Chem.* **2009,** *113,* 1252–1259. doi:10.1016/j.foodchem.2008.08.027

License and Terms

Beilstein Journal of Organic Chemistry

Mutational analysis of a phenazine biosynthetic gene cluster in *Streptomyces anulatus* 9663

Orwah Saleh[1], Katrin Flinspach[1], Lucia Westrich[1], Andreas Kulik[2], Bertolt Gust[1], Hans-Peter Fiedler[2] and Lutz Heide[*1,§]

Full Research Paper

Open Access

Address:
[1]Pharmaceutical Institute, University of Tübingen, Auf der Morgenstelle 8, 72076 Tübingen, Germany and [2]Institute of Microbiology and Infection Medicine, University of Tübingen, Auf der Morgenstelle 28, 72076 Tübingen, Germany

Email:
Lutz Heide[*] - heide@uni-tuebingen.de

* Corresponding author
§ Fax: +497071295250

Keywords:
phenazine; gene cluster; gene inactivation

Beilstein J. Org. Chem. **2012,** *8,* 501–513.
doi:10.3762/bjoc.8.57

Received: 02 January 2012
Accepted: 06 March 2012
Published: 04 April 2012

This article is part of the Thematic Series "Biosynthesis and function of secondary metabolites".

Guest Editor: J. S. Dickschat

Abstract

The biosynthetic gene cluster for endophenazines, i.e., prenylated phenazines from *Streptomyces anulatus* 9663, was heterologously expressed in several engineered host strains derived from *Streptomyces coelicolor* M145. The highest production levels were obtained in strain M512. Mutations in the *rpoB* and *rpsL* genes of the host, which result in increased production of other secondary metabolites, had no beneficial effect on the production of phenazines. The heterologous expression strains produced, besides the known phenazine compounds, a new prenylated phenazine, termed endophenazine E. The structure of endophenazine E was determined by high-resolution mass spectrometry and by one- and two-dimensional NMR spectroscopy. It represented a conjugate of endophenazine A (9-dimethylallylphenazine-1-carboxylic acid) and L-glutamine (L-Gln), with the carboxyl group of endophenazine A forming an amide bond to the α-amino group of L-Gln. Gene inactivation experiments in the gene cluster proved that *ppzM* codes for a phenazine *N*-methyltransferase. The gene *ppzV* apparently represents a new type of TetR-family regulator, specifically controlling the prenylation in endophenazine biosynthesis. The gene *ppzY* codes for a LysR-type regulator and most likely controls the biosynthesis of the phenazine core. A further putative transcriptional regulator is located in the vicinity of the cluster, but was found not to be required for phenazine or endophenazine formation. This is the first investigation of the regulatory genes of phenazine biosynthesis in *Streptomyces*.

Introduction

Phenazine natural products have important biological activities comprising antibacterial, antifungal, antitumor, antimalarial, antioxidant and antiparasitic activities, and as inhibitors of angiotensin converting enzyme (ACE) or testosterone-5-α-reductase [1]. The synthetic phenazine clofazimine has been approved for human therapy in the treatment of leprosy. Some of the other naturally occurring phenazines are bacterial virulence factors [1]. Natural phenazines are secondary metabolites,

produced mainly by different species of the proteobacterium *Pseudomonas* and of the actinobacterium *Streptomyces*. While *Pseudomonas* strains produce phenazine derivatives with relatively simple structures, more complex phenazines are produced by *Streptomyces* strains [1]. The biosynthesis of phenazine-1-carboxylic acid (PCA) and its derivatives has been studied extensively in *Pseudomonas* [2-5]. The biosynthesis of PCA requires a set of seven genes named *phzABCDEFG* [3,6]. PhzC codes for DAHP (3-deoxy-D-arabinoheptulosonate-7-phosphate) synthase, the first enzyme of the shikimate pathway, and ensures the flow of primary metabolites towards chorismic acid. Chorismic acid is the branch point at which the biosynthesis of PCA, catalyzed by the enzymes PhzABDEFG, branches off from the shikimate pathway. These seven core phenazine biosynthesis genes could be identified in nearly all investigated bacterial strains that produce phenazine compounds [3,6]. Other genes have been shown to play a role in the regulation of phenazine biosynthesis. In *P. fluorescens*, the transcriptional regulation involves the quorum sensing proteins PhzR/PhzI, the positive two-component regulator system GacS/GacA, and the negative two-component regulator system RpeA/RpeB [7,8]. Additional regulatory genes have been identified in *P. chlororaphis*, including the transcriptional regulator gene *pip* and post-transcriptional regulators encoded by *rsmA* and *rsmZ* [7,9,10]. Although many different phenazines are produced by *Streptomyces* strains, only two gene clusters have been identified in *Streptomyces* so far, i.e., the phenazine biosynthetic gene clusters from *S. anulatus* [11] and from *S. cinnamonensis* [12,13]. In *Streptomyces*, it is as yet completely unknown which genes are involved in the regulation of the biosynthesis of phenazine natural products.

In a previous study, we described the biosynthetic gene cluster for prenylated phenazines from *Streptomyces anulatus* (Figure 1) [11]. This cluster contained the seven core phenazine biosynthesis genes, the mevalonate pathway genes and a prenyltransferase gene, and further genes with unknown functions. Heterologous expression of this cluster, contained in cosmid ppzOS04, in *Streptomyces coelicolor* M512 yielded similar phenazine compounds as formed by the wild-type producer strain, with PCA and endophenazine A as the dominant compounds, and endophenazine B as a minor product (Figure 1) [11].

In the present study, we carried out inactivation experiments of genes on cosmid ppzOS04, followed by heterologous expres-

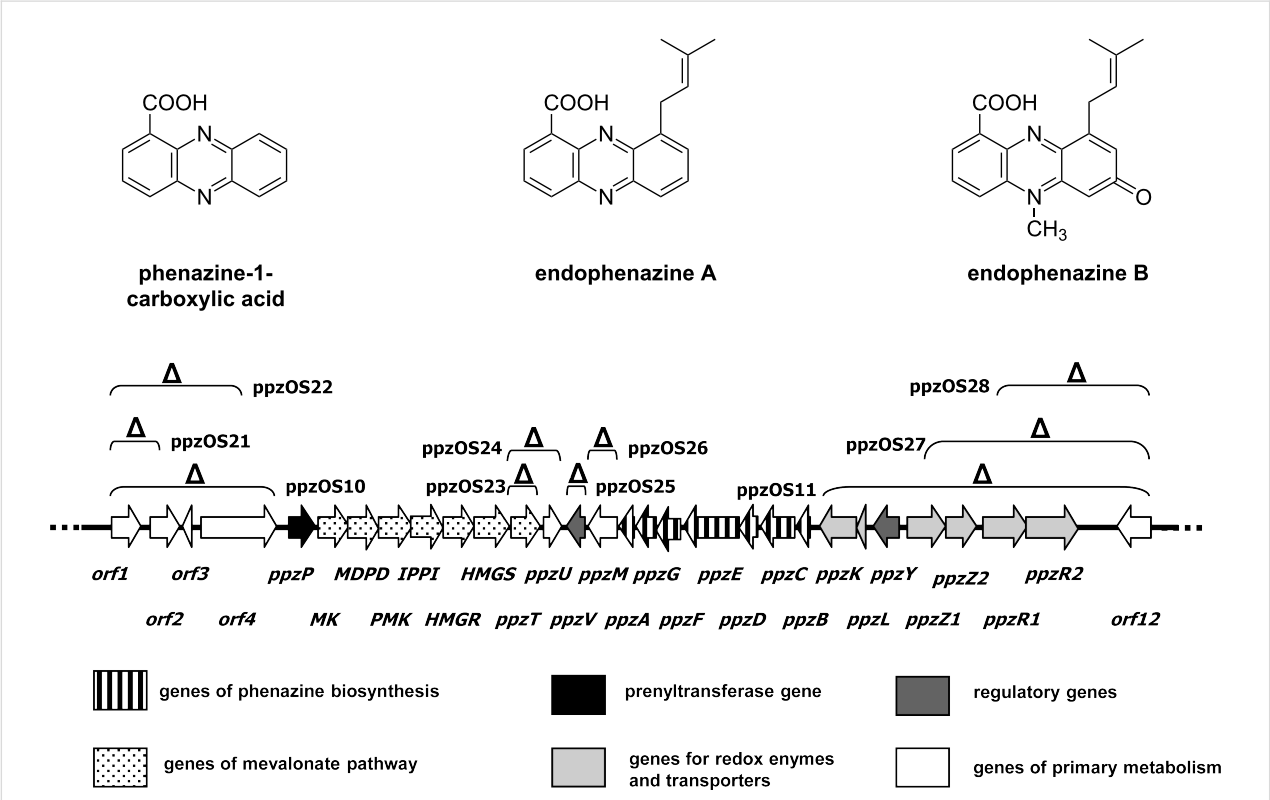

Figure 1: The endophenazine biosynthetic gene cluster from *Streptomyces anulatus* 9663 and the structures of phenazine-1-carboxylic acid and endophenazines A and B. The depicted sequence corresponds to the insert of cosmid ppzOS04. The gene deletions carried out in this study and the names of the resulting constructs are indicated.

sion of the modified clusters and chemical analysis of secondary metabolite formation. This allowed us to investigate the function of individual genes of this cluster for the biosynthetic pathway and for its regulation. The genes inactivated in this study are summarized in Table 1, and a complete list of the genes contained in the insert of cosmid ppzOS04 is given in Table S1 of Supporting Information File 1.

Results and Discussion

Production of prenylated phenazines by cultivation of the heterologous producer strain in 24 square deep-well plates

One important aspect of the current study was the investigation of the influence of putative regulatory genes on the production of endophenazines. Therefore, it was important to assess quantitative differences in production reliably. We decided to use cultivation in 24 square deep-well plates (EnzyScreen BV, The Netherlands). Previous studies have shown that this greatly reduces the variability of secondary metabolite production in comparison to cultivation in Erlenmeyer flasks [14]. In order to obtain a uniform inoculum, precultures were harvested at a defined growth stage, i.e., before reaching the stationary phase. The mycelia were finely dispersed by brief treatment with a Potter homogenizer, frozen in the presence of peptone and stored at −70 °C. Aliquots of this inoculum were used to inoculate individual wells of the deep-well plates, with each well containing 3 mL medium. In initial experiments, the medium was supplemented with 0.6% (w/v) of the siloxylated ethylene oxide/propylene oxide copolymer Q2-5247 (Dow Corning, USA), which acts as an oxygen carrier and has been shown to increase the production of certain antibiotics [14].

Of each mutant obtained in this study, usually three independent clones were isolated, and secondary metabolite production was determined in three parallel cultivations for

Table 1: Genes investigated in this study.

gene	aa	proposed function	orthologue identified by BLAST search	identity/ similarity %	acc. number
orf1	333	serine protease	putative serine protease, *Streptomyces roseosporus* NRRL 15998	93/98	ZP_04708306
orf2	342	aspartate-semialdehyde dehydrogenase	ASD2, *Streptomyces griseus* subsp. griseus NBRC 13350	97/99	YP_001826399
orf3	115	putative transcriptional modulator	*Streptomyces roseosporus* NRRL 11379	71/87	ZP_04708308
orf4	870	aminopeptidase N	*Streptomyces griseus* subsp. griseus NBRC 13350	98/99	YP_001826397
(prenyltransferase gene *ppzP* and six genes of the mevalonate pathway)					
ppzT	327	putative acetoacetyl-CoA synthase	*Streptomyces* sp. KO-3988	79/87	BAD86806
ppzU	221	flavodoxin	flavoprotein WrbA, *Streptomyces violaceusniger* Tü 4113	63/79	YP_004814680
ppzV	206	putative TetR-family regulator	EpzV, *Streptomyces cinnamonensis*	64/76	ADQ43382
ppzM	340	*N*-Methyltransferase	EpzM, *Streptomyces cinnamonensis*	77/86	ADQ43384
(genes *ppzBCDEFGA* of phenazine-1-carboxylic acid biosynthesis)					
ppzK	419	FAD-dependent oxidoreductase	FAD-dependent pyridine nucleotide-disulfide oxidoreductase	55/66	YP_295688
ppzL	107	ferredoxin	ferredoxin, *Rhodopseudomonas palustris* HaA2	55/68	YP_487220
ppzY	290	transcriptional regulator	transcriptional regulator, *Streptomyces lividans* TK24	61/74	ZP_06530228
ppzZ1	430	cytochrome d ubiquinol oxidase, subunit I	cytochrome d ubiquinol oxidase, subunit I, *Stackebrandtia nassauensis* DSM 44728	54/66	YP_003509915
ppzZ2	344	cytochrome d ubiquinol oxidase, subunit II	cytochrome d ubiquinol oxidase, subunit II, *Stackebrandtia nassauensis* DSM 44728	48/60	YP_003509914
ppzR1	563	ABC transporter	cysteine ABC transporter permease, *Thermobispora bispora* DSM 43833	55/68	YP_003653341
ppzR2	585	ABC transporter	cysteine ABC transporter permease, *Streptosporangium roseum* DSM 43021	52/65	YP_003338959
orf12	384	allantoicase	putative allantoicase, *Streptomyces griseus* subsp. griseus NBRC 13350	98/99	YP_001826394

each clone. The variability of production between different clones, and between parallel cultivations of the same clone, was relatively low (average standard deviation of 19.2%).

Expression of the endophenazine gene cluster in different host strains

Previous heterologous expression experiments of the endophenazine gene cluster have been carried out using *Streptomyces coelicolor* M512 as a host strain [11]. Recently, new heterologous expression strains were generated from *S. coelicolor* M145, the parental strain of M512. These new strains include M1146, in which the entire biosynthetic gene clusters of actinorhodin, undecylprodigiosine and calcium-dependent antibiotic, as well as the so-called *cpk* cluster, have been deleted, and which also lacks plasmids SCP1 and SCP2. Furthermore, strain M1154 was generated from strain M1146 by introducing mutations into the genes *rpoB* and *rpsL*, which has been shown to result in an increased production of certain antibiotics [15]. We have now introduced cosmid ppzOS04, which contains the entire gene cluster of the endophenazines [11], into these two strains. However, as depicted in Figure 2, the highest production was achieved in strain M512. Therefore, the *rpoB* and *rpsL* mutations, and the deletion of the other biosynthetic gene cluster, have no beneficial effect on the production of phenazines, and all further experiments in this study were carried out by using M512 as the heterologous expression strain.

Identification of a new phenazine natural product

As shown in Figure 2 and Figure 3, heterologous expression of cosmid ppzOS04 did not only result in the formation of endophenazine A, but also of another compound with the typical absorption spectrum of phenazines. This compound was termed endophenazine E. In M1146 and M1154, endophenazine E was the dominant product in all investigated samples. In M512, endophenazine E was a minor compound after five days of cultivation in the presence of the oxygen carrier Q2-5247 (Figure 2). In the absence of Q2-5247, endophenazine E was a minor compound after three days of cultivation, but became the dominant compound after five days. The time course of the formation of endophenazine A and E during seven days of cultivation is depicted in Figure S1 (Supporting Information File 1).

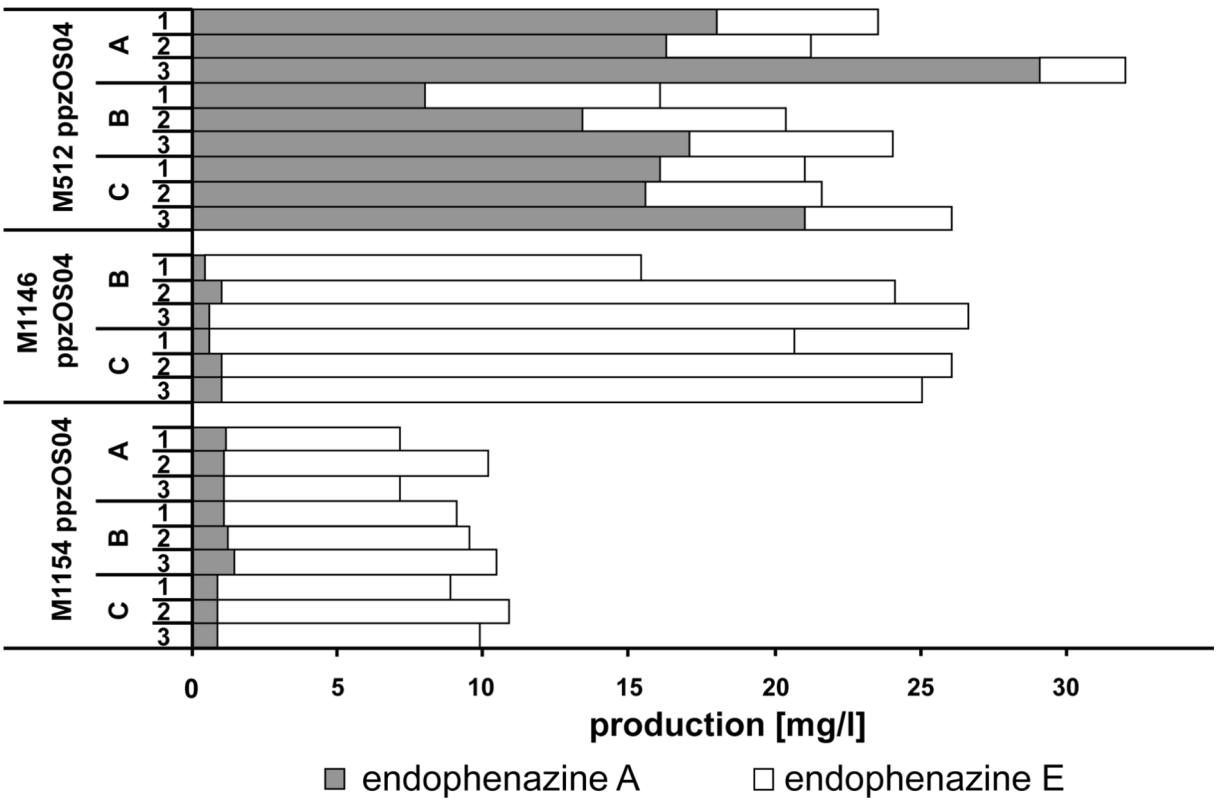

Figure 2: Production of prenylated phenazines after heterologous expression of the endophenazine gene cluster in different expression hosts. From each expression host, two to three independent clones were obtained (A–C), and production was determined in three parallel cultivations of each clone (1–3). Cultivation was carried out in 24 square deep-well plates. In the experiments depicted here, the culture medium was supplemented with 0.6% of the oxygen carrier Q2-5247.

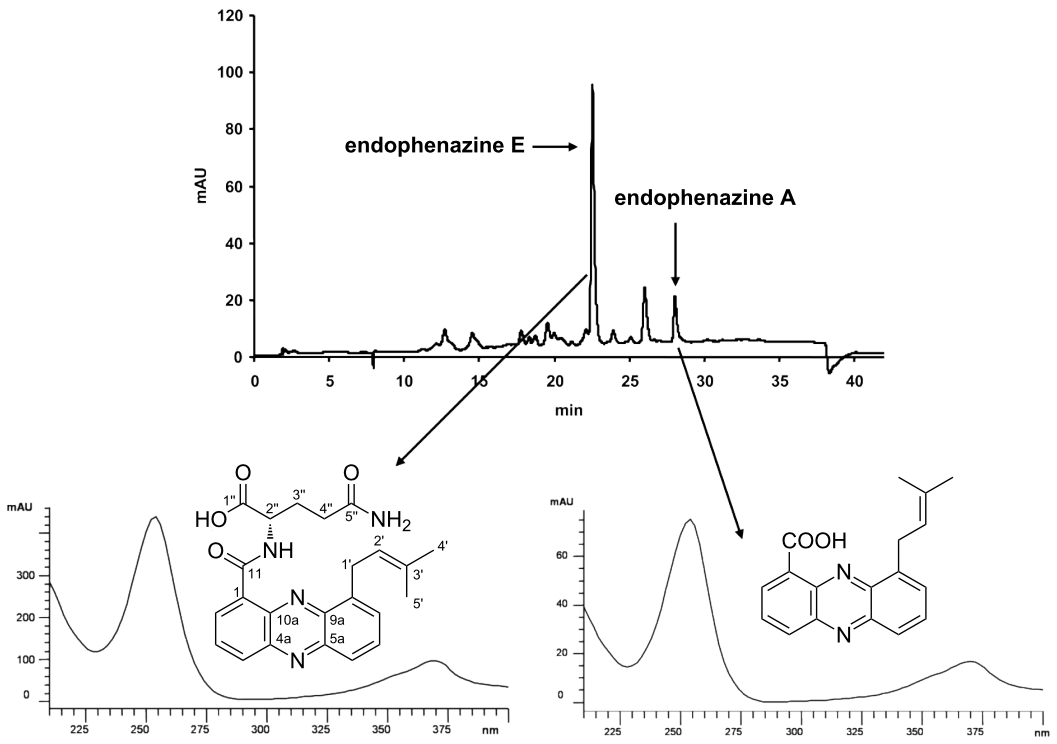

Figure 3: HPLC analysis of mycelia of the heterologous expression strain *S. coelicolor* M512(ppzOS04) after five days of cultivation. The oxygen carrier Q2-5247 was not included in the culture medium in this experiment. Detection wavelength: 365 nm. The lower panels show the UV spectra of endophenazine A and endophenazine E.

Endophenazine E showed a molecular ion at *m*/*z* 421 ($[M + H]^+$). Positive-ion-mode high-resolution mass spectrometry showed an exact mass of 421.186790 Dalton, indicating a molecular formula of $C_{23}H_{24}N_4O_4$ (calculated mass 420.1870317 Dalton, Δ = 0.57 ppm), different from any phenazine derivative described previously.

To identify the structure of the new product, the heterologous expression strain *S. coelicolor* M512(ppzOS04) carrying the phenazine biosynthetic gene cluster was cultivated in a 10 L fermenter. Endophenazine E was purified from the mycelia by chromatography on Sephadex LH-20 and by preparative reversed-phase HPLC. Sixty milligrams of a yellow solid compound was obtained and 7 mg were investigated by unidimensional (^{1}H and ^{13}C) and multidimensional (COSY, HSQC and HMBC) NMR spectroscopy, in comparison to PCA. This showed signals for a phenazine core and for a prenyl group, very similar to those shown by endophenazine A. The additional signals showed that the carboxyl group of endophenazine A was attached to the α-amino group of the amino acid glutamine. The ^{1}H and ^{13}C NMR data of the compound are summarized in Table 2, and the ^{1}H-^{1}H COSY, HSQC and HMBC correlations are depicted in Figure S2 (Supporting Information File 1).

The configuration at the α-carbon of the amino acid was determined as L-Gln by enantioselective HPLC analysis [16] (see Experimental section). The specific rotation was determined as $[\alpha]_D^{20} = +16.8$ (*c* = 0.33, MeOH).

Endophenazine E is a new natural product. The conjugation of a phenazine to *N*-acetylcysteine has been described previously [17]. In that case, conjugation occurred through the thiol group of cysteine and led to the loss of the antibacterial activity of the phenazine. A similar *N*-acetylcysteine adduct has been described for a polyketide antibiotic, also leading to a loss of biological activity; therefore, the conjugation has been suggested as representing a detoxification mechanism [18].

The extent of the conversion of endophenazine A to endophenazine E in cultures of *S. coelicolor* M512(ppzOS04) depended on the cultivation conditions. Only small amounts of endophenazine E are formed by cultivation in Erlenmeyer flasks. Upon cultivation in 24 square deep-well plates, endophenazine E is still a minor compound if the oxygen supply is improved by the inclusion of the oxygen carrier Q2-5247. If Q2-5247 is omitted from the medium, however, endophenazine E becomes the dominant product once the culture has reached the stationary growth phase. Q2-5247 did

Table 2: Full ^{1}H and ^{13}C NMR spectroscopic data of endophenazine E. Chemical shifts are expressed in δ values with the solvent as the internal standard.

position	^{13}C NMR data (100.6 MHz, MeOD) δ_C [ppm]	^{1}H NMR data (400 MHz, MeOD) δ_H [ppm]	^{1}H NMR data (400 MHz, d_6-DMSO) δ_H [ppm]
1	130.0	—	—
2	136.3	8.83, 1H, dd, *J* = 7.2, 1.4 Hz	8.80, 1H, dd, *J* = 7.2, 1.5 Hz
3	131.1	8.01, 1H, dd, *J* = 8.7, 7.2 Hz	8.10, 1H, dd, *J* = 8.7, 7.2 Hz
4	135.0	8.38, 1H, dd, *J* = 8.7, 1.4 Hz	8.46, 1H, dd, *J* = 8.7, 1.5 Hz
4a	144.0	—	—
5a	144.6	—	—
6	128.3	8.06, 1H, bd, *J* = 8.7 Hz	8.15, 1H, dd, *J* = 8.1, 0.7 Hz
7	132.9	7.87, 1H, dd, *J* = 8.7, 6.8 Hz	7.95, 1H, dd, *J* = 8.7, 6.7 Hz
8	131.3	7.75, 1H, dd, *J* = 6.8, 1.0 Hz	7.80, 1H, dd, *J* = 6.7, 0.7 Hz
9	141.7	—	—
9a	141.9	—	—
10a	140.9	—	—
11	166.8	—	—
1′	30.8	4.17, 2H, d, *J* = 7.3 Hz	4.13, 2H, dd, *J* = 7.2, 7.2 Hz
2′	122.4	5.58, 1H, dddd, *J* = 7.3, 7.3, 1.0, 1.0 Hz	5.57, 1H, dddd, *J* = 7.2, 7.2, 1.2, 1.2 Hz
3′	135.7	—	—
4′	26.0	1.82, 3H, bs	1.73, 3H, bs
5′	18.1	1.80, 3H, bs	1.73, 3H, bs
1″	174.8	—	—
2″	54.0	4.96, 1H, dd, *J* = 9.1, 4.1 Hz	4.74, ddd, 1H, *J* = 8.7, 8.7, 3.9 Hz
2″-NH			10.9, d, *J* = 8.7 Hz
3″	29.8	2.18–2.30, $1H_a$, m 2.16–2.36, $1H_b$, m	1.93–2.09, $1H_a$, m 2.22–2.38, $1H_b$, m
4″	33.2	2.16–2.36, 2H, m	2.22–2.38, 2H, m
5″	177.4	—	—
5″-NH_2		—	6.73, $1H_a$, bs 7.27, $1H_b$, sb

not affect the total amount of prenylated phenazines formed, and we omitted it from the culture medium in all subsequent experiments.

The conversion of endophenazine A to endophenazine E was almost complete in strains M1146 and M1154, in contrast to strain M512 (Figure 2). In the former two strains, the entire biosynthetic gene clusters of actinorhodin, undecylprodigiosine and calcium-dependent antibiotic as well as the so-called *cpk* cluster have been deleted. However, it is unknown how these deletions are connected to the conversion of endophenazine A to endophenazine E.

Determination of the borders of the endophenazine cluster

The left side of the endophenazine gene cluster depicted in Figure 1 contains the phenazine prenyltransferase gene *ppzP* and, downstream thereof, the genes of the mevalonate pathway for supply of the isoprenoid precursor dimethylallyl diphosphate (DMAPP). Upstream of *ppzP*, four genes, *orf1*-*orf4,* could be identified. Database comparisons by using BLAST and Pfam searches gave no obvious clues as to whether or not they are involved in the biosynthesis of secondary metabolites. The gene *orf1* (1002 bp) showed similarities to serine proteases, and *orf2* (1029 bp) to aspartate-semialdehyde dehydrogenases. The gene *orf3* (348 bp) showed homology to transcriptional modulators of the PemK-like protein family [19]; PemK binds to the promoter region of the Pem operon in *E. coli.* Finally, *orf4* (2613 bp) showed homology to aminopeptidases.

λ-RED recombination was used to delete the entire coding sequence of *orf1* and the first 437 nucleotides of *orf2* from the insert of cosmid ppzOS04 (Figure 1). After recombination of the pIJ773 cassette harbouring an apramycin resistance gene, the disruption cassette was excised by FLP recombinase. The correct sequence of the resulting cosmid ppzOS21 was confirmed by restriction analysis and PCR. Cosmid ppzOS21 was introduced into *S. coelicolor* M512 by triparental mating, and stably integrated into the *attB* site of the genome. Three independent integration mutants were obtained, and their sec-

ondary metabolite production was investigated by HPLC in comparison to a strain harbouring the unmodified cosmid ppzOS04 (Table 3). Both strains produced similar amounts of prenylated phenazines (162 or 201 µmol/L, respectively), besides smaller amounts of nonprenylated phenazines. This proved that *orf1* and *orf2* are not required for the formation of endophenazines.

However, when we deleted a DNA fragment comprising all four genes from *orf1* to *orf4* by the same procedure, the resulting strain, i.e., *S. coelicolor* M512(ppzOS10) showed a strongly reduced formation of prenylated phenazines (23 µmol/L). At the same time, the production of nonprenylated phenazines was increased, indicating that the mutation affected the formation or attachment of the prenyl moiety of the endophenazines. Two alternative hypotheses may explain this observation: The regulatory gene *orf3* may be involved in the regulation of the prenylation; or the deletion of the entire *orf4* sequence may have affected the promoter of the prenyltransferase gene *ppzP*, which is situated downstream of *orf4*. In order to distinguish between these two possibilities, an additional λ-RED-mediated gene inactivation was carried out (Figure 1). The genes *orf1*, *orf2, orf3* and the first 1092 bp of *orf4* were deleted, resulting in cosmid ppzOS22. In this construct, the regulator *orf3* is deleted, but the promoter region of *ppzP* is expected to be intact, even if it would extend into the coding sequence of *orf4*. Integration of this cosmid into the heterologous expression host resulted in a strain, which again produced endophenazines (113 µmol/L) (Table 3). These results show that *orf3* and *orf4* are not essential for the production of prenylated phenazines. The strong reduction of prenylated phenazine production in mutant *S. coelicolor*(ppzOS10) is most likely due to the absence of *ppzP* promoter sequences located within the coding sequence of the gene *orf4*. In a previous study, we have already shown that deletion of the prenyltransferase gene *ppzP* results in a complete abolishment of the production of prenylated phenazines [11]. Therefore, *ppzP* (including its promoter region) may represent the left border of this cluster.

The right side of the endophenazine gene cluster depicted in Figure 1 contains the operon of phenazine biosynthesis genes, *ppzBCDEFGA*, oriented in the opposite direction to the mevalonate biosynthesis genes. Upstream of *ppzB*, seven genes are found (*ppzK* to *ppzR2*), the function of which is unclear. Orthologues for these seven genes, arranged in exactly the same order and orientation, were also identified next to the endophenazine gene cluster of *S. cinnamonensis* DSM 1042 [12].

The gene *ppzK* shows similarities to FAD-dependent oxidoreductases, and *ppzL* to ferredoxin. The gene *ppzY* is similar to the transcriptional regulator SCO3435 of *Streptomyces coelicolor* A3(2). The genes *ppzZ1* and *ppzZ2* have similarities to the two subunits of cytochrome d ubiquinol oxidase, and *ppzR1* and *ppzR2* to ABC transporters. The next gene, *orf12*, shows very high similarities to the primary metabolic enzyme allantoicase (allantoate amidohydrolase, EC 3.5.3.4), an enzyme of purine catabolism. It is separated from *ppzR2* by a gap of 1.3 kb and oriented in the opposite direction.

In order to determine the border of the gene cluster, we carried out three parallel inactivation experiments, in which either all genes from *ppzK* to *orf12*, or the genes from *ppzZ1* to *orf12*, or only the genes from *ppzR1* to *orf12* were deleted from cosmid ppzOS04, by using λ-RED recombination and the same procedure as described above. Analysis of the secondary metabolite production in the Δ*ppzR1-orf12* mutant showed that the formation of prenylated phenazines was reduced to 31 µmol/L, i.e., to approximately 17% of the amount formed in the strain with the

Table 3: Production of nonprenylated and of prenylated phenazines in the heterologous expression strain *Streptomyces coelicolor* M512, carrying either the complete endophenazine gene cluster (ppzOS04) or clusters in which individual genes had been deleted. Data represent mean values ±SD.

integrated construct	description	nonprenylated phenazines [µmol/L] (phenazine-1-carboxylic acid and phenazine-1-carboxylic acid methyl ester)	prenylated phenazines [µmol/L] (endophenazine A, B and E)
ppzOS04	complete cluster	17.8 ± 4.0	200.8 ± 42.7
ppzOS21	Δ(*orf1* − *orf2*)	6.7 ± 2.4	161.5 ± 35.9
ppzOS10	Δ(*orf1* − *orf4*)	54.9 ± 4.2	23.3 ± 1.6
ppzOS22	Δ(*orf1* − middle of *orf4*)	12.4 ± 1.9	112.8 ± 20.4
ppzOS23	Δ*ppzT*	7.3 ± 1.6	103.9 ± 16.8
ppzOS24	Δ(*ppzT* + *ppzU*)	6.1 ± 1.7	2.4 ± 0.9
ppzOS25	Δ*ppzV*	58.3 ± 21.0	<0.1
ppzOS26	Δ*ppzM*	4.5 ± 0.5	165.5 ± 60
ppzOS11	Δ(*ppzK* − *orf12*)	1.1 ± 0.3	0.4 ± 0.2
ppzOS27	Δ(*ppzZ1* − *orf12*)	17.5 ± 3.5	3.1 ± 1.07
ppzOS28	Δ(*ppzR1* − *orf12*)	14.8 ± 5.2	31.4 ± 5.1

intact cosmid; production of nonprenylated phenazines was similar in both strains. The most likely explanation of this result is that the ABC transporters encoded by *ppzR1* and *ppzR2* are involved in the export of endophenazines, and therefore their inactivation reduces but does not completely prevent the production of these compounds. In the Δ*ppzZ1-orf12* mutant, the production of prenylated phenazines was reduced even further (to 3.1 µmol/L), while the production of nonprenylated phenazines was similar to that of the strain with the intact cluster (17.5 µmol/L). This suggests that *ppzZ1* and *ppzZ2*, encoding proteins similar to the two subunits of prokaryotic cytochrome d ubiquinol oxidase, play a role in the formation of prenylated phenazines. Cytochrome d ubiquinol oxidase reduces ubiquinone to ubiquinol, a reaction similar to the reduction of PCA to 5,10-dihydro-PCA (Figure S3, Supporting Information File 1). The compound 5,10-dihydro-PCA, but not PCA, is the substrate for prenylation by the prenyltransferase PpzP [11]. This may explain why the deletion of *ppzZ1-ppzZ2* resulted in a reduced formation of prenylated phenazines.

In the Δ*ppzK-orf12* mutant, finally, the production of both prenylated and nonprenylated phenazines was nearly abolished. A possible explanation is that the putative regulatory gene *ppzY* plays a role in the regulation of phenazine biosynthesis. PpzY is similar to transcriptional regulators of the LysR family, the most abundant type of transcriptional regulators in the prokaryotic kingdom [20]. The LysR-like protein PqsR from *Pseudomonas* sp. M18 is involved in the regulation of phenazine biosynthesis. Inactivation of *pqsR* resulted in almost complete abolishment of the transcription of the phenazine biosynthesis genes [21]. It may therefore be speculated that *ppzY* codes for a positive regulator of PCA biosynthesis.

Based on these results, the large intergenic region between the ABC transporter gene *ppzR2* and the primary metabolic gene *orf12* (allantoicase) is likely to represent the right border of the endophenazine cluster.

Functional investigation of the four genes *ppzTUVM*, situated in the center of the endophenazine cluster

In between the mevalonate pathway genes and the dihydro-PCA biosynthesis genes, four further genes are situated, i.e., *ppzTUVM* (Figure 1). The gene *ppzM* (1023 bp) shows similarities to PhzM from *Pseudomonas aeruginosa* PAO1, a putative phenazine-specific methyltransferase that catalyzes the *N*-methylation reaction during the biosynthesis of pyocyanine in *Pseudomonas*. Also, *Streptomyces anulatus* produces an *N*-methylated phenazine, i.e., endophenazine B [22]. The heterologous expression strain *S. coelicolor* M512 containing the endophenazine cluster from *S. anulatus* produces very low amounts of endophenazine B, such that detection requires LC-MS analysis (Figure 4). We deleted *ppzM* using λ-RED recombination and the resulting construct, ppzOS26, was introduced into *S. coelicolor* M512. HPLC-UV analysis of cultures of the resulting strain showed a similar production of prenylated and nonprenylated phenazines to that observed in the strain with the intact cluster (Table 3). HPLC-ESI-MS analysis, however, revealed that the production of endophenazine B had been abolished by the *ppzM* deletion (Figure 4 and Figure S4, Supporting Information File 1). The gene *ppzM* is thereby the first phenazine *N*-methyltransferase gene identified in *Streptomyces*.

We expressed the protein PpzM in *E. coli* and purified it using Ni^{2+} affinity chromatography. However, incubation of PpzM

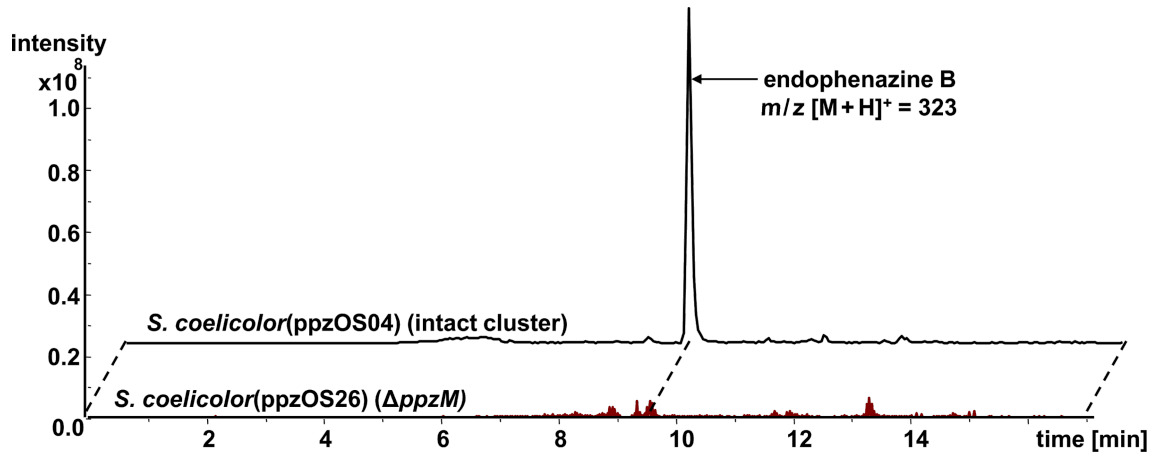

Figure 4: Extracted ion chromatograms for the mass of endophenazine B (*m*/*z* [M + H]$^+$ = 323) in *S. coelicolor* M512(ppzOS04), and the mutant *S. coelicolor* M512(ppzOS26). The deletion of the gene *ppzM* reveals the abolishment of the production of endophenazine B.

with *S*-adenosylmethionine and either PCA or dihydro-PCA did not result in the formation of any methylated derivatives. It has been reported that, likewise, PhzM from *P. aeroginosa* was not active when incubated with PCA and SAM alone; methylating activity was only detected when the hydroxylase PhzS and its cofactor NADH were also included in the incubation [23,24]. The endophenazine biosynthetic gene cluster from *S. anulatus* does not contain an orthologue of PhzS. Possibly, PpzM requires association with another protein for its activity, but it cannot be decided at present which protein this may be.

The function of *ppzT* (984 bp) was unknown when we first published the sequence of the endophenazine gene cluster [11]. The predicted protein PpzT showed similarities to putative 3-oxoacyl-[acyl-carrier-protein] synthases. Recently, Okamura et al. [25] proved that *nphT7*, a gene that is highly similar to *ppzT*, is responsible for catalysing the first step of the mevalonate pathway in naphterpin biosynthesis, i.e., the biosynthesis of acetoacetyl-CoA from malonyl-CoA and acetyl-CoA. In many other organisms, acetoacetyl-CoA for mevalonate biosynthesis is produced by a different reaction, i.e., by acetyl-CoA acetyltransferase (= acetoacetyl-CoA thiolase). We deleted *ppzT* from cosmid ppzOS04 and heterologously expressed the resulting cosmid ppzOS23. Analysis of the obtained strain showed that the formation of prenylated phenazines was reduced by approximately 50% in comparison to the strain containing the intact cluster. Since the heterologous host strain *S. coelicolor* M512 contains several putative acetyl-CoA acetyltransferase genes, which may generate acetoacetyl-CoA, a reduction, but not an abolishment, of the formation of prenylated phenazines was indeed the expected result after inactivation of *ppzT*. It should also be noted that *Streptomycetes* synthesize DMAPP for primary metabolism via the nonmevalonate pathway (MEP pathway), enabling a further route to prenylated phenazines in the Δ*ppzT* mutant [26].

The gene *ppzU* (348 bp) shows high similarity to flavodoxin from *Streptomyces roseosporus* NRRL 15998 and to the closely related flavoprotein WrbA from *Streptomyces flavogriseus* ATCC 33331. Flavodoxins are mobile electron carriers containing a flavin mononucleotide as the prosthetic group and mediating redox processes among a promiscuous set of donors and acceptors. For unknown reasons, the individual deletion of *ppzU* from cosmid ppzOS04 was unsuccessful. However, we did succeed in the deletion of the DNA fragment comprising both *ppzT* and *ppzU,* resulting in cosmid ppzOS24. Strains expressing this cosmid showed an almost complete abolishment of the production of prenylated phenazines, while the production of nonprenylated phenazine derivatives was not different from the Δ*ppzT* single mutant (Table 3). This suggests that *ppzU* plays a role for the prenylation in endophenazine biosynthesis. For instance, it could act as an electron carrier for the above-mentioned heterodimeric redox enzyme PpzZ1/PpzZ2, which may catalyze the reduction of PCA to 5,10-dihydro-PCA and thereby generate the substrate of the prenyltransferase PpzP. In *E. coli*, WrbA has been suggested to carry out a regulatory function in addition to its biochemical function [27], but this hypothesis is controversial [28].

The gene *ppzV* (621 bp) shows similarities in BLAST searches to *ovmZ*, a gene with unknown function in the biosynthetic gene cluster of oviedomycin from *Streptomyces antibioticus* [29]. Orthologs of *ovmZ* are found in the gene clusters of several prenylated secondary metabolites, e.g., *fnq22* in the furanonaphthoquinone/phenazine biosynthesis gene cluster from *Streptomyces cinnamonensis* [13], *napU1* in the napyradiomycin biosynthesis gene cluster from *S. aculeolatus* [30], and *fur18* in the biosynthetic gene cluster of furaquinocin A from *Streptomyces* sp. KO-3988 [31]. A similar gene, *aur1O*, is found in the biosynthetic gene cluster of the polyketide antibiotic auricin from *S. aureofaciens* [32]. The function of these proteins is unknown. Pfam searches do not show any match to known protein domains. Therefore, the possible function of *ppzV* was obscure. We deleted *ppzV* using λ-RED recombination and the resulting construct ppzOS25 was introduced into *S. coelicolor* M512. Unexpectedly, the resulting strains showed a nearly complete abolishment of the formation of prenylated phenazines, while the production of nonprenylated phenazines increased (Table 3). This suggests that *ppzV* inactivation had drastically and specifically affected the prenylation step in endophenazine biosynthesis. This prompted us to carry out further bioinformatic investigations on *ppzV*. We carried out a protein-fold recognition search using the Phyre server [33]. Unexpectedly, this showed that PpzV possesses protein-fold homology to the TetR family of transcriptional regulators. Members of the TetR-family, e.g., PsrA [34], are involved in the regulation of phenazine biosynthesis in *Pseudomonas* and in the regulation of the biosynthesis of many secondary metabolites in *Streptomyces*. It therefore appears likely that PpzV is a new member of the TetR transcriptional regulators, despite its low sequence similarity to previously characterized members of this group. Based on the results of our inactivation experiments, it is tempting to speculate that PpzV is a positive regulator of the transcription of the prenyltransferase gene *ppzP* and/or of the mevalonate pathway genes.

Conclusion

Our study showed that the endophenazine biosynthetic gene cluster comprises the 27 kb DNA region stretching from the phenazine prenyltransferase gene *ppzP* to the ABC transporters *ppzR1* and *ppzR2*. Inactivation experiments provided initial genetic insights into the regulation of phenazine biosynthesis in

Streptomyces. While the complicated network responsible for the regulation of phenazine biosynthesis in *Pseudomonas* has been investigated in some detail [9,21,34,35], in *Streptomyces* none of the regulatory genes involved in the biosynthesis of phenazines or prenylated phenazines have been identified previously. Our mutational study now shows the involvement of several regulatory genes in this pathway. The gene *ppzV*, coding for a new type of TetR-related regulator, is likely to regulate the prenylation of the phenazine core. The gene *ppzY*, coding for a LysR-type regulator, appears to regulate the biosynthesis of the phenazine core, although further studies are required to confirm its precise role. In contrast, *orf3*, which codes for a protein similar to transcriptional modulators of the PemK-like family, is not required for endophenazine biosynthesis and is apparently situated outside of the endophenazine biosynthetic gene cluster. Our inactivation experiments identified *ppzM* as the first phenazine *N*-methyltransferase gene investigated in *Streptomyces*. We identified a new phenazine natural product, endophenazine E, and elucidated its structure. Endophenazine E represents a conjugate between the prenylated phenazine, endophenazine A, and L-glutamine.

Experimental

Bacterial strains, plasmids, and culture conditions

S. anulatus 9663 was isolated previously from the gut of a wood louse [22]. It was grown in liquid YMG medium [36] or on solid MS medium [36]. For the production of secondary metabolites, the medium described by Sedmera et al. [37] was used. *Escherichia coli* XL1 Blue MRF, *E. coli* SURE (Stratagene, Heidelberg, Germany), *E. coli* BW 25113, and *E. coli* ET 12567 (pUB307) were used for cloning and were grown in liquid or on solid (1.5% agar) Luria-Bertani or SOB medium at 37 °C. The REDIRECT technology kit for PCR targeting was obtained from Plant Bioscience Limited (Norwich, UK). For inactivation experiments, the *aac*(3)IV/*ori*T (apramycin resistance) cassette from pIJ773 [38] was used. Carbenicillin (50–100 μg·mL^{-1}), apramycin (50 μg·mL^{-1}), kanamycin (50 μg·mL^{-1}), chloramphenicol (25 μg·mL^{-1}), and nalidixic acid (20 μg·mL^{-1}) were used for the selection of recombinant strains.

Chemicals

Kanamycin and carbenicillin were purchased from Genaxxon BioSciences GmbH (Biberach, Germany) and phenazine 1-carboxylic acid was from InFormatik. IPTG, Tris, NaCl, glycerol, dithiothreitol, $MgCl_2$, formic acid, sodium dodecyl sulfate, polyacrylamide, and EDTA were from Carl Roth, Karlsruhe, Germany. Apramycin, nalidixic acid, methanol, Tween 20 and imidazole were from Sigma Aldrich, Steinheim, Germany. Merck supplied chloramphenicol, dipotassium hydrogen phosphate, potassium dihydrogen phosphate, sodium carbonate, sodium hydrogen carbonate and β-mercaptoethanol. Lysozyme was from Boehringer Ingelheim, Heidelberg, Germany.

Genetic procedures

Standard methods for DNA isolation and manipulation were performed as described by Kieser et al. [36] and Sambrook et al. [39]. DNA fragments were isolated from agarose gels by using a PCR purification kit (Amersham Biosciences). Genomic DNA was isolated by lysozyme treatment and phenol/chloroform extraction as described by Kieser et al. [36]. The construction, screening and heterologous expression of the phenazine biosynthetic gene cluster from *S. anulatus* was previously described [11].

Construction of cosmids ppzOS10, ppzOS11, ppzOS21-28

An apramycin resistance cassette (*aac(3)IV*) was amplified from plasmid pUG019 [40] using the corresponding primers mentioned in Table S2. The resulting 1077-bp PCR product was used to replace the desired genes on cosmid ppzOS04 by λ-RED-mediated recombination. Deletion of the *aac(3)IV* cassette from the resulting cosmids was carried out by using FLP-recombinase [41]. The resulting constructs were introduced into *S. coelicolor M512* by triparental mating [36].

Production and analysis of secondary metabolites

Culture methods and analysis techniques were adapted from Saleh et al. [11]. For the culture in Erlenmyer flasks, exconjugants of all mutants as well as wild type *S. anulatus* were precultured for 48 h in liquid YMG medium (50 mL). Then, 50 mL of production medium was inoculated with 2.5 mL of the precultures. The flasks were agitated on a rotary shaker at 30 °C and 200 rpm for 72–120 h.

For isolation of endophenazine A and endophenazine E, mycelia from 50 mL cultures were centrifuged at 3500 × *g* for 10 min. The cells were extracted with methanol (10 mL) by vortexing. The extract was mixed with sodium acetate buffer (10 mL; 1 M, pH 4.0) and extracted with dichloromethane (5 mL). After separation of the organic phase, the solvent was evaporated, and the residue was redissolved in methanol (0.5 mL). For the extraction of nonprenylated phenazines, the supernatant of the 50 mL cultures was adjusted to pH 4.0 by using 1 M HCl and extracted with 50 mL ethylacetate. After vortexing, the organic solvent was evaporated and the residue was dissolved in 500 μL methanol.

For the production in 24 square deep-well plates, homogenized and frozen inoculums, as described by Siebenberg et al. [14], were prepared from each mutant, inoculated into 3 mL of

production media in each deep well and incubated for five days at 30 °C. For the analysis of the secondary metabolites, 1 mL was extracted as described above and analyzed by HPLC. For the analysis of the secondary metabolite profile over time, 100 µL from each deep well was collected after three, five and seven days and extracted as described above.

The extracts from supernatant and from mycelia were analyzed with HPLC (Agilent 1200 series; Waldbronn, Germany) by using an Eclipse XDB-C18 column (4.6 × 150 mm, 5 µm; Agilent) at a flow rate of 1 mL·min^{-1} with a linear gradient from 40 to 100% of solvent B in 20 min (solvent A: water/formic acid (999:1); solvent B, methanol) and detection at 252 and 365 nm. Additionally, a UV spectrum from 200 to 400 nm was logged by a photodiode array detector. The absorbance at 365 nm was used for quantitative analysis, employing an authentic reference sample of PCA as the external standard.

Analysis by LC–MS

The extracts were examined with LC–MS and LC–MS^2 analysis by using a Nucleosil 100-C_{18} column (2 × 100 mm, 3 µm) coupled to an ESI mass spectrometer (LC/MSD Ultra Trap System XCT 6330; Agilent Technology). Analysis was carried out at a flow rate of 0.4 mL·min^{-1} with a linear gradient from 10 to 100% of solvent B in 15 min (solvent A: water/formic acid (999:1); solvent B: acetonitrile/formic acid (999.4:0.6)). Detection was carried out at 230, 260, 280, 360, and 435 nm. Electrospray ionization (positive and negative ionization) in Ultra Scan mode with capillary voltage of 3.5 kV and drying gas temperature of 350 °C was used for LC–MS analysis. For LC–MS^2 and LC–MS^3, the analysis was carried out in positive ionization mode with a capillary voltage of 3.5 kV at 350 °C.

Preparative isolation of endophenazine E

The strain *S. coelicolor*(ppzOS04) was precultured in 500 mL production medium for 48 h at 27 °C. This culture was inoculated into a 10 L fermenter containing the same production media and grown at 27 °C for 144 h. The cultures were then filtrated under vacuum by using 3% celite. The mycelia supernatant was discarded and the mycelia was extracted with methanol/acetone (1:1). The extract was concentrated in vacuo to an aqueous residue, adjusted to pH 4.0 by using HCl and extracted with ethyl acetate. The ethyl acetate extract was first treated with petrol ether. After evaporation, the extract residue was fractioned by using a liquid chromatography system with a Sephadex LH20 column (2.5 × 90 cm) and methanol as the mobile phase. The fractions containing endophenazine E as the main product were pooled and the solvents were evaporated. The residue was redissolved in methanol and applied to a preparative HPLC system with Reprosil Basic C18 column (250 × 20 mm). The separation was carried out with a linear gradient from 70 to 85% of solvent B in 15 min (solvent A: water/formic acid (999:1); solvent B: methanol) and the fractions containing pure endophenazine E were pooled and dried by lyophilisation, resulting in 50 mg of pure endophenazine E being extracted.

Identification of the stereochemical configuration of endophenazine E

The configuration of the amino acid glutamine in the structure of PCA-Gln was determined as described by Lämmerhofer and Lindner [16], by using an enantioselective HPLC system with two complementary chiral columns, which contained either quinine (QN) or quinidine (QD) derivatives as chiral selectors. To produce reference substances, 5 mg *N*,*N*′-dicyclohexylcarbodiimide (DCC) dissolved in 10 µL acetonitrile was added to 1 mg endophenazine A in 200 µL acetonitrile. The tube was heated to 60 °C for 1 h. Then, 2 mg *N*-hydroxysuccinimide, dissolved in 10 µL acetonitrile, was added to the reaction. The mixture was kept at 60 °C for 24 h. After being cooled to room temperature, acetonitrile was added to give a final volume of 300 µL. To a 100 µL aliquot of this solution, 1 mg D-glutamine in 100 µL carbonate buffer (0.1 M $NaHCO_3$/0.1 M Na_2CO_3; 2:1 (v/v)) was added. To a further aliquot of 100 µL, 1 mg L-glutamine in 100 µL carbonate buffer was added. To a third aliquot of 50 µL, 50 µL carbonate buffer without glutamine was added. All three tubes were kept at 25 °C for three days and subsequently air dried at 25 °C. The residues were taken up in 100 µL MeOH and analysed by HPLC by using Chiralpak QN-AX and Chiralpak QD-AX columns (5 µm, 150 × 4 mm ID) (Chiral Technologies Europe, Illkirch, France). A mixture of methanol/acetic acid/ammonium acetate (99:1:0.25 (v/v/w)) was used as the mobile phase with an isocratic flow rate of 1 mL·min^{-1} and a column temperature of 25 °C. UV detection was carried out at 220, 250, 350 and 370 nm. On the QN-AX and QD-AX columns, the isolated compound PCA-Gln showed retention times of 9.3 min and 7.5 min, respectively, identical to the reference compound synthesized from L-Gln.

Overexpression and purification of PpzM Protein

Analogous to the method used for PpzP protein by Saleh et al. [11], the gene *ppzM* was amplified by using the primers *ppzM*_pHis_F (5′- CCG CCC ATG AGG AGA GGA TCC ATG AGT ACC GAC ATC GCA C-3′) and *ppzM*_pHis_R (5′- GTC GCC GGC CGT CGG CAC CTC GAG GTC AGC CGG CCG GGG TCA GG -3′). The underlined letters represent BamHI and XhoI restriction sites, respectively. The resulting PCR fragment was digested with BamHI and XhoI and ligated into plasmid pHis8 [42], digested with the same restriction enzymes. The resulting plasmid, pHis8-OS03, was verified by restriction mapping and sequencing. *E. coli* BL21(DE3)pLysS cells harbouring plasmid pHis8-OS03 were cultivated in 2 L of liquid TB medium containing 50 µg·mL^{-1} kanamycin and

grown at 37 °C to an A_{600} of 0.6. The temperature was lowered to 20 °C, and isopropyl-1-thio-β-D-galactopyranoside was added to a final concentration of 0.5 mM. The cells were cultured for a further 10 h at 20 °C and harvested. Then, 30 mL of lysis buffer (50 mM Tris-HCl, pH 8.0, 1 M NaCl, 10% glycerol, 10 mM β-mercaptoethanol, 20 mM imidazole, 0.5 mg·mL^{-1} lysozyme, 0.5 mM phenylmethylsulfonyl fluoride) was added to the pellet (40 g). After being stirred at 4 °C for 30 min, cells were ruptured with a Branson sonifier at 4 °C. The lysate was centrifuged (55,000 × *g*, 45 min). Affinity chromatography with 4 mL of Ni^{2+}-nitrilotriacetic acid-agarose resin (Qiagen, Hilden, Germany) was carried out according to the manufacturer's instructions, by using 2 × 2.5 mL of 250 mM imidazole (in 50 mM Tris-HCl, pH 8.0, 1 M NaCl, 10% glycerol, 10 mM β-mercaptoethanol) for elution. Subsequently, a buffer exchange was carried out by PD10 columns (Amersham Biosciences), which were eluted with 50 mM Tris-HCl, pH 8.0, 1 M NaCl, 10% glycerol, and 2 mM 1,4-dithiothreitol. Approximately 30 mg of purified PpzM was obtained from 2 L of cultures.

Supporting Information

Supporting Information File 1

Analytical data, complete list of genes in cosmid ppzOS04, and PCR primers.
[http://www.beilstein-journals.org/bjoc/content/supplementary/1860-5397-8-57-S1.pdf]

Acknowledgements

We thank Nadja Burkard and Stefanie Grond for the NMR analysis, Dorothee Wistuba for HRMS analysis, and Stefan Polnick and Michael Lämmerhofer for the determination of the configuration of glutamine in the structure of endophenazine E. This work was supported by a grant from the German Ministry for Education and Research (BMBF/ERA-IB, Project GenoDrug) (to L. H.) and by a scholarship from Tishrin University, Syria (to O. S.).

References

1. Laursen, J. B.; Nielsen, J. *Chem. Rev.* **2004,** *104,* 1663–1686. doi:10.1021/cr020473j
2. Mavrodi, D. V.; Bonsall, R. F.; Delaney, S. M.; Soule, M. J.; Phillips, G.; Thomashow, L. S. *J. Bacteriol.* **2001,** *183,* 6454–6465. doi:10.1128/JB.183.21.6454-6465.2001
3. Mavrodi, D. V.; Blankenfeldt, W.; Thomashow, L. S. *Annu. Rev. Phytopathol.* **2006,** *44,* 417–445. doi:10.1146/annurev.phyto.44.013106.145710
4. Ahuja, E. G.; Janning, P.; Mentel, M.; Graebsch, A.; Breinbauer, R.; Hiller, W.; Costisella, B.; Thomashow, L. S.; Mavrodi, D. V.; Blankenfeldt, W. *J. Am. Chem. Soc.* **2008,** *130,* 17053–17061. doi:10.1021/ja806325k
5. McDonald, M.; Mavrodi, D. V.; Thomashow, L. S.; Floss, H. G. *J. Am. Chem. Soc.* **2001,** *123,* 9459–9460. doi:10.1021/ja011243+
6. Mavrodi, D. V.; Peever, T. L.; Mavrodi, O. V.; Parejko, J. A.; Raaijmakers, J. M.; Lemanceau, P.; Mazurier, S.; Heide, L.; Blankenfeldt, W.; Weller, D. M.; Thomashow, L. S. *Appl. Environ. Microbiol.* **2010,** *76,* 866–879. doi:10.1128/AEM.02009-09
7. Pierson, L. S.; Pierson, E. A. *Appl. Microbiol. Biotechnol.* **2010,** *86,* 1659–1670. doi:10.1007/s00253-010-2509-3
8. Girard, G.; van Rij, E. T.; Lugtenberg, B. J. J.; Bloemberg, G. V. *Microbiology (Reading, U. K.)* **2006,** *152,* 43–58. doi:10.1099/mic.0.28284-0
9. Girard, G.; Barends, S.; Rigali, S.; van Rij, E. T.; Lugtenberg, B. J. J.; Bloemberg, G. V. *J. Bacteriol.* **2006,** *188,* 8283–8293. doi:10.1128/JB.00893-06
10. Ge, Y.; Yang, S.; Fang, Y.; Yang, R.; Mou, D.; Cui, J.; Wen, L. *FEMS Microbiol. Lett.* **2007,** *268,* 81–87. doi:10.1111/j.1574-6968.2006.00562.x
11. Saleh, O.; Gust, B.; Boll, B.; Fiedler, H. P.; Heide, L. *J. Biol. Chem.* **2009,** *284,* 14439–14447. doi:10.1074/jbc.M901312200
12. Seeger, K.; Flinspach, K.; Haug-Schifferdecker, E.; Kulik, A.; Gust, B.; Fiedler, H. P.; Heide, L. *Microb. Biotechnol.* **2011,** *4,* 252–262. doi:10.1111/j.1751-7915.2010.00234.x
13. Haagen, Y.; Glück, K.; Fay, K.; Kammerer, B.; Gust, B.; Heide, L. *ChemBioChem* **2006,** *7,* 2016–2027. doi:10.1002/cbic.200600338
14. Siebenberg, S.; Bapat, P. M.; Lantz, A. E.; Gust, B.; Heide, L. *J. Biosci. Bioeng.* **2010,** *109,* 230–234. doi:10.1016/j.jbiosc.2009.08.479
15. Gomez-Escribano, J. P.; Bibb, M. J. *Microb. Biotechnol.* **2011,** *4,* 207–215. doi:10.1111/j.1751-7915.2010.00219.x
16. Lämmerhofer, M.; Lindner, W. Liquid Chromatographic Enantiomer Separation and Chiral Recognition by Cinchona Alkaloid-Derived Enantioselective Separation Materials. In *Advances in Chromatography;* Grinberg, N.; Grushka, E., Eds.; CRC Press: Boca Raton, FL, 2008; Vol. 46, pp 1–107. doi:10.1201/9781420060263.ch1
17. Gilpin, M. L.; Fulston, M.; Payne, D.; Cramp, R.; Hood, I. *J. Antibiot.* **1995,** *48,* 1081–1085. doi:10.7164/antibiotics.48.1081
18. Schulz, D.; Nachtigall, J.; Riedlinger, J.; Schneider, K.; Poralla, K.; Imhoff, J. F.; Beil, W.; Nicholson, G.; Fiedler, H.-P.; Süssmuth, R. D. *J. Antibiot.* **2009,** *62,* 513–518. doi:10.1038/ja.2009.64
19. Masuda, Y.; Miyakawa, K.; Nishimura, Y.; Ohtsubo, E. *J. Bacteriol.* **1993,** *175,* 6850–6856.
20. Maddocks, S. E.; Oyston, P. C. F. *Microbiology (Reading, U. K.)* **2008,** *154,* 3609–3623. doi:10.1099/mic.0.2008/022772-0
21. Lu, J.; Huang, X.; Li, K.; Li, S.; Zhang, M.; Wang, Y.; Jiang, H.; Xu, Y. *J. Biotechnol.* **2009,** *143,* 1–9. doi:10.1016/j.jbiotec.2009.06.008
22. Gebhardt, K.; Schimana, J.; Krastel, P.; Dettner, K.; Rheinheimer, J.; Zeeck, A.; Fiedler, H.-P. *J. Antibiot.* **2002,** *55,* 794–800. doi:10.7164/antibiotics.55.794
23. Greenhagen, B. T.; Shi, K.; Robinson, H.; Gamage, S.; Bera, A. K.; Ladner, J. E.; Parsons, J. F. *Biochemistry* **2008,** *47,* 5281–5289. doi:10.1021/bi702480t
24. Parsons, J. F.; Greenhagen, B. T.; Shi, K.; Calabrese, K.; Robinson, H.; Ladner, J. E. *Biochemistry* **2007,** *46,* 1821–1828. doi:10.1021/bi6024403

25. Okamura, E.; Tomita, T.; Sawa, R.; Nishiyama, M.; Kuzuyama, T. *Proc. Natl. Acad. Sci. U. S. A.* **2010,** *107,* 11265–11270. doi:10.1073/pnas.1000532107
26. Kuzuyama, T.; Seto, H. *Nat. Prod. Rep.* **2003,** *20,* 171–183. doi:10.1039/B109860H
27. Yang, W.; Ni, L.; Somerville, R. L. *Proc. Natl. Acad. Sci. U. S. A.* **1993,** *90,* 5796–5800.
28. Grandori, R.; Khalifah, P.; Boice, J. A.; Fairman, R.; Giovanielli, K.; Carey, J. *J. Biol. Chem.* **1998,** *273,* 20960–20966. doi:10.1074/jbc.273.33.20960
29. Lombó, F.; Braña, A. F.; Salas, J. A.; Méndez, C. *ChemBioChem* **2004,** *5,* 1181–1187. doi:10.1002/cbic.200400073
30. Winter, J. M.; Moffitt, M. C.; Zazopoulos, E.; McAlpine, J. B.; Dorrestein, P. C.; Moore, B. S. *J. Biol. Chem.* **2007,** *282,* 16362–16368. doi:10.1074/jbc.M611046200
31. Kawasaki, T.; Hayashi, Y.; Kuzuyama, T.; Furihata, K.; Itoh, N.; Seto, H.; Dairi, T. *J. Bacteriol.* **2006,** *188,* 1236–1244. doi:10.1128/JB.188.4.1236-1244.2006
32. Novakova, R.; Homerova, D.; Feckova, L.; Kormanec, J. *Microbiology (Reading, U. K.)* **2005,** *151,* 2693–2706. doi:10.1099/mic.0.28019-0
33. Kelley, L. A.; Sternberg, M. J. E. *Nat. Protoc.* **2009,** *4,* 363–371. doi:10.1038/nprot.2009.2
34. Chin-A-Woeng, T. F. C.; van den Broek, D.; Lugtenberg, B. J. J.; Bloemberg, G. V. *Mol. Plant-Microbe Interact.* **2005,** *18,* 244–253. doi:10.1094/MPMI-18-0244
35. Heeb, S.; Haas, D. *Mol. Plant-Microbe Interact.* **2001,** *14,* 1351–1363. doi:10.1094/MPMI.2001.14.12.1351
36. Kieser, T.; Bibb, M. J.; Buttner, M. J.; Chater, K. F.; Hopwood, D. A. *Practical Streptomyces genetics;* John Innes Foundation: Norwich, UK, 2000.
37. Sedmera, P.; Pospíšil, S.; Novák, J. *J. Nat. Prod.* **1991,** *54,* 870–872. doi:10.1021/np50075a022
38. Gust, B.; Chandra, G.; Jakimowicz, D.; Yuqing, T.; Bruton, C. J.; Chater, K. F. *Adv. Appl. Microbiol.* **2004,** *54,* 107–128. doi:10.1016/S0065-2164(04)54004-2
39. Sambrook, J.; Russell, D. W. *Molecular Cloning. A Laboratory Manual;* Cold Spring Harbor Laboratory Press: New York, 2001.
40. Eustáquio, A. S.; Gust, B.; Galm, U.; Li, S.-M.; Chater, K. F.; Heide, L. *Appl. Environ. Microbiol.* **2005,** *71,* 2452–2459. doi:10.1128/AEM.71.5.2452-2459.2005
41. Gust, B.; Challis, G. L.; Fowler, K.; Kieser, T.; Chater, K. F. *Proc. Natl. Acad. Sci. U. S. A.* **2003,** *100,* 1541–1546. doi:10.1073/pnas.0337542100
42. Jez, J. M.; Ferrer, J.-L.; Bowman, M. E.; Dixon, R. A.; Noel, J. P. *Biochemistry* **2000,** *39,* 890–902. doi:10.1021/bi991489f

License and Terms

Beilstein Journal of Organic Chemistry

Synthesis of szentiamide, a depsipeptide from entomopathogenic *Xenorhabdus szentirmaii* with activity against *Plasmodium falciparum*

Friederike I. Nollmann[1], Andrea Dowling[2,§], Marcel Kaiser[3,§], Klaus Deckmann[4,§], Sabine Grösch[4,§], Richard ffrench-Constant[2,§] and Helge B. Bode[*1]

Letter

Open Access

Address:
[1]Stiftungsprofessur für Molekulare Biotechnologie, Institut für Molekulare Biowissenschaften, Goethe Universität Frankfurt, Max-von-Laue-Straße 9, D-60438 Frankfurt a. M., Germany, [2]Biosciences, University of Exeter in Cornwall, Tremough Campus, Penryn, Cornwall TR10 9EZ, United Kingdom, [3]Swiss Tropical and Public Health Institute, Parasite Chemotherapy, Socinstr. 57, P.O. Box, CH-4002 Basel, Switzerland and [4]Institut für klinische Pharmakologie, Uniklinik Frankfurt, Theodor-Stern-Kai 7, D-60590 Frankfurt a. M., Germany

Email:
Helge B. Bode[*] - h.bode@bio.uni-frankfurt.de

* Corresponding author
§ Bioactivity testing

Keywords:
cyclic depsipeptide; esterification; natural product; szentiamide; *Xenorhabdus*

Beilstein J. Org. Chem. **2012,** *8,* 528–533.
doi:10.3762/bjoc.8.60

Received: 08 February 2012
Accepted: 15 March 2012
Published: 11 April 2012

This article is part of the Thematic Series "Biosynthesis and function of secondary metabolites".

Guest Editor: J. S. Dickschat

Abstract

The synthesis of the recently characterized depsipeptide szentiamide (**1**), which is produced by the entomopathogenic bacterium *Xenorhabdus szentirmaii*, is described. Whereas no biological activity was previously identified for **1**, the material derived from the efficient synthesis enabled additional bioactivity tests leading to the identification of a notable activity against insect cells and *Plasmodium falciparum*, the causative agent of malaria.

Introduction

Bacteria of the genus *Xenorhabdus* live in symbiosis with nematodes of the genus *Steinernema* and together they form an entomopathogenic complex that can infect and kill several insect larvae. During this complex life cycle the bacteria produce secondary metabolites, which may be involved in and/or may be required for different stages of this life cycle, including the symbiotic stage (towards the nematode) or pathogenic stage (towards the insect prey) [1-3]. Until three years ago, the natural products extracted from *Xenorhabdus* and its close neighbour *Photorhabdus* were only low-molecular-weight

compounds with UV chromophores (e.g., isopropylstilbenes [4], anthraquinones [4], or xenorhabdines [5]. However, bioactivity-based or MS-based screening of crude extracts and culture supernatants led to the identification of larger compounds, such as the PAX peptides [6], the xenortides [7], xenematide [8] and the GameXPeptides [9]. Analysis of the genome sequences of the fully sequenced members of *Xenorhabdus* and *Photorhabdus* [10,11] has revealed that several additional compounds and especially even much larger compounds await isolation and structure elucidation. Recently, szentiamide (**1**) has been isolated, representing only the second depsipeptide (Figure 1) from these bacteria [12]. It is composed of six amino acids having a formylated *N*-terminus and raised our interest as it is produced by *X. szentirmaii*, whose crude extract shows a very high biological activity in several different bioassays (unpublished data). Nevertheless, no bioactivity has been described for **1** so far. Since we believe that **1** must have a biological function that is simply awaiting its identification, and since the peptide can only be found in small amounts when *X. szentirmaii* is grown in Luria–Bertani media, we wanted to synthesize it and make it accessible for additional bioactivity tests.

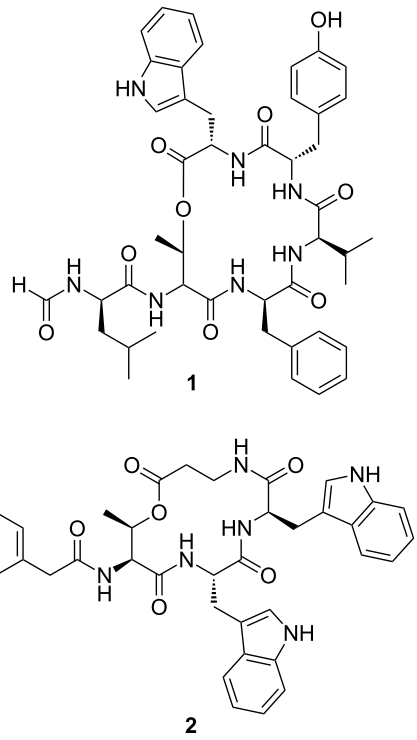

Figure 1: Structure of depsipeptides szentiamide (**1**) [12] and xenematide (**2**) [8] identified in *Xenorhabdus* strains.

Results and Discussion

Synthesis

As previous syntheses of depsipeptides showed that lactamization was preferred over lactonization [13,14], the synthesis of **1** was performed as follows: briefly, the linear peptide was synthesized using solid-phase peptide synthesis, followed by esterification and subsequent cleavage from the resin, deprotection and cyclization to yield **1**, assisted by microwave irradiation at every stage with the exception of the esterification (Scheme 1).

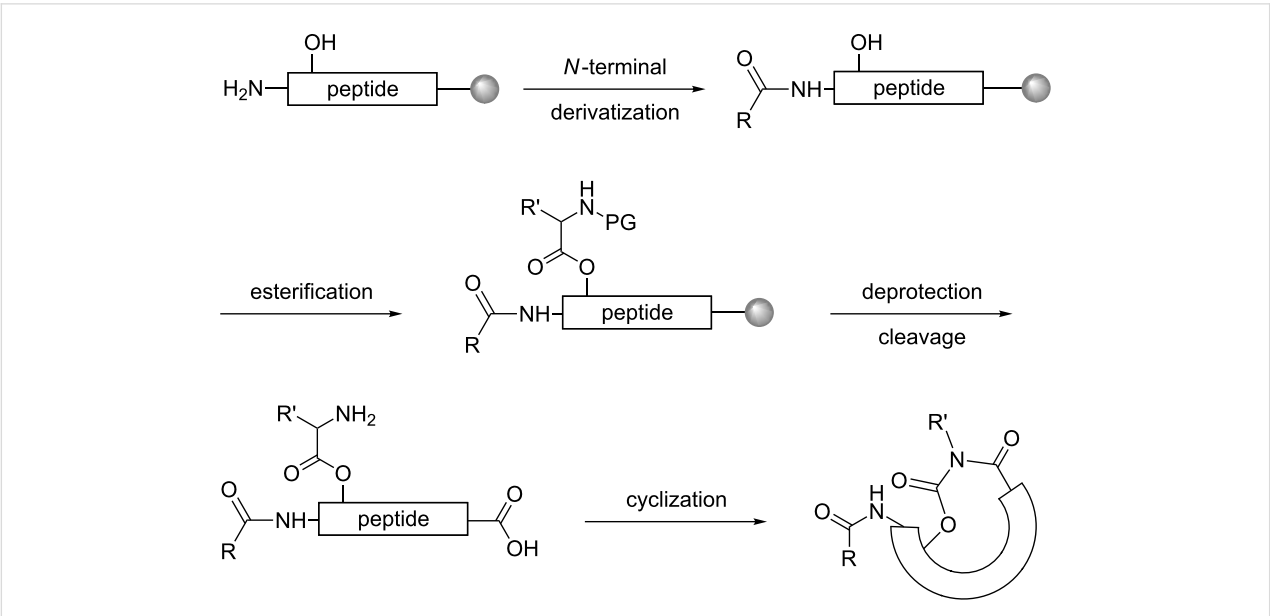

Scheme 1: Overview of the synthetic strategy.

In detail, a preloaded 2-chlorotrityl chloride resin was used in order to avoid nonspecific interaction in the cyclization process. Prior to the synthesis, the resin was reactivated [15] and then loaded with Fmoc-L-Tyr(*t*-Bu)-OH [16], followed by the build-up of the linear sequence **3** (Scheme 2) with *O*-benzotriazole-*N,N,N',N'*-tetramethyluronium hexafluorophosphate (HBTU) in dimethylformamide (DMF) and *N*,*N*-diisopropylethylamine (DIEA) in *N*-methylpyrrolidone (NMP), assisted by microwave irradiation. After the final Fmoc-deprotection with 20% piperidine in DMF, the *N*-terminus was formylated with *para*-nitrophenyl formate (*p*NPF) in the presence of *N*-methylmorpholine (NMM) at 4 °C, affording the synthetic intermediate **4**.

The attempts to form the ester bond by using catalytic amounts of 4-dimethylaminopyridine (DMAP) with 1-ethyl-3-(3-dimethylaminopropyl)carbodiimide (EDC), DMAP together with *N,N'*-diisopropylcarbodiimide (DIC), or a mixture of the DMAP hydrochloride and DMAP together with DIC all turned out to be unsuccessful. However, we were then able to establish the ester bond in **5** using modified Yamaguchi conditions [17]. Subsequently, the Fmoc-protecting group was removed at room temperature, and the peptide was cleaved from the resin with 3% hexafluoroisopropanol (HFIP) in dichloromethane (DCM) in order to preserve the side-chain protecting group. Following this, the peptide was cyclized in solution by using *O*-(7-azabenzotriazol-1-yl)-*N,N,N',N'*-tetramethyluronium hexafluorophosphate (HATU) and DIEA in DMF, assisted by microwave irradiation. Afterwards, the remaining side-chain protecting group was removed by incubation with a common cleavage cocktail for 60 min at room temperature to give the crude product **1**, which was purified by preparative reversed-phase HPLC (yield: 14% from the resin (B = 0.84 mmol/g)). In order to compare the synthetic to the natural product we isolated **1** from *Xenorhabdus szentirmaii* DSM 16338 as described previously [12]. Briefly, the strain was cultivated in a shake flask containing Luria–Bertani media and 2% Amberlite XAD-16 adsorber resin. After cultivation for three days at 30 °C, the resin was collected and the bound substances were eluted with methanol (MeOH) repeatedly. The resulting brown, oily crude extract was fractionated by normal-phase flash chromatography, followed by the isolation of compound **1** by preparative reversed-phase HPLC. In contrast to already published data [12] we were able to isolate 26.8 mg from a 2 L culture, which corresponds to a yield of 0.015 % (m/v). Thus, the addition of Amberlite XAD-16 adsorber resin led to a 150-fold increase of the production of **1** in comparison to cultures cultivated without XAD-16 [12]. In fact the productivity was even higher, since it was obtained from a three-day instead of the described eight-day cultivation of *X. szentirmaii*. Comparison of the LC–MS (Figure 2b and c) and NMR data (Figure S1, S2 and Table S1 in Supporting Information File 1) proved the synthetic **1** to be identical to the natural product.

Biological testing

The cyclic depsipeptide **1** was tested against different Gram-positive (*Micrococcus luteus, Bacillus subtilis, Staphylococcus aureus*) and Gram-negative (*Escherichia coli, Pseudomonas aeroginosa*) bacteria, as well as yeast (*Candida albicans, Saccharomyces cerivisiae*). However, consistent with the published data [12], no antibacterial or antifungal activity was detected. Additionally, the peptide **1** was tested against several parasites (*Trypanosoma brucei rhodesiense, Trypanosoma*

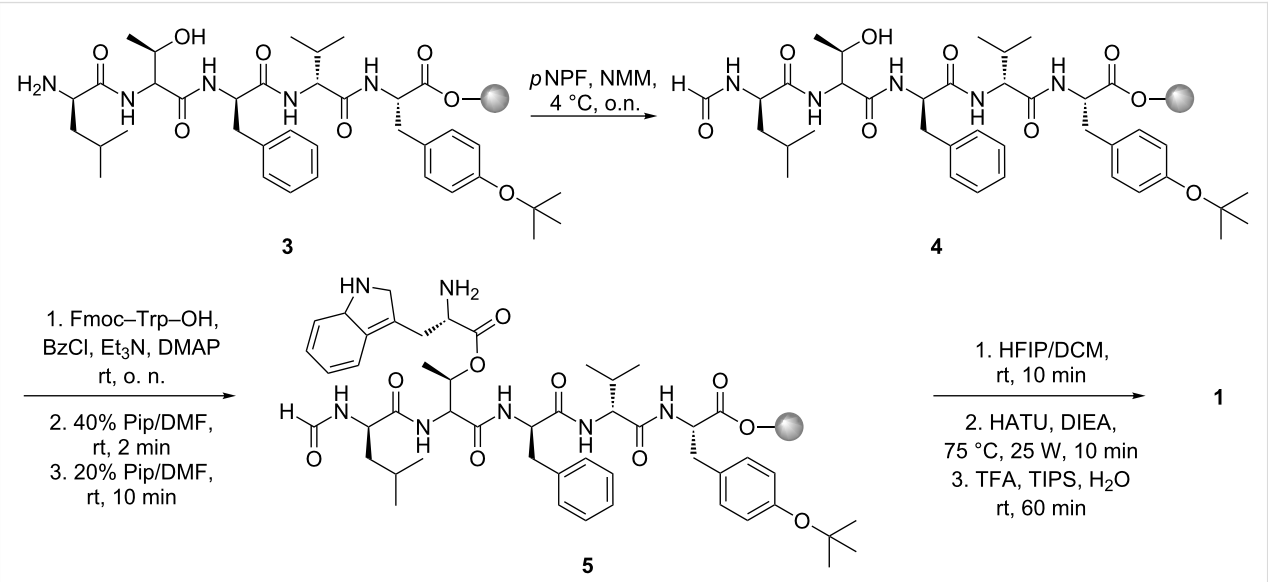

Scheme 2: Synthesis of compound **1**.

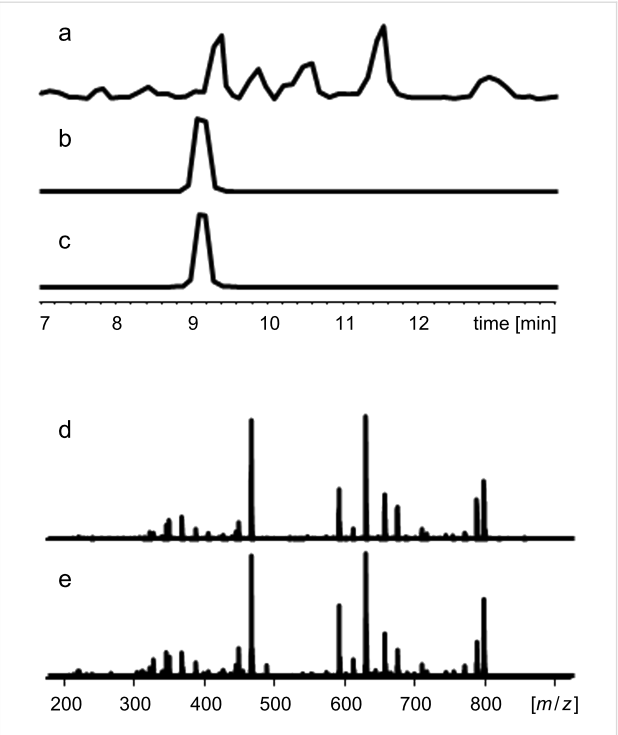

Figure 2: HPLC–MS data of an XAD-extract of *X. szentirmaii* (a; base-peak chromatogram), the natural **1** (b; extracted-ion chromatogram) and synthetic **1** (c; extracted-ion chromatogram) with their MS^2-spectra (d, natural **1**, and e, synthetic **1**).

cruzi, Leishmania donovani, Plasmodium falciparum) being the causative agents of the neglected tropical diseases [18] sleeping sickness, leishmaniasis and malaria. Interestingly, a good activity against the malaria-causing parasite *P. falciparum* (IC_{50} = 0.995 µg/mL) was observed, but only a 50- to 80-fold weaker cytotoxicity (L6 cells, IC_{50} = 57.4 µg/mL and HeLa cells, IC_{50} > 80 µg/mL). Only a weak activity was observed against *T. b. rhodesiense* and *L. donovani* with IC_{50} = 10.0 µg/mL and IC_{50} = 11.0 µg/mL, respectively. Additionally, we also tested **1** against hemocytes of *Galleria mellonella* and could detect a LD_{50} value of 59.7 µg/mL.

Conclusion

The establishment of an efficient synthesis route for the depsipeptide szentiamide (**1**) from *X. szentirmaii* revealed its biological activity against insect cells and protists such as *P. falciparum*. The rationale behind this bioactivity may be that **1** adds to the overall insecticidal activity of *Xenorhabdus* bacteria. Protists such as amoeba are common soil inhabitants, which may feed on the dead insect cadaver. Thus, compounds such as **1** may protect the insect cadaver against these food competitors and "accidentally" may also target pathogenic protists such as *Plasmodium*, which is a global human threat. Therefore, the bioactivity of **1** revealed in this study highlights the potential of *Xenorhabdus* bacteria as producers of bioactive natural products and the importance of a broad bioactivity testing of isolated compounds in order to find a biological activity and thus a biological function of such natural products. Work in the Bode lab currently concentrates on the identification of the mode of action of **1** in insects and protists in order to also understand its molecular function.

Experimental

Synthesis

Unless otherwise stated, we used the chemicals in their highest available purity. The progress of the synthesis was monitored with MALDI–MS as well as RP-UPLC coupled with ESI–MS.

Solid-phase peptide synthesis. The linear sequence was synthesized on a preloaded 2-chlorotrityl chloride resin (Carbolution Chemicals, Germany) on a 50 µmol scale with the Discover CEM System by using standard 9-fluorenylmethoxycarbonyl/*tert*-butyl (Fmoc/*t*-Bu) chemistry. An amount of 6 equiv of amino-acid derivatives (>98%; Iris Biotech, Germany/Carbolution Chemicals; *c* = 0.2 mol/L) was activated in situ with 5 equiv *O*-benzotriazole-*N,N,N′,N′*-tetramethyluronium hexafluorophosphate (HBTU; Iris Biotech) in dimethylformamide (DMF; Acros Organics, Belgium; *c* = 0.5 mol/L) in the presence of 10 equiv *N*,*N*-diisopropylethylamine (DIEA; Novabiochem, Darmstadt, Germany) in *N*-methylpyrrolidone (NMP; VWR, Germany; *c* = 2 mol/L). Fmoc protecting groups were cleaved with 20% piperidine in DMF by using microwave irradiation as well.

Formylation. The free *N*-terminus was formylated with 5 equiv *para*-nitrophenyl formate (*p*NPF; Sigma Aldrich, Germany) and 3 equiv *N*-methylmorpholine (NMM; Sigma Aldrich, Germany) in DMF (*c* = 12.5 mmol/L) at 4 °C over night.

Ester bond formation. The depsipeptide bond was formed by using 20 equiv Fmoc-protected amino acid, 20 equiv benzoyl chloride (BzCl, Sigma Aldrich, Germany) and 40 equiv (Et_3N, Sigma Aldrich, Germany) in DCM (*c* = 62.5 mmol/L) first at 0 °C then with warming to room temperature overnight. After the quantitative reaction, the Fmoc-protecting group was cleaved by using 40% piperidine in DMF for 2 min and then 20% piperidine in DMF for 10 min at room temperature.

Cleavage and cyclization. The protected branched peptide was cleaved with 3% hexafluoroisopropanol (HFIP; Carbolution Chemicals, Germany) in dichloromethane (DCM; VWR, Germany) and cyclized in solution (20 min, 25 W; 75 °C) by using *O*-(7-azabenzotriazol-1-yl)-*N,N,N′,N′*-tetramethyluronium hexafluorophosphate (HATU; Carbolution Chemicals, Germany) and DIEA in DMF (*c* = 4 mmol/L). The cyclized product was fully deprotected by incubation with 95% trifluo-

roacetic acid (TFA; Iris Biotech, Germany) and 2.5% triisopropylsilane (TIPS, Alfa Aesar, Germany) in deionized water at room temperature for at least 60 min. Then the cleavage cocktail was evaporated and the peptide dissolved in MeOH in order to purify it by HPLC–MS (Waters® Purification™ System, Waters Corporation, USA; Jupiter Proteo, Phenomenex, Germany). The purity was determined by RP-UPLC coupled with ESI–MS.

Fermentation. *Xenorhabdus szentirmaii* was cultivated at 30 °C and 280 rpm on a rotary shaker in two 5 L Erlenmeyer flasks each containing 1 L of Luria–Bertani (LB) broth (pH 7.0) and 2% (v/v) of XAD-16 (Sigma-Aldrich, Germany). These cultures were inoculated with 1% (v/v) of an 18 h preculture in the same medium without XAD-16. Cultures were harvested after three days, and XAD beads were separated from the supernatant by sieving.

Isolation. After washing with H_2O the XAD beads where extracted with MeOH (2 × 50 mL), followed by concentration to dryness under reduced pressure, yielding a brown oily residue and amorphous precipitate. This was dissolved in 4 mL MeOH, centrifuged for 10 min and 13000 rpm at room temperature and the pure compound isolated from the supernatant by HPLC-MS.

Biological testing

Disk diffusion Test. The nonpathogenic strains *E. coli* BL21, *M. luteus, B. subtilis* and *S. cerevisae* PK113 were cultured overnight at 30 °C in LB and YPD media. Agar plates were overlaid with an inoculum (turbidity equivalent to the optical density of 0.5 measured at 600 nm) of the different strains. Cellulose disks (100% cotton linter; Carl Roth, Karlsruhe, Germany) were loaded with 100 µg of the peptide. The dried disks were applied to the prepared agar plates and incubated for 24 h. Then the inhibition zones were measured following NCCLS criteria [19].

Hemocyte cytotoxicity analysis [20]. Last instar *Galleria mellonella* (Greater wax moth) larvae (Livefoods, UK) were anaesthetized by chilling on ice for 30 min. The larvae were surface sterilized with 70% ethanol before one of the first prolegs was excised with micro-scissors. Approximately 1.5 mL of out-flowing hemolymph was collected from the larvae directly into 10 mL chilled supplemented Graces Insect Medium (GIM) (Gibco, Invitrogen) and mixed rapidly by inversion. The hemocyte suspension was then centrifuged at 200 *g* for 5 min, the supernatant aspirated and the hemocyte pellet gently resuspended in 1 mL GIM before being made up to a final 10 mL dilution. The hemocyte suspension was arrayed into black microplates (Greiner microclear) and then incubated at 28 °C undisturbed for 60 min to allow the cells to settle and adhere. The monolayers were washed with GIM before the addition of GIM containing 100, 10 or 1 µg/mL of each of the compounds, which were co-incubated with the hemocytes for 4 h. Following incubation, the GIM and compounds mixture was aspirated and replaced with GIM containing 500 nM Mitotracker CMH_2XRos for 45 min at 28 °C (Molecular Probes, Invitrogen). Hemocyte monolayers were washed with 1× PBS and fixed with 4% paraformaldehyde for 15 min before permeabilizing with 0.2% Triton X-100 in PBS for 10 min. Cells were stained with FITC-conjugated phalloidin and Hoechst 33258 and finally washed with PBS. The plate was imaged by using the IN Cell Analyzer 2000 (GE Healthcare) and analyzed with the IN Cell Analyzer 1000 Workstation software. Estimates of LD_{50} values were calculated by using the R statistical package [21].

Cell viability assay. HeLa cells: The water-soluble tetrazolium-1 salt (WST-1; Roche Diagnostics, Germany) was used to determine the cell viability after treatment of cells with the compounds. HeLa cells were seeded at a density of 3×10^3 cells in 100 µL culture medium containing 10% FCS into 96-well microplates and incubated for 24 h at 37 °C. The medium was removed and HeLa cells were treated with increasing concentrations of the compound (10, 50 and 100 µM) or dimethyl sulfoxide. After 24 h, 10 µL of WST-1 reagent was added to each well and the cells were incubated for a further 90–150 min. The formation of the formazan was measured at 450 nm against a reference wavelength of 620 nm by using a 96-well spectrophotometric plate reader (SpectraFluor Plus, Tecan, Crailsheim, Germany). **L6-cells:** Assays were performed in 96-well microtiter plates, each well containing 100 µL of RPMI 1640 medium supplemented with 1% L-glutamine (200 mM) and 10% fetal bovine serum, and 4×10^4 L6 cells (a primary cell line derived from rat skeletal myoblasts). Serial drug dilutions of seven three-fold dilution steps, covering a range from 90 to 0.123 µg/mL, were prepared. After 72 h of incubation, the plates were inspected under an inverted microscope to assure growth of the controls and sterile conditions, 10 µL of Alamar Blue solution was then added to each well and the plates were incubated for another 2 h. Then the plates were read with a Spectramax Gemini XS microplate fluorometer with an excitation wavelength of 536 nm and an emission wavelength of 588 nm. Data were analysed by using the microplate-reader software Softmax Pro.

Activity testing against parasitic protozoa. Bioactivity against the four protozoan parasites *P. falciparum* (NF54), *T. cruzi* (Tulahuen C4), *T. b. rhodesiense* (STIB900), and *L. donovani* (MHOM-ET-67/L82) was determined as previously described [22].

Supporting Information

Supporting Information File 1

NMR-data of szentiamide (**1**).
[http://www.beilstein-journals.org/bjoc/content/supplementary/1860-5397-8-60-S1.pdf]

Acknowledgements

The research leading to these results has been funded by the European Community's Seventh Framework Program (FP7/2007-2013) under grant agreement no. 223328, and the Deutsche Forschungsgemeinschaft (DFG). Work in the Bode lab is additionally funded by the BMBF, the research funding program "LOEWE – Landes-Offensive zur Entwicklung Wissenschaftlich-ökonomischer Exzellenz" of Hessen's Ministry of Higher Education, Research, and the Arts, and the Frankfurt Initiative for Microbial Sciences (FIMS).

References

1. Goodrich-Blair, H. *Curr. Opin. Microbiol.* **2007,** *10,* 225–230. doi:10.1016/j.mib.2007.05.006
2. Herbert, E. E.; Goodrich-Blair, H. *Nat. Rev. Microbiol.* **2007,** *5,* 634–646. doi:10.1038/nrmicro1706
3. Bode, H. B. *Curr. Opin. Chem. Biol.* **2009,** *13,* 224–230. doi:10.1016/j.cbpa.2009.02.037
4. Richardson, W. H.; Schmidt, T. M.; Nealson, K. H. *Appl. Environ. Microbiol.* **1988,** *54,* 1602–1605.
5. McInerney, B. V.; Gregson, R. P.; Lacey, M. J.; Akhurst, R. J.; Lyons, G. R.; Rhodes, S. H.; Smith, D. R. J.; Engelhardt, L. M.; White, A. H. *J. Nat. Prod.* **1991,** *54,* 774–784. doi:10.1021/np50075a005
6. Fuchs, S. W.; Proschak, A.; Jaskolla, T. W.; Karas, M.; Bode, H. B. *Org. Biomol. Chem.* **2011,** *9,* 3130–3132. doi:10.1039/c1ob05097d
7. Lang, G.; Kalvelage, T.; Peters, A.; Wiese, J.; Imhoff, J. F. *J. Nat. Prod.* **2008,** *71,* 1074–1077. doi:10.1021/np800053n
8. Crawford, J. M.; Portmann, C.; Kontnik, R.; Walsh, C. T.; Clardy, J. *Org. Lett.* **2011,** *13,* 5144–5147. doi:10.1021/ol2020237
9. Bode, H. B.; Reimer, D.; Fuchs, S. W.; Kirchner, F.; Dauth, C.; Kegler, C.; Lorenzen, W.; Brachmann, A. O.; Grün, P. *Chem.–Eur. J.* **2012,** *18,* 2342–2348. doi:10.1002/chem.201103479
10. Chaston, J. M.; Suen, G.; Tucker, S. L.; Andersen, A. W.; Bhasin, A.; Bode, E.; Bode, H. B.; Brachmann, A. O.; Cowles, C. E.; Cowles, K. N.; Darby, C.; de Léon, L.; Drace, K.; Du, Z.; Givaudan, A.; Herbert Tran, E. E.; Jewell, K. A.; Knack, J. J.; Krasomil-Osterfeld, K. C.; Kukor, R.; Lanois, A.; Latreille, P.; Leimgruber, N. K.; Lipke, C. M.; Liu, R.; Lu, X.; Martens, E. C.; Marri, P. R.; Médigue, C.; Menard, M. L.; Miller, N. M.; Morales-Soto, N.; Norton, S.; Ogier, J.-C.; Orchard, S. S.; Park, D.; Park, Y.; Qurollo, B. A.; Sugar, D. R.; Richards, G. R.; Rouy, Z.; Slominski, B.; Slominski, K.; Snyder, H.; Tjaden, B. C.; van der Hoeven, R.; Welch, R. D.; Wheeler, C.; Xiang, B.; Barbazuk, B.; Gaudriault, S.; Goodner, B.; Slater, S. C.; Forst, S.; Goldman, B. S.; Goodrich-Blair, H. *PLoS One* **2011,** *6,* e27909. doi:10.1371/journal.pone.0027909
11. Duchaud, E.; Rusniok, C.; Frangeul, L.; Buchrieser, C.; Givaudan, A.; Taourit, S.; Bocs, S.; Boursaux-Eude, C.; Chandler, M.; Charles, J.-F.; Dassa, E.; Derose, R.; Derzelle, S.; Freyssinet, G.; Gaudriault, S.; Médigue, C.; Lanois, A.; Powell, K.; Siguier, P.; Vincent, R.; Wingate, V.; Zouine, M.; Glaser, P.; Boemare, N.; Danchin, A.; Kunst, F. *Nat. Biotechnol.* **2003,** *21,* 1307–1313. doi:10.1038/nbt886
12. Ohlendorf, B.; Simon, S.; Wiese, J.; Imhoff, J. F. *Nat. Prod. Commun.* **2011,** *6,* 1247–1250.
13. Zhang, W.; Ding, N.; Li, Y. *J. Pept. Sci.* **2011,** *17,* 533–539. doi:10.1002/psc.1361
14. Horton, A. E.; May, O. S.; Elsegood, M. R. J.; Kimber, M. C. *Synlett* **2011,** 797–800. doi:10.1055/s-0030-1259915
15. Harre, M.; Nickisch, K.; Tilstam, U. *React. Funct. Polym.* **1999,** *41,* 111–114. doi:10.1016/S1381-5148(99)00039-5
16. Barlos, K.; Gatos, D.; Kapolos, S.; Papaphotiu, G.; Schäfer, W.; Yao, W. Q. *Tetrahedron Lett.* **1989,** *30,* 3947–3950. doi:10.1016/S0040-4039(00)99291-8
17. Hung, K. Y.; Harris, P. W. R.; Heapy, A. M.; Brimble, M. A. *Org. Biomol. Chem.* **2011,** *9,* 236–242. doi:10.1039/c0ob00315h
18. Feasey, N.; Wansbrough-Jones, M.; Mabey, D. C. W.; Solomon, A. W. *Br. Med. Bull.* **2010,** *93,* 179–200. doi:10.1093/bmb/ldp046
19. Velasco, D.; del Mar Tomas, M.; Cartelle, M.; Beceiro, A.; Perez, A.; Molina, F.; Moure, R.; Villanueva, R.; Bou, G. *J. Antimicrob. Chemother.* **2005,** *55,* 379–382. doi:10.1093/jac/dki017
20. Proschak, A.; Schultz, K.; Herrmann, J.; Dowling, A. J.; Brachmann, A. O.; ffrench-Constant, R.; Müller, R.; Bode, H. B. *ChemBioChem* **2011,** *12,* 2011–2015. doi:10.1002/cbic.201100223
21. R Development Core Team *R: A Language and Enviroment for Statistical Computing;* R Foundation for Statistical Computing: Vienna, Austria, 2010.
22. Orhan, I.; Sener, B.; Kaiser, M.; Brun, R.; Tasdemir, D. *Mar. Drugs* **2010,** *8,* 47–58. doi:10.3390/md8010047

License and Terms

Beilstein Journal of Organic Chemistry

Volatile organic compounds produced by the phytopathogenic bacterium *Xanthomonas campestris* pv. *vesicatoria* 85-10

Teresa Weise[1], Marco Kai[1,2], Anja Gummesson[3], Armin Troeger[4], Stephan von Reuß[4,5], Silvia Piepenborn[1], Francine Kosterka[1], Martin Sklorz[3], Ralf Zimmermann[3], Wittko Francke[4] and Birgit Piechulla[*1,§]

Full Research Paper

Open Access

Address:
[1]University of Rostock, Institute of Biological Sciences, Albert-Einstein-Str. 3, 18059 Rostock, Germany, [2]present address: Max-Planck Institute for Chemical Ecology, Hans-Knoell-Str. 8, 07745 Jena, Germany, [3]Joint Mass Spectrometry Centre of the University of Rostock, Chair of Analytical Chemistry, Albert-Einstein-Str. 1, 18059 Rostock, Germany and the Cooperation group „Comprehensive Molecular Profiling“, Helmholtz Zentrum München, Ingolstädter Landstraße 1, 85764 Oberschleißheim, Germany, [4]University of Hamburg, Institute of Organic Chemistry, Martin-Luther-King-Platz 6, 20146 Hamburg, Germany and [5]present address: Boyce Thompson Institute, Cornell University, 1 Tower Road, Ithaca, NY, 14853, USA

Email:
Birgit Piechulla[*] - birgit.piechulla@uni-rostock.de

* Corresponding author
§ Tel: 0049 381 4986130; Fax: 0049 381 4986132

Keywords:
Aspergillus nidulans; *Fusarium solani*; growth inhibition and promotion; methylketones; 10-methylundecan-2-one; *Rhizoctonia solani*; volatile organic compound (VOC); *Xanthomonas campestris* pv. *vesicatoria*

Beilstein J. Org. Chem. **2012,** *8,* 579–596.
doi:10.3762/bjoc.8.65

Received: 09 February 2012
Accepted: 19 March 2012
Published: 17 April 2012

This article is part of the Thematic Series "Biosynthesis and function of secondary metabolites".

Guest Editor: J. S. Dickschat

Abstract

Xanthomonas campestris is a phytopathogenic bacterium and causes many diseases of agricultural relevance. Volatiles were shown to be important in inter- and intraorganismic attraction and defense reactions. Recently it became apparent that also bacteria emit a plethora of volatiles, which influence other organisms such as invertebrates, plants and fungi. As a first step to study volatile-based bacterial–plant interactions, the emission profile of *Xanthomonas c.* pv. *vesicatoria* 85-10 was determined by using GC/MS and PTR–MS techniques. More than 50 compounds were emitted by this species, the majority comprising ketones and methylketones. The structure of the dominant compound, 10-methylundecan-2-one, was assigned on the basis of its analytical data, obtained by GC/MS and verified by comparison of these data with those of a synthetic reference sample. Application of commercially available decan-2-one, undecan-2-one, dodecan-2-one, and the newly synthesized 10-methylundecan-2-one in bi-partite Petri dish bioassays

revealed growth promotions in low quantities (0.01 to 10 μmol), whereas decan-2-one at 100 μmol caused growth inhibitions of the fungus *Rhizoctonia solani*. Volatile emission profiles of the bacteria were different for growth on media (nutrient broth) with or without glucose.

Introduction

Plant surfaces are inhabited by diverse and complex communities of microorganisms, although these habitats may be hostile environments, e.g. [1-6]. Bacteria are the most dominant inhabitants, e.g., more than 10^7 cells per cm^2 of leaf surface are present, but also filamentous fungi and yeasts are found [7,8]. One of the most abundant bacterial genera in the phyllosphere is *Xanthomonas*; *X. campestris* is the dominant species, and at least 141 pathovars invasive against several plant species are known, including many of agricultural relevance [9]. Prominent and widespread diseases caused by *Xanthomonas* species include diseases such as bacterial spot on peppers and tomatoes, citrus canker, and bacterial blight disease in rice [9,10]. Unravelling the mechanisms for phytopathogenicity and virulence of *X. campestris* resulted in the identification of a type-three secretion system through which bacterial effector proteins enter the plant cells to interfere with cellular processes, to the benefit of the bacterium [11]. However, some plants react to the effector proteins by local cell death, a hypersensitive response, and are able to escape bacterial spreading and invasion. Apart from these cell-to-cell-based interactions, additional modes of action of *X. campestris* may influence growth of the plant directly or indirectly. Although antagonistic features of *Xanthomonas* spp. against fungi have been only sparsely studied, it is known that *Xanthomonas* competes with fungi [3]. The bacteria take up nutrients more rapidly and in larger amounts as compared to the germ tubes of fungi. This could be advantageous for *Xanthomonas* during competition for nutrients. Furthermore, some antagonistic activity of two *Xanthomonas* isolates against *Verticillium dahliae* was documented [12]. Since only a little or no production of lytic enzymes or siderophores could be observed, other mechanisms must exist that promote bacterial growth versus fungal growth. It was shown that 11-methyldodec-2*Z*-enoic acid, known as quorum-sensing signal, produced by *X. campestris* pv. *campestris* repressed hyphal development in *Candida albicans* [13], and Hogan et al. [14] concluded that either the bacteria modulate the fungal behavior or that *C. albicans* (or related fungi) responded to the presence of antagonistic bacteria in such a way that it was advantageous for the bacteria.

Volatiles were also shown to support and facilitate cross-kingdom interactions, such as plant–insect communications as bi- and tritrophic attractions and defenses [15]. For example, volatiles emitted by vegetative plant tissues suppress the growth of microorganisms, both in the case of bacteria and fungi [16-19]. Recently, a new field of interest emerged, when it became apparent that also bacteria emit a plethora of volatiles, which may influence other organisms, such as invertebrates, plants and fungi [20,21]. There is increasing information about those volatiles emitted by bacteria, especially rhizobacteria, e.g., [22-25], which influence the growth of fungi [22,23,26,27]. In most cases the bacterial volatiles showed inhibitory activities (reviewed in [20]). We, therefore, hypothesized that volatile compounds emitted by *Xanthomonas campestris* pv. *vesicatoria* 85-10 may also play a role as antagonistic weapons against competitive fungi. As a first approach in our investigations, we analysed the profiles of its volatiles. Only two volatile organic compounds released by *X. campestris* have so far been described: 11-methyldodec-2*Z*-enoic acid [13] and γ-butyrolactone [28]. To extend this preliminary information we carried out GC/MS and proton transfer reaction (PTR)–MS analyses with *X. c.* pv. *vesicatoria* 85-10. In addition, we aimed at structure elucidation and on temporal variation of profiles of volatiles produced upon growth on different media.

Results and Discussion

Effect of *Xanthomonas campestris* pv. *vesicatoria* volatiles on fungal growth

So far neglected in former investigations was the possibility that volatiles emitted from *X. c.* pv. *vesicatoria* 85-10 may influence plant growth directly or indirectly, e.g., through fungi. As a first step to investigate whether *Xanthomonas* volatiles effect other organisms, three fungi, *Aspergillus nidulans*, *Fusarium solani* and *Rhizoctonia solani,* were cocultivated with *X. c.* pv. *vesicatoria* 85-10 in compartmentalized Petri dishes (Figure 1). This ensures that only volatiles can diffuse between the compartments to act on the fungal test organisms. Since it is known that growth media influence the pattern of bacterial volatiles [29], nutrient broth with and without the addition of glucose, NBG and NB, respectively, were investigated. Figure 1A–D demonstrates the effects of *Xanthomonas* volatiles on *R. solani* in such a culture system. In the absence of bacteria the fungus exhibits circular mycelium growth (control, Figure 1A and Figure 1C), while growth was retarded when *X. c.* pv. *vesicatoria* 85-10 was growing in the other compartment (Figure 1B and Figure 1D). Growth of *R. solani* was more inhibited when *X. c.* pv. *vesicatoria* 85-10 grew on NB compared to less inhibition when it was grown on NBG (98% vs 55%, Figure 1B and Figure 1D, respectively). The same tendency was observed for the growth of *A. nidulans* and *F. solani*.

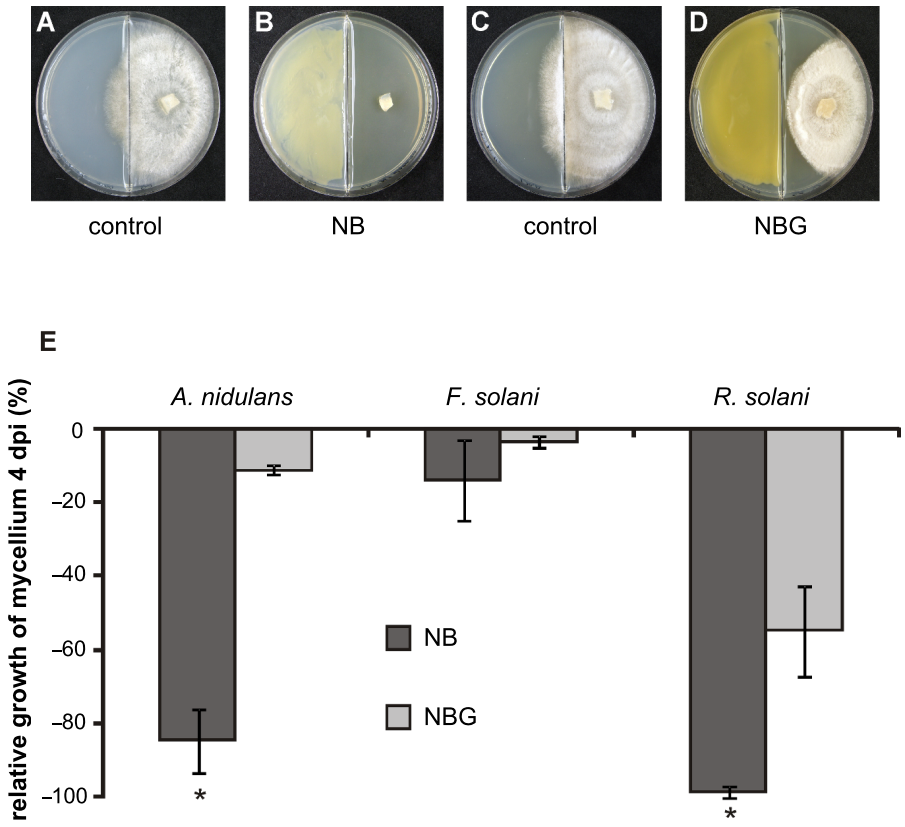

Figure 1: Cocultivation of *Xanthomonas campestris* pv. *vesicatoria* 85-10 with three fungi on different media. (A) Control experiment: Cultivation of *Rhizoctonia solani* on NB (day 4). (B) Cocultivation of *X. c.* pv. *vesicatoria* 85-10 on NB with *Rhizoctonia solani* (day 4). (C) Control experiment: Cultivation of *Rhizoctonia solani* on NBG (day 4). (D) Cocultivation of *X. c.* pv. *vesicatoria* 85-10 on NBG with *Rhizoctonia solani* (day 4). (E) Quantification of the inhibition of fungal mycelium growth during cocultivation with *X. c.* pv. *vesicatoria* 85-10, either grown on NB (black column) or NBG (grey column). Fungi: *Aspergillus nidulans, Fusarium solani* and *Rhizoctonia solani*. (4 dpi: four days after inoculation; NBG: nutrient broth (NB) II agar plus 1.1% glucose; *: growth significantly different compared to the control, $p < 0.01$ according to t-test).

When *X. c.* pv. *vesicatoria* 85-10 grew on NB, *A. nidulans* was inhibited by 85% and *F. solani* by 14%, while the inhibition of both fungi on NBG was only 11% and 3.5%, respectively. The inhibitory potential of *X. c.* pv. *vesicatoria* 85-10 volatiles on fungi was less pronounced when the bacteria grew on glucose-containing media (Figure 1E), indicating that growth suppression depended on the supplied nutrient source. Fiddaman and Rossall [29] described similar results, since the addition of D-glucose but not L-glucose lead to the formation of inhibitory volatiles by *Bacillus subtilis*. The milder inhibitory potential of *X. c.* pv. *vesicatoria* 85-10 growing on NBG, may be explained by the suggestions that (i) inhibitory volatiles were produced in higher amounts when grown on NB medium, (ii) inhibitory volatiles were only produced in the peptone-rich NB medium, (iii) glucose suppressed the production of inhibitory volatiles, for example through catabolite repression, or (iv) the emission of inhibitory volatiles was delayed.

Interestingly, *Fusarium solani* was only weakly influenced by the volatiles of *X. c.* pv. *vesicatoria* 85-10, indicating species-specific reactions. Similar results were obtained when ten different rhizobacteria were tested with various fungi [27]. Most of the tested fungi, including *R. solani*, *Verticillium dahliae*, *Paecilomyces carneus* and *Sclerotinia sclerotiorum* were strongly inhibited by the rhizobacteria (*Serratia* spp., *Pseudomonas* spp., *Stenotrophomonas* spp.), and only *F. solani* appeared to be resistant against the bacterial volatiles. Also *Muscodor albus* volatiles only partially influence the growth of *F. solani*, while other fungi are much more severely inhibited [30]. Bacterial volatiles may also directly influence plant growth. *Arabidopsis thaliana* and *Physcomitrella patens* were exposed to mixtures of volatiles emitted by various bacteria. Depending on the bacterial species or experimental setup, either promotion or inhibition of plant growth was observed [25,27,31-35]. Individual compounds such as acetoin and 2,3-butanediol acted as plant-growth-promoting agents [31], while dimethyl disulfide and 2-phenylethanol inhibited plant growth [34,36]. The inhibitory potential of volatiles of different *Xanthomonas campestris* species/isolates on *Caenorhabditis elegans* and on bacteria was also shown [20,37].

Volatile emissions of *Xanthomonas campestris* pv. *vesicatoria* 85-10

GC/MS analysis of volatiles released by *X. c.* pv. vesicatoria 85-10

The volatiles emitted by *X. c.* pv. *vesicatoria* 85-10 showed strong effects on the tested fungi (Figure 1). Therefore, it was interesting to carry out investigations on the qualitative and quantitative profiles of volatiles produced by *X. c.* pv. *vesicatoria* 85-10. Samples of volatiles were obtained by growing the bacteria in 10 L of liquid medium and trapping the volatiles on SuperQ. Upon application of GC/MS, more than 50 compounds were identified among a large number of components present in only very small amounts (Figure 2, Figure 3, Table 1). Contaminants (see Table 1) are marked in Figure 2. The scent released by *X. c.* pv. *vesicatoria* 85-10 was shown to be particularly rich in ketones and corresponding alcohols. In addition to straight-chain methylketones from hexan-2-one (compound **1** in Figure 3 and Table 1) to pentadecan-2-one (**50**), several branched-chain methylketones could be identified (Figure 3, Table 1). The volatiles were found to be largely dominated by a substance (Figure 2, compound **34**) showing a mass spectrum that was very similar to that of dodecan-2-one. A slightly later-eluting minor component furnished an almost identical mass spectrum. As both compounds eluted between undecan-2-one (**31**) and dodecan-2-one (**38**) (small amounts of which were found to be present among the natural volatiles), retention indices with methylketones as reference standards were calculated. Corresponding data published for methyl-branched hydrocarbons and increment calculations strongly suggested *iso*-branching for the main compound and *anteiso*-branching for the later-eluting isomer [38-40]. In fact, mass spectra and retention times (co-injection) of 10-methylundecan-2-one (**34**) and 9-methylundecan-2-one (**35**) synthesized in our lab (Scheme 1) matched those of the respective natural products. Small amounts of the corresponding alcohols, 10-methylundecan-2-ol (**36**) and 9-methylundecan-2-ol (**37**) (stereochemistry not determined) were also detected by GC/MS and co-injection. As the headspace volatiles contained a continuous row of homologous straight-chain methylketones, identification of additional compounds with similar structures was largely facilitated: the unbranched ketones were found to be always accompanied by the *iso*-branched isomers and in some cases also by the *anteiso*-branched ones. Corresponding methylcarbinols could also be detected. The position of the double bond in a pentadecen-2-one (**49**), a member of the identified suite of methylketones, remained unassigned.

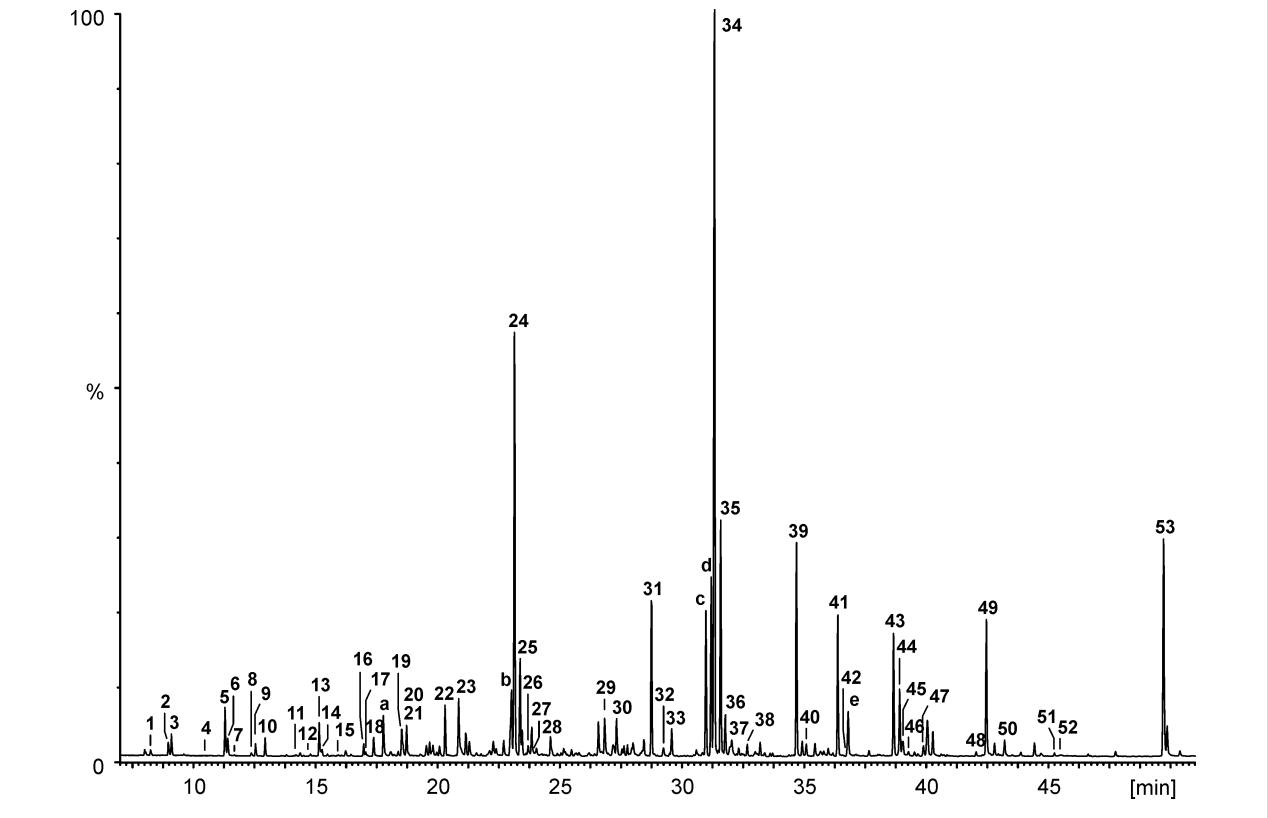

Figure 2: GC/MS-chromatogram (total ion current) of the headspace of *X. c.* pv. *vesicatoria* 85-10 grown in 10 L liquid nutrient broth without glucose. Compound labels are the same throughout this paper.

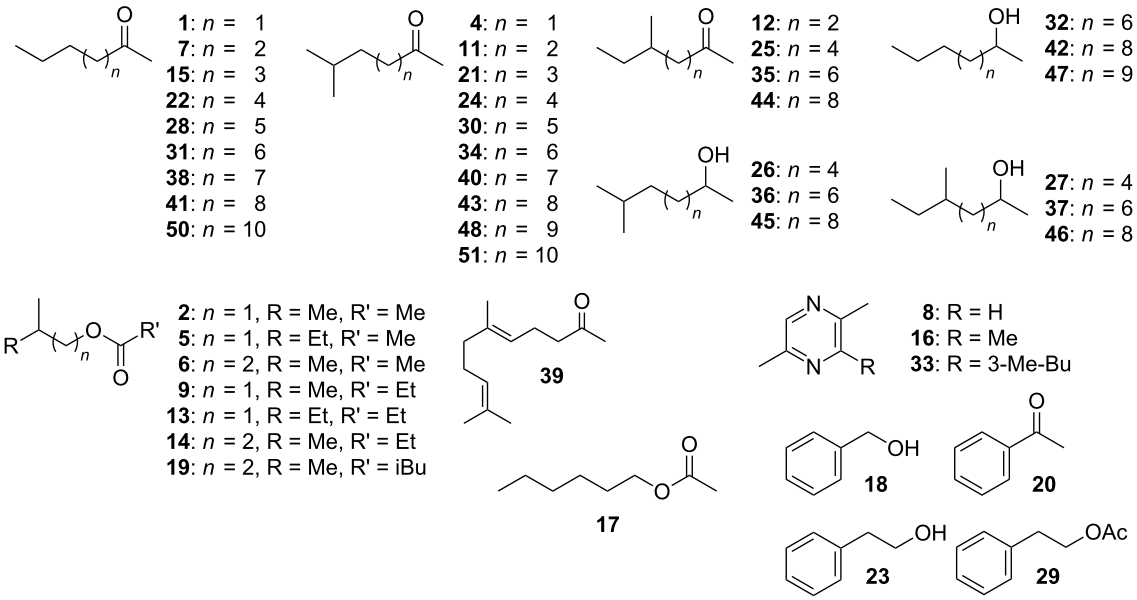

Figure 3: Structures of compounds emitted by *Xanthomonas campestris* pv. *vesicatoria* 85-10. Compound labels are the same throughout this paper.

Table 1: GC/MS analysis of Super-Q trapped volatiles emitted by *Xanthomonas campestris* pv. *vesicatoria* 85-10 grown in 10 L nutrient broth without glucose. Compound labels are the same throughout this paper.

compound	t_R [min]	retention index I	rel. area [%]	compound
1	8.23	778	0.7	hexan-2-one
2	8.96	795	1.6	2-methylpropyl acetate
3	9.10	798	2.5	*n*-octane
4	10.50	830	tr	5-methylhexan-2-one
5	11.28	848	5.4	2-methylbutyl acetate
6	11.40	851	2.4	3-methylbutyl acetate
7	11.67	857	0.2	heptan-2-one
8	12.36	873	0.4	2,5-dimethylpyrazine
9	12.53	877	1.4	2-methylpropyl propionate
10	12.92	886	2.0	*n*-nonane
11	14.36	919	0.5	6-methylheptan-2-one
12	14.78	929	tr	5-methylheptan-2-one
13	15.14	938	3.9	2-methylbutyl propionate
14	15.26	940	0.7	3-methylbutyl propionate
15	15.88	955	tr	octan-2-one
16	16.22	963	0.9	2,3,5-trimethylpyrazine
17	16.97	981	1.3	hexyl acetate
18	17.37	990	2.5	benzylalcohol
19	18.51	1018	4.0	3-methylbutyl 3-methylbutyrate
20	18.71	1022	3.7	acetophenone
21	18.71	1022	tr	7-methyloctan-2-one
22	20.29	1061	5.6	nonan-2-one
23	20.85	1074	8.4	2-phenylethanol
24	23.13	1131	52.8	8-methylnonan-2-one
25	23.37	1137	11.6	7-methylnonan-2-one
26	23.69	1145	1.4	8-methylnonan-2-ol
27	23.99	1152	tr	7-methylnonan-2-ol

Table 1: GC/MS analysis of Super-Q trapped volatiles emitted by *Xanthomonas campestris* pv. *vesicatoria* 85-10 grown in 10 L nutrient broth without glucose. Compound labels are the same throughout this paper. (continued)

28	24.60	1168	2.9	decan-2-one
29	26.82	1224	5.5	2-phenylethyl acetate
30	27.31	1237	4.9	9-methyldecan-2-one
31	28.73	1274	19.7	undecan-2-one
32	29.23	1287	1.4	undecan-2-ol
33	29.56	1296	3.7	3,6-dimethyl-2-(3-methylbutyl)pyrazine
34	31.32	1344	100.0	10-methylundecan-2-one
35	31.58	1351	28.3	9-methylundecan-2-one
36	31.76	1356	4.9	10-methylundecan-2-ol
37	32.02	1363	4.0	9-methyundecan-2-ol
38	32.66	1380	1.4	dodecan-2-one
39	34.68	1437	25.0	geranylacetone
40	35.08	1448	1.7	11-methyldodecan-2-one
41	36.37	1485	17.5	tridecan-2-one
42	36.76	1496	tr	tridecan-2-ol
43	38.64	1552	15.7	12-methyltridecan-2-one
44	38.89	1559	8.8	11-methyltridecan-2-one
45	39.03	1563	3.0	12-methyltridecan-2-ol
46	39.27	1570	0.7	11-methyltridecan-2-ol
47	39.87	1589	1.4	tetradecan-2-ol
48	42.02	1655	0.6	13-methyltetradecan-2-one
49	42.45	1668	17.7	pentadecen-2-one
50	43.19	1691	2.1	pentadecan-2-one
51	45.24	1757	0.5	14-methylpentadecan-2-one
52	45.48	1765	0.4	13-methylpentadecan-2-one
53	49.69	1907	29.8	terpenoid?
contaminants, also in blank				
a	17.76	1000	5.1	2-ethylhexanol
b	23.01	1128	8.8	2-ethylhexyl acetate
c	30.97	1334	17.8	hydrocarbon
d	31.19	1340	20.5	hydrocarbon
e	36.79	1497	6.7	2,4-bis-*tert*-butylphenol

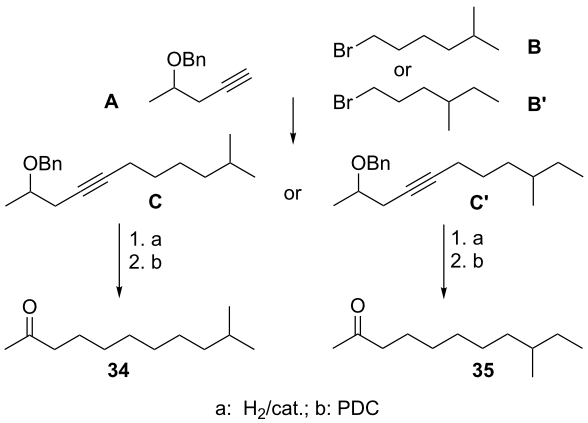

Scheme 1: Synthesis of 10-methylundecan-2-one (**34**) and 9-methylundecan-2-one (**35**).

Some of the identified ketones released by *X. c.* pv. *vesicatoria* 85-10 were known to be emitted by other bacteria, e.g., undecan-2-one (**31**) was emitted from *Serratia* sp. 2675, *Pseudomanas fluorescens*, *P. chlororaphis*, *P. aurantiaca* and *P. corrugata* [22,41]. Dodecan-2-one (**38**) was found among the volatiles of *Serratia* strains [41], and decan-2-one (**28**) was released by an epilithic cyanobacterial biofilm of *Rivularia* sp. and *Calothrix parietina* [42]. The main component among the volatile compounds released by *X. c.* pv. *vesicatoria* 85-10, namely 10-methylundecan-2-one (**34**), has been reported from plants [43-46] and bacteria, e.g., from the myxobacterium *Stigmatella aurantiaca* and arctic bacteria of the *cytophaga-flavobacterium-bacteroides* group [47,48]. In some of these bacteria a pattern of methylketones similar to that of *X. c.* pv. *vesicatoria* 85-10 was found: A continuous row of homologous straight-chain methylketones accompanied by *iso*-branched isomers, showing 10-methylundecan-2-one (**34**) as a major

component. To the best of our knowledge, the isomeric 9-methylundecan-2-one (**35**) has not been identified from a natural source before.

Possible biosynthesis of methylketones found in *Xanthomonas campestris* pv. *vesicatoria* 85-10

While odd-numbered, unbranched methylketones are clearly biosynthesized from straight-chain even-numbered fatty acids originating from the acetate pool, the biosynthesis of even-numbered congeners may start from propionate, a C3-unit. Consequently, odd-numbered fatty acids will yield even-numbered straight-chain methylketones. Leucine or valine may serve as the starters for the biosyntheses of *iso*-branched compounds [47-49], which, in this case, is supported by the presence of three esters of 3-methylbutanol and one of 2-methylbutanol. Similarly, *iso*-leucine (its involvement in biosynthesis being supported by the presence of esters of 2-methylbutanol) will give rise to *anteiso*-branching. However, due to the general principles of chain elongation with acetate/malonate units, in *X. c.* pv. *vesicatoria* 85-10 the corresponding methylketones showed an odd number of carbons along the chain. Consequently, the *anteiso*-branched isomers of compounds **21**, **30**, **40**, and **48** (Table 1) were absent among the natural volatiles.

It is interesting to note that 10-methylundecan-2-one (**34**), the main component among the less volatile compounds emitted by *X. c.* pv. *vesicatoria* 85-10, shows a close biogenetic relation to 11-methyldodec-2*Z*-enoic acid (compound **V** in Scheme 2), which has been described earlier as a metabolite produced by *Xanthomonas* [13]. Possible biogenetic pathways to the two compounds are shown in Scheme 2. Chain elongation of 3-methylbutyryl-SCoA (**I**), produced from leucine, will give rise to the formation of (ω−1)-methylcarboxylic acids [47,50], and 10-methylundecan-2-one (**34**) may be either a degradation product of a longer branched-chain carboxylic acid or formed during an anabolic process. In any case, 11-methyl-3-oxodecanoyl-SCoA (**III**) will be the key compound in the formation of **34**. Starting from **I**, three complete cycles of chain elongation with malonyl-SCoA produces 9-methyldecanoyl-SCoA (**II**), which will yield **III** upon condensation with another malonyl-SCoA. After hydrolysis and decarboxylation, **III** will directly form **34**. On the other hand, reduction of **III** would

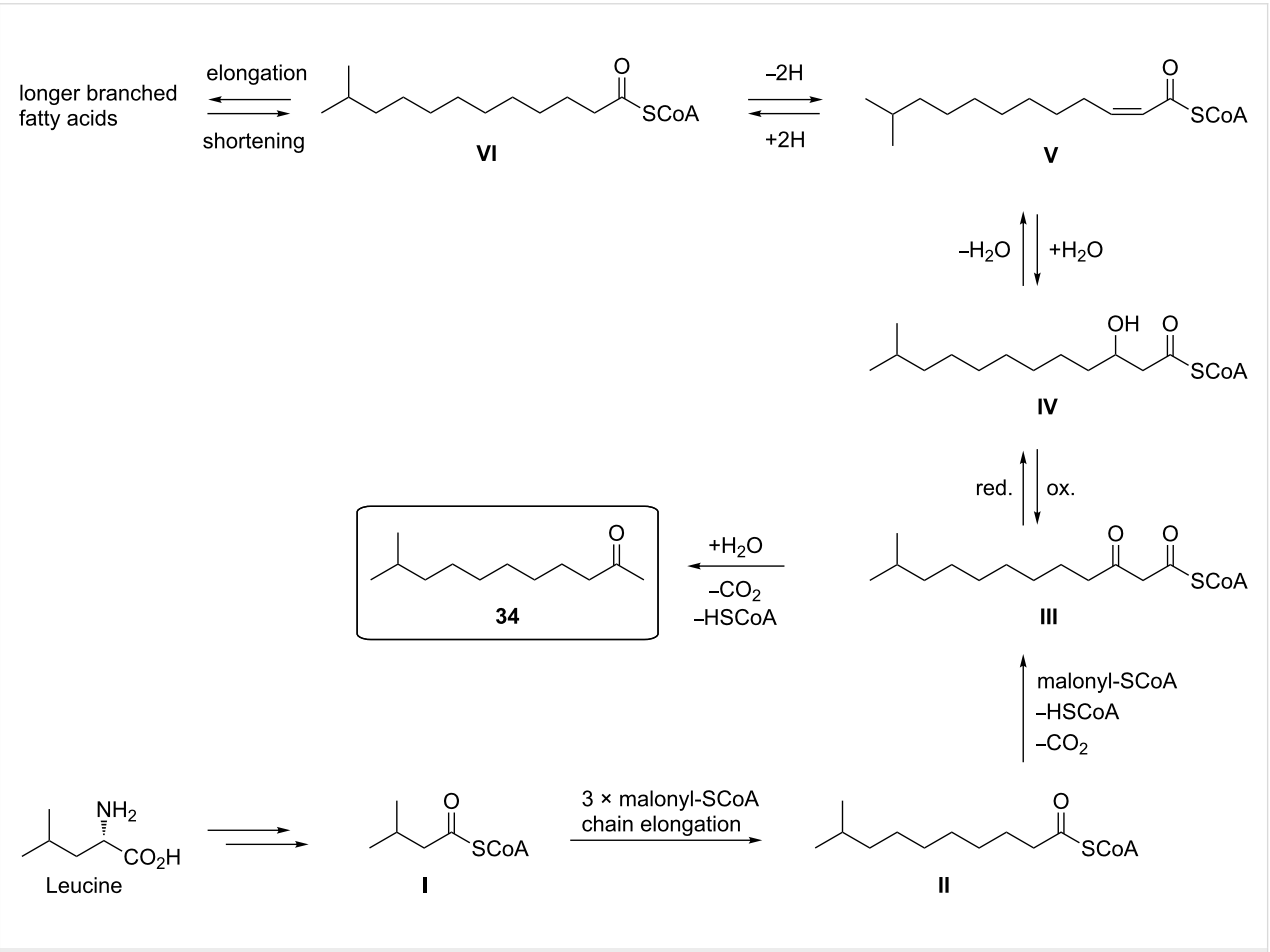

Scheme 2: Suggested biosynthesis of methylketones found in *Xanthomonas campestris* pv. *vesicatoria* 85-10.

furnish **IV**, and subsequent elimination of water would lead to **V**, the immediate precursor of 11-methyldodec-2*Z*-enoic acid. However, **V** may also be formed upon dehydrogenation of 11-methyldodecanoyl-SCoA (**VI**), which, in turn, may be produced by chain shortening of 13-methyltetradecanoyl-SCoA. Further steps during β-oxidation will afford **III** via **IV**.

With the exception of 8-methylnonan-2-one (**24**), an important component of the female-produced sex pheromone of the desert spider *Agelenopsis aperta* [51], no significant biological activities have yet been reported for the identified branched methylketones and methylcarbinols.

Various other volatiles are present in the profile of *X. c.* pv. *vesicatoria* 85-10

In addition to these methylketones and methylcarbinols, trace amounts of esters, such as 3-methylbutyl acetate (**6**) and 3-methylbutyl propionate (**14**), and the corresponding 2-methylbutyl esters **5** and **13** as well as 3-methylbutyl 3-methylbutyrate (**19**) could be identified. Trace amounts of benzylalcohol (**18**), acetophenone (**20**) and 2-phenylethanol (**23**) and its acetate (**29**) along with the three alkylated pyrazines **8**, **16**, **33** were the only aromatic components found in the bouquet, while geranylacetone (**39**) and a later-eluting yet unidentified compound, showing a mass spectrum somewhat resembling that of farnesylacetone, represented terpenoid structures among the volatiles produced by *X. c.* pv. *vesicatoria* 85-10.

PTR–MS of highly volatile compounds released by *X. c.* pv. *vesicatoria* 85-10

In our previous studies it became evident that the analysis of volatile profiles by GC/MS has its technical limitations for the detection of highly volatile compounds [34,52]. To extend the spectrum of volatiles of *X. c.* pv. *vesicatoria* 85-10, proton transfer reaction mass spectrometry (PTR–MS) was additionally used. The analyses of volatiles emitted by *X. c.* pv. *vesicatoria* 85-10 were performed after three days of incubation on NB and NBG in Petri dishes (Figure 4A and Figure 4B, respectively). At least 27 *m*/*z* values were found in the mass range between 30 and 250 with signals that were significantly enhanced (5% confidence level) compared to those of the blank control samples. If the proton affinity of an analyte molecule is higher than the one of H_3O^+ the proton transfer reaction is more or less quantitative (quasi-first-order reaction kinetics). Thus the detection efficiency of compounds is rather independent of the nature of the analyzed molecule [53] and the signal obtained by normalization of the measured count rate to the primary ion count rate is roughly proportional to the concentration. The headspace concentrations measured by online PTR–MS during the incubation experiments cover about four orders of magnitude. The most abundant *m*/*z* values $(M + H)^+$ were 59, 30, 33, 41, 43, 57, 71, 73 and higher masses such as 157, 171 and 185 (Figure 4). As PTR–MS only provides molecular mass information, an unambiguous structure elucidation is impossible. However, the tentative assignments of some volatiles are strongly supported by the results obtained during GC/MS analysis (Figure 2, Table 1). The intensive signal at *m*/*z* 157 may be attributed to the sum of decan-2-one (**28**), 7-methylnonan-2-one (**25**) and 8-methylnonan-2-one (**24**); that at *m*/*z* 171 to the sum of undecan-2-one (**31**) and 9-methyldecan-2-one (**30**); and that at *m*/*z* 185 to the sum of dodecan-2-one (**38**), 9-methylundecan-2-one (**35**) and 10-methylundecan-2-one (**34**). As the instrument is tuned to maximum sensitivity, even the soft ionization by H_3O^+ could lead to some fragmentation due to the relatively high setting of the extraction/drift-tube voltages. Therefore, the *m*/*z* values of 41, 43, 57, 71, especially, may be fragments of short-chain alkylketones and aldehydes, as reported by Blake et al. in 2006 [54].

Changes in the compositions of headspace volatiles of *Xanthomonas campestris* pv. *vesicatoria* 85-10 during growth on different media

Different intensities of reactions of the three tested fungi were observed when *X. c.* pv. *vesicatoria* 85-10 was either grown on NB or NBG (Figure 1). To trace this phenomenon, we applied solid-phase micro-extraction (SPME)–GC/MS as well as PTR–MS to monitor the patterns of headspace volatiles under two different growth conditions as well as at two different time points. The profiles of volatiles produced by *X. c.* pv. *vesicatoria* 85-10 growing on agar composed of NB and NBG were investigated at day 3 and day 6 after inoculation (Figure 5). A complex pattern of volatiles could be detected when *X. c.* pv. *vesicatoria* 85-10 was grown on the NB medium (Figure 5A). The pattern did not change much between day 3 and day 6 (Figure 5A and Figure 5C, Table 2). The volatile profile of *X. c.* pv. *vesicatoria* 85-10 grown on the NBG medium (day 3) proved to be simpler, both with respect to qualitative and quantitative composition, since only a few compounds could be traced (Figure 5B, Table 2). Interestingly, the number of detectable compounds increased after six days on NBG (Figure 5D, Table 2). By comparison of the bouquets released by *X. c.* pv. *vesicatoria* 85-10 growing on NB and NBG, only three overlapping compounds above a threshold level of 2×10^6 were observed at day 3, whereas during continued incubation the compositions of bacterial volatiles became more alike, since eight compounds appeared in both chromatograms (Figure 5E, Table 2). This observation suggested a delay of volatile emission for *X. c.* pv. *vesicatoria* 85-10 grown on NBG. Two scenarios may explain this observation: (i) catabolite repression by glucose inhibited the synthesis of certain volatiles; or (ii) the easily accessible glucose was catabolized before other components of the medium were utilized.

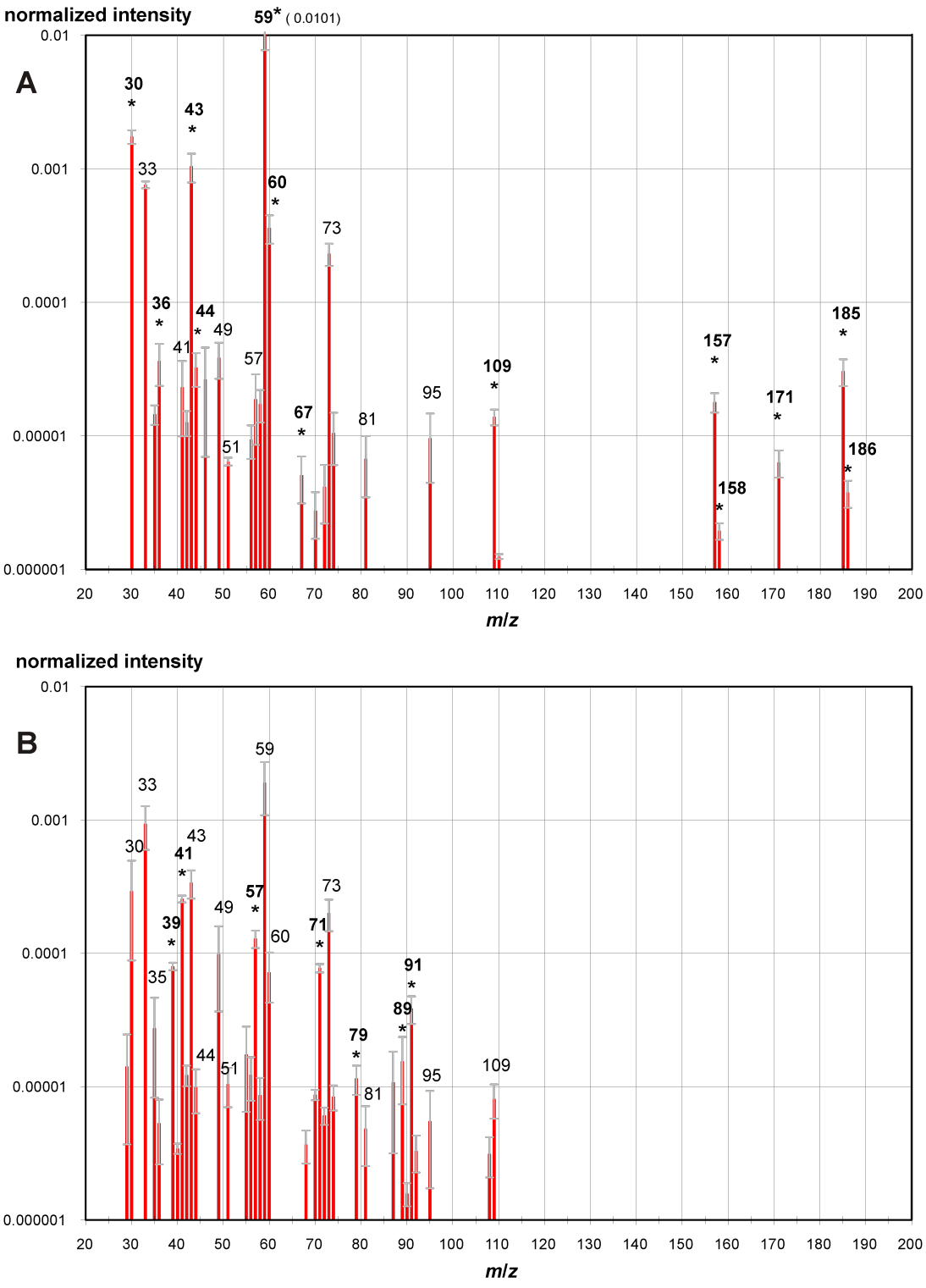

Figure 4: PTR–MS mass spectra of *Xanthomonas campestris* pv. *vesicatoria* 85-10 volatiles after three days of incubation. (A) PTR–MS profile scan of headspace volatiles of *X. c.* pv. *vesicatoria* 85-10 growing in a Petri dish with NB. (B) PTR–MS profile scan of headspace volatiles of *X. c.* pv. *vesicatoria* 85-10 growing in a Petri dish with NBG. Spectra are normalized to the primary ion signal (H_3O^+) and are blank corrected (i.e., spectra recorded from the respective media without bacteria are subtracted). Signals that are significantly influenced by the growth media (5% confidence level) are labeled by *. Only significant signals (mean subtracted by standard deviation) higher than 10^{-6} are shown and a log-scale on the ordinate axis is used. Note that missing signals therefore do not necessarily indicate zero concentration but may also be due to the variance of the sample or a blank signal higher than the mean value.

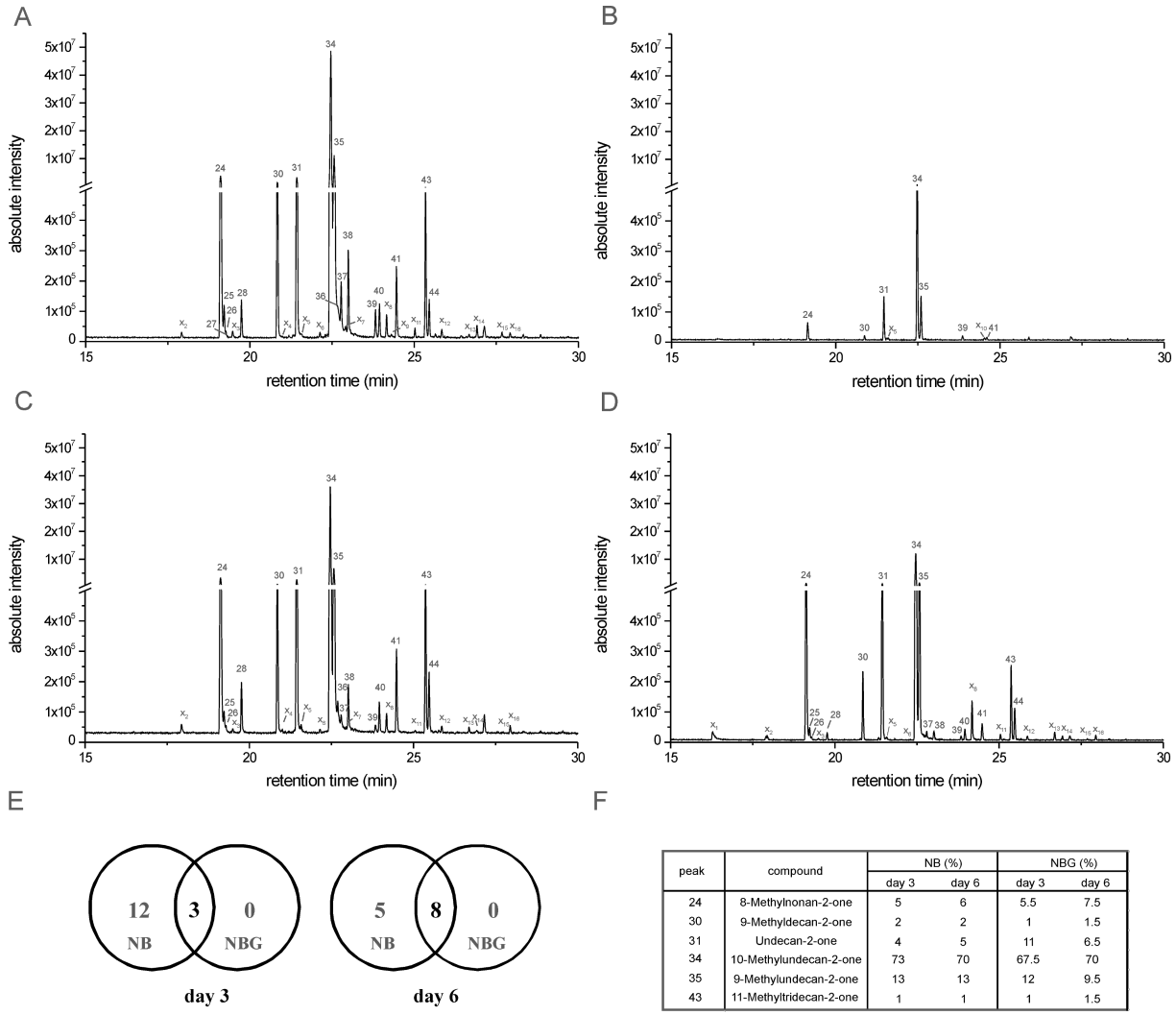

peak	compound	NB (%)		NBG (%)	
		day 3	day 6	day 3	day 6
24	8-Methylnonan-2-one	5	6	5.5	7.5
30	9-Methyldecan-2-one	2	2	1	1.5
31	Undecan-2-one	4	5	11	6.5
34	10-Methylundecan-2-one	73	70	67.5	70
35	9-Methylundecan-2-one	13	13	12	9.5
43	11-Methyltridecan-2-one	1	1	1	1.5

Figure 5: GC/MS analysis of volatiles emitted by *Xanthomonas campestris* pv. *vesicatoria* 85-10 grown on different media. (A) GC/MS-profile of headspace volatiles of *X. c.* pv. *vesicatoria* 85-10 grown on NB at day 3. (B) GC/MS-profile of headspace volatiles of *X. c.* pv. *vesicatoria* 85-10 grown on NBG at day 3. (C) GC/MS-profile of headspace volatiles of *X. c.* pv. *vesicatoria* 85-10 grown on NB at day 6. (D) GC/MS-profile of headspace volatiles of *X. c.* pv. *vesicatoria* 85-10 grown on NBG at day 6. (E) Registration of volatiles reaching a threshold level >1 × 10^5 when *X. c.* pv. *vesicatoria* 85-10 grew on NB (left circle) and NBG (right circle) (day 3: left panel, day 6: right panel). (F) Relative contribution (%) of the six major volatiles emitted by *Xanthomonas campestris* pv. *vesicatoria* 85-10 at day 3 and 6 grown on NB and NBG.

Table 2: GC/MS analysis of SPME trapped volatiles emitted from *Xanthomonas campestris* pv. *vesicatoria* 85-10 grown in a Petri dish on NB or NBG.[a]

compound	identification	NB		NBG	
		day 3	day 6	day 3	day 6
x_1	—	—	—	—	+
x_2	—	+	+	—	+
24	8-methylnonan-2-one	+++	+++	+	+++
25	7-methylnonan-2-one	++	++	—	+
26	8-methylnonan-2-ol	+	+	—	+
27	7-methylnonan-2-ol	+	—	—	—
x_3	—	+	+	—	+

Table 2: GC/MS analysis of SPME trapped volatiles emitted from *Xanthomonas campestris* pv. *vesicatoria* 85-10 grown in a Petri dish on NB or NBG.[a] (continued)

28	decan-2-one	++	++	—	+
30	9-methyldecan-2-one	+++	+++	+	++
x_4	—	+	+	—	—
31	undecan-2-one	+++	+++	++	+++
x_5	—	+	+	+	+
x_6	—	+	+	—	+
34	10-methylundecan-2-one	++++	++++	+	++++
35	9-methylundecan-2-one	++++	++++	++	+++
36	10-methylundecan-2-ol	++	+++	—	—
37	9-methylundecan-2-ol	++	+	—	+
x_7	—	+	+	—	—
38	dodecan-2-one	++	++	—	+
39	geranylacetone	++	+	+	+
40	11-methyldodecan-2-one	++	++	—	+
x_8	—	++	+	—	++
x_9	—	+	—	—	—
x_{10}	—	—	—	+	—
41	tridecan-2-one	++	++	+	+
x_{11}	—	+	+	—	+
43	12-methyltridecan-2-one	++	++	—	++
44	11-methyltridecan-2-one	++	++	—	++
x_{12}	—	+	+	—	+
x_{13}	—	+	+	—	+
x_{14}	—	+	+	—	+
x_{15}	—	+	+	—	+
x_{16}	—	+	+	—	+

[a]x_1–x_{16}: compounds not identified; + = 0–10^5 counts; ++ = 10^5–10^6 counts; +++ = 10^6–10^7 counts; ++++ = 10^7–10^8 counts.

We also determined the contribution (%) of each of the six major volatiles during bacterial growth (Figure 5F). The dominant compound, 10-methylundecan-2-one (**34**) comprised about 70% under the four growth conditions, followed by 10–12% of 9-methylundecan-2-one (**35**), about 5–7% of 8-methylnonan-2-one (**24**), 4–6% undecan-2-one (**31**), and 1–2% 9-methyldecan-2-one (**30**) and 11-methyltridecan-2-one (**44**). All other compounds contributed less than 1% to the bouquets. It is interesting to note, that the ratios of the six major compounds did not significantly vary (except for undecan-2-one (**31**) at day 3 on NBG), indicating that the same metabolic pathways were active and only larger quantities/fluxes of the volatiles were emitted under the four different growth conditions.

Similarly, as performed with the GC/MS analysis, PTR–MS volatile profiles where obtained when *X. c.* pv. *vesicatoria* was grown on NB and NBG at day 3 and 6. The PTR–MS pattern of *X. c.* pv. *vesicatoria* grown on NB for three (Figure 4A) and six days were quite similar (data not shown). It is remarkable that, in comparison, the signals for the later-eluting alkanones, i.e., *m*/*z* 157, 171 and 185 especially, were absent or significantly lower when bacteria grew on NBG for three days (Figure 4B). Furthermore, *m*/*z* = 30, 36, 43, 44, 59, 60, 67 and 109 appeared at higher levels in NB compared to NBG. Conversely, when bacteria were grown on NBG, the signals at *m*/*z* = 39, 41, 57, 71, 79 as well as 89 and 91 were enhanced. When the incubation time on NBG was prolonged to six days, even the alkanones contributed significantly, but still in about five-fold lower amounts.

Individual volatiles of *Xanthomonas campestris* pv. *vesicatoria* 85-10 marginally influence fungal growth

As demonstrated in Figure 1, *X. c.* pv. *vesicatoria* 85-10 strongly inhibited the growth of *Rhizoctonia solani* and *Aspergillus nidulans* and to a certain extent that of *Fusarium solani*. The inhibition was stronger when *X. c.* pv. *vesicatoria* 85-10 was grown on NB as compared to NBG. Both methods, GC/MS and PTR–MS, indicated the emission of a multitude of volatile compounds, including many ketones. Decan-2-one (**28**), undecan-2-one (**31**), dodecan-2-one (**38**) and 10-methylundecan-2-one (**34**) were identified as major products of *X. c.* pv. *vesicatoria* 85-10. Since the ketones were released in

different quantities from both media, we tested these ketones individually in different amounts or in combination, to find out whether the identified ketones influence the fungal growth (Figure 6). They were applied repetitively every 24 h at concentrations of 0.01, 0.1, 1.0, 10 and 100 µmol in 50 µL pentane (10-methylundecan-2-one (**34**) was applied at 0.01, 0.1 and 1 µmol in 50 µL pentane). The area of the fungal mycelium was determined after four days of cocultivation. Only at a concentration of 100 µmol decan-2-one (**28**) the growth of *R. solani* was inhibited, by 30% (Figure 6), while the other ketones did not significantly influence the development of *R. solani* at any of the tested concentrations. Surprisingly, undecan-2-one (**31**) promoted the growth of *R. solani* by 10–15% at concentrations from 0.01 to 10 µmol in 50 µL and dodecan-2-one (**38**) at 0.01 and 0.1 µmol in 50 µL. 10-Methylundecan-2-one (**34**) had no effect on the growth of *R. solani*. An additional bioassay, performed with a mixture of the four synthetic compounds (decan-2-one (**28**), undecan-2-one (**31**), dodecan-2-one (**38**), 10-methylundecan-2-one (**34**)) in the ratios that were emitted by the bacteria growing in the Petri dish (6.7%:5.5%:87.2%:0.6%), revealed 10% inhibition at 9 µmol in 50 µL and slight promotion (ca. 6%) at 0.09 µmol in 50 µL. These results indicate that the individual ketones neither acted additively nor synergistically, and they were most likely not significantly responsible for inhibitory effects on the growth (Figure 1) of the fungi by *X. c.* pv. *vesicatoria* volatiles. We concluded that either the experimental design of the bioassay was not appropriate or other volatiles account for the inhibitory effects. In the literature, contradictory results were found for undecan-2-one (**31**). It is likely to be involved in the inhibition of sapstain fungi [40], while *Sclerotinia sclerotiorum* was not affected by **31** [22]. It must also be considered that it is not known whether the emitted volatile blends change qualitatively and quantitatively during the growth of *X. c.* pv. *vesicatoria* 85-10 [34]. Hence, to find the inhibitory component(s) and the bioactive concentrations, the emitted blends of volatiles must be investigated more comprehensively.

In addition, inorganic compounds have to be considered, including hydrogen cyanide (HCN) and ammonia. HCN is produced, e.g., by *Pseudomonas* spp. [55] and, due to its slightly higher proton affinity than water, it should be detectable down to a concentration lower than 100 ppb by PTR–MS [56,57]. Nevertheless in our experiments with *X. c.* pv. *vesicatoria* 85-10 we did not detect any significant signal at $m/z = 28$ corresponding to HCN. Ammonia emissions by *X. vesicatoria*

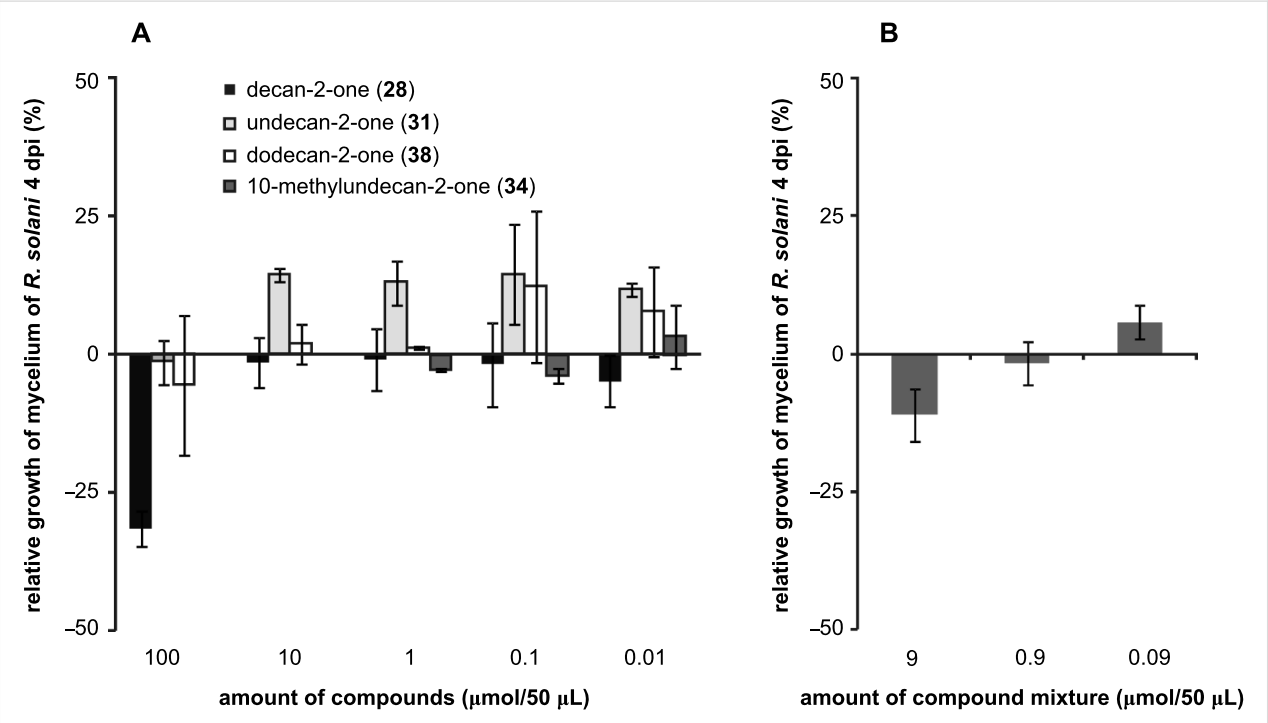

Figure 6: Testing synthetic volatiles on the growth of *Rhizoctonia solani*. Synthetic commercially available and chemically synthesized ketones were dissolved in pentane and applied on a filter-paper disc in aliquots of 50 µL. The filter paper was placed in the opposite compartment to the *R. solani* in a bi-partite Petri dish. Defined dilutions or mixtures were applied every 24 h. At day 4 the diameter of the mycelium was measured and compared to control plates containing pentane. Positive values represent growth promotion and negative values growth inhibition of *R. solani* compared to the control. Data are from two experiments each replicated three times; the standard deviation is presented. (A) Decan-2-one (**28**) (black), undecan-2-one (**31**) (light grey), dodecan-2-one (**38**) (white), and 10-methylundecan-2-one (**34**) (dark grey) were individually applied in 50 µL aliquots each day (day 0 to day 4). (B) A mixture of **28**, **31**, **38** and **34** (6.7%:5.5%:0.6%:87.2%) was applied in 50 µL aliquots every day (day 0 to day 4).

and of two *Bacillus subtilis* strains in cocultivation with *Neurospora crassa* were described [58,59]. Ammonia is of course an important nitrogen source for organisms, but recently other roles were also attributed to ammonia. Nijland and Burgess [60] suggested that ammonia acts as an olfactory cue in the communication of *Bacillus licheniformis* strains, and Bernier et al. [61] showed that elevated ammonia levels lead to increased polyamine levels in *E. coli* with consequences for the membrane permeability and increased antibiotic resistance. Other volatiles such as CO, CH_4, CH_2O and NO were not detectable with the applied methods. However, the PTR provides evidence for the emission of sulfur-containing compounds such as H_2S (m/z = 35) and methanethiol (m/z = 49), as has been suggested for other microorganisms [52]. The compound producing m/z = 33 was tentatively assigned to be methanol in accordance with published data [52]. Methanol is so far not known as a prominent compound released by bacteria. In addition to the *Enterobacteriaceae E.coli, Shigella flexneri*, and *Salmonella enterica* also *X. vesicatoria* may emit methanol. The release of CO_2 due to the active tricarboxylic acid cycle is very likely, but CO_2 does not accumulate at higher than ambient concentrations in the open experimental system [62] and, therefore, cannot be considered as a growth-promoting or -inhibitory component.

Considerations concerning methodological approaches

It is quite obvious that further research is necessary to identify the bioactive compounds, especially those sensitive and/or highly volatile substances that escaped conventional GC/MS-analysis. During our investigations on volatiles of *Xanthomonas* we noticed a discrepancy in the number of compounds detected in the headspace of a 10 L liquid-medium culture versus growth on solid medium (Petri dish). Beside the known physiological adaptations of bacteria growing on liquid and solid media, the different trapping material (Super-Q versus polydimethylsiloxane) and the experimental procedure (30 hour trapping versus 2 hour trapping) most likely account for those differences. As discussed above, the suitability of PTR–MS for compound identification is limited. Therefore, structure assignments are based on comparison with GC/MS data (i.e., as performed also in this work) and literature-based information. Selectivity may be enhanced by using ammonia as the primary ion-source gas. Ammonia has a higher proton affinity than water, and therefore, some substance classes can be ionized selectively (e.g., nitrogen-containing compounds). Further information to discriminate nominally isobaric compounds could be obtained by using proton-transfer-reaction ion-trap mass spectrometry (PIT–MS), which allows tandem mass spectrometric experiments (MS/MS) [63,64], or by high-resolution PTR–TOF–MS for the determination of exact molecular masses and assignment of atomic compositions. Regarding quantitative analysis, some striking differences between results obtained with extracts or solid-phase micro extraction (SPME) applying conventional GC/MS and PTR–MS, respectively, have been observed. As an example, in PTR–MS analyses the signal at m/z = 109 is about as intensive as those produced by the methyl ketones at m/z = 157, m/z = 171, and m/z = 185 (Figure 4A). In contrast, in our GC/MS analyses the sum of 2,5-dimethylpyrazine (**8**) and benzylalcohol (**18**) (Figure 2, Table 1), which may give rise to m/z = 109 (provided that there is no abundant compound that did not survive GC), never exceeded 5% of 10-methylundecan-2-one (**34**). These discrepancies require further investigations. The most important future analytical aspect will be online PTR–MS, tracing the dynamics in the emission of volatiles during incubation time, considering both qualitative and quantitative compositions of the profiles. In addition, gas-chromatographic analyses of highly volatile compounds, by using either direct headspace injection or solid-phase adsorption/thermodesorption separation on thick film capillaries connected to a GC/MS system, will have to be carried out.

Conclusion

Profiles of volatiles emitted by *Xanthomonas c.* pv. *vesicatoria* 85-10 were investigated by using GC/MS and PTR–MS techniques. More than 50 compounds were emitted by this species, the majority comprising ketones and methylketones, including 10-methylundecan-2-one (**34**) as the largely dominant component. The emission profiles differed depending on whether the bacteria were grown on a medium with or without glucose. To better understand the involvement of *X. c.* pv. *vesicatoria* volatiles in antagonistic processes against fungi, more ecological information is required. Most obviously it needs to be addressed as to whether *X. c.* pv. *vesicatoria* 85-10 emits volatiles while growing in the phyllosphere and whether the emission occurs continuously. Continuous volatile perception by the plant may be a prerequisite to induce signal cascades in the plant, similarly to the behavior shown for repetitive wounding in contrast to single cuts in plants [65]. Furthermore, a possible role of volatiles in achieving a better colonization of the aerial parts by *X. c.* pv. *vesicatoria* has to be considered. Another question of concern is whether and how the plants are directly affected by the volatiles of *X. c.* pv. *vesicatoria* 85-10. Plant growth promotion as well as inhibition is reflected at the molecular and physiological level of *Arabidopsis thaliana* and of *Physcomitrella patens* [23,27,31,34,62,66]. However, in most of these studies the bioactive compound(s) need to be determined. Therefore, future tasks must focus on (i) the comprehensive determination of volatile profiles of bacteria of the phyllosphere as well as in the rhizosphere and (ii) the identification of biologically active volatiles.

Experimental

Bacterial cultures

Xanthomonas campestris pv. *vesicatoria* 85-10 was originally isolated from *Capsicum* sp. The bacterial strain was kindly provided by Prof. U. Bonas (University of Halle/Wittenberg). It was stored in frozen stocks at −70 °C and grown on nutrient broth (NB) II agar (SIFIN, Berlin) either with or without 1.1% glucose (Merck, Darmstadt) at 30 °C.

Fungal isolates

Aspergillus nidulans (FGCS A4) was kindly provided by Dr. S. Busch (University of Göttingen). *Fusarium solani* and *Rhizoctonia solani* KÜHN (RHI S0 WE) were obtained from the Strain Collection of Antagonistic Microorganisms (SCAM; University of Rostock, Microbiology). Fungal mycelium was grown on Sabouraud agar (Dinkelberg Analytics GmbH, Regensburg) with a mycelia plug from stock cultures stored at −70 °C. To maintain the fungi, every seventh day a mycelium disk was transferred from the edge of an actively growing fungus to a new agar plate. Cultures were incubated at 20 °C in the dark.

Cocultivation of *Xanthomonas campestris* pv. *vesicatoria* 85-10 with fungi

Bacteria were grown on nutrient agar (NB II; peptone from casein 3.5 $g \cdot L^{-1}$, peptone from meat 2.5 $g \cdot L^{-1}$, peptone from gelatin 2.5 $g \cdot L^{-1}$, yeast extract 1.5 $g \cdot L^{-1}$, NaCl 5 $g \cdot L^{-1}$, agar-agar 15 $g \cdot L^{-1}$, pH 7.2), and nutrient agar with glucose (NBG; NB plus 11 $g \cdot L^{-1}$ glucose) at 30 °C. Cocultivations of bacteria and fungi were performed in bi-partite Petri dishes. One milliliter of the overnight cultures of *Xanthomonas* grown on NB or NBG was transferred into 100 mL fresh medium in 250 mL chicane flasks and incubated by shaking overnight at 30 °C. Fifty microliters of these cultures were plated onto nutrient agar, with or without glucose, in one compartment of the Petri dish and cultivated at 30 °C. Three days later (day 0 of cocultivation) a seven-day-old 6 mm disk of actively grown mycelium of the tested fungus was transferred to Sabouraud agar in the other compartment of the Petri dish. Cocultivation was performed at 20 °C in the dark. Digital images were taken after four days. Growth of fungi was determined by measuring the diameter of the mycelium and compared to the control (without adjacent bacterial growth). Average values were calculated based on three experiments each with three to five replicates.

Analysis of volatiles produced by *Xanthomonas campestris* pv. *vesicatoria* 85-10

Cultivation in liquid medium: A single colony of *X. c.* pv. *vesicatoria* was picked and suspended in 6 mL of NB medium. After incubation for 24 h at 30 °C and shaking at 180 rpm, 1 mL (OD_{600} = 0.8–1.4) was used as inoculum for a 250 mL NB culture. The preculture (100 mL) was used to inoculate 10 L of the culture medium in a 20 L Duran® wide-necked glass flask closed with a specially designed glass cap (equipped with an inlet and an outlet). During growth, the bacterial culture was stirred with a magnetic stir bar at 600 rpm and incubated at 30 °C. A diaphragm pump (Denver Gardner, Puchheim, Germany) pulled charcoal-purified, sterile air at a flow of 3 L/min through the system. Volatiles released during a 30 hours growth of *X. c.* pv. *vesicatoria* were trapped on Super-Q (100 mg, Alltech Associates, Deerfield, IL, USA). The collected volatiles were eluted three times with 500 µL dichloromethane and further analysed. Gas chromatography coupled with mass spectrometry (GC/MS) was carried out by linking a gas chromatograph HP 5890 (Hewlett Packard, Palo Alto, US) to a double-focusing spectrometer (VG-7070/250SE, Vacuum Generators, Manchester, UK). By using helium as the carrier gas, separations were achieved with a 50 m × 0.25 mm id CPSil5 fused silica column (Chrompack, Middleburg, The Netherlands) under the following conditions: injector temperature 250 °C, 1 min splitless, 1 min at 50 °C, then programmed to increase to 290 °C at a rate of 3.5 °C/min. Identification of volatiles was based on comparison of their mass spectra with those reported in the literature [67,68] as well as with the analytical data of commercially available or specifically synthesized reference compounds (co-injection). Synthetic 10-methylundecan-2-one and 9-methylundecan-2-one served as standards for the structure assignments of other branched-chain methyl ketones on the basis of their mass spectra and retention indices.

Cultivation on solid medium: In another analytical approach, solid-phase micro extraction (SPME) was applied to trap volatiles, which were subsequently analyzed by GC/MS. Bi-partite glass Petri dishes with a borehole (1 mm diameter) at the side of one compartment were used for SPME. The preculture (1 mL) was used to inoculate 100 mL NB or NBG medium in a 250 mL chicane flask. After 24 h of incubation at 30 °C, 50 µL was plated on NB or NBG agar on one side of the compartmentalized Petri dish. Similarly to the cocultivation tests, the inoculated plate was incubated for three days at 30 °C under darkness. The collection of volatiles was performed at day 3 and day 6 after inoculation at 20 °C in the dark. A 100 µm polydimethylsiloxane (PDMS; SUPELCO, Bellefonte, USA) coated SPME-fiber was preconditioned to remove all contaminants (30 min, 250 °C). Subsequently, the SPME needle was introduced into the Petri dish through the hole, and the fiber was extended into the headspace. The time for the adsorption and accumulation of bacterial volatiles was set to 2 h. Volatile compounds were thermally desorbed and analyzed by using a GC/MS-QP5000 (Shimadzu; Kyoto, Japan, injection port set at 250 °C). The initial temperature of the DB5-MS column

(60 m × 0.25 mm × 0.25 μm; J&W Scientific, Folsom, California, USA) was kept at 35 °C for 5 min, increased to 280 °C at a rate of 10 °C/min, and then kept constant for 15 min. Helium at a flow rate of 1.1 mL/min was used as the carrier gas with a linear velocity of 28 cm/s. Electron ionization (EI) mass spectra were taken at 70 eV. The mass range was m/z = 40–280. Compounds were identified by using available reference compounds and the library of the National Institute of Standards and Technology (NIST147) for the comparison of mass spectra, retention times and Kovats indices [69]. Analysis of the volatile emissions was replicated twice, and compounds emitted by the NB or NBG agar (blank) were subtracted.

Highly volatile components produced by *X. campestris* pv. *vesicatoria* 85-10 were monitored by proton transfer reaction mass spectrometry (PTR–MS). This technique allows continuous online monitoring of mixtures of volatiles at the parts-per-billion (ppb) level. The method is a special variant of the well-established chemical ionization mass spectrometry. In PTR–MS, the hydronium ion H_3O^+ is the primary species to generate the protonated analyte $(M + H)^+$, which is recorded by the detector. The PTR–MS (Ionicon, Innsbruck, Austria) used in this investigation has been described elsewhere [70]. As a modification to this original PTR–MS a heated inlet system was installed to prevent condensation and to enable also a qualitative analysis of less volatile compounds. It consists of a deactivated 2 m long GC capillary (ID 0.53 mm, MXT Guard Column, BGB-Analytik, Schlossboeckelheim, Germany) integrated in a 1/8 inch copper tube and maintained at a temperature of 60 °C by using a heating hose (Horst GmbH, Lorsch, Germany). The sample flow through the capillary is 80 mL/min. Drift tube pressure was set to 2.0 mbar and drift voltage to 600 V. These settings resulted in very sensitive measurements, but some side reactions led to fragmentation of, e.g., aldehydes, as described for a SWIFT instrument by Blake et al. [54]. Mass-to-charge ratios from 20 to 250 unified mass units (m/z) were run by using a quadrupole at a dwell time of 100 ms per m/z resulting in a repetition rate of about two full mass spectra per minute. Generally 100 spectra were recorded. For PTR-analysis the Petri dish with growing bacteria were placed at day 3 and 6, without the lid, into a glass compartment (Petri dish, 145 x 30 mm) with an in- and outlet. Charcoal-purified air was passed over the culture and entered the PTR instrument through the inlet. All analyses of bacterial metabolites were carried out in triplicate. Blank samples of NB and NBG were analyzed twice to identify compounds directly related to outgasing of the nutrient agar. For data evaluation, raw spectra of each measurement (100 spectra) were first normalized to the signal of the primary ion (H_3O^+), to enable a semiquantitative data evaluation and a direct comparison of spectra that were obtained at different days with a slightly different sensitivity. As a second step these normalized raw spectra were averaged and blank-value corrected. Statistical analyses of bacterial metabolites on NB and NBG were performed by using a variant of the T-test, with a 5% confidence level [71].

Syntheses of reference compounds

The syntheses of 10-methylundecan-2-one (**34**) and 9-methylundecan-2-one (**35**) proceeded straightforwardly, following a conventional alkyne approach (Scheme 1). Commercially available (Aldrich) 4-pentyne-2-ol was reacted with benzyl chloride to yield the corresponding benzyl ether **A**. Subsequently, **A** was coupled to commercially available (Aldrich) 1-bromo-5-methylhexane (**B**) according to the standard procedure [72]. The resulting 2-benzyloxy-10-methylundec-4-yne (**C**) was hydrogenated over 10% Pd/C-catalyst at 1 atm. The crude secondary alcohol was oxidized with pyridinium dichromate [73,74] to yield the corresponding ketone. Purification by column chromatography on silica (ICN, pore size 60 Å, particle size 32–63 μm) with cyclohexane/ethyl acetate 20:1 followed by Kugelrohr distillation at 20 mmHg afforded 10-methylundecan-2-one (**34**) in a purity of 98%. Analytical data of the product were identical to those reported in the literature [47]. Following the same route as for the synthesis of **34** (Scheme 1), 9-methylundecan-2-one (**35**), was prepared by coupling 1-bromo-4-methylhexane (**B′**) [75] to **A**. Hydrogenation of the obtained **C′** followed by oxidation of the obtained alcohol yielded **35**.

Synthesis of 9-methylundecan-2-one (35): To a stirred, ice-cooled solution of 2.0 g (23.8 mmol) *rac*-4-pentyne-2-ol in 50 mL dry THF was slowly added 1.20 g (49.9 mmol) sodium hydride. The reaction mixture was warmed to room temperature, and stirring was continued until the formation of hydrogen ceased. Subsequently, a solution of 4.27 g (25.0 mmol) benzyl bromide in 50 mL dry THF was added slowly. After 3 h stirring at RT, 150 mL water was added, and the mixture was extracted with three portions of diethyl ether at 50 mL each. The combined organic solutions were washed with a saturated aqueous solution of sodium hydrogen carbonate and brine and dried over magnesium sulfate. The solvent was removed in vacuo, and the residue was submitted to flash chromatography (silica; cyclohexane/ethyl acetate 40:1) yielding 2.44 g (29.8 mmol, 83%) of 2-benzyloxypent-3-yne (**A**).

A solution of 2.70 g (15.5 mmol) of **A** in 50 mL dry THF was cooled to −78 °C and deprotonated with 10.6 mL of a 1.6 M solution of butyl lithium in hexane, which was added slowly. After warming to RT, 3.05 g (17.0 mmol) of 1-bromo-4-methylhexane (**B'**), dissolved in 15 mL dry THF, was added dropwise. After heating under reflux for 12 h, the mixture was cooled to RT, and 150 mL of a saturated aqueous solution of ammonium chloride was added. After separation, the aqueous layer was

extracted with three portions of diethyl ether at 50 mL each. The combined organic solutions were washed with brine and dried over magnesium sulfate. The solvent was removed in vacuo, and the residue was submitted to flash chromatography (silica; cyclohexane/ethyl acetate 40:1) to yield 2.7 g (10.0 mmol, 64%) of 2-benzyloxy-9-methylundec-4-yne (**C′**). A solution of 2.53 g (9.3 mmol) of crude **C′** in 50 mL methanol was hydrogenated overnight at 20 bar by using 20% PD/C-catalyst. The mixture was filtered over silica, and the solvent was removed in vacuo.

To a solution of 950 mg (5.1 mmol) of the crude 9-methylundecane-2-ol in 50 mL dichloromethane was added 2.3 g (1.2 equiv) pyridinium dichromate, and the mixture was vigorously stirred for 12 h at RT. As a gas-chromatographic control revealed the reaction to be incomplete, another 1.2 equiv of pyridinium dichromate was added, and the mixture was heated under reflux for 6 h. After filtration over silica and concentration in vacuo, the crude ketone was purified by column chromatography on silica with cyclohexane/diethyl ether 20:1. A final Kugelrohr distillation of 20 mmHg afforded 855 mg (4.6 mmol) of 9-methylundecan-2-one (**35**). The total yield over four steps was about 45%, the obtained product showing a purity of ca. 98%. ^{1}H NMR (500 MHz, $CDCl_3$) δ 0.83 (d, J = 6.1 Hz, 3H, CH_3 C12), 0.85 (t, J = 7.2 Hz, 3H, CH_3 C11), 1.03–1.10/1.22–1.30 (2m, 2H, CH_2 C8), 1.06–1.17/1.20–1.30 (2m, 2H, CH_2 C10), 1.21–1.32 (m, 6H, 3×CH_2 C5-C7), 1.24–1.33 (m, 1H, CH C9), 1.52–1.61 (m, 2H, CH_2 C4), 2.13 (s, 3H, CH_3 C1), 2.41 (t, J = 7.5 Hz, 2H, CH_2 C3) ppm; ^{13}C NMR (101 MHz, C_6D_6) δ 11.54 (q, C11), 19.35 (q, C12), 24.04 (t, C4), 27.06 (t, C7), 29.38 (t, C5), 29.62 (t, C10), 29.90 (t, C6), 29.99 (q, C1), 34.52 (d, C9), 36.70 (t, C8), 43.99 (t, C3), 209.16 (s, C2) ppm; GC/MS (EI, 70 eV) *m*/*z* (% relative intensity): 39 (8), 41 (35), 42 (6), 43 (100), 56 (7), 57 (23), 58 (94), 59 (37), 67 (4), 68 (3), 69 (9), 70 (11), 71 (49), 81 (6), 82 (8), 83 (6), 85 (11), 95 (9), 96 (14), 97 (8), 109 (5), 110 (3), 124 (4), 126 (4), 127 (4), 137 (4), 166 (2), 169 (1), 184 (4); Anal. calcd for $C_{12}H_{24}O$: C, 78.20; H, 13.12; found: C, 77.52; H, 13.16.

Influence of individual volatiles of *Xanthomonas campestris* pv. *vesicatoria* 85-10 on the growth of different fungi

Synthetic ketones identified as volatiles of *Xanthomonas* (decan-2-one (**28**), undecan-2-one (**31**), 10-methylundecan-2-one (**34**), dodecan-2-one (**38**)) were assayed in bi-partite Petri dishes with *R. solani* as the test organism. A seven-day-old 6 mm disk of actively grown mycelium was transferred to Sabouraud agar, to one compartment of the Petri dish. Pentane solutions of synthetic compounds were prepared in different concentrations in decade steps (0.01–100 µmol in 50 µL). In addition, a blend of the four synthetic compounds in defined ratios (**28**:**31**:**34**:**38** 6.7%:5.5%:87.2%:0.6%) was tested as well. Fifty microliters of each mixture (0.09–9 µmol) were applied on filter paper (1 cm^2), which was deposited at the other compartment of the Petri dish. Control experiments were performed with pentane alone. Similarly to the cocultivation test, the bioassay with individual compounds was performed at 20 °C in the dark. Every 24 h the filter paper was replaced by a freshly prepared filter paper with 50 µL of the respective test solution. Growth inhibition of fungi was determined by measuring the diameter of the mycelium at day 4 of the experiment and by comparison to the control experiment (pure pentane). Average values were calculated based on two repeat experiments each with three replicates.

Acknowledgements

The authors thank the DFG for financial support (Pi153/26 resp. FR507/19-1). We are grateful to Dr. Ulla Bonas for providing Xcv 85-10 and Dr. S. Busch for *Aspergillus nidulans* (FGCS A4). We like to thank Claudia Dinse for technical assistance.

References

1. Ruinen, J. *Plant Soil* **1961,** *15,* 81–109. doi:10.1007/BF01347221
2. Last, F. T.; Deighton, F. C. *Trans. Br. Mycol. Soc.* **1965,** *48,* 83–99. doi:10.1016/S0007-1536(65)80011-0
3. Blakeman, J. P.; Fokkema, N. J. *Annu. Rev. Phytopathol.* **1982,** *20,* 167–190. doi:10.1146/annurev.py.20.090182.001123
4. Preece, T. F.; Dickinson, C. H., Eds. *Ecology of leaf surface microorganisms;* Academic Press: London, 1971.
5. Hirano, S. S.; Upper, C. D. *Microbiol. Mol. Biol. Rev.* **2000,** *64,* 624–653. doi:10.1128/MMBR.64.3.624-653.2000
6. Yang, C. H.; Crowley, D. E.; Borneman, J.; Keen, N. T. *Proc. Natl. Acad. Sci. U. S. A.* **2001,** *98,* 3889–3894. doi:10.1073/pnas.051633898
7. Lindow, S. E.; Leveau, J. H. J. *Curr. Opin. Biotechnol.* **2002,** *13,* 238–243. doi:10.1016/S0958-1669(02)00313-0
8. Lindow, S. E.; Brandl, M. T. *Appl. Environ. Microbiol.* **2003,** *69,* 1875–1883. doi:10.1128/AEM.69.4.1875-1883.2003
9. Doidge, E. M. J. *Dep. Agric., Union S. Afr.* **1921,** *1,* 718–721.
10. Hayward, A. C. The hosts of Xanthomonas. In *Xanthomonas;* Swings, J. G.; Civerolo, E. L., Eds.; Chapmann & Hall: London, 1993; pp 1–119.
11. Gürlebeck, D.; Thieme, F.; Bonas, U. *J. Plant Physiol.* **2006,** *163,* 233–255. doi:10.1016/j.jplph.2005.11.011
12. Opelt, K.; Berg, G. *Appl. Environ. Microbiol.* **2004,** *70,* 6569–6579. doi:10.1128/AEM.70.11.6569-6579.2004
13. Wang, L.; He, Y.; Gao, Y.; Wu, J. E.; Dong, Y.; He, C.; Wang, S. X.; Weng, L.; Xu, J.; Tay, L.; Fang, R. X.; Zhang, L. *Mol. Microbiol.* **2004,** *51,* 903–912. doi:10.1046/j.1365-2958.2003.03883.x
14. Hogan, D. A.; Vik, A.; Kolter, R. *Mol. Microbiol.* **2004,** *54,* 1212–1223. doi:10.1111/j.1365-2958.2004.04349.x
15. Rasmann, S.; Köllner, T. G.; Degenhardt, J.; Hiltpold, I.; Toepfer, S.; Kuhlmann, U.; Gershenzon, J.; Turlings, T. C. J. *Nature* **2005,** *434,* 732–737. doi:10.1038/nature03451

16. Hamilton-Kemp, T. R.; McCracken, C. T., Jr.; Loughrin, J. H.; Andersen, R. A.; Hildebrand, D. F. *J. Chem. Ecol.* **1992,** *18,* 1083–1091. doi:10.1007/BF00980064
17. Pandey, V. N.; Dubey, N. K. *Biol. Plant.* **1992,** *34,* 143–147. doi:10.1007/BF02925809
18. Trombetta, D.; Castelli, F.; Sarpietro, M. G.; Venuti, V.; Cristani, M.; Daniele, C.; Saija, A.; Mazzanti, G.; Bisignano, G. *Antimicrob. Agents Chemother.* **2005,** *49,* 2474–2478. doi:10.1128/AAC.49.6.2474-2478.2005
19. Wink, M. Importance of plant secondary metabolites for protection against insects and microbial infections. In *Naturally occurring bioactive compounds;* Carpinella, M. C.; Rai, M., Eds.; Advances in Phytomedicine, Vol. 3; Elsevier: Amsterdam, 2006; pp 251–268.
20. Kai, M.; Haustein, M.; Molina, F.; Petri, A.; Scholz, B.; Piechulla, B. *Appl. Microbiol. Biotechnol.* **2009,** *81,* 1001–1012. doi:10.1007/s00253-008-1760-3
21. Wenke, K.; Kai, M.; Piechulla, B. *Planta* **2010,** *231,* 499–506. doi:10.1007/s00425-009-1076-2
22. Fernando, W. G. D.; Ramarathnam, R.; Krishnamoorthy, A. S.; Savchuk, S. C. *Soil Biol. Biochem.* **2005,** *37,* 955–964. doi:10.1016/j.soilbio.2004.10.021
23. Kai, M.; Effmert, U.; Berg, G.; Piechulla, B. *Arch. Microbiol.* **2007,** *187,* 351–360. doi:10.1007/s00203-006-0199-0
24. Schulz, S.; Dickschat, J. S. *Nat. Prod. Rep.* **2007,** *24,* 814–842. doi:10.1039/b507392h
25. Kai, M.; Piechulla, B. *Plant Signal. Behav.* **2010,** *5,* 444–446. doi:10.4161/psb.5.4.11340
26. Fiddaman, P. J.; Rossall, S. *J. Appl. Microbiol.* **1993,** *74,* 119–126. doi:10.1111/j.1365-2672.1993.tb03004.x
27. Vespermann, A.; Kai, M.; Piechulla, B. *Appl. Environ. Microbiol.* **2007,** *73,* 5639–5641. doi:10.1128/AEM.01078-07
28. Chun, W.; Cui, J.; Poplawsky, A. *Physiol. Mol. Plant Pathol.* **1997,** *51,* 1–14. doi:10.1006/pmpp.1997.0096
29. Fiddaman, P. J.; Rossall, S. J. *Appl. Bacteriol.* **1994,** *76,* 395–405. doi:10.1111/j.1365-2672.1994.tb01646.x
30. Strobel, G. A.; Dirkse, E.; Sears, J.; Markworth, C. *Microbiology (Reading, U. K.)* **2001,** *147,* 2943–2950.
31. Ryu, C. M.; Farag, M. A.; Hu, C. H.; Reddy, M. S.; Wie, H. X.; Pare, P. W.; Kloepper, J. W. *Proc. Natl. Acad. Sci. U. S. A.* **2003,** *100,* 4927–4932. doi:10.1073/pnas.0730845100
32. Zhang, H.; Kim, M. S.; Krishnamachari, V.; Payton, P.; Sun, Y.; Grimson, M.; Farag, M. A.; Ryu, C. M.; Allen, R.; Melo, I. S.; Pare, P. W. *Planta* **2007,** *226,* 839–851. doi:10.1007/s00425-007-0530-2
33. Zhang, H.; Xie, X.; Kim, M. S.; Kornyeyev, D. A.; Holaday, S.; Pare, P. W. *Plant J.* **2008,** *56,* 264–273. doi:10.1111/j.1365-313X.2008.03593.x
34. Kai, M.; Crespo, E.; Cristescu, S. M.; Harren, F. J. M.; Francke, W.; Piechulla, B. *Appl. Microbiol. Biotechnol.* **2010,** *88,* 965–976. doi:10.1007/s00253-010-2810-1
35. Blom, D.; Fabbri, C.; Eberl, L.; Weisskopf, L. *Appl. Environ. Microbiol.* **2011,** *77,* 1000–1008. doi:10.1128/AEM.01968-10
36. Wenke, K.; Weise, T.; Warnke, R.; Valverde, C.; Wanke, D.; Kai, M.; Piechulla, B. Bacterial Volatiles Mediating Information Between Bacteria and Plants. In *Bio-Communication in Plants;* Witzany, G.; Baluska, F., Eds.; Signaling and Communication in Plants, Vol. 14; Springer: Berlin, 2012; pp 327–347. doi:10.1007/978-3-642-23524-5
37. Ryan, R. P.; Dow, J. M. *Microbiology (Reading, U. K.)* **2008,** *154,* 1845–1858. doi:10.1099/mic.0.2008/017871-0
38. Katritzky, A. R.; Chen, K. *Anal. Chem.* **2000,** *72,* 101–109. doi:10.1021/ac990800w
39. Schulz, S. *Lipids* **2001,** *36,* 637–647. doi:10.1007/s11745-001-0768-7
40. Junkes, B. S.; Amboni, R. D. M. C.; Heinzen, V. E. F.; Yunes, R. A. *Chromatographia* **2002,** *55,* 707–713. doi:10.1007/BF02491786
41. Bruce, A.; Verrall, S.; Hackett, C. A.; Wheatley, R. E. *Holzforschung* **2004,** *58,* 193–198. doi:10.1515/HF.2004.029
42. Höckelmann, C.; Moens, T.; Jüttner, F. *Limnol. Oceanogr.* **2004,** *49,* 1809–1819. doi:10.4319/lo.2004.49.5.1809
43. Tressl, R.; Friese, L. Z. *Lebensm.-Unters. Forsch.* **1978,** *166,* 350–354. doi:10.1007/BF01181504
44. Joulain, D.; Laurent, R.; Fourniol, Y. P.; Yaacob, K. B. J. *Essent. Oil Res.* **1991,** *3,* 355–357.
45. Schlumpberger, B. O.; Clery, R. A.; Barthlott, W. *Plant Biol.* **2006,** *8,* 265–270. doi:10.1055/s-2005-873045
46. Altintas, A.; Koca, U.; Demirci, B.; Husnu Can Baser, K. *Asian J. Chem.* **2010,** *22,* 4711–4716.
47. Dickschat, J. S.; Bode, H. B.; Wenzel, S. C.; Müller, R.; Schulz, S. *ChemBioChem* **2005,** *6,* 2023–2033. doi:10.1002/cbic.200500174
48. Dickschat, J. S.; Helmke, E.; Schulz, S. *Chem. Biodiversity* **2005,** *2,* 318–353. doi:10.1002/cbdv.200590014
49. Dickschat, J. S.; Wenzel, S. C.; Bode, H. B.; Müller, R.; Schulz, S. *ChemBioChem* **2004,** *5,* 778–787. doi:10.1002/cbic.200300813
50. Francke, W.; Schulz, S. Pheromones. In *Miscellaneous Natural Products Including Marine Natural Products, Pheromones, Plant Hormones, and Aspects of Ecology;* Barton, D.; Nakanishi, K., Eds.; Comprehensive Natural Products Chemistry, Vol. 8; Elsevier: Amsterdam, 1999; pp 197–261. doi:10.1016/B978-0-08-091283-7.00052-7
51. Papke, M. D.; Riechert, S. E.; Schulz, S. *Anim. Behav.* **2001,** *61,* 877–886. doi:10.1006/anbe.2000.1675
52. Bunge, M.; Araghipour, N.; Mikoviny, T.; Dunkl, J.; Schnitzhofer, R.; Hansel, A.; Schinner, F.; Wisthaler, A.; Margesin, R.; Märk, T. D. *Appl. Environ. Microbiol.* **2008,** *74,* 2179–2186. doi:10.1128/AEM.02069-07
53. Lindinger, W.; Hansel, A.; Jordan, A. *Int. J. Mass Spectrom. Ion Processes* **1998,** *173,* 191–241. doi:10.1016/S0168-1176(97)00281-4
54. Blake, R. S.; Wyche, K. P.; Ellis, A. M.; Monks, P. S. *Int. J. Mass Spectrom.* **2006,** *254,* 85–93. doi:10.1016/j.ijms.2006.05.021
55. Knowles, C. J. *Bacteriol. Rev.* **1976,** *40,* 652–680.
56. Hunter, E. P. L.; Lias, S. G. *J. Phys. Chem. Ref. Data* **1998,** *27,* 413–656. doi:10.1063/1.556018
57. Knighton, W. B.; Fortner, E. C.; Midey, A. J.; Viggiano, A. A.; Herndon, S. C.; Wood, E. C.; Kolb, C. E. *Int. J. Mass Spectrom.* **2009,** *1–3,* 112–121. doi:10.1016/j.ijms.2009.02.013
58. Ryan, F. J.; Schneider, L. K. *J. Bacteriol.* **1947,** *54,* 209–211.
59. Stall, R. E.; Hall, C. B.; Cook, A. A. *Phytopathology* **1972,** *62,* 882–886. doi:10.1094/Phyto-62-882
60. Nijland, R.; Burgess, J. G. *Biotechnol. J.* **2010,** *5,* 974–977. doi:10.1002/biot.201000174
61. Bernier, S. P.; Létoffé, S.; Delepierre, M.; Ghigo, J. M. *Mol. Microbiol.* **2011,** *81,* 705–716. doi:10.1111/j.1365-2958.2011.07724.x
62. Kai, M.; Piechulla, B. *FEBS Lett.* **2009,** *583,* 3473–3477. doi:10.1016/j.febslet.2009.09.053
63. Steeghs, M. M. L.; Crespo, E.; Harren, F. J. M. *Int. J. Mass Spectrom.* **2007,** *263,* 204–212. doi:10.1016/j.ijms.2007.02.011

64. Crespo, E.; Cristescu, S. M.; de Ronde, H.; Kuijper, S.; Kolk, A. H. J.; Anthony, R. M.; Harren, F. J. M. *J. Microbiol. Methods* **2011,** *86,* 8–15. doi:10.1016/j.mimet.2011.01.025
65. Bricci, I.; Leitner, M.; Foti, M.; Mithöfer, A.; Boland, W.; Maffei, M. E. *Planta* **2010,** *232,* 719–729. doi:10.1007/s00425-010-1203-0
66. Kai, M.; Vespermann, A.; Piechulla, B. *Plant Signal. Behav.* **2008,** *3,* 482–484. doi:10.4161/psb.3.7.5681
67. McLafferty, F. W.; Stauffer, D. B. *The Wiley/NBS Registry of Mass Spectral Data;* Wiley: New York, 1989.
68. Adams, R. P. *Identification of Essential Oil Components by Gas Chromatography/Mass Spectometry,* 4th ed.; Allured Publ. Corp.: Carol Stream, U.S.A., 2007.
69. Kováts, E. sz. *Fresenius' Z. Anal. Chem.* **1961,** *181,* 351–364. doi:10.1007/BF00466597
70. Hansel, A.; Jordan, A.; Holzinger, R.; Prazeller, P.; Vogel, W.; Lindinger, W. *Int. J. Mass Spectrom. Ion Processes* **1995,** *149–150,* 609–619. doi:10.1016/0168-1176(95)04294-U
71. de V. Weir, J. B. *Nature* **1960,** *187,* 438. doi:10.1038/187438a0
72. Brandsma, L. *Preparative Acetylenic Chemistry;* Elsevier: Amsterdam, 1988.
73. Corey, E. J.; Schmidt, G. *Tetrahedron Lett.* **1979,** *20,* 399–402. doi:10.1016/S0040-4039(01)93515-4
74. Cernecki, S.; Georgoulis, C.; Stevens, C. L.; Vijayakumaran, K. *Tetrahedron Lett.* **1985,** *26,* 1699–1702. doi:10.1016/S0040-4039(00)98314-X
75. Sonnet, P. E.; Carney, R. L.; Henrick, C. *J. Chem. Ecol.* **1985,** *11,* 1371–1387. doi:10.1007/BF01012138

License and Terms

Beilstein Journal of Organic Chemistry

Phytoalexins of the Pyrinae: Biphenyls and dibenzofurans

Cornelia Chizzali and Ludger Beerhues*§

Review

Open Access

Address:
Institut für Pharmazeutische Biologie, Technische Universität Braunschweig, Mendelssohnstr. 1, 38106 Braunschweig, Germany

Email:
Cornelia Chizzali - c.huettner@tu-bs.de; Ludger Beerhues* - l.beerhues@tu-bs.de

* Corresponding author
§ Tel.: +49-531-3915689; fax: +49-531-3918104

Keywords:
biphenyls; dibenzofurans; phytoalexins; Pyrinae; *Sorbus aucuparia*

Beilstein J. Org. Chem. **2012,** *8,* 613–620.
doi:10.3762/bjoc.8.68

Received: 27 January 2012
Accepted: 20 March 2012
Published: 20 April 2012

This article is part of the Thematic Series "Biosynthesis and function of secondary metabolites".

Guest Editor: J. S. Dickschat

Abstract

Biphenyls and dibenzofurans are the phytoalexins of the Pyrinae, a subtribe of the plant family Rosaceae. The Pyrinae correspond to the long-recognized Maloideae. Economically valuable species of the Pyrinae are apples and pears. Biphenyls and dibenzofurans are formed de novo in response to infection by bacterial and fungal pathogens. The inducible defense compounds were also produced in cell suspension cultures after treatment with biotic and abiotic elicitors. The antimicrobial activity of the phytoalexins was demonstrated. To date, 10 biphenyls and 17 dibenzofurans were isolated from 14 of the 30 Pyrinae genera. The most widely distributed compounds are the biphenyl aucuparin and the dibenzofuran γ-cotonefuran. The biosynthesis of the two classes of defense compounds is not well understood, despite the importance of the fruit crops. More recent studies have revealed simultaneous accumulation of biphenyls and dibenzofurans, suggesting sequential, rather than the previously proposed parallel, biosynthetic pathways. Elicitor-treated cell cultures of *Sorbus aucuparia* served as a model system for studying phytoalexin metabolism. The key enzyme that forms the carbon skeleton is biphenyl synthase. The starter substrate for this type-III polyketide synthase is benzoyl-CoA. In apples, biphenyl synthase is encoded by a gene family, members of which are differentially regulated. Metabolism of the phytoalexins may provide new tools for designing disease control strategies for fruit trees of the Pyrinae subtribe.

Review

Diversity of biphenyl and dibenzofuran phytoalexins

Within the plant family Rosaceae, the subtribe Pyrinae consists of 30 genera and approximately 1000 species, which include a number of economically important fruit trees, such as apple (*Malus domestica*) and pear (*Pyrus communis*) [1]. The subtribe Pyrinae corresponds to the long-recognized subfamily Maloideae, in which the fruit type is generally a pome. In response to biotic and abiotic stress factors, the Pyrinae produce biphenyls and dibenzofurans as phytoalexins, i.e., de novo

formed antimicrobial compounds [2]. To date, 10 biphenyls and 17 dibenzofurans have been detected in 14 genera of the Pyrinae (Figure 1) [3-23]. The majority of these inducible defense compounds were found as a result of fungal attack. Six biphenyls (**3**, **5**, **6**, **8**–**10**) and 15 dibenzofurans (**11**–**17**, **19**, **21**–**27**) accumulated in Pyrinae plants after either natural infection or artificial inoculation [3-9,13-19,21]. A single publication reports biphenyl and dibenzofuran formation in response to bacterial challenge [12]. Inoculation of an apple cultivar with the fire-blight-causing bacterium, *Erwinia amylovora*, led to

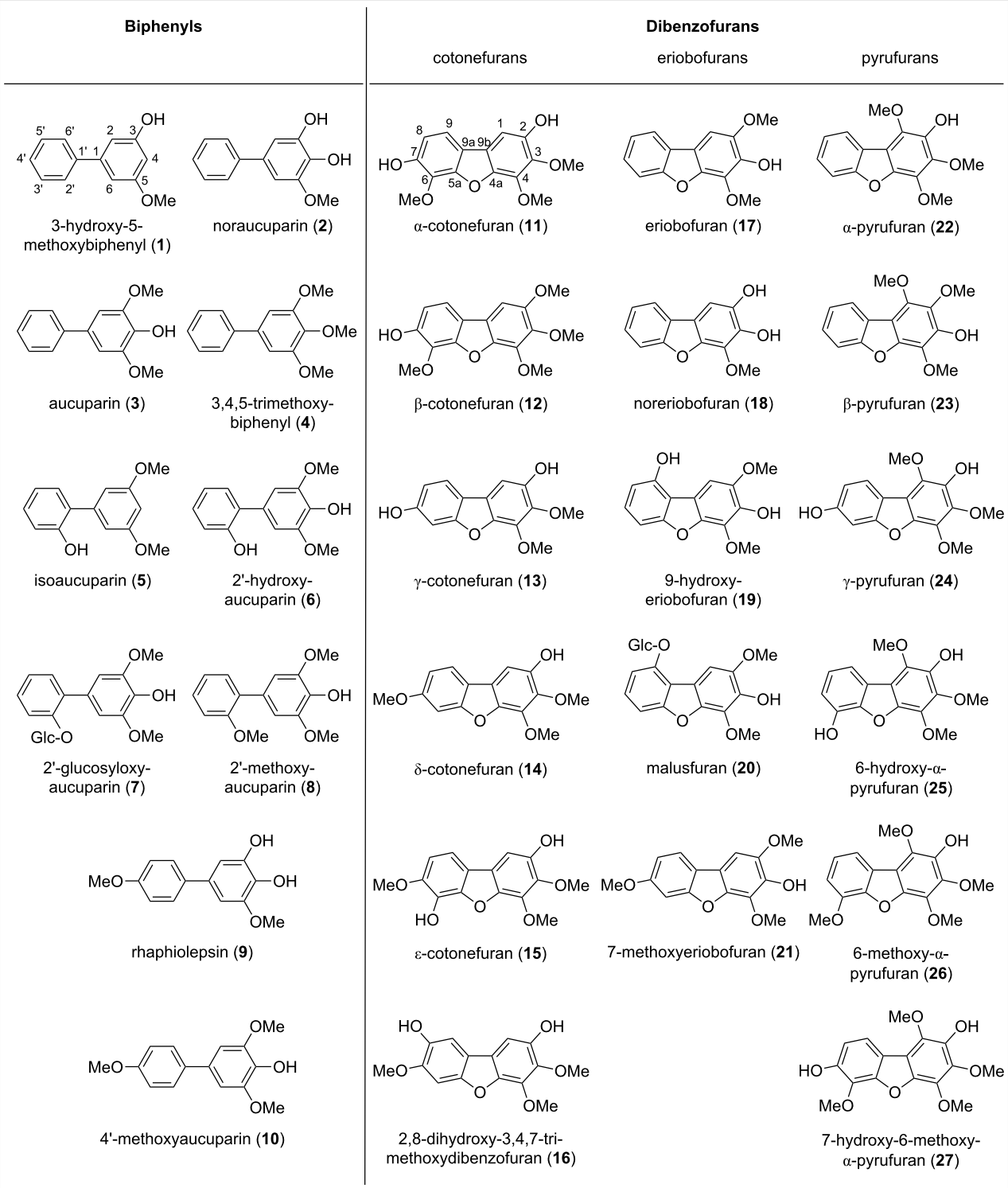

Figure 1: Biphenyl and dibenzofuran phytoalexins isolated from the Pyrinae.

accumulation of four biphenyls (**1**–**3**, **6**) and two dibenzofurans (**17**, **18**). In a fire-blight-infected pear cultivar, three biphenyls (**3**, **4**, **6**) and one dibenzofuran (**18**) were formed. When copper as an abiotic elicitor was applied to leaves of 130 Rosaceae species, including 34 species of the Pyrinae, only *Sorbus aucuparia* formed a phytoalexin, namely aucuparin (**3**) [20]. Another abiotic elicitor, mercury, caused accumulation of 4'-methoxyaucuparin (**10**) in *Rhaphiolepis umbellata* at concentrations higher than after fungal infection [14,19]. So far, no glycosides of biphenyls and dibenzofurans were detected in intact plants of the Pyrinae; however, cell cultures of an apple cultivar accumulated the biphenyl derivative 2'-glucosyloxyaucuparin (**7**) and the dibenzofuran glucoside malusfuran (**20**) [10,11].

The most widely distributed biphenyl is aucuparin (**3**), which was detected as a defense compound in eight Pyrinae species belonging to the six genera *Aronia*, *Chaenomeles*, *Eriobotrya*, *Malus*, *Pyrus*, and *Sorbus*. In contrast, there are biphenyl phytoalexins that are unique to a single species, such as 3-hydroxy-5-methoxybiphenyl (**1**) and 2'-glucosyloxyaucuparin (**7**) in *M. domestica* [11,12], 3,4,5-trimethoxybiphenyl (**4**) in *P. communis* [12], rhaphiolepsin (**9**) in *R. umbellata* [18], and isoaucuparin (**5**) in *S. aucuparia* [21]. Similar observations were made with dibenzofurans. γ-Cotonefuran (**13**) was found as phytoalexin in 11 species of the four genera *Cotoneaster*, *Crataegus*, *Pyrus*, and *Sorbus* [3,4]. In contrast, the following dibenzofurans were detected only in one Pyrinae species: Malusfuran (**20**) in *M. domestica* [10], 7-methoxyeriobofuran (**21**) in *Photinia davidiana* [3], 9-hydroxyeriobofuran (**19**) in *Pyracantha coccinea* [3], α-, β-, and γ-pyrufurans (**22**–**24**) in *P. communis* [3,16,17], and 6-hydroxy-α-pyrufuran (**25**), 6-methoxy-α-pyrufuran (**26**), and 7-hydroxy-6-methoxy-α-pyrufuran (**27**) in *Mespilus germanica* [13].

The number of biphenyl and dibenzofuran phytoalexins strongly varies between the Pyrinae species (Table 1 and Table 2). Some species produced a remarkable array of compounds, whereas others accumulated only a single phytoalexin. For example, five dibenzofurans (**11**–**15**) were observed in *Cotoneaster acutifolius* [3,4], whereas a single dibenzofuran was detected in *C. lactea* (**11**) and *C. veitchii* (**13**) [3,5]. Six genera (*Cotoneaster*, *Crataegus*, *Cydonia*, *Mespilus*, *Pseudocydonia*, and *Pyracantha*) lack biphenyls but contain dibenzofurans [3-5,13,15]. Conversely, three genera (*Aronia*, *Chaenomeles*, and *Rhaphiolepis*) lack dibenzofurans but contain biphenyls [3,18,19]. In 16 of the 30 Pyrinae genera, neither biphenyls nor dibenzofurans were detected.

Outside the subtribe Pyrinae, biphenyls and dibenzofurans were also found in a number of species. However, they do not function as phytoalexins, i.e., de novo formed defense compounds after microbial infection. They occur as preformed constituents (phytoanticipins), which are present before any challenge by microorganisms or herbivores and provide a constitutive barrier.

Table 1: Occurrence of biphenyl phytoalexins in species of the Pyrinae.

Species	Biphenyls[a]										Reference
	1	**2**	**3**	**4**	**5**	**6**	**7**	**8**	**9**	**10**	
Aronia											
A. arbutifolia			+					+		+	[3]
Chaenomeles											
C. cathayensis			+					+		+	[3]
C. japonica								+		+	[3]
Eriobotrya											
E. japonica			+								[6,7]
Malus											
M. domestica	+	+	+			+	+	+			[3,9,11,12]
M. sieversii			+					+			[3]
M. silvestris			+					+		+	[3]
Photinia											
P. glabra								+		+	[14]
Pyrus											
P. communis			+	+		+					[12]
Rhaphiolepis											
R. umbellata									+	+	[18,19]
Sorbus											
S. aucuparia		+	+		+	+		+		+	[3,20-23]

[a]**1**: 3-hydroxy-5-methoxybiphenyl, **2**: noraucuparin, **3**: aucuparin, **4**: 3,4,5-trimethoxybiphenyl, **5**: isoaucuparin, **6**: 2'-hydroxyaucuparin, **7**: 2'-glucosyloxyaucuparin, **8**: 2'-methoxyaucuparin, **9**: rhaphiolepsin, **10**: 4'-methoxyaucuparin.

Table 2: Occurrence of dibenzofuran phytoalexins in species of the Pyrinae.

Species	Dibenzofurans[a]																	Reference
	11	**12**	**13**	**14**	**15**	**16**	**17**	**18**	**19**	**20**	**21**	**22**	**23**	**24**	**25**	**26**	**27**	
Cotoneaster																		
C. acutifolius	+	+	+	+	+													[3,4]
C. divaricatus	+	+	+															[3]
C. henryanus	+	+	+															[3]
C. horizentalis	+	+	+		+													[3]
C. lactea	+																	[3,5]
C. splendens	+		+															[3]
C. veitchii			+															[3]
Crataegus																		
C. monogyna	+		+															[3]
Cydonia																		
C. oblonga				+	+	+												[3]
Eriobotrya																		
E. japonica							+											[8]
Malus																		
M. domestica							+	+		+								[10,12]
Mespilus																		
M. germanica	+														+	+	+	[3-5,13]
Photinia																		
P. davidiana							+				+							[3,15]
Pseudocydonia																		
P. sinensis					+													[3]
Pyracantha																		
P. coccinea							+		+									[3,15]
Pyrus																		
P. communis						+		+				+	+	+				[3,16,17]
P. nivalis			+			+												[3]
P. ussuriensis			+			+												[3]
P. pyraster						+												[3]
Sorbus																		
S. aucuparia							+	+										[23]
S. chamaemespilus			+															[3]
S. domestica			+															[3]

[a]**11**: α-cotonefuran, **12**: β-cotonefuran, **13**: γ-cotonefuran, **14**: δ-cotonefuran, **15**: ε-cotonefuran, **16**: 2,8-dihydroxy-3,4,7-trimethoxydibenzofuran, **17**: eriobofuran, **18**: noreriobofuran, **19**: 9-hydroxyeriobofuran, **20**: malusfuran, **21**: 7-methoxyeriobofuran, **22**: α-pyrufuran, **23**: β-pyrufuran, **24**: γ-pyrufuran, **25**: 6-hydroxy-α-pyrufuran, **26**: 6-methoxy-α-pyrufuran, **27**: 7-hydroxy-6-methoxy-α-pyrufuran.

Antimicrobial properties

Antifungal activity of biphenyls and dibenzofurans was demonstrated in a number of studies [4,7-10,12-15,18,19,21]. Spore germination, germ-tube development, and mycelial growth were inhibited by the phytoalexins at concentrations that are supposed to be present at local infection sites [10]. For example, the effective dose 50% (ED_{50}) for inhibition of *Fusarium culmorum* ranged from 12 to 84 μg/mL [4,13,15,21]. When the dibenzofuran eriobofuran (**17**) and its *O*-glucoside malusfuran (**20**) were tested for their inhibitory effect on the scab-causing fungus, *Venturia inaequalis*, the aglycone exhibited significantly stronger antifungal activity than the glucoside [10]. This finding agrees with the observation that the accumulated phytoalexins are commonly aglycones of biphenyls and dibenzofurans.

The antibacterial activity of biphenyls and dibenzofurans is less well studied [24,25]. Recently, a number of the Pyrinae-specific phytoalexins were tested for in vitro antibacterial activity against *E. amylovora*, the fire-blight-causing agent [12]. 3,5-Dihydroxybiphenyl was the most active compound with a minimum inhibitory concentration (MIC) of 115 μg/mL. While this concentration was bactericidal, a concentration approximately ten times lower led to 50% growth inhibition (MIC_{50} = 17 μg/mL). Biphenyls exhibited somewhat stronger antibacterial activity than structurally related dibenzofurans did [12], whereas the opposite tendency was observed for antifungal activity [26]. However, more biphenyls and dibenzofurans need to be tested for their antibacterial and antifungal potentials in order to allow for reliable conclusions concerning structure–activity relationships. The array of phytoalexins accu-

mulated in response to infection in a number of Pyrinae species appears to provide protection from both bacterial and fungal pathogens, such as *E. amylovora* and *V. inaequalis*, respectively. The mechanism of antimicrobial action of biphenyls and dibenzofurans has not yet been established.

Co-occurrence of biphenyls and dibenzofurans

In a previous study [3], it was concluded that Pyrinae species produce either biphenyls or dibenzofurans. No plant was known to simultaneously produce both classes of phytoalexins. *Malus* was a biphenyl producer and *Pyrus* was a dibenzofuran producer. *Eriobotrya japonica* was found to form the biphenyl aucuparin (**3**) and the dibenzofuran eriobofuran (**17**); however, the former compound was present in the cortex and the latter in the leaves [6-8]. Generally, species of the same genus produce the same class of phytoalexins, except for *Photinia glabra*, which contained biphenyls (**8**, **10**), and *P. davidiana*, which formed dibenzofurans (**17**, **21**) [3,14,15]. Based on the lack of co-occurrence of biphenyl and dibenzofuran phytoalexins, parallel, rather than sequential, biosynthetic pathways were proposed [3]. Later, the simultaneous formation of biphenyls and dibenzofurans was observed in elicitor-treated cell cultures of a scab-resistant apple cultivar, which formed the biphenyls aucuparin (**3**), 2'-hydroxyaucuparin (**6**), and 2'-glucosyloxyaucuparin (**7**) in addition to the dibenzofuran malusfuran (**20**) [10,11]. For intact plants, co-occurrence of the two classes of defense compounds has only recently been observed in fire-blight-infected stems of apple and pear [12]. While the pear cultivar accumulated three biphenyls (**3**, **4**, **6**) and one dibenzofuran (**18**), the apple cultivar formed four biphenyls (**1**–**3**, **6**) and two dibenzofurans (**17**, **18**) [12]. Along with the previously isolated compounds, apple species produce seven biphenyls (**1**–**3**, **6**–**8**, **10**) and three dibenzofurans (**17**, **18**, **20**) [3,9-12], whereas pear species form three biphenyls (**3**, **4**, **6**) and six dibenzofurans (**13**, **16**, **18**, **22**–**24**) [3,12,16,17].

Elicitor-treated cell cultures as a model system

Cell suspension cultures treated with elicitors are widely used to investigate microbe-induced processes in systems of reduced complexity, as compared to natural interactions between differentiated plants and intact pathogens [22,27-32]. The phytoalexin response in elicitor-treated cell cultures is magnified relative to that at local infection sites of plant organs. Furthermore, the disruption of cultured cells to extract phytoalexins, as well as enzymes and transcripts, is easier than homogenization of intact, woody plants. However, cell cultures fail to provide insight into the organ and tissue specificities of the biosynthetic pathway.

We have established cell cultures of *S. aucuparia* as a model system for studying biphenyl and dibenzofuran formation after elicitor treatment [22,23]. *S. aucuparia* cell cultures respond to the addition of elicitors with the accumulation of both biphenyls (**2**, **3**, **6**) and dibenzofurans (**17**, **18**). Simultaneous formation of the two classes of defense compounds has thus been observed with *M. domestica*, *P. communis*, and *S. aucuparia*, although intact *S. aucuparia* plants contain only biphenyls [3,20-22]. The pattern of phytoalexins formed in *S. aucuparia* cell cultures varied with the type of elicitor added [23]. Yeast extract mainly induced the formation of aucuparin (**3**), whereas chitosan, although being a relatively poor elicitor, primarily stimulated the production of noraucuparin (**2**). Maximum phytoalexin levels were observed after the addition of autoclaved suspensions of the fire-blight bacterium, *E. amylovora*, and the scab-causing fungus, *V. inaequalis*. Eriobofuran (**17**) was the major inducible defense compound. The total biphenyl and dibenzofuran concentrations were 8.5 and 9.5 µg/g dry weight, respectively, and did not appreciably differ after treatment with the scab fungus and the fire-blight bacterium (Figure 2). These two pathogens along with the powdery mildew-causing fungus are responsible for the most destructive diseases affecting the Pyrinae, which lead to significant yield losses and crop failures in apple and pear production (Figure 3) [33].

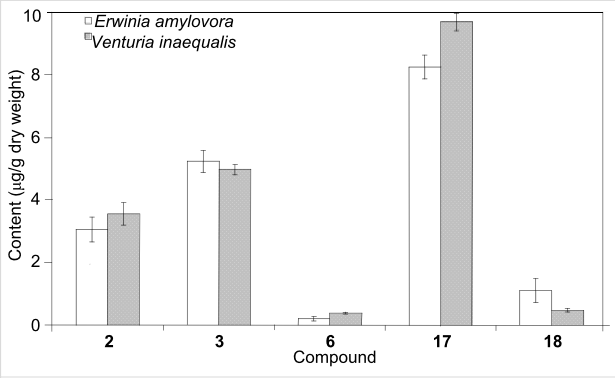

Figure 2: Biphenyl and dibenzofuran concentrations determined in *S. aucuparia* cell cultures after treatment with *E. amylovora* and *V. inaequalis* [23]. Data are average values ± SD (*n* = 3).

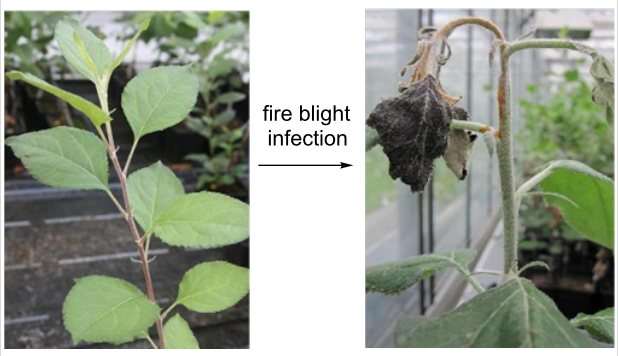

Figure 3: Greenhouse-grown apple shoots inoculated with the fire-blight-causing bacterium, *E. amylovora*.

Biosynthesis of biphenyls and dibenzofurans

The key enzyme of the biosynthetic pathway is biphenyl synthase (BIS) [22]. This type-III polyketide synthase (PKS) catalyzes the iterative condensation of benzoyl-CoA with three acetyl units from the decarboxylation of malonyl-CoA to form a linear tetraketide intermediate, which undergoes intramolecular C2→C7 aldol condensation and decarboxylative elimination of the terminal carboxyl group to give 3,5-dihydroxybiphenyl (Figure 4). BIS activity was first detected in cell cultures of *S. aucuparia* treated with yeast extract as an elicitor [22]. A BIS cDNA was cloned, and the recombinant enzyme was functionally expressed in *Escherichia coli* and characterized [34]. Recently, four cDNAs encoding BIS isoenzymes were cloned from fire-blight-infected shoots of apple plants, heterologously expressed, and functionally analyzed [35]. Expression of the four BIS genes was differentially regulated in response to fire-blight infection. While the BIS3 gene was expressed in stems, leading to the accumulation of four biphenyls (**1**–**3**, **6**) and two dibenzofurans (**17**, **18**), the BIS2 gene was transcribed in leaves. However, leaves failed to accumulate immunodetectable amounts of BIS protein, which was consistent with the absence of phytoalexins from the leaves [35]. In cell cultures of apple, three BIS genes were expressed after treatment with an autoclaved suspension of the fire-blight bacterium. Immunofluorescence localization in cross sections of apple stems revealed the occurrence of the BIS protein in the parenchyma of the bark [35]. Interestingly, dot-shaped immunofluorescence was confined to the junctions between neighboring cortical parenchyma cells, suggesting an association of BIS with plasmodesmata.

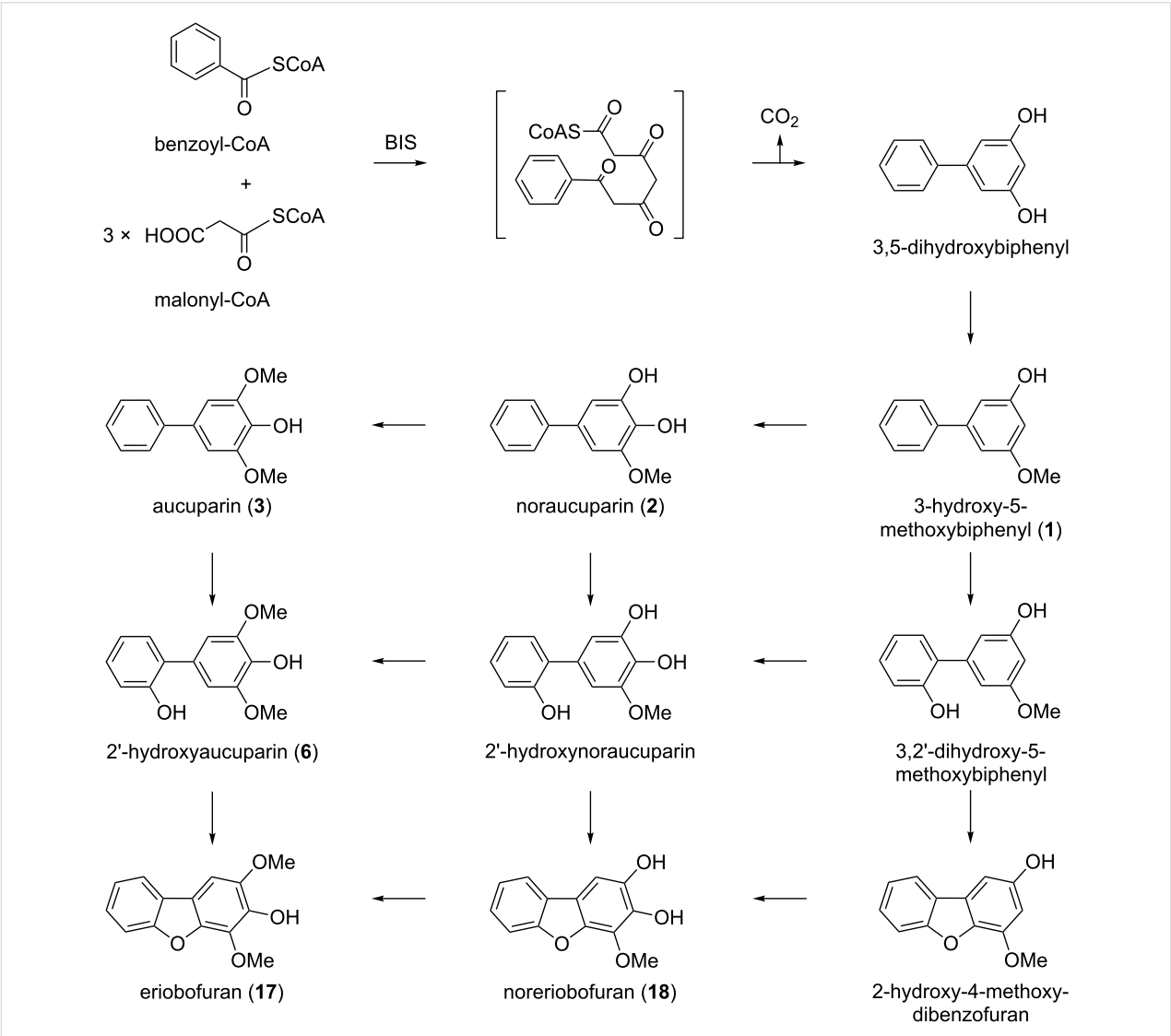

Figure 4: Established formation of 3,5-dihydroxybiphenyl by biphenyl synthase (BIS) [34] and proposed biosynthetic reactions leading to biphenyl and dibenzofuran phytoalexins in elicitor-treated *S. aucuparia* cell cultures [23].

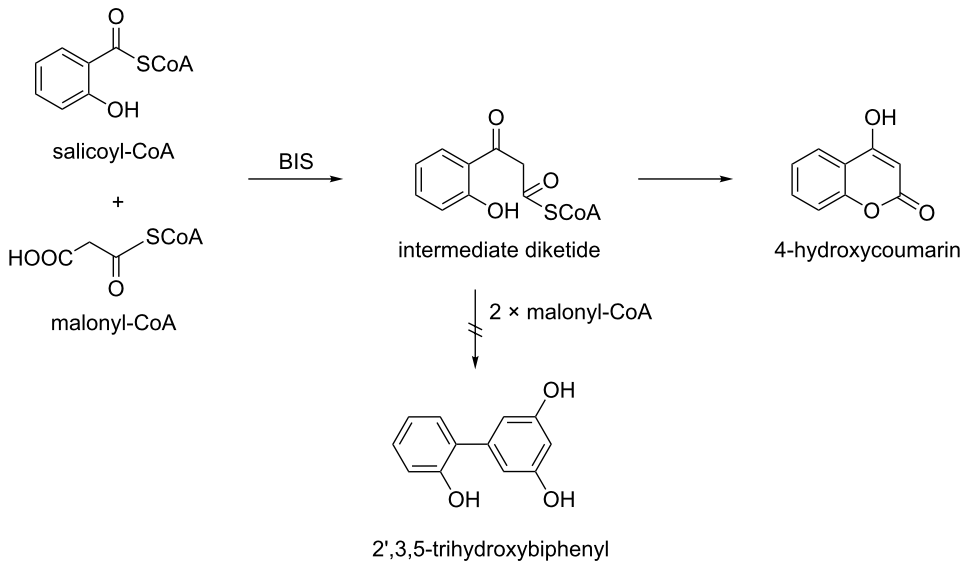

Figure 5: In vitro biosynthesis of 4-hydroxycoumarin by biphenyl synthase (BIS). No formation of 2',3,5-trihydroxybiphenyl was observed [35,36].

The simultaneous formation of biphenyls and dibenzofurans in *M. domestica* [3,9-12], *P. communis* [3,12,16,17], and *S. aucuparia* [3,20-23] led us to propose sequential, rather than parallel, pathways of biphenyl and dibenzofuran biosynthesis (Figure 4) [23]. BIS thus appears to form the carbon skeleton of both classes of defense compounds. The product of the BIS reaction, 3,5-dihydroxybiphenyl, undergoes O-methylation to give 3-hydroxy-5-methoxybiphenyl (**1**), as recently detected in elicitor-treated *S. aucuparia* cell cultures (Khalil and Beerhues, unpublished). Subsequent 4-hydroxylation and additional O-methylation yield noraucuparin (**2**) and aucuparin (**3**), respectively. The dibenzofurans noreriobofuran (**18**) and eriobofuran (**17**) have been proposed to arise from 2'-hydroxylated intermediates, one of which, 2'-hydroxyaucuparin (**6**), was isolated from *S. aucuparia* cell cultures [23]. Interestingly, the 2'-hydroxylated intermediates do not originate from salicoyl-CoA as a starter substrate [35,36]. All BIS enzymes studied so far released 4-hydroxycoumarin after a single condensation with malonyl-CoA rather than 2',3,5-trihydroxybiphenyl after three additions of acetyl units (Figure 5). Intramolecular cyclization converting 2'-hydroxylated intermediates to dibenzofurans has not yet been demonstrated biochemically (Figure 4).

Conclusion

Upon attack by pathogens, species of the Pyrinae form biphenyl and dibenzofuran phytoalexins. The biosynthesis of these two classes of defense compounds is poorly understood, although the Pyrinae include apple, pear, and related fruit trees. Plant diseases, such as fire blight, scab, and powdery mildew, lead to dramatic losses of fruits and trees. Engineering of the phytoalexin metabolism may provide new tools for enhancing disease resistance in economically important cultivars. However, this approach requires a detailed knowledge of biphenyl and dibenzofuran biosynthesis at the metabolic, enzymatic, and genetic levels. Data obtained with elicitor-treated cell cultures as a simplified experimental system lay the foundation for the study of the more complex interaction of differentiated plants and intact pathogens.

Acknowledgements

Work in our laboratory was supported by the Deutsche Forschungsgemeinschaft (DFG).

References

1. Potter, D.; Eriksson, T.; Evans, R. C.; Oh, S.; Smedmark, J. E. E.; Morgan, D. R.; Kerr, M.; Robertson, K. R.; Arsenault, M.; Dickinson, T. A.; Campbell, C. S. *Plant Syst. Evol.* **2007,** *266,* 5–43. doi:10.1007/s00606-007-0539-9
2. Paxton, J. D. *J. Phytopathol.* **1981,** *101,* 106–209. doi:10.1111/j.1439-0434.1981.tb03327.x
3. Kokubun, T.; Harborne, J. B. *Phytochemistry* **1995,** *40,* 1649–1654. doi:10.1016/0031-9422(95)00443-B
4. Kokubun, T.; Harborne, J. B.; Eagles, J.; Waterman, P. G. *Phytochemistry* **1995,** *38,* 57–60. doi:10.1016/0031-9422(94)00636-8
5. Burden, R. S.; Kemp, M. S.; Wiltshire, C. W.; Owen, J. D. *J. Chem. Soc., Perkin Trans. 1* **1984,** 1445–1448. doi:10.1039/P19840001445
6. Morita, A.; Nonaka, F.; Makizumi, K. *Ann. Phytopath. Soc. Japan* **1980,** *46,* 386.
7. Watanabe, K.; Ishiguri, Y.; Nonaka, F.; Morita, A. *Agric. Biol. Chem.* **1982,** *46,* 567–568. doi:10.1271/bbb1961.46.567
8. Miyakodo, M.; Watanabe, K.; Ohno, N.; Nonaka, F.; Morita, A. J. *Pestic. Sci.* **1985,** *10,* 101–106. doi:10.1584/jpestics.10.101

9. Kemp, M. S.; Holloway, P. J.; Burden, R. S. *J. Chem. Res.* **1985,** 1848–1876.
10. Hrazdina, G.; Borejsza-Wysocki, W.; Lester, C. *Phytopathology* **1997,** *87,* 868–876. doi:10.1094/PHYTO.1997.87.8.868
11. Borejsza-Wysocki, W.; Lester, C.; Attygalle, A. B.; Hrazdina, G. *Phytochemistry* **1999,** *50,* 231–235. doi:10.1016/S0031-9422(98)00509-3
12. Chizzali, C.; Khalil, M. N. A.; Beuerle, T.; Schuehly, W.; Richter, K.; Flachowsky, H.; Peil, A.; Hanke, M.-V.; Liu, B.; Beerhues, L. *Phytochemistry* **2012,** *77,* 179–185. doi:10.1016/j.phytochem.2012.01.023
13. Kokubun, T.; Harborne, J. B.; Eagles, J.; Waterman, P. G. *Phytochemistry* **1995,** *39,* 1039–1042. doi:10.1016/0031-9422(95)00160-9
14. Widyastuti, S. M.; Nonaka, F.; Watanabe, K.; Sako, N.; Tanaka, K. *Ann. Phytopath. Soc. Japan* **1992,** *58,* 228–233. doi:10.3186/jjphytopath.58.228
15. Kokubun, T.; Harborne, J. B.; Eagles, J.; Waterman, P. G. *Phytochemistry* **1995,** *39,* 1033–1037. doi:10.1016/0031-9422(95)00128-T
16. Kemp, M. S.; Burden, R. S.; Loeffler, S. T. *J. Chem. Soc., Perkin Trans. 1* **1983,** 2267–2272. doi:10.1039/P19830002267
17. Kemp, M. S.; Burden, R. S. *J. Chem. Soc., Perkin Trans. 1* **1984,** 1441–1443. doi:10.1039/P19840001441
18. Watanabe, K.; Widyastuti, S. M.; Nonaka, F. *Agric. Biol. Chem.* **1990,** *54,* 1861–1862. doi:10.1271/bbb1961.54.1861
19. Widyastuti, S. M.; Nonaka, F.; Watanabe, K.; Maruyama, E.; Sako, N. *Ann. Phytopath. Soc. Japan* **1991,** *57,* 232–238. doi:10.3186/jjphytopath.57.232
20. Kokubun, T.; Harborne, J. B. *Z. Naturforsch., C: J. Biosci.* **1994,** *49,* 628–634.
21. Kokubun, T.; Harborne, J. B.; Eagles, J.; Waterman, P. G. *Phytochemistry* **1995,** *40,* 57–59. doi:10.1016/0031-9422(95)00307-S
22. Liu, B.; Beuerle, T.; Klundt, T.; Beerhues, L. *Planta* **2004,** *218,* 492–496. doi:10.1007/s00425-003-1144-y
23. Hüttner, C.; Beuerle, T.; Scharnhop, H.; Ernst, L.; Beerhues, L. *J. Agric. Food Chem.* **2010,** *58,* 11977–11984. doi:10.1021/jf1026857
24. Garcia Cortez, D. A.; Abreu Filho, B. A.; Nakamura, C. V.; Dias Filho, B. P.; Marston, A.; Hostettmann, K. *Pharm. Biol.* **2002,** *40,* 485–489. doi:10.1076/phbi.40.7.485.14687
25. Shiu, W. K. P.; Gibbons, S. *Phytochemistry* **2009,** *70,* 403–406. doi:10.1016/j.phytochem.2008.12.016
26. Harborne, J. B. *Nat. Prod. Rep.* **1997,** *14,* 83–98. doi:10.1039/np9971400083
27. Hahlbrock, K.; Scheel, D. *Annu. Rev. Plant Physiol. Plant Mol. Biol.* **1989,** *40,* 347–369. doi:10.1146/annurev.pp.40.060189.002023
28. Daniel, S.; Barz, W. *Planta* **1990,** *182,* 279–286. doi:10.1007/BF00197122
29. Dietrich, A.; Mayer, J. E.; Hahlbrock, K. *J. Biol. Chem.* **1990,** *265,* 6360–6368.
30. Fischer, D.; Ebenau-Jehle, C.; Grisebach, H. *Arch. Biochem. Biophys.* **1990,** *276,* 390–395. doi:10.1016/0003-9861(90)90737-J
31. Kutchan, T. M.; Dittrich, H.; Bracher, D.; Zenk, M. H. *Tetrahedron* **1991,** *47,* 5945–5954. doi:10.1016/S0040-4020(01)86487-5
32. Chappell, J. *Plant Physiol.* **1995,** *107,* 1–6.
33. Gessler, C.; Patocchi, A. *Adv. Biochem. Eng. Biotechnol.* **2007,** *107,* 113–132. doi:10.1007/10_2007_053
34. Liu, B.; Raeth, T.; Beuerle, T.; Beerhues, L. *Planta* **2007,** *225,* 1495–1503. doi:10.1007/s00425-006-0435-5
35. Chizzali, C.; Gaid, M. M.; Belkheir, A. K.; Hänsch, R.; Richter, K.; Flachowsky, H.; Peil, A.; Hanke, M.-V.; Liu, B.; Beerhues, L. *Plant Physiol.* **2012,** *158,* 864–875. doi:10.1104/pp.111.190918
36. Liu, B.; Raeth, T.; Beuerle, T.; Beerhues, L. *Plant Mol. Biol.* **2010,** *72,* 17–25. doi:10.1007/s11103-009-9548-0

License and Terms

Beilstein Journal of Organic Chemistry

Identification and isolation of insecticidal oxazoles from *Pseudomonas* spp.

Florian Grundmann[1], Veronika Dill[1], Andrea Dowling[2], Aunchalee Thanwisai[3], Edna Bode[1], Narisara Chantratita[3], Richard ffrench-Constant[2] and Helge B. Bode[*1]

Letter

Open Access

Address:
[1]Department of Molecular Biotechnology, Goethe-Universität Frankfurt, Max-von-Laue-Str. 9, 60438 Frankfurt am Main, Germany, [2]Biosciences, University of Exeter, Penryn, Cornwall, TR10 9EZ, UK and [3]Faculty of Tropical Medicine, Mahidol University, 420/6 Ratchawithi Road, Ratchathewi, Bangkok 10400, Thailand

Email:
Helge B. Bode[*] - h.bode@bio.uni-frankfurt.de

* Corresponding author

Keywords:
insecticidal activity; labradorin; oxazole; *Pseudomonas*; secondary metabolite

Beilstein J. Org. Chem. **2012,** *8,* 749–752.
doi:10.3762/bjoc.8.85

Received: 18 March 2012
Accepted: 02 May 2012
Published: 18 May 2012

This article is part of the Thematic Series "Biosynthesis and function of secondary metabolites".

Guest Editor: J. S. Dickschat

Abstract

Two new and five known oxazoles were identified from two different *Pseudomonas* strains in addition to the known pyrones pseudopyronine A and B. Labeling experiments confirmed their structures and gave initial evidence for a novel biosynthesis pathway of these natural oxazoles. In order to confirm their structure, they were synthesized, which also allowed tests of their bioactivity. Additionally, the bioactivities of the synthesis intermediates were also investigated revealing interesting biological activities for several compounds despite their overall simple structures.

Findings

During our search for novel natural products from entomopathogenic bacteria, strain PB22.5 was isolated from a soil sample collected in Thailand by using the baiting technique for the isolation of entomopathogenic bacteria and/or entomopathogenic nematodes, as described previously [1-4]. HPLC–MS analysis of extracts from strain PB22.5 grown in LB showed several peaks (Supporting Information File 1, Figure S1) that have not been detected in other entomopathogenic bacteria (data not shown). Subsequent large scale cultivation and purification of the main components led to the isolation of five major compounds, which were subjected to structure elucidation by MS (Supporting Information File 1, Figure S2) and NMR analysis (Supporting Information File 1, Tables S1–S6). Whereas the structures **1** and **2** could be identified as pseudopyronines A (**1**, 267.4 *m/z* $[M + H]^+$, $C_{16}H_{26}O_3$) and B (**2**, 295.4 *m/z* $[M + H]^+$, $C_{18}H_{30}O_3$) [5-7], three other compounds were identified as the

known oxazole derivatives labradorin 1 (**3**, 241.1 *m/z* $[M + H]^+$, $C_{15}H_{16}N_2O$), labradorin 2 (**4**, 255.2 *m/z* $[M + H]^+$, $C_{16}H_{18}N_2O$) and pimprinaphine (**5**, 275.1 *m/z* $[M + H]^+$, $C_{18}H_{14}N_2O$) (Figure 1) [8,9].

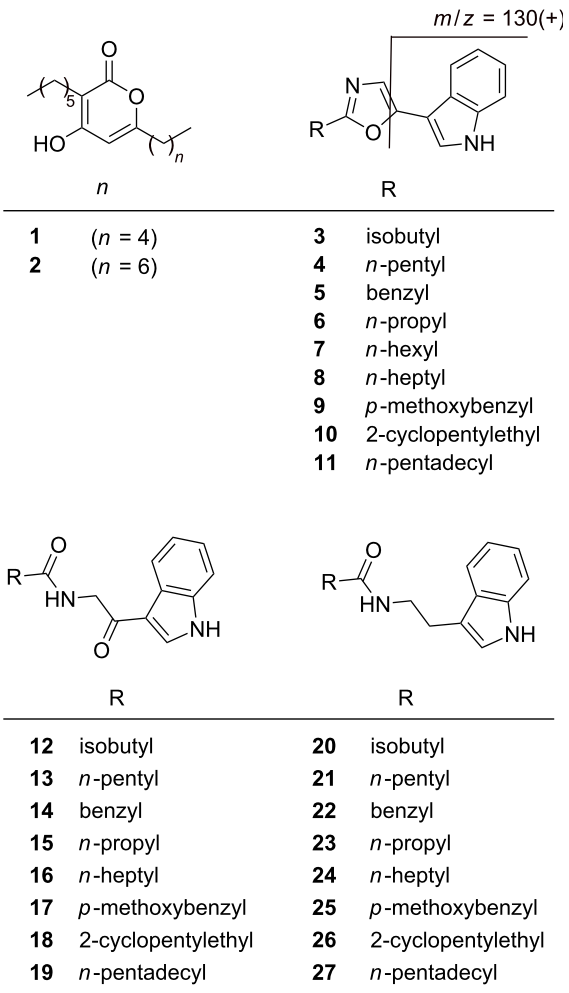

Figure 1: Structures of pseudopyronines A (**1**) and B (**2**) and natural oxazoles (**3**–**8**) as well as synthetic oxazole derivatives (**9**–**11**). All natural and synthetic oxazoles show the characteristic MS fragment 130 *m/z* $[M + H]^+$. The intermediates of the oxazole syntheses (**12**–**27**) are also shown as they were also tested for their biological activity.

Detailed analysis of the HPLC–MS data showed WS-30581 A (**6**, 227.1 *m/z* $[M + H]^+$, $C_{14}H_{14}N_2O$) [10] as an additional oxazole derivative, but which was only produced in minute amounts. WS-30581 A (**6**) was identified by comparing the retention time and the MS fragmentation (Supporting Information File 1, Figure S2) of the product contained in the extract, with a synthesized compound. All oxazoles showed a characteristic fragment ion of 130 *m/z* $[M + H]^+$ (Supporting Information File 1, Figure S2), and labeling experiments (Supporting Information File 1, Figure S3) enabled the elucidation of this ion as 3-methylidene-3*H*-indolium (Figure 1).

In order to determine the genus of the producing strain PB22.5, we sequenced its 16S-rRNA gene revealing it to be a *Pseudomonas* sp. with closest homology to *P. putida* (100% similarity: Supporting Information File 1, Figure S4) [11-14].

As judged on the basis of high-resolution MALDI–MS and LC–ESIMS/MS data the well-known entomopathogenic *P. entomophila* [15,16] also produces compounds **3**–**6** but not **1** and **2**. Furthermore two novel oxazole derivatives named labradorin 3 (**7**, 268.4 *m/z* $[M + H]^+$, $C_{17}H_{20}N_2O$) and labradorin 4 (**8**, 283.2 *m/z* $[M + H]^+$, $C_{18}H_{22}N_2O$) were detected, but they could not be isolated due to their very low production.

Labeling experiments were performed in order to confirm the oxazole structures and to reveal their biosynthesis. Therefore, both strains were cultivated in fully labeled ^{13}C or ^{15}N media and ^{12}C precursors were added (Figure 2).

Five carbons of leucine are incorporated in compound **3**, while eight carbons of compound **5** originate from phenylalanine**,** which confirms these moieties to be amino-acid derived (Figure 3).

Ten carbons and one nitrogen of tryptophan were incorporated in all oxazoles, confirming the indole moiety to be derived from tryptophan. Surprisingly, no incorporation of carbon from tryptamine was observed, and the fact that nitrogen labeling also occurs when ^{14}N-tryptamine, leucine or phenylalanine is fed indicates an efficient transaminase activity in both strains, as one would indeed expect for a bacterial strain living on proteinogenic substrates such as insects. Indole acetaldehyde was also fed in ^{13}C-labeled medium, but, in this case as well, no incorporation was observed (data not shown).

Thus, indolepyruvate or an unknown degradation product thereof is proposed as a precursor for the indole moiety. Unfortunately, the production of **7** and **8** was insufficient for analysis in the labeled media, but the nature of the side chains was concluded from a fatty-acid analysis of the producing strain, which showed only straight-chain fatty acids (data not shown).

In order to confirm the structure of all oxazole derivatives, to compare their retention times, and to provide enough material for bioactivity tests, oxazoles **3**–**6** and **8** were synthesized. Briefly, the respective tryptamine derivatives were formed, which were then oxidized at the alpha-position with the help of 2,3-dichloro-5,6-dicyano-1,4-benzoquinone (DDQ) and cyclized to give the oxazoles by using phosphorylchloride as described [9]. Additionally, three nonnatural derivatives were

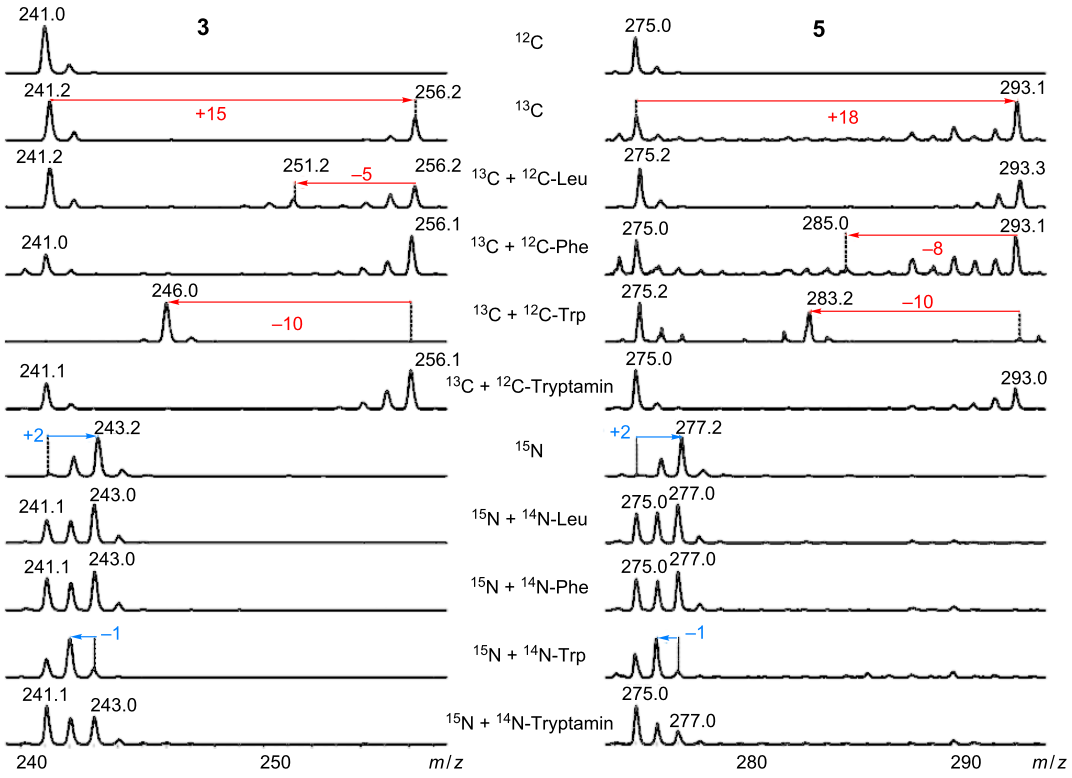

Figure 2: MS data from strain PB22.5, which was cultivated in [U-^{13}C] and [U-^{15}N] medium background and LB medium as a control. Feeding experiments with ^{12}C and ^{14}N amino acids confirmed structures **3** and **5** and gave initial insights into the biosynthesis.

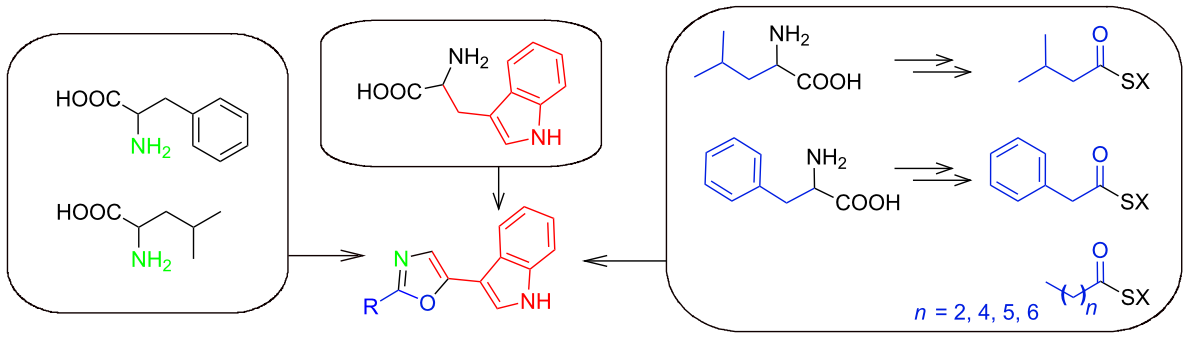

Figure 3: All incorporated biosynthetic precursors of the oxazoles are shown in color. The nitrogen shown in green is derived from transamination as part of the amino acid metabolism. SX = activated ester, which may be coenzyme A or enzyme (acyl carrier protein or polyketide synthase or nonribosomal peptide synthetase) bound.

synthesized to get a more diverse set of oxazole derivatives differing from the natural compounds by unusual (compound **9** and **10**) or very long (compound **11**) acyl chains.

Additionally, the synthetic intermediates were also tested as precursors in labeling experiments as described above, but again no incorporation could be observed. Thus, the biosynthesis via tryptamine amides, which are subsequently oxidized and cyclized to give the oxazoles, can be excluded and more experiments are needed to fully elucidate the biosynthesis of these simple heterocyclic compounds.

All synthesized compounds and intermediates thereof were tested for their biological activity, as a broad range of activities has already been described for these oxazoles, including anticonvulsant and antithrombotic activity as well as activity against human lung and pancreas cancer cell lines [9,10,17].

We tested the bioactivity against the human breast-cancer cell line MCF-7, using the XTT assay [18], and against insect hemocytes from the greater wax moth *Galleria melonella* according to the method described by Proschak et al. [19]. Three oxazole compounds show LD_{50} [μg ml^{-1}] values against *Galleria* hemocytes of 30 (compound **3**), 1.7 (compound **6**), and 103 (compound **9**) (Table S7). Compounds **3**, **5**, **6**, and **9** are active in the MCF-7 assay with EC_{50} [μg ml^{-1}] values of 58, 363, 26, and 34, respectively. Similar to previous results [19], several tryptamine amide derivatives (**20**–**24**, **26**) showed cytotoxic activity against the MCF-7 cells with **24** being the most potent compound (1.02 μg ml^{-1}). Interestingly, **26** also showed activity against *Galleria* hemocytes, although its oxazole derivative **10** did not, which may point to different targets for both compound classes.

The class of oxazole compounds, which were identified in this article, are not only prevalent in *Pseudomonas* but also in other bacteria such as *Streptomyces* [20] or *Streptoverticillium* [8,10], suggesting a biological relevance also in these bacteria. However, as concluded from the observed activity against insect cells, they could significantly add to the overall insecticidal activity of the investigated *Pseudomonas* strains.

Supporting Information

Supporting Information File 1

General experimental procedures, isolation of the strain and taxonomic identification, cultivation and extraction, isolation, labeling experiments, synthesis, bioactivity results and compound characterization.
[http://www.beilstein-journals.org/bjoc/content/supplementary/1860-5397-8-85-S1.pdf]

Acknowledgements

Work in the Bode lab was supported by the LOEWE Schwerpunkt Insektenbiotechnologie, the European Community's Seventh Framework Programme (FP7/2007-2013) under grant agreement no. 223328, which also supported work in the ffrench-Constant and Chantratita labs, and the Deutsche Forschungsgemeinschaft (DFG).

References

1. Akhurst, R. J. *J. Gen. Microbiol.* **1980,** *121,* 303–309.
2. Bedding, R. A.; Akhurst, R. J. *Nematologica* **1975,** *21,* 109–110.
3. White, G. F. *Science* **1927,** *66,* 302–303. doi:10.1126/science.66.1709.302-a
4. Woodring, L. J. H.; Kaya, K. H. *Steinernematid and Heterorhabditid nematodes. A Handbook of biology and techniques;* Southern Cooperative Series Bulletin, Arkansas Agricultural Experimental Station: Fayetteville Arkansas, USA, 1988.
5. Chu, M.; Mierzwa, R.; Xu, L.; He, L.; Terracciano, J.; Patel, M.; Zhao, W.; Black, T. A.; Chan, T. M. *J. Antibiot.* **2002,** *55,* 215–218.
6. Kong, F.; Singh, M. P.; Carter, G. T. *J. Nat. Prod.* **2005,** *68,* 920–923. doi:10.1021/np050038v
7. Singh, M. P.; Kong, F. M.; Janso, J. E.; Arias, D. A.; Suarez, P. A.; Bernan, V. S.; Petersen, P. J.; Weiss, W. J.; Carter, G.; Greenstein, M. *J. Antibiot.* **2003,** *56,* 1033–1044.
8. Koyama, Y.; Yokose, K.; Dolby, L. J. J. *Agric. Biol. Chem.* **1981,** *45,* 1285–1287.
9. Pettit, G. R.; Knight, J. C.; Herald, D. L.; Davenport, R.; Pettit, R. K.; Tucker, B. E.; Schmidt, J. M. *J. Nat. Prod.* **2002,** *65,* 1793–1797. doi:10.1021/np020173x
10. Umehara, K.; Yoshida, K.; Okamoto, M.; Iwami, M.; Tanaka, H.; Kohsaka, M.; Imanaka, H. *J. Antibiot.* **1984,** *37,* 1153–1160.
11. Kimura, M. *J. Mol. Evol.* **1980,** *16,* 111–120. doi:10.1007/BF01731581
12. Saitou, N.; Nei, M. *Mol. Biol. Evol.* **1987,** *4,* 406–425.
13. Tamura, K.; Dudley, J.; Nei, M.; Kumar, S. *Mol. Biol. Evol.* **2007,** *24,* 1596–1599. doi:10.1093/molbev/msm092
14. Thompson, J. D.; Higgins, D. G.; Gibson, T. J. *Nucleic Acids Res.* **1994,** *22,* 4673–4680. doi:10.1093/nar/22.22.4673
15. Vodovar, N.; Vinals, M.; Liehl, P.; Basset, A.; Degrouard, J.; Spellman, P.; Boccard, F.; Lemaitre, B. *Proc. Natl. Acad. Sci. U. S. A.* **2005,** *102,* 11414–11419. doi:10.1073/pnas.0502240102
16. Vodovar, N.; Vallenet, D.; Cruveiller, S.; Rouy, Z.; Barbe, V.; Acosta, C.; Cattolico, L.; Jubin, C.; Lajus, A.; Segurens, B.; Vacherie, B.; Wincker, P.; Weissenbach, J.; Lemaitre, B.; Médigue, C.; Boccard, F. *Nat. Biotechnol.* **2006,** *24,* 673–679. doi:10.1038/nbt1212
17. Naik, S. R.; Harindran, J.; Varde, A. B. *J. Biotechnol.* **2001,** *88,* 1–10. doi:10.1016/S0168-1656(01)00244-9
18. Scudiero, D. A.; Shoemaker, R. H.; Paull, K. D.; Monks, A.; Tierney, S.; Nofziger, T. H.; Currens, M. J.; Seniff, D.; Boyd, M. R. *Cancer Res.* **1988,** *48,* 4827–4833.
19. Proschak, A.; Schultz, K.; Herrmann, J.; Dowling, A. J.; Brachmann, A. O.; ffrench-Constant, R.; Müller, R.; Bode, H. B. *ChemBioChem* **2011,** *12,* 2011–2015. doi:10.1002/cbic.201100223
20. Joshi, B. S.; Taylor, W. I.; Bhate, D. S.; Karmarkar, S. S. *Tetrahedron* **1963,** *19,* 1437–1439. doi:10.1016/S0040-4020(01)98569-2

License and Terms

Beilstein Journal of Organic Chemistry

Unprecedented deoxygenation at C-7 of the ansamitocin core during mutasynthetic biotransformations

Tobias Knobloch[1], Gerald Dräger[1], Wera Collisi[2], Florenz Sasse[2] and Andreas Kirschning[*1]

Full Research Paper

Open Access

Address:
[1]Institute of Organic Chemistry and Center of Biomolecular Drug Research (BMWZ), Leibniz University Hannover, Schneiderberg 1b, 30167 Hannover, Germany and [2]Department of Chemical Biology, Helmholtz Center for Infectious Research (HZI), Inhoffenstraße 7, D-38124 Braunschweig, Germany

Email:
Andreas Kirschning[*] - andreas.kirschning@oci.uni-hannover.de

* Corresponding author

Keywords:
ansamitocins; antibiotics; antitumor agents; mutasynthesis; natural products

Beilstein J. Org. Chem. **2012,** *8,* 861–869.
doi:10.3762/bjoc.8.96

Received: 23 April 2012
Accepted: 16 May 2012
Published: 11 June 2012

This article is part of the Thematic Series "Biosynthesis and function of secondary metabolites".

Guest Editor: J. S. Dickschat

Abstract

We describe the unprecedented formation of six ansamitocin derivatives that are deoxygenated at C-7 of the ansamitocin core, obtained during fermentation experiments by employing a variety of *Actinosynnema pretiosum* mutants and mutasynthetic approaches. We suggest that the formation of these derivatives is based on elimination at C-7/C-8 followed by reduction(s) of the intermediate enone. In bioactivity tests, only ansamitocin derivatives bearing an ester side chain at C-3 showed strong antiproliferative activity.

Introduction

Natural products still play an important role as lead structures for the treatment of infectious diseases and cancer. However, natural products have lost some of their attraction for the development of pharmaceuticals because of their structural complexity and the difficulties associated with accessing analogues for structure–activity relationship studies. Total synthesis approaches are still a tour de force and are hardly employed, while commonly semisynthesis as well as biotechnological approaches are widely pursued in industrial research [1-3]. Investigations into the biosynthesis of natural products have not only allowed us to understand the synthetic principles that nature pursues, but have also provided tools, mainly based on genetic engineering, which can be exploited in natural product synthesis [4].

Producer strains genetically blocked in the biosynthesis of important and complex natural products can serve as such new tools. The synthetic concept based on these blocked mutants is

termed "mutational biosynthesis", or in short mutasynthesis, and it relies on the cellular uptake of modified biosynthetic intermediates, sometimes termed mutasynthons, and their incorporation into complex secondary metabolites [5-7].

When making use of mutants that are blocked in early stages of a given biosynthesis pathway, the concept of mutasynthesis may be compared to a (partial) natural product total synthesis. When further modification of an advanced biosynthetic intermediate with an established core structure towards bioactive natural products and analogues is conducted, mutasynthesis may be regarded as the "endgame" of a total synthesis [4].

The ansamitocins (maytansinoids) **3**–**5** are ideally suited for mutasynthetic modifications and the creation of new analogues because they are highly potent antitumor active compounds that inhibit the growth of different leukemia cell lines as well as human solid tumors at very low concentrations (10^{-3} to 10^{-7} μg/mL) [8]. In contrast to colchicine, maytansinoids such as ansamitocins bind to β-tubulin monomers at a site overlapping the vinca alkaloid binding site [9].

Recently, we disclosed several mutasynthetic studies aimed at the production of derivatives of ansamitocins **3**–**5** [10-12] as well as of geldanamycin (**6**), utilizing mutant strains of *Actinosynnema pretiosum*, the ansamitocin producer [13-17], and *Streptomyces hygroscopicus*, the geldanamycin producer [18,19]. These engineered strains are unable to biosynthesize 3-amino-5-hydroxybenzoic acid (**1**) [20], the common starter unit for both polyketide synthases (PKS) (Scheme 1). These assembly-line-type multienzymes are responsible for setting up the complete carbon backbone of both ansamycin antibiotics [21-24].

More precisely, the biosynthesis of ansamitocins relies on a type I modular polyketide synthase (PKS), with 3-amino-5-hydroxybenzoic acid (**1**, AHBA) [20] as the starter unit followed by chain extension by one "glycolate", three propionate and three acetate units. The last PKS module holds *seco*-proansamitocin, which is released and cyclized, presumably by an ansamycin amide synthase (Asm9) [21-24], to yield the 19-membered macrocyclic lactam proansamitocin (**2**). Proansamitocin (**2**) is transformed into bioactive compounds **3**–**5** by a set of post-PKS tailoring steps, following a predetermined, only partly flexible logic (Scheme 1) [16].

Complementing our studies with mutant strain *A. pretiosum* HGF073, blocked in the biosynthesis of the PKS starter unit AHBA **1** [13-16], we recently reported the use of a mutant of *A. pretiosum* blocked in Asm12 (chlorination) and Asm21

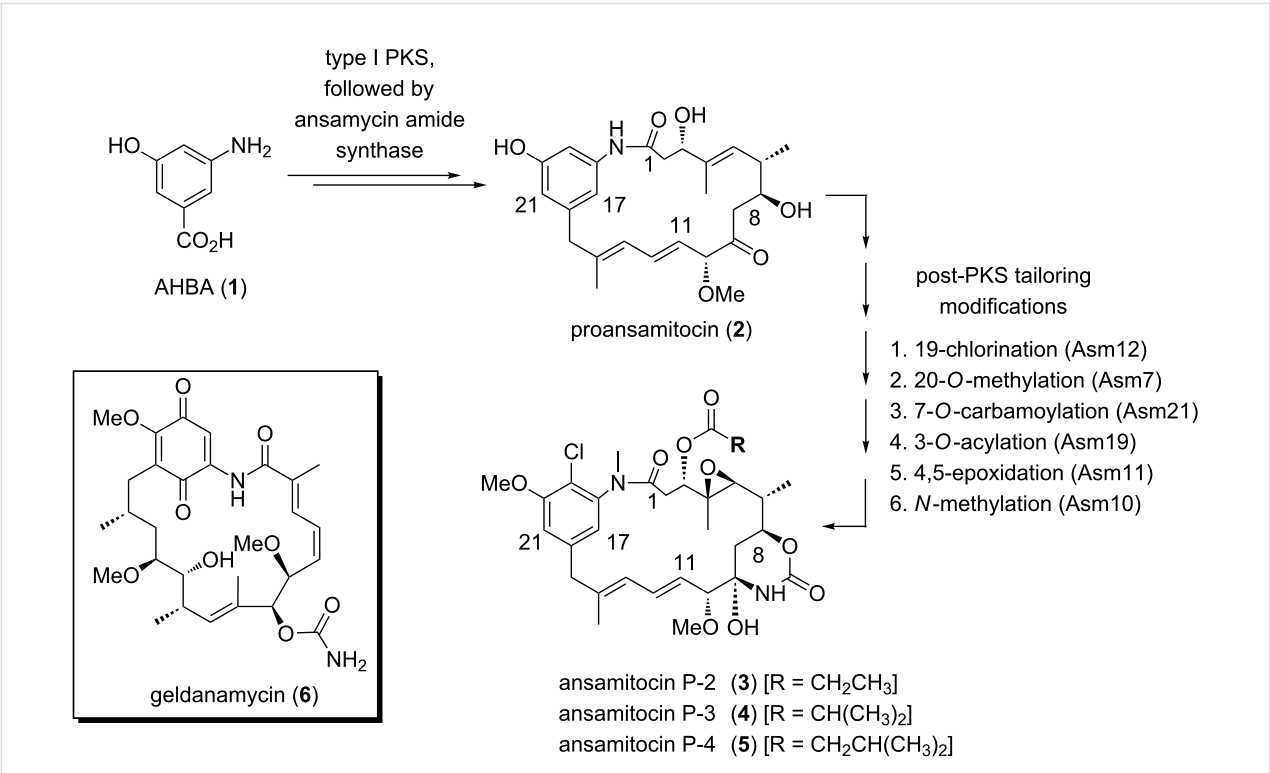

Scheme 1: Summary of ansamitocin biosynthesis and structure of the related ansamycin antibiotic geldanamycin (**6**).

(carbamoylation) and therefore producing proansamitocin (**2**) in good yield (up to 106 mg/L of fermentation broth) [17]. Additionally, we isolated small amounts of *O*-methyl proansamitocin **7** (2.3 mg/L), 10-*epi*-proansamitocin **8** (3.5 mg/L) and two diastereomeric byproducts **9a** and **9b** (7.6 mg/L; 1:1 ratio) from the fermentation broth of *A. pretiosum* Δasm12/21 (Figure 1). We also showed that none of these proansamitocin derivatives exhibit antiproliferative activity.

Herein, we describe the unprecedented formation of ansamitocin derivatives that are deoxygenated at C-7 of the ansamitocin core, obtained by us during fermentation experiments using a variety of *A. pretiosum* mutants and mutasynthetic approaches.

Results and Discussion

In the course of our well-established mutasynthesis experiments with *A. pretiosum* HGF073, a mutant that is unable to produce the essential starter unit AHBA (**1**) by itself, we achieved the generation of several novel ansamitocin derivatives, among other things, based on the simple mutasynthon 3-amino-5-chlorobenzoic acid (**10**, Scheme 2).

With the exception of proansamitocin analogue **11a**, all new metabolites were isolated on a preparative scale and fully characterized. These compounds correspond to the known stepwise sequence of postketide synthase tailoring transformations, and those products and similar compounds have been reported by us before [16]. As evident from the variety of compounds isolated, proansamitocin analogues resulting from supplementation of AHBA analogue **10** to *A. pretiosum* HGF073 were not efficiently processed by the enzymes involved in post-PKS tailoring. In addition to the ordinary compounds **11a**–**e**, the experiment yielded three compounds of an unprecedented type (**11f**–**h**) whose appearance could not be attributed to the known tailoring transformations. Herein, we now describe for the first time the isolation and characterization of compounds **11f**–**h** sharing, in contrast to all other (pro)ansamitocin derivatives known so far, the common feature of deoxygenation at C-7. In addition, proansamitocin derivatives **11g**–**h** are notable for their C-9 alcohol, while **11h** shows additional carbamoylation of the unusual alcohol moiety. The extraordinary proansamitocin derivatives **11f**–**h** were fully characterized, except for the configuration at C-9 in **11g** and **11h** (single diastereomer). Overlap with other signals in the ^{1}H NMR spectra hampered complete assignment of all coupling constants at C-9 except for $J_{9,10}$ = 7.2 Hz, which, however, is not diagnostic.

In continuation of our experiments with advanced biosynthetic intermediates, such as proansamitocin (**2**) [25] and *seco*-acid derivatives [26,27] serving as mutasynthons in experiments with early-stage-blocked mutants, we also tested the unusual metabolites **9a** and **9b** [17] as precursors for further processing by the AHBA(−)-mutant of the ansamitocin producer (Scheme 3).

Originally obtained by fermentation of a mutant blocked to the greatest extent in the post-PKS transformation sequence (*A. pretiosum* Δasm12/21) [17], it was questionable whether these compounds, differing substantially from proansamitocin (**2**) both by a rearranged diene system and an alcohol moiety at C-14, would be accepted by the tailoring enzymes. Surprisingly, when the rearranged oxidation products **9a** and **9b** were each supplemented to cultures of *A. pretiosum* HGF073, new products were formed. While the carbamoylated derivative **12** resulting from biotransformation of alcohol **9b** can be attributed to the activity of the carbamoyltransferase Asm21, thereby providing an indication pertaining to its substrate flexibility, products **13a** and **13b** obtained from both experiments are more unusual and differ from the starting material by being deoxygenated at C-7.

However, the structure of compound **12** strongly contrasts with all of the other 7-*O*-carbamoylated (pro)ansamitocin derivatives that we have obtained with this kind of feeding experiment so far [17]. In the case of compound **12**, the carbinol-

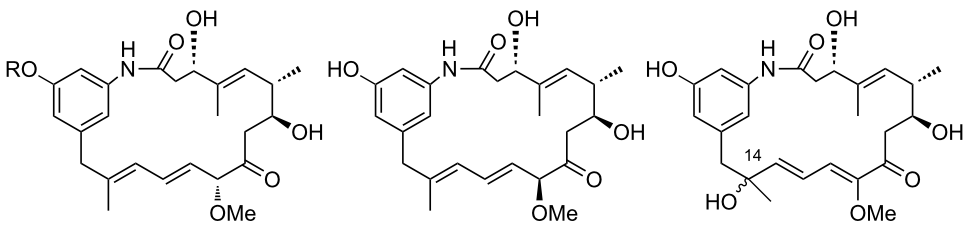

2 R = H (106 mg/L)
7 R = Me (2.3 mg/L)
8 (3.5 mg/L)
9a (3.7 mg/L)
9b (3.9 mg/L)

Figure 1: Fermentation products, proansamitocin (**2**) and derivatives **7**–**9**, of the Asm12 and Asm21-blocked (chlorination, carbamoylation) mutant strain *A. pretiosum* Δasm12/21 (yields given as isolated product per volume of fermentation broth) [17].

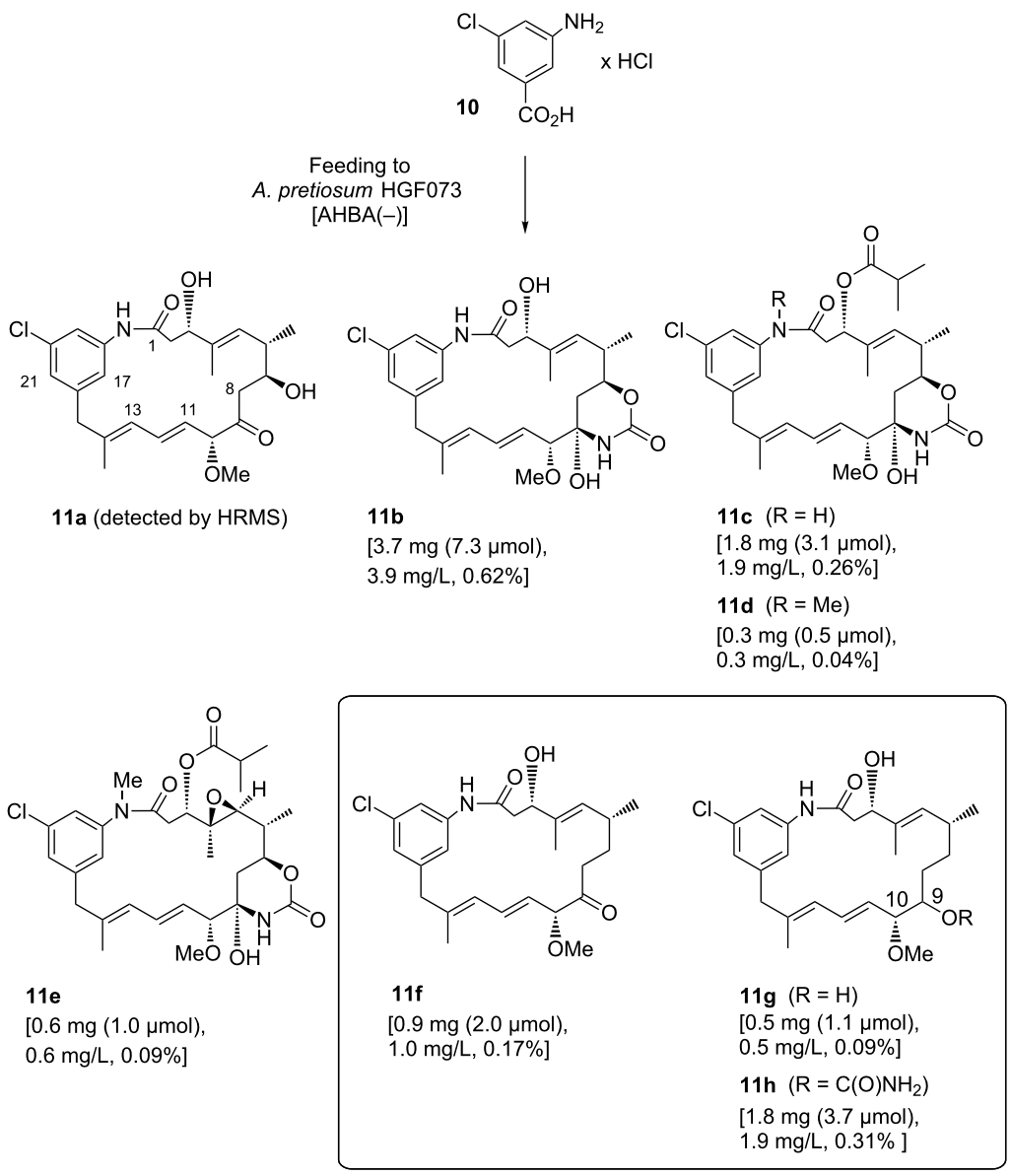

Scheme 2: Mutasynthetic preparation of ansamitocin derivatives **11a**–**h** by using 3-amino-5-chlorobenzoic acid (**10**) as a mutasynthon (yields in % are calculated with reference to the amount of mutasynthon **10** fed).

amide moiety is not present in a cyclic halfaminal form ($\delta_{C\text{-}9}$ ~197 ppm instead of ~82 ppm), despite the fact that the keto group at C-9 is still present. This result may be attributed to the keto group at C-9 being in conjugation with the diene system, resulting in a reduced activity of the carbonyl group and an alteration of the macrolactam ring conformation.

We based the determination of deoxygenation at C-7 in **13a** and **13b** on MS data and the appearance of a secondary carbon atom in exchange of the tertiary carbinol at C-7 on phase-sensitive ^{1}H–^{13}C-correlation NMR spectra (HSQC). It needs to be noted that NOE-analysis combined with molecular modeling did not allow elucidation of the absolute configuration at C-14 for the new derivatives **13a** and **13b**, as it did not allow for the starting compounds **9a** and **9b** [17].

In order to shed light on the sequence of events leading to deoxygenation, the carbamoylated derivative **12** was again fed to a culture of *A. pretiosum* HGF073, and the formation of new products was analyzed by UPLC-HRMS of the partially purified crude extract (Scheme 3). Indeed, the expected deoxygenated product **13b** could be detected, but was also accompanied by the formation of alcohol **9b**. Compound **9b** may either have resulted from Michael addition of water to the suspected

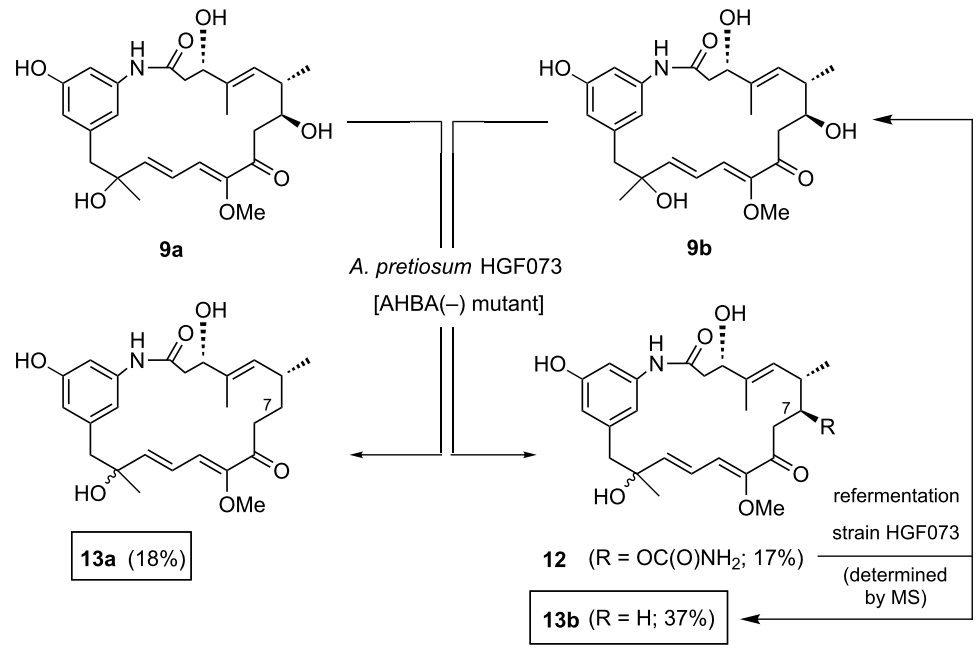

Scheme 3: Mutasynthetic biotransformation of proansamitocin derivatives **9a** and **9b** with AHBA(−) mutant *A. pretiosum* HGF073 (starting materials could be reisolated: **9a**: 77% reisolated, **9b**: 23% reisolated).

intermediate enone **17** (see later in Scheme 5) or from hydrolytic cleavage of the carbinolamide **12**.

A blocked mutant of *A. pretiosum* that is unable to carry out acylation of the C-3 alcohol of the carbamoylated proansamitocin derivative precursor due to genetic inactivation of the acyl transferase Asm19, was reported by Floss et al. [21,28]. It was known that mutant strain *A. pretiosum* HGF059 produces the expected ansamitocin derivative **14** in good yield (Scheme 4) [28]. Besides the ester side chain, compound **14** also lacks the

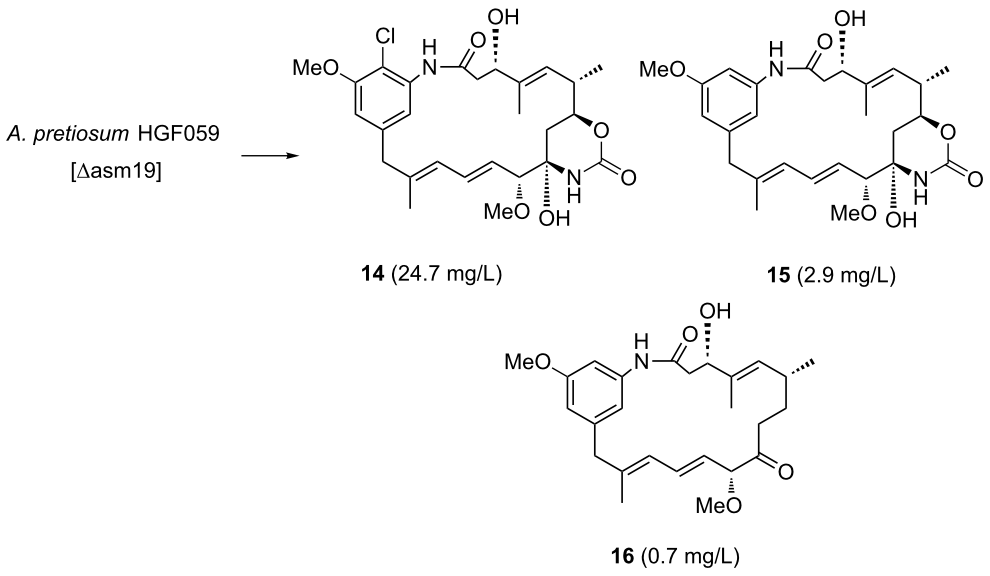

Scheme 4: Fermentation products **14**–**16** of acyl transferase Asm19-blocked mutant *A. pretiosum* HGF059 (Δasm19) (yields given as isolated product per volume of fermentation broth).

epoxy functionality and the *N*-methyl group. These two tailoring steps finalize the biosynthesis of ansamitocin P-3 (AP-3, **4**) and occur only after acylation has taken place (Scheme 1).

While examining the fermentation extract for byproducts we were able to identify two new metabolites, **15** and **16**. Formation of compound **15** can be traced back to inefficient chlorination, a phenomenon that we have encountered before in other feeding experiments with proansamitocin [25]. More unusual is metabolite **16,** which is yet another example of a case in which deoxygenation at C-7 has taken place.

In summary, deoxygenation may occur when the AHBA-blocked mutant *A. pretiosum* HGF073 or the acyl transferase Asm19-blocked mutant *A. pretiosum* HGF059 are employed, whereas the reduction process does not occur with the blocked mutant *A. pretiosum* Δasm12/21. The major difference between these three mutants is the presence (HGF073, HGF059) or absence (Δasm12/21) of the carbamoyl transferase Asm21. Carbamoylation of proansamitocin derivatives at C-7 (e.g. **11a**, **9a**/**b** and **7**) introduces a fairly good leaving group β-positioned to the keto group, thereby facilitating elimination to enones **17** (Scheme 5).

In the case of compound **12,** which predominantly exists in a form lacking the typical cyclized carbinolamide moiety, the C-9 keto group can preserve its electronic properties, thus facilitating the elimination step. Finally, the activity of a tailoring reductase, which in all likelihood is not part of the PKS, catalyzes the reduction of the α,β-unsaturated bond, yielding the deoxygenated derivatives (**11f**, **13a/b**, **16**). Diastereoselective reduction of the C-9 keto group and carbamoylation of intermediate **11f** would then result in compounds **11g** and **11h**, respectively.

A factor contributing to the formation of deoxygenated proansamitocin derivatives is likely the usage of the carbamoylated precursors by the Asm19 acyl transferase. Acylation is a crucial bottleneck step in the otherwise partly flexible sequence of post-PKS transformations. When this step cannot occur due to the absence of an active acyl transferase (as in *A. pretiosum* HGF059), or if the transformation is inefficient (e.g., compound **11b**) or even nonexistent due to an unusual substrate (e.g., compound **12**), carbamoylated intermediates accumulate. Indeed, the carbamoylated product **11b** was the major product of the mutasynthesis experiment with mutasynthon **10**. The carbamoylated compounds may then be channeled into the pathway leading to deoxygenated products. Depending on the substrate, this process may be quite efficient. For instance, no carbamoylated product could be isolated after the biotransformation of compound **9a**, indicating an efficient transformation of the suspected carbamoylated intermediate to the final product **13a**.

All (pro)ansamitocin derivatives fully characterized by NMR were also subjected to in vitro biological testing with different human cell lines derived from tumors or the umbilical vein. The results from these tests are given as values for the half-maximal inhibitory concentration of the respective ansamitocin deriva-

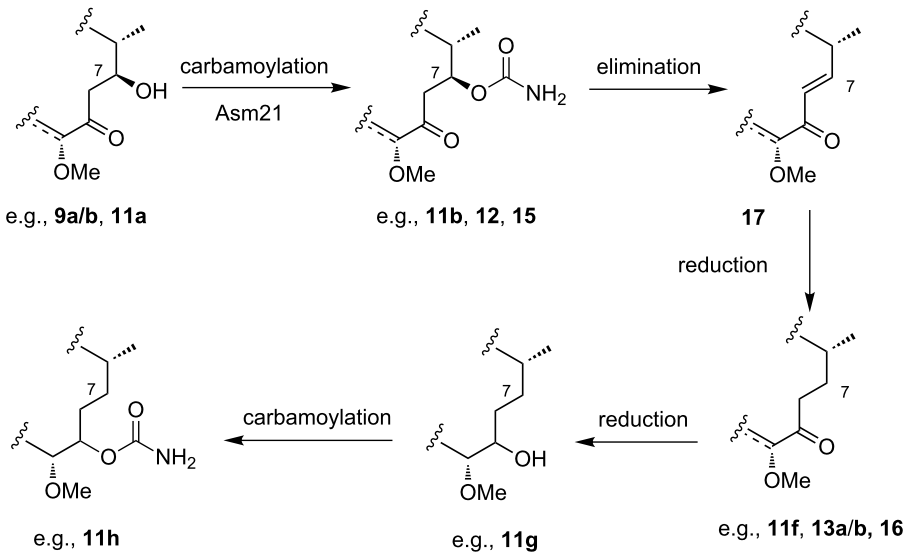

Scheme 5: Possible mechanism of deoxygenation at C-7 of proansamitocin derivatives.

tives in comparison to the "gold standard" ansamitocin P-3 (**4**, Table 1). As expected [14], all (pro)ansamitocin derivatives lacking the ester side chain at C-3 (**11b**, **11g–h**, **12–16**) do not show any antiproliferative activity (IC_{50} > 800 nM) for at least two of the cell lines listed in Table 1.

Compounds **11c–e**, bearing the ester side chain at C-3, predominantly showed activities in the pM range. As seen also with AP-3 (**4**), there is no significant difference between cancerous and healthy cells. The most active compound was the *N*-methyl derivative **11d**, which reached the activity of the standard AP-3 (**4**) for selected cell lines.

Conclusion

In conclusion, we disclose the isolation and chemical and antiproliferative activity characterization of several novel ansamitocin derivatives that are deoxygenated at C-7. We used three different *A. pretiosum* mutants and a variety of mutasynthetic approaches. These preliminary studies on the deoxygenation at C-7 suggest that it occurs by elimination at C-7/C-8 after carbamoylation has taken place, followed by reduction mediated by an unknown reductase, which is not part of the main assembly line PKS. As expected, all ansamitocin compounds bearing the ester side chain at C-3 predominantly showed activities in the pM range.

Experimental

Analytical details are given in the Supporting Information File 1.

Cultivation

In general, cultivation of microbial strains on agar plates was conducted in a Heraeus incubator at 30 °C, while cultivation in a shake flask was performed in a multilevel New Brunswick Scientific Innova 4900 gyratory multi-shaker at 200 rpm at 29 °C.

Unless otherwise noted, the cultivation media were prepared using distilled water and sterilized by autoclaving: YMG medium – 10 g/L malt extract (Sigma), 4 g/L yeast extract (Bacto), 4 g/L D(+)- glucose·H_2O; YMG agar – YMG medium plus 22 g/L agar (Bacto); K-medium [29], basal composition (final start concentration in the main culture corresponds to 5/6 of the values given for this medium due to dilution) – 60 g/L dextrin from maize starch (Fluka), 30 g/L D(+)-maltose·H_2O (Fluka), 5.25 g/L cottonseed flour (Proflo), 5 g/L $CaCO_3$, 4.5 g/L yeast extract (Bacto), 300 mg/L K_2HPO_4 (Fluka, TraceSelect), 2 mg/L $FeSO_4 \cdot 7H_2O$. K-medium, additive – autoclaved and added separately: 3 g/L L-valine (final start concentration in the main culture, from a 3% (w/v) stock solution). *A. pretiosum* HGF073 is a replicate of strain HGF056 reported in [22].

Fermentation of *A. pretiosum* strains

A. pretiosum strains (HGF073, HGF059, Δasm12/21) were stored as spore suspensions in 40% (v/v) glycerol/water at −80 °C, and used for the inoculation of YMG agar plates. Following incubation of the plates for 4 d at 30 °C, 5–8 well-sporulated colonies were transferred to a 1.5 mL tube charged with 1 mL of sterile distilled water and filled to approx. 50% height with sterile glass beads (Ø = 2 mm, washed with dilute hydrochloric acid). After vortex-mixing, the resulting suspension was used for the inoculation of precultures in bottom-baffled 250 mL Erlenmeyer flasks charged with YMG medium (50 mL per flask, with additional steel spring). Precultures were shaken for 2 d at 29 °C before inoculation of main production cultures (1/15 dilution). Cultivations were performed in K-medium with additives – 42 mL K-medium with L-valine, 3 mL preculture and one drop of SAG 471 anti-foam (GE Bayer Silicones) [30] – by using nonbaffled 250 mL Erlenmeyer flasks (final volume: 35–60 mL per flask, with additional steel spring). Shaking was continued at 29 °C for a total cultivation time of 7–10 days.

Table 1: Antiproliferative activity IC_{50} [nmol/L] of **11c–e** in comparison to AP-3 (**4**).[a]

compound	cell line					
	U-937	A-431	SK- OV-3	PC-3	MCF-7	HUVEC
AP-3 (**4**)	0.01	0.08	0.05	0.06	n.d.	0.02
11c	0.5	1.58	0.66	0.30	0.90	0.32
11d	0.05	0.10	0.05	0.16	0.11	0.08
11e	0.18	0.35	0.21	0.53	0.41	0.21

[a]Values shown are means of two determinations in parallel; human cell lines: U-937 (histiocytic lymphoma), A-431 (epidermoid carcinoma), SK-OV-3 (ovary adenocarcinoma), PC-3 (prostate adenocarcinoma), MCF-7 (breast adenocarcinoma), HUVEC (umbilical vein endothelial cells); n.d. = not determined.

For detection of novel products from test cultures, samples of the culture broth (200 µL) were mixed with ethanol (200 µL), centrifuged (20800*g*, 3 min, 4 °C) and the clear supernatant subjected to UPLC-ESIMS analysis. Failing detection of novel products, the culture broth was extracted three times with ethyl acetate, dried over $MgSO_4$, concentrated in vacuo, and filtered over silica gel with ethyl acetate, and the solvent was removed in vacuo. The residue was dissolved in methanol (1 mL) and subjected to UPLC-ESIMS analysis.

For isolation of novel products from (large-scale) fermentations, the combined fermentation broth was extracted with ethyl acetate as described above, and the crude extract subjected to a sequence of chromatographic purifications (Supporting Information File 1).

Mutasynthesis with *A. pretiosum* HGF073

In mutasynthesis experiments with *A. pretiosum* HGF073, production cultures were shaken for 2 d after inoculation (see above) before mutasynthons were added (**9a**, **9b**, **10** or **12**). For novel mutasynthons, productivity of the strain was first monitored by parallel feeding of mutasynthons for which acceptance was known (e.g., the natural starter building block: 3-Amino-5-hydroxybenzoic acid, hydrochloride salt (**1**)). Mutasynthons were dissolved in DMSO/water [preferably 1:1; volume of feeding solution not exceeding 10% (v/v) with respect to the recipient culture] and sterilized by filtration.

Mutasynthon **10** (1.25 mmol/L of fermentation broth) was added to production cultures with a combined volume of 945 mL continuously (drop-wise) over the time-course of 3.5 d, by using autoclavable, syringe pump-driven feeding capillaries – Braintree Scientific BS-9000-8 syringe pump with Upchurch Scientific high-purity Teflon® PFA tubing (1/16" OD, 0.1" ID) and Tefzel® connectors.

Biotransformation of the proansamitocin derivatives **9a**, **9b** and **12** was carried out by supplementing a production culture of *A. pretiosum* HGF073 (45 mL final volume; K-medium; see above) with the respective derivative [**9a**/**b** (each*:* 4.5 mg, 9.8 µmol, dissolved in 2 mL DMSO:H_2O = 1:1); **12** (0.1 mg, 0.2 µmol, dissolved in 1 mL DMSO)] in a single portion after 2.5 (for **12**) to 3.5 d (for **9a**/**b**) of shaking.

Following biotransformation (refermentation) of proansamitocin derivative **12**, only UPLC-ESIMS analysis of the silica-gel-filtered ethyl acetate extract taken up in methanol (see above) was carried out. The retention times and mass spectra of the detected product derivatives **9b** and **13b** were identical to those of the previously isolated materials (Supporting Information File 1).

Supporting Information

The supporting information provides purification protocols of fermentations, a short description of the cell proliferation assay, analytical descriptions of new metabolites and copies of ^1H and ^{13}C NMR spectra.

Supporting Information File 1

Analytical details and compound spectra.
[http://www.beilstein-journals.org/bjoc/content/supplementary/1860-5397-8-96-S1.pdf]

Acknowledgements

This work was supported by the Deutsche Forschungsgemeinschaft (Grant Ki-397, 13-1) and the Fonds der Chemischen Industrie.

References

1. Cragg, G. M.; Grothaus, P. G.; Newman, D. J. *Chem. Rev.* **2009,** *109,* 3012–3043. doi:10.1021/cr900019j
2. Newman, D. J.; Cragg, G. M. *J. Nat. Prod.* **2007,** *70,* 461–477. doi:10.1021/np068054v
3. von Nussbaum, F.; Brands, M.; Hinzen, B.; Weigand, S.; Häbich, D. *Angew. Chem.* **2006,** *118,* 5194–5254. doi:10.1002/ange.200600350
Angew. Chem. Int. Ed. **2006,** *45,* 5072–5129. doi:10.1002/anie.200600350.
4. Kirschning, A.; Hahn, F. *Angew. Chem.* **2012,** *124,* 4086–4096. doi:10.1002/ange.201107386
Angew. Chem. Int. Ed. **2012,** *51,* 4012–4022. doi:10.1002/anie.201107386.
5. Weist, S.; Süssmuth, R. D. *Appl. Microbiol. Biotechnol.* **2005,** *68,* 141–150. doi:10.1007/s00253-005-1891-8
6. Kirschning, A.; Taft, F.; Knobloch, T. *Org. Biomol. Chem.* **2007,** *5,* 3245–3295. doi:10.1039/b709549j
7. Kennedy, J. *Nat. Prod. Rep.* **2008,** *25,* 25–34. doi:10.1039/B707678A
8. Funayama, S.; Cordell, G. A. In *Studies in Natural Product Chemistry;* Rahman, A.-U., Ed.; Elsevier Science B. V.: Amsterdam, 2000; Vol. 23, pp 51–106.
9. Hamel, E. *Pharmacol. Ther.* **1992,** *55,* 31–51. doi:10.1016/0163-7258(92)90028-X
10. Cassady, J. M.; Chan, K. K.; Floss, H. G.; Leistner, E. *Chem. Pharm. Bull.* **2004,** *52,* 1–26. doi:10.1248/cpb.52.1
11. Kirschning, A.; Harmrolfs, K.; Knobloch, T. *C. R. Chim.* **2008,** *11,* 1523–1543. doi:10.1016/j.crci.2008.02.006
12. Floss, H. G.; Yu, T.-W.; Arakawa, K. *J. Antibiot.* **2011,** *64,* 35–44. doi:10.1038/ja.2010.139
13. Taft, F.; Brünjes, M.; Floss, H. G.; Czempinski, N.; Grond, S.; Sasse, F.; Kirschning, A. *ChemBioChem* **2008,** *9,* 1057–1060. doi:10.1002/cbic.200700742
14. Kubota, T.; Brünjes, M.; Frenzel, T.; Xu, J.; Kirschning, A.; Floss, H. G. *ChemBioChem* **2006,** *7,* 1221–1225. doi:10.1002/cbic.200500506
15. Taft, F.; Brünjes, M.; Knobloch, T.; Floss, H. G.; Kirschning, A. *J. Am. Chem. Soc.* **2009,** *131,* 3812–3813. doi:10.1021/ja8088923

16. Knobloch, T.; Harmrolfs, K.; Taft, F.; Thomaszewski, B.; Sasse, F.; Kirschning, A. *ChemBioChem* **2011,** *12,* 540–547. doi:10.1002/cbic.201000608
17. Eichner, S.; Knobloch, T.; Floss, H. G.; Fohrer, J.; Harmrolfs, K.; Hermane, J.; Schulz, A.; Sasse, F.; Spiteller, P.; Taft, F.; Kirschning, A. *Angew. Chem.* **2012,** *124,* 776–781. doi:10.1002/ange.201106249 *Angew. Chem. Int. Ed.* **2012,** *51,* 752–757. doi:10.1002/anie.201106249.
18. Eichner, S.; Floss, H. G.; Sasse, F.; Kirschning, A. *ChemBioChem* **2009,** *10,* 1801–1805. doi:10.1002/cbic.200900246
19. Eichner, S.; Eichner, T.; Floss, H. G.; Fohrer, J.; Hofer, E.; Sasse, F.; Zeilinger, C.; Kirschning, A. *J. Am. Chem. Soc.* **2012,** *134,* 1673–1679. doi:10.1021/ja2087147
20. Walsh, C. T.; Haynes, S. W.; Ames, B. D. *Nat. Prod. Rep.* **2012,** *29,* 37–59. doi:10.1039/c1np00072a
21. Spiteller, P.; Bai, L.; Shang, G.; Carroll, B. J.; Yu, T.-W.; Floss, H. G. *J. Am. Chem. Soc.* **2003,** *125,* 14236–14237. doi:10.1021/ja038166y
22. Yu, T.-W.; Bai, L.; Clade, D.; Hoffmann, D.; Toelzer, S.; Trinh, K. Q.; Xu, J.; Moss, S. J.; Leistner, E.; Floss, H. G. *Proc. Natl. Acad. Sci. U. S. A.* **2002,** *99,* 7968–7973. doi:10.1073/pnas.092697199
23. Arakawa, K.; Müller, R.; Mahmud, T.; Yu, T.-W.; Floss, H. G. *J. Am. Chem. Soc.* **2002,** *124,* 10644–10645. doi:10.1021/ja0206339
24. Yu, T.-W.; Müller, R.; Müller, M.; Zhang, X.; Dräger, G.; Kim, C.-G.; Leistner, E.; Floss, H. G. *J. Biol. Chem.* **2001,** *276,* 12546–12555. doi:10.1074/jbc.M009667200
25. Meyer, A.; Brünjes, M.; Taft, F.; Frenzel, T.; Sasse, F.; Kirschning, A. *Org. Lett.* **2007,** *9,* 1489–1492. doi:10.1021/ol0702270
26. Frenzel, T.; Brünjes, M.; Quitschalle, M.; Kirschning, A. *Org. Lett.* **2006,** *8,* 135–138. doi:10.1021/ol052588q
27. Harmrolfs, K.; Brünjes, M.; Dräger, G.; Floss, H. G.; Sasse, F.; Taft, F.; Kirschning, A. *ChemBioChem* **2010,** *11,* 2517–2520. doi:10.1002/cbic.201000422
28. Moss, S. J.; Bai, L.; Toelzer, S.; Caroll, B. J.; Mahmud, T.; Yu, T.-W.; Floss, H. G. *J. Am. Chem. Soc.* **2002,** *124,* 6544–6545. doi:10.1021/ja020214b
29. Bandi, S.; Kim, Y. J.; Sa, S. O.; Chang, Y.-K. *J. Microbiol. Biotechnol.* **2005,** *15,* 930–937.
30. Chung, J.; Byng, G. S. Mutant Actinosynnema pretiosum strain with increased maytansinoid production. U.S. Patent 6,790,954, Sept 14, 2004.
Use of SAG 471 anti-foam for fermentation of *A. pretiosum* was suggested.

License and Terms

Beilstein Journal of Organic Chemistry

Algicidal lactones from the marine *Roseobacter* clade bacterium *Ruegeria pomeroyi*

Ramona Riclea[1], Julia Gleitzmann[1], Hilke Bruns[1], Corina Junker[2], Barbara Schulz[2] and Jeroen S. Dickschat[*1]

Full Research Paper

Open Access

Address:
[1]Institut für Organische Chemie, Technische Universität Braunschweig, Hagenring 30, D-38106 Braunschweig, Germany and [2]Institut für Mikrobiologie, Technische Universität Braunschweig, Spielmannstraße 7, D-38106 Braunschweig, Germany

Email:
Jeroen S. Dickschat[*] - j.dickschat@tu-braunschweig.de

* Corresponding author

Keywords:
bacteria-algae symbiosis; lactones; *Roseobacter*; synthesis; volatiles

Beilstein J. Org. Chem. **2012,** *8,* 941–950.
doi:10.3762/bjoc.8.106

Received: 04 April 2012
Accepted: 06 June 2012
Published: 25 June 2012

This article is part of the Thematic Series "Biosynthesis and function of secondary metabolites".

Associate Editor: S. Flitsch

Abstract

Volatiles released by the marine *Roseobacter* clade bacterium *Rugeria pomeroyi* were collected by use of a closed-loop stripping headspace apparatus (CLSA) and analysed by GC–MS. Several lactones were found for which structural proposals were derived from their mass spectra and unambiguously verified by the synthesis of reference compounds. An enantioselective synthesis of two exemplary lactones was performed to establish the enantiomeric compositions of the natural products by enantioselective GC–MS analyses. The lactones were subjected to biotests to investigate their activity against several bacteria, fungi, and algae. A specific algicidal activity was observed that may be important in the interaction between the bacteria and their algal hosts in fading algal blooms.

Introduction

Bacteria of the *Roseobacter* clade form one of the most abundant lineages of marine bacteria that occur globally in marine ecosystems from polar to tropical regions [1,2]. They are present in costal and open ocean environments, in surface waters and in the water column; are found as algal symbionts [3,4] or associated with molluscs [5]; and can form biofilms [6]. Particularly interesting from an ecological point of view is their association with marine algae, such as dinoflagellates and coccolithophores, which produce large amounts of the sulfur metabolite dimethylsulfoniopropionate (**1**, DMSP, Figure 1). DMSP is used as an osmolyte and cryoprotectant by marine phytoplankton, various macroalgae, and also a few angiosperms, and is produced at an estimated annual rate of 1000 Tg (10^{15} g) [7]. The microalgal phytoplankton frequently forms massive blooms, which can even be observed by satellites from space [8], sometimes covering large areas of $>10^5$ km^2 and containing more than 10^6 cells mL^{-1}. During these blooms bacteria from the *Roseobacter* clade have been observed as the

predominant prokaryotic species accounting for more than half of the total bacterial community [3,4]. DMSP is also an attractant for *Ruegeria* sp. TM1040 and causes flagella-mediated chemotactic behaviour [9], suggesting an important role of DMSP in the symbiosis between the algae and bacteria. Upon lysis of ageing blooms by viruses, or cell disruption by grazing, the intracellular DMSP is released, making the dissolved DMSP available for bacterial degradation to methanethiol (MeSH) [10] or dimethyl sulfide (DMS) [11-15]. The bacterial production of DMS is important for the global sulfur cycle [16,17] and the planet's climate [18,19], while the alternative DMSP degradation product MeSH controls the bioavailability of metal ions by the formation of metal–MeSH complexes [7] and can be used for the biosynthesis of various sulfur-containing secondary metabolites [20].

A sulfur-containing metabolite, for which the direct sulfur precursor has not been determined yet, is the antibiotic tropodithietic acid (TDA, **2**), which may have an important function in mutualistic symbioses of *P. gallaeciensis* and marine algae by protecting the algal host from pathogenic bacteria in emerging blooms. In ageing blooms *p*-coumaric acid (**5**) is released from lysing algal cells as a lignin breakdown product. This compound causes a switch in *P. gallaeciensis* from exhibiting mutualistic to pathogenic properties mediated by the algicidal roseobacticides, which are only produced upon induction by **5** [21,22]. Roseobacticide A (**4**) was suggested to arise from tropone (**3**), *p*-hydroxyphenylacetic acid, which is potentially formed from **5**, and MeSH [21]. In addition, **5** can be taken up and used by some bacteria, including *R. pomeroyi* for the biosynthesis of the autoinducer *N*-coumaroyl-L-homoserine lactone (**6**) [23], but it is unknown whether **6** or any other molecule plays a regulatory function for the genetic activation of the biosynthesis of **4**, or whether formation of the roseobacticides is just activated because the required building block is available from **5**.

All of these recently obtained insights support a strong interaction between marine algae and bacteria of the *Roseobacter* clade, which is mediated by small and diffusible molecules. Herein we describe the identification and synthesis of volatile lactones from *R. pomeroyi* and their specific algicidal activity, which may also play a role in the interaction between the *Roseobacter* clade bacteria and their algal hosts in fading blooms.

Results and Discussion

Analysis of volatiles released by *Ruegeria pomeroyi*

The volatiles emitted by agar plate cultures of *Ruegeria pomeroyi* DSS-3 grown on ½ YTSS medium were collected on charcoal by using a closed-loop stripping apparatus (CLSA) [24]. After a collection time of about one day the adsorbed compounds were eluted with analytically pure dichloromethane, and the obtained extracts were analysed by GC–MS. A representative chromatogram of a headspace extract of *R. pomeroyi* is shown in Figure 2A.

The sulfur volatiles dimethyl disulfide, dimethyl trisulfide, and *S*-methyl methanethiosulfonate, previously reported from several other bacteria of the *Roseobacter* clade and also from various other species [25], were readily identified according to their mass spectra and by comparison with synthetic standards. However, the volatiles **7**–**11**, including the main compound **8**, could not immediately be identified by their mass spectra alone. The mass spectrum of **8** (Figure 3) showed strong similarities to the mass spectrum of 2-methylpentan-4-olide, which is included in our electronic mass-spectra libraries [26,27]. Compound **7**, which is released only in small amounts, showed an almost identical mass spectrum, suggesting the volatiles **7** and **8** to be the *cis*- and *trans*-diastereoisomers of 2-methylpentan-4-olide, but it was impossible to assign the structure of a distinct diastereomer. The compounds **9** and **10** also showed highly similar

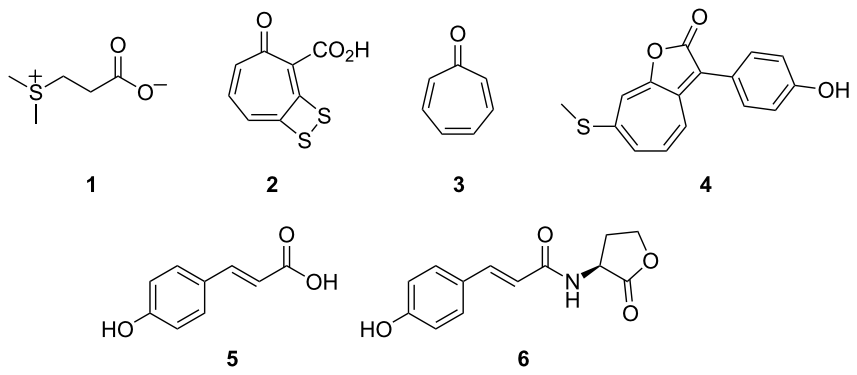

Figure 1: Important metabolites in the interaction of bacteria from the *Roseobacter* clade with marine algae.

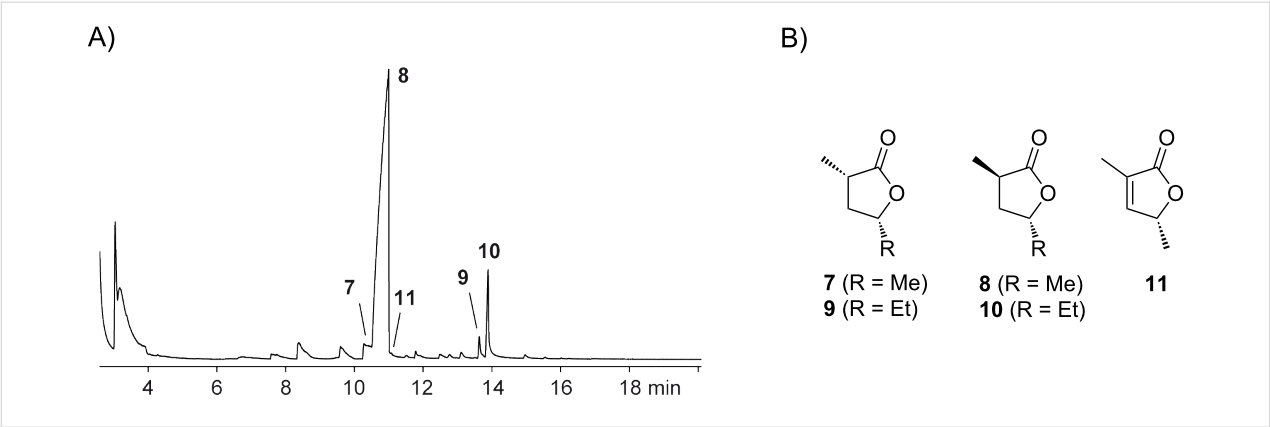

Figure 2: (A) Total ion chromatogram of a headspace extract from *R. pomeroyi*, (B) structures of lactones released by *R. pomeroyi*.

mass spectra and both a molecular ion at m/z = 128. Due to the increase by 14 amu compared to the molecular ions of **7** and **8**, the volatiles **9** and **10** were assumed to represent higher homologues by the addition of one methylene unit. The base peak at m/z = 99 furthermore supported the structures of methylated butanolides, leading to the structural suggestions of *cis*- and *trans*-2-methylhexan-4-olide. The alternative structures of *cis*- and *trans*-2-ethylpentan-4-olide seemed less likely since these

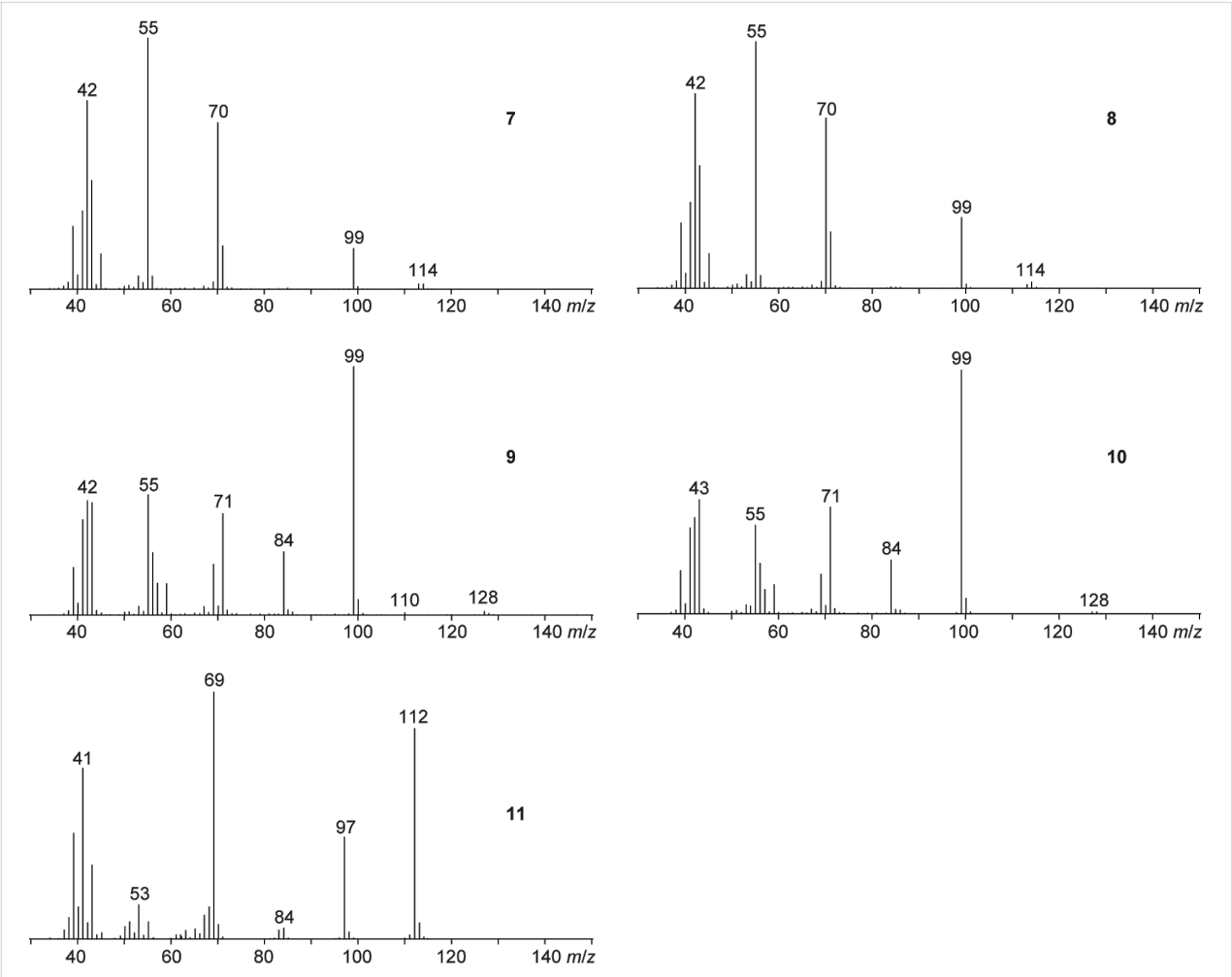

Figure 3: Mass spectra of the compounds **7**–**11** emitted by *R. pomeroyi*.

lactones were assumed to undergo a McLafferty rearrangement that should result in significant fragment ions at m/z = 100 by the neutral loss of ethene. Finally, compound **11** exhibited a mass spectrum with a molecular ion at m/z = 112, which, together with the fragment ion at m/z = 97, suggested the structure of a dimethylbutenolide. Compound **11** may be the precursor of, or derived from, **7** and **8**, resulting in the proposed structure of 2-methylpent-2-en-4-olide.

To prove the structural suggestions unambiguously, syntheses of reference compounds were carried out (Scheme 1). Methacryloyl chloride (**12**) was esterified with but-3-en-2-ol (**13**) in the presence of triethylamine to yield but-3-en-2-yl methacrylate (**15**). Ring-closing metathesis with Grubbs catalyst of the second generation gave 2-methylpent-2-en-4-olide (**11**) that upon catalytic hydrogenation yielded *cis*-2-methylpentan-4-olide (**7**) as a single diastereomer, as reported previously [28]. Under prolonged treatment with KO*t*-Bu in *t*-BuOH under reflux, partial isomerisation to *trans*-2-methylpentan-4-olide (**8**) was achieved. Longer reaction times did not result in higher yields of the *trans* isomer, but instead in loss of material due to decomposition, and therefore the isomerisation was stopped after one day. By using the same approach starting from **12** and pent-1-en-3-ol (**14**) pure *cis*-2-methylhexan-4-olide (**9**) was obtained by esterification to pent-1-en-3-yl methacrylate (**16**), ring-closing metathesis to 2-methylhex-2-en-4-olide (**17**), and catalytic hydrogenation. The isomerisation of **9** with KO*t*-Bu in *t*-BuOH again provided a mixture of **9** and its diastereomer *trans*-2-methylhexan-4-olide (**10**). Comparison of GC retention times and mass spectra of the synthetic material to those of the natural compounds revealed that the first-eluting minor diastereomer of 2-methylpentan-4-olide emitted by *R. pomeroyi* is the *cis*-diastereomer **7** and the main compound is the *trans*-diastereomer **8**. Accordingly, the structures of the *cis*- and *trans*-diastereomers **9** and **10** were assigned to the first- and the second-eluting diastereomers of 2-methylhexan-4-olide, respectively. Furthermore, the trace compound **11**, found in the headspace extract, was identical to the synthetic intermediate obtained en route to **7** and **8**.

To determine the enantiomeric compositions of the lactones from *R. pomeroyi*, an enantioselective synthesis of **7** and **8** was carried out (Scheme 2). For this purpose the lactone (2*S*,3*R*,4*R*)-2,4-dimethyl-5-oxotetrahydrofuran-3-yl 2-ethylpentanoate (**18**), a derivative of the antimycin degradation product blastmycinone, which has recently been obtained in an enantioselective synthesis in our laboratory [29], was used as a starting material. The elimination of 2-ethylpentanoic acid was achieved by treat-

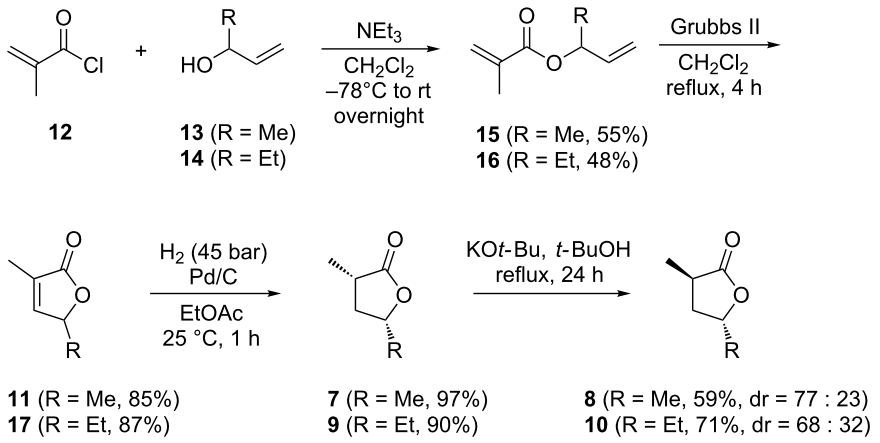

Scheme 1: Synthesis of compounds **7**–**11**. For these target structures the relative configurations are shown.

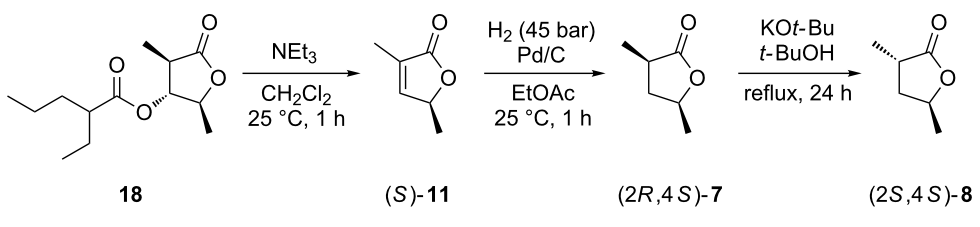

Scheme 2: Enantioselective synthesis of (2*R*,4*S*)-**7** and (2*S*,4*S*)-**8**.

ment with triethylamine to yield (*S*)-**11**. As described above for the racemic compounds, catalytic hydrogenation afforded (2*R*,4*S*)-**7**, which was isomerised to (2*S*,4*S*)-**8**. Enantioselective GC-analyses clearly demonstrated that the lactones from *R. pomeroyi* have the opposite absolute configurations as these synthetic lactones (Figure 4). Therefore, the lactones from *R. pomeroyi* are identified as (2*S*,4*R*)-**7** and (2*R*,4*R*)-**8**. The bacterial headspace extracts did not contain sufficient amounts

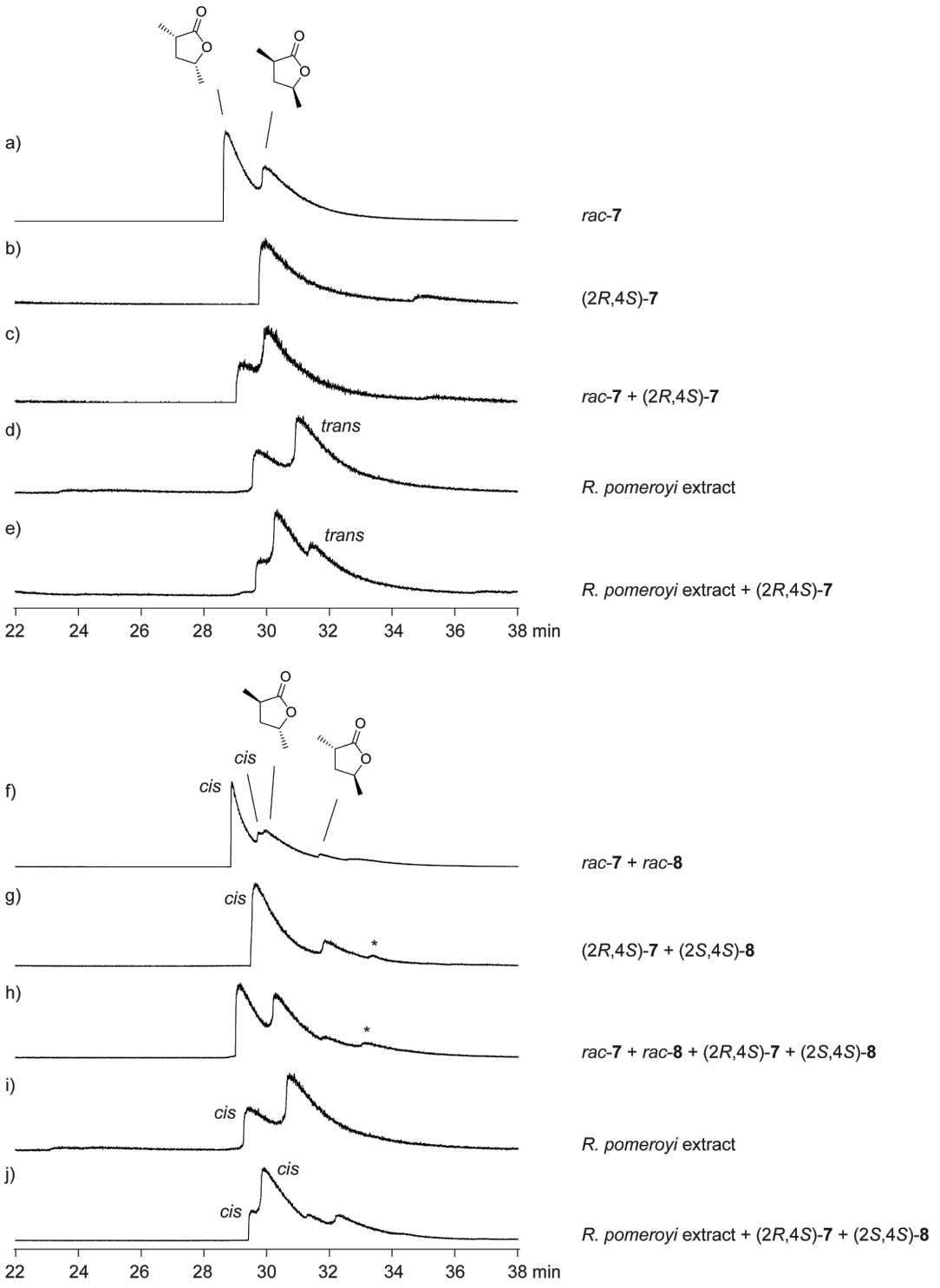

Figure 4: Enantioselective GC analyses for the assignment of the enantiomeric compositions of natural (2*S*,4*R*)-**7** and (2*R*,4*R*)-**8** from *R. pomeroyi*.

of **11** for elucidation of its absolute configuration by using synthetic racemic and (*S*)-**11**. However, the absolute configurations of the other lactones are most likely related to those of **7** and **8**, leading to the suggested structures of (2*S*,4*R*)-**9**, (2*R*,4*R*)-**10**, and (*R*)-**11**. As can be seen in an accompanying paper in this Thematic Series by Francke and co-workers on the synthesis and absolute configurations of iridomyrmecins from the parasitoid wasp *Alloxysta victrix*, the expected stereochemical relationships between structurally similar natural products from one species are not always met [30], and therefore, these suggestions should be taken with care.

To investigate the possible biological function of the lactones emitted by *R. pomeroyi* an agar diffusion assay with the synthetic compounds was carried out (Table 1). Since the headspace extracts from *R. pomeroyi* contained mixtures of the diastereomers **7**/**8** and **9**/**10**, respectively, these compounds were also tested as diastereomeric mixtures as obtained in the isomerisation procedures with **7** and **9**. Tests were performed with bacteria, including the Gram-negative *Escherichia coli* and the Gram-positive *Bacillus megaterium*, fungi, represented by the basidiomycete *Microbotryum violaceum* and the ascomycete *Botrytis cinerea*, and the fresh water alga *Chlorella fusca*. These microorganisms were chosen because they are nonpathogenic and are accurate initial test organisms for antibacterial, antifungal, and antialgal/herbicidal activities. All the lactones specifically showed partial inhibition of the alga *C. fusca*, but no activity against the bacteria and fungi.

Conclusion

More and more data are accumulated demonstrating that bacteria of the marine *Roseobacter* clade produce bioactive secondary metabolites. In the present work, we have identified five lactones in the volatile fraction of *R. pomeroyi*. The structures of these lactones have been unambiguously assigned by comparison to synthetic standards. In agar diffusion assays the synthetic lactones showed specific activity against algae, but not against bacteria or fungi, suggesting that the lactones may have an ecological function in the interaction between the bacteria and the algae in fading algal blooms, similar to the recently described roseobacticides from *P. gallaeciensis*, which are active against *Emiliana huxleyi*. In the present work we have performed initial tests to investigate the bioactivity of the *Ruegeria* lactones against bacteria, fungi, and the fresh water alga *Chlorella fusca*. Further tests will have to be performed with marine algae, including *E. huxleyi* and related species, to investigate the significance of these findings within the ecological context of the bacterial lactone producers.

Experimental

Strains, media, and growth conditions. *Ruegeria pomeroyi* DSS-3 was grown in ½ YTSS liquid medium (2 g L^{-1} yeast extract, 1.25 g L^{-1} tryptone, 20 g L^{-1} sea salts (Sigma-Aldrich)) at 28 °C. After full growth of the culture (ca. 3 d), an agar plate with YTSS medium was inoculated by plating of 100 µL of liquid culture. Plates were incubated for three days and then subjected to headspace analysis.

Collection of volatiles. The volatiles released by the *R. pomeroyi* agar plate cultures were collected by use of a closed-loop stripping apparatus (CLSA) as described previously [24]. The headspace extracts were immediately analysed by GC–MS and stored at −80 °C.

GC–MS. GC–MS analyses were carried out with a HP7890A gas chromatograph connected to a HP5975C mass-selective detector. The GC was equipped with a HP-5 MS fused silica capillary column (30 m × 0.22 mm i.d., 0.25 µm film, Hewlett-Packard, Wilmington, USA) or with a hydrodex-6-TBDMS fused silica capillary column (50 m, 0.25 mm i.d., 0.25 µm film, Macherey-Nagel) for enantioselective GC analyses. Conditions were as follows: inlet pressure: 67 kPa, He 23.3 mL min^{-1}; injection volume: 1 µL; injector: 250 °C; transfer line: 300 °C; electron energy: 70 eV; carrier gas (He): 1.2 mL min^{-1}. The GC

Table 1: Agar diffusion assay with the lactones released by *Ruegeria pomeroyi*.[a]

Compound	*E. coli*[b]	*B. megaterium*[c]	*M. violaceum*[d]	*B. cinerea*[e]	*C. fusca*[f]
7/**8**[g]	0	0	0	0	6 (pi)
9/**10**[g]	0	0	0	0	6 (pi)
11	0	0	0	0	7 (pi)
penicillin	nt	18	0	nt	0
tetracycline	nt	18	0	nt	10 (pi)
nystatin	nt	0	20	nt	0
actidione	nt	0	50	nt	35
MeOH	0	0	0	0	0

[a]Radius of inhibition zones in mm, pi = partial inhibition, nt = not tested; [b]*Escherichia coli* K12; [c]*Bacillus megaterium*; [d]*Microbotryum violaceum*; [e]*Botrytis cinerea*; [f]*Chlorella fusca*; [g]diastereomeric mixtures as obtained in the isomerisations of **7** and **9** were used.

was programmed as follows: standard GC analyses: 50 °C (5 min isothermic), increasing at 5 °C min^{-1} to 320 °C; enantioselective GC analyses: 35 °C, increasing at 0.75 °C min^{-1} to 65 °C, followed by 20 °C min^{-1} to 220 °C. Retention indices were determined from a homologous series of *n*-alkanes (C_8–C_{32}). For compound identification commercially available mass-spectrum libraries were used [26,27].

General synthetic methods: The syntheses of the reference compounds **7**/**8** and **9**/**10** were performed by using the same route. In the following paragraphs general procedures are given in which the molar ratios of the starting materials are given in equivalents (equiv). Concentrations refer to the transformed starting material, which was set to 1.0 equiv in the appropriate solvents. All reactions were performed in flame-dried glassware in a nitrogen atmosphere. Solvents were dried according to standard methods. All chemicals were obtained from commercial suppliers (Sigma-Aldrich or Acros) and used without further purification.

General procedure for the preparation of methacrylate esters: A 0.3 M solution of the appropriate alcohol **13** or **14** (1.0 equiv) and NEt_3 (1.38 equiv) in dry dichloromethane was cooled to 0 °C followed by the slow addition of methacryloyl chloride (**12**, 1.0 equiv). The mixture was stirred at room temperature overnight and then quenched by the addition of an equal volume of 1 N HCl. The layers were separated and the aqueous layer was extracted three times with dichloromethane. The combined organic layers were washed with saturated aqueous $NaHCO_3$ and brine, dried over $MgSO_4$, and concentrated under reduced pressure. The residue was purified by column chromatography on silica gel (hexane/ethyl acetate 20:1) to yield the esters as colourless oils.

But-3-en-2-yl methacrylate (15): Yield: 0.92 g (6.6 mmol, 55%). TLC (hexane/ethyl acetate 20:1): R_f 0.50; GC (BPX-5): *I* = 909; ^{1}H NMR (400 MHz, $CDCl_3$) δ 6.11 (m, 1H, CH_2), 5.86 (ddd, $^3J_{H,H}$ = 5.8, 10.5, 16.3 Hz, 1H, CH), 5.54 (quin, $^2J_{H,H}$ = $^4J_{H,H}$ = 1.6 Hz, 1H, CH_2), 5.43–5.35 (m, 1H, CH), 5.24 (dt, $^2J_{H,H}$ = 1.2 Hz, $^3J_{H,H}$ = 17.2 Hz, 1H, CH_2), 5.12 (dt, $^2J_{H,H}$ = 1.2 Hz, $^3J_{H,H}$ = 10.5 Hz, 1H, CH_2), 1.93 (dd, $^4J_{H,H}$ = 1.1, 1.6 Hz, 3H, CH_3), 1.34 (d, $^3J_{H,H}$ = 6.5 Hz, $^1J_{C,H}$ = 127.8 Hz, 3H, CH_3); ^{13}C NMR (100 MHz, $CDCl_3$) δ 166.4 (CO), 137.7 (CH), 136.6 (C_q), 125.4 (CH_2), 115.5 (CH_2), 77.1 (CH), 19.9 (CH_3), 18.2 (CH_3); MS (EI, 70 eV) *m*/*z* (%): 140 (<1) [M^+], 111 (16), 95 (18), 69 (96), 55 (100), 53 (19), 43 (21), 41 (92), 40 (20); IR (ATR) $\tilde{\nu}$: 2985 (w), 2933 (w), 2847 (w), 1731 (m), 1677 (m), 1450 (w), 1376 (w), 1344 (w), 1284 (m), 1242 (w), 1202 (m), 1181 (m), 1152 (s), 1110 (s), 1036 (s), 990 (m), 924 (m), 834 (w), 761 (w), 696 (w), 553 (w) cm^{-1}; UV–vis λ_{max} (log ε): 240 (2.22) nm.

Pent-1-en-3-yl methacrylate (16): Yield: 3.0 g (19.4 mmol, 48%). TLC (hexane/ethyl acetate 10:1): R_f 0.29; GC (BPX-5): *I* = 988; ^{1}H NMR (400 MHz, $CDCl_3$) δ 6.11 (m, 1H, CH_2), 5.81 (ddd, $^3J_{H,H}$ = 17.0, 10.5, 6.5 Hz, 1H, CH), 5.54–5.52 (m, 1H, CH_2), 5.25–5.19 (m, 2H, CH, CH_2), 5.17–5.13 (m, 1H, CH_2), 1.93 (d, $^4J_{H,H}$ = 1.0 Hz, 3H, CH_3), 1.69 (quintd, $^3J_{H,H}$ = 7.3 Hz, $^4J_{H,H}$ = 2.7 Hz, 2H, CH_2), 0.90 (t, $^3J_{H,H}$ = 7.4 Hz, $^1J_{C,H}$ = 126.2 Hz, CH_3); ^{13}C NMR (100 MHz, $CDCl_3$) δ 166.7 (CO), 136.6 (C_q), 136.3 (CH), 125.1 (CH_2), 116.5 (CH_2), 76.0 (CH), 27.2 (CH_2), 18.3 (CH_3), 9.3 (CH_3); MS (EI, 70 eV) *m*/*z* (%): 154 (<1) [M^+], 125 (8), 111 (7), 109 (6), 69 (100), 67 (14), 41 (44), 39 (22); IR (ATR) $\tilde{\nu}$: 3087 (w), 2696 (m), 2931 (m), 2879 (w), 1721 (s), 1640 (w), 1456 (w), 1381 (w), 1294 (w), 1261 (w), 1164 (m), 1078 (w), 1059 (w), 990 (w), 930 (m), 810 (w), 657 (w) cm^{-1}; UV–vis: λ_{max} (log ε): 228 (2.83) nm.

General procedure for the ring-closing metathesis to butenolides: Grubbs catalyst of the second generation (0.05 equiv) was added to a solution of the ester **15** or **16** (1.0 equiv) in dry dichloromethane (0.05 M). The mixture was stirred under reflux for 5 d. The solvent was removed under reduced pressure and the residue was purified by column chromatography on silica gel (pentane/diethyl ether 3:1) to give the butenolides as colourless oils.

2-Methylpent-2-en-4-olide (11): Yield: 0.48 g (3.96 mmol, 85%). TLC (hexane/ethyl acetate 3:1): R_f 0.27; GC (BPX-5): *I* = 1017; ^{1}H NMR (400 MHz, $CDCl_3$) δ 7.02 (quint, $^3J_{H,H}$ = $^4J_{H,H}$ = 1.6 Hz, $^1J_{C,H}$ = 171.3 Hz, 1H, CH), 5.01–4.94 (m, 1H, CH), 1.90 (dd, $^4J_{H,H}$ = $^5J_{H,H}$ = 1.6 Hz, $^1J_{C,H}$ = 128.8 Hz, 3H, CH_3), 1.39 (d, $^3J_{H,H}$ = 6.8 Hz, $^1J_{C,H}$ = 129.0 Hz, 3H, CH_3); ^{13}C NMR (100 MHz, $CDCl_3$) δ 173.9 (CO), 149.6 (CH), 129.3 (C_q), 77.1 (CH), 18.7 (CH_3), 10.2 (CH_3); MS (EI, 70 eV) *m*/*z* [%]: 112 (28), 98 (16), 84 (4), 69 (42), 52 (24), 41 (78), 39 (100); IR (ATR) $\tilde{\nu}$: 3382 (br, w), 3084 (w), 2985 (w), 2933 (w), 1743 (s), 1659 (w), 1448 (w), 1376 (w), 1342 (w), 1321 (w), 1209 (w), 1188 (w), 1103 (m), 1082 (s), 1048 (m), 1028 (m), 997 (s), 929 (m), 866 (m), 763 (m), 610 (m), 574 (w), 540 (m) cm^{-1}; UV–vis λ_{max} (log ε): 228 (2.70), 221 (2.03) nm. NMR spectroscopic data are in agreement with previously published data [31].

2-Methylhex-2-en-4-olide (17): Yield: 0.24 g (1.89 mmol, 97%). TLC (hexane/ethyl acetate 3:1): R_f 0.25; GC (BPX-5): *I* = 1113; ^{1}H NMR (400 MHz, $CDCl_3$) δ 7.02 (quint, $^3J_{H,H}$ = $^4J_{H,H}$ = 1.6 Hz, 1H, CH), 4.84–4.79 (m, 1H, CH), 1.89 (t, $^4J_{H,H}$ = 1.8 Hz, 3H, CH_3), 1.80–1.69 (m, 1H, CH_2), 1.65 (dquin, $^2J_{H,H}$ = 14.4 Hz, $^3J_{H,H}$ = 7.2 Hz, 1H, CH_2), 0.97 (t, $^3J_{H,H}$ = 7.4 Hz, 3H, CH_3); ^{13}C NMR (100 MHz, $CDCl_3$) δ 174.3 (CO), 148.4 (CH), 130.0 (C_q), 82.0 (CH), 26.5 (CH_2), 10.5 (CH_3), 9.0 (CH_3); MS (EI, 70 eV) *m*/*z* (%): 126 (41), 111 (28), 97 (100),

83 (3), 69 (64), 57 (17), 53 (6), 51 (5), 41 (56), 39 (35); IR (ATR) $\tilde{\nu}$: 2973 (w), 2932 (w), 2882 (w), 1744 (s), 1660 (w), 1459 (w), 1343 (w), 1281 (w), 1208 (w), 1086 (s), 1047 (m), 1022 (m), 959 (m), 856 (m), 786 (m), 761 (w), 612 (w), 555 (w) cm^{-1}; UV–vis λ_{max} (log ε): 229 (2.83) nm. NMR spectroscopic data are in agreement with previously published data [32].

General procedure for the catalytic hydrogenation of butenolides: To a solution of the lactone **11** or **17** (1.0 equiv) in ethyl acetate (0.15 M) Pd on charcoal (10% Pd, 0.1 equiv) was added. The mixture was stirred in a hydrogen atmosphere (45 bar) for 1 h at 25 °C. The catalyst was removed by filtration, the solvent was evaporated under reduced pressure, and the residue was purified by column chromatography on silica gel (pentane/diethyl ether 3:1) to yield the butanolides as colourless oils.

***cis*-2-Methylpentan-4-olide (7):** Yield: 0.38 g (3.28 mmol, 97%). TLC (hexane/ethyl acetate 2:1): R_f 0.48; GC (BPX-5): I = 1005; ^{1}H NMR (400 MHz, $CDCl_3$) δ 4.40 (ddq, $^3J_{H,H}$ = 5.4, 11.5, 6.1 Hz, 1H, CH), 2.66 (ddq, $^3J_{H,H}$ = 8.5, 12.1, 7.1 Hz, 1H, CH), 2.49 (ddd, $^2J_{H,H}$ = 12.4 Hz, $^3J_{H,H}$ = 5.4, 8.5 Hz, 1H, CH_2), 1.49 (dt, $^2J_{H,H}$ = $^3J_{H,H}$ = 12.3 Hz, $^3J_{H,H}$ = 10.4 Hz, 1H, CH_2), 1.39 (d, $^3J_{H,H}$ = 6.1 Hz, 3H, CH_3), 1.23 (d, $^3J_{H,H}$ = 7.0 Hz, 3H, CH_3); ^{13}C NMR (100 MHz, $CDCl_3$) δ 179.5 (CO), 74.9 (CH), 39.1 (CH_2), 36.3 (CH), 20.9 (CH_3), 15.1 (CH_3); MS (EI, 70 eV) *m*/*z* (%): 114 (<1) [M^+], 99 (6), 70 (34), 55 (100), 42 (72), 39 (69); IR (ATR) $\tilde{\nu}$: 2977 (w), 2935 (w), 2878 (w), 1762 (s), 1454 (w), 1387 (w), 1349 (w), 1293 (w), 1177 (s), 1121 (m), 1069 (m), 1042 (s), 994 (w), 949 (s), 922 (w), 872 (w), 775 (w), 704 (w), 625 (m), 569 (w) cm^{-1}; UV–vis λ_{max} (log ε): 239 (1.22), 232 (0.69) nm. NMR spectroscopic data are in agreement with previously published data [33].

***cis*-2-Methylhexan-4-olide (9):** Yield: 0.19 g (1.41 mmol, 90%). TLC (hexane/ethyl acetate 3:1): R_f 0.36; GC (BPX-5): I = 1099; ^{1}H NMR (400.1 MHz, $CDCl_3$) δ 4.30–4.23 (m, 1H, CH), 2.65 (ddq, $^3J_{H,H}$ = 8.5, 12.0, 7.0 Hz, 1H, CH), 2.47 (ddd, $^3J_{H,H}$ = 5.4, 8.6 Hz, $^2J_{H,H}$ = 12.4 Hz, 1H, CH_2), 1.77 (dquin, $^2J_{H,H}$ = 14.4 Hz, $^3J_{H,H}$ = 7.2 Hz, 1H, CH_2), 1.68–1.57 (m, 1H, CH_2), 1.48 (dt, $^2J_{H,H}$ = $^3J_{H,H}$ = 12.2 Hz, $^3J_{H,H}$ = 10.4 Hz, 1H, CH_2), 1.25 (d, $^3J_{H,H}$ = 7.1 Hz, $^1J_{C,H}$ = 128.3 Hz, 3H, CH_3), 0.98 (t, $^3J_{H,H}$ = 7.5 Hz, $^3J_{H,H}$ = 126.4, 3H, CH_3); ^{13}C NMR (100 MHz, $CDCl_3$) δ (major compound) 179.6 (CO), 79.8 (CH), 36.8 (CH_2), 35.9 (CH), 28.4 (CH_2), 15.1 (CH_3), 9.4 (CH_3); MS (EI, 70 eV) *m*/*z* (%): 128 (<1) [M^+], 127 (1), 99 (49), 84 (24), 71 (23), 69 (29), 56 (30), 55 (69), 41 (100), 39 (92); IR (ATR) $\tilde{\nu}$: 3082 (w), 2973 (w), 2934 (w), 2883 (w), 1746 (s), 1659 (w), 1460 (w), 1383 (w), 1344 (w), 1281 (w), 1209 (w), 1087 (s), 1046 (w), 1023 (m), 1009 (m), 959 (m), 892 (m), 857 (m), 786 (m), 762 (w), 612 (w), 555 (w) cm^{-1}; UV–vis: λ_{max} (log ε): 228 (1.44), 222 (0.90) nm.

General procedure for the *cis*/*trans* isomerisation: To a solution of the *cis*-substituted lactone **7** or **9** (1.0 equiv) in *t*-BuOH (0.2 M), KO*t*-Bu (2.0 equiv) was added. The mixture was stirred under reflux for 24 h and then quenched by the addition of an equal volume of HCl (0.5 M). The mixture was extracted three times with diethyl ether. The combined organic layers were dried over $MgSO_4$ and concentrated under reduced pressure. Column chromatography of the residue on silica gel (pentane/diethyl ether 3:1) yielded mixtures of the *cis*- and *trans*-configured lactones as colourless oils, which were inseparable by chromatographic means.

***trans*-2-Methylpentan-4-olide (8):** Yield: 0.30 g (2.63 mmol, 59%, dr = 77:23, *cis*/*trans*), TLC (hexane/ethyl acetate 2:1): R_f 0.48; GC (BPX-5): GC: I = 1006; ^{1}H NMR (400 MHz, $CDCl_3$) δ 4.63 (ddq, $^3J_{H,H}$ = 5.0, 7.0, 6.4 Hz, 1H, CH), 2.74–2.62 (m, 1H, CH), 2.08–1.96 (m, 2H, CH_2), 1.33 (d, $^3J_{H,H}$ = 6.4 Hz, 3H, CH_3), 1.24 (d, $^3J_{H,H}$ = 7.3 Hz, 3H, CH_3); ^{13}C NMR (100 MHz, $CDCl_3$) δ 179.9 (CO), 74.5 (CH), 36.9 (CH_2), 33.9 (CH), 20.9 (CH_3), 15.6 (CH_3); MS (EI, 70 eV) *m*/*z* (%): 114 (<1) [M^+], 99 (8), 70 (38), 55 (100), 42 (80), 39 (75); IR (ATR) $\tilde{\nu}$: 2977 (w), 2936 (w), 2879 (w), 1763 (s), 1455 (w), 1386 (w), 1349 (w), 1178 (s), 1122 (m), 1068 (w), 1042 (m), 996 (w), 950 (s), 922 (w), 872 (w), 774 (w), 704 (w), 625 (w), 570 (w) cm^{-1}; UV–vis λ_{max} (log ε): 239 (1.20), 232 (0.53) nm. NMR spectroscopic data are in agreement with previously published data, apart from the chemical shifts of the ^{13}C NMR signals for the methyl groups, which were previously reported at 20.7 and 26.3 ppm [33], but found at 15.6 and 20.9 ppm in our spectrum.

***trans*-2-Methylhexan-4-olide (10):** Yield: 0.08 g (0.63 mmol, 71%, dr = 68:32, *cis*/*trans*). TLC (hexane/ethyl acetate 3:1): R_f 0.36; GC (BPX-5): I = 1105; ^{1}H NMR (400 MHz, $CDCl_3$) δ 4.43–4.36 (m, 1H, CH), 2.69–2.60 (m, 1H, CH), 2.12–2.04 (m, 1H, CH), 1.95 (dt, $^2J_{H,H}$ = 12.9 Hz, $^3J_{H,H}$ = 7.6 Hz, 1H, CH_2), 1.74–1.50 (m, 2H, CH_2), 1.26 (d, $^3J_{H,H}$ = 7.2 Hz, 3H, CH_3), 0.94 (t, $^3J_{H,H}$ = 7.4 Hz, 3H, CH_3); ^{13}C NMR (100 MHz, $CDCl_3$) δ 180.0 (CO), 79.6 (CH), 34.8 (CH_2), 33.9 (CH), 28.2 (CH_2), 15.8 (CH_3), 9.5 (CH_3); MS (EI, 70 eV) *m*/*z* (%): 128 (1) [M^+], 99 (54), 84 (25), 71 (27), 69 (31), 55 (57), 41 (100), 39 (87); IR (ATR) $\tilde{\nu}$: 2971 (w), 2983 (w), 2881 (w), 1762 (s), 1457 (w), 1378 (w), 1354 (w), 1291 (w), 1177 (s), 1134 (w), 1053 (w), 1024 (w), 996 (m), 960 (m), 929 (m), 868 (w), 755 (w), 733 (w), 583 (w) cm^{-1}; UV–vis λ_{max} (log ε): 238 (1.30), 233 (0.92) nm.

Enantioselective synthesis of (2*R*,4*S*)-7 and (2*S*,4*S*)-8. Treatment of (2*S*,3*R*,4*R*)-**18** (15 mg, 0.06 mmol; its synthesis is published elsewhere [29]) with Et_3N (12 mg, 0.12 mmol, 2 equiv) in dry CH_2Cl_2 (1 mL) for 1 h at room temperature was followed by acidic work-up with 2 N HCl (5 mL) and extrac-

tion with diethyl ether (3 × 5 mL). The combined organic layers were dried with $MgSO_4$ and concentrated. The crude product was purified by chromatography over silica gel (hexane/EtOAc 3:1). Due to its volatility and the low amounts of material used for the synthesis, the solvent was not completely removed. The product (+)-**11** was identical to racemic **11** by GC–MS analysis (lit.: $[\alpha]_D^{25}$ +91.5 (*c* 1.24, $CHCl_3$), [34]). Compound **11** (6 mg) was dissolved in methanol (1 mL) and a small amount of $Pd(OH)_2$ (ca. 1 mg, 10% Pd) was added. The catalytic hydrogenation was carried out in a H_2 atmosphere (1 bar) at 20 °C for 24 h. The reaction mixture was filtered through silica gel and concentrated to yield (2*R*,4*S*)-**7**. The product was used in the next step without purification. Treatment of (2*R*,4*S*)-**7** with potassium *tert*-butoxide (5 mg) in *tert*-butanol (1 mL) under reflux for 6 h gave a mixture of (2*R*,4*S*)-**7** and (2*S*,4*S*)-**8**, which was used for enantioselective GC analyses.

Agar diffusion assay for antimicrobial activity. The substances were dissolved in MeOH at a concentration of 2 mg/mL. Twenty-five microlitres of the solutions (equal to 50 μg of the compounds) was pipetted onto a sterile filter disk (Schleicher & Schuell, 9 mm), which was placed onto an appropriate agar growth medium for the respective test organism and subsequently sprayed with a suspension of the test organism. The bacteria *Escherichia coli* and *Bacillus megaterium* were grown on Luria-Bertani (LB) medium (10 g L^{-1} peptone, 5 g L^{-1} yeast extract, 5 g L^{-1} NaCl, 20 g L^{-1} agar), the fungus *Microbotryum violaceum* and the alga *Chlorella fusca* were grown on MPY medium (20 g L^{-1} malt extract, 2.5 g L^{-1} peptone, 2.5 g L^{-1} yeast extract, 20 g L^{-1} agar), and *B. cinerea* was grown on biomalt agar (30 g L^{-1} biomalt, 20 g L^{-1} agar) [35]. Reference substances were penicillin, nystatin, actidione, and tetracycline, and negative controls were performed with MeOH alone. Commencing at the middle of the filter disk, the radius of the zone of inhibition was measured in millimeters.

Acknowledgements

This work was funded by the Deutsche Forschungsgemeinschaft (DFG) within the Transregional Collaborative Research Centre “Ecology, Physiology and Molecular Biology of the *Roseobacter* clade” (SFB-TR 51). We thank Andrew Johnston (Norwich) for strain *Ruegeria pomeroyi* DSS-3 and Stefan Schulz (Braunschweig) for his support.

References

1. Buchan, A.; González, J. M.; Moran, M. A. *Appl. Environ. Microbiol.* **2005,** *71,* 5665–5677. doi:10.1128/AEM.71.10.5665-5677.2005
2. Giovannoni, S. J.; Stingl, U. *Nature* **2005,** *437,* 343–348. doi:10.1038/nature04158
3. González, J. M.; Simó, R.; Massana, R.; Covert, J. S.; Casamayor, E. O.; Pedrós-Alió, C.; Moran, M. A. *Appl. Environ. Microbiol.* **2000,** *66,* 4237–4246. doi:10.1128/AEM.66.10.4237-4246.2000
4. Zubkov, M. V.; Fuchs, B. M.; Archer, S. D.; Kiene, R. P.; Amann, R.; Burkill, P. H. *Environ. Microbiol.* **2001,** *3,* 304–311. doi:10.1046/j.1462-2920.2001.00196.x
5. Ruiz-Ponte, C.; Cilia, V.; Lambert, C.; Nicolas, J. L. *Int. J. Syst. Bacteriol.* **1998,** *48,* 537–542. doi:10.1099/00207713-48-2-537
6. Bruhn, J. B.; Gram, L.; Belas, R. *Appl. Environ. Microbiol.* **2007,** *73,* 442–450. doi:10.1128/AEM.02238-06
7. Kiene, R. P.; Linn, L. J.; Bruton, J. A. *J. Sea Res.* **2000,** *43,* 209–224. doi:10.1016/S1385-1101(00)00023-X
8. Holligan, P. M.; Viollier, M.; Harbour, D. S.; Camus, P.; Champagne-Philippe, M. *Nature* **1983,** *304,* 339–342. doi:10.1038/304339a0
9. Miller, T. R.; Belas, R. *Environ. Microbiol.* **2006,** *8,* 1648–1659. doi:10.1111/j.1462-2920.2006.01071.x
10. Howard, E. C.; Henriksen, J. R.; Buchan, A.; Reisch, C. R.; Bürgmann, H.; Welsh, R.; Ye, W.; González, J. M.; Mace, K.; Joye, S. B.; Kiene, R. P.; Whitman, W. B.; Moran, M. A. *Science* **2006,** *314,* 649–652. doi:10.1126/science.1130657
11. Todd, J. D.; Rogers, R.; Li, Y. G.; Wexler, M.; Bond, P. L.; Sun, L.; Curson, A. R. J.; Malin, G.; Steinke, M.; Johnston, A. W. B. *Science* **2007,** *315,* 666–669. doi:10.1126/science.1135370
12. Todd, J. D.; Curson, A. R. J.; Nikolaidou-Katsaraidou, N.; Brearley, C. A.; Watmough, N. J.; Chan, Y.; Page, P. C. B.; Sun, L.; Johnston, A. W. B. *Environ. Microbiol.* **2010,** *12,* 327–343. doi:10.1111/j.1462-2920.2009.02071.x
13. Curson, A. R. J.; Rogers, R.; Todd, J. D.; Brearley, C. A.; Johnston, A. W. B. *Environ. Microbiol.* **2008,** *10,* 757–767. doi:10.1111/j.1462-2920.2007.01499.x
14. Todd, J. D.; Curson, A. R. J.; Dupont, C. L.; Nicholson, P.; Johnston, A. W. B. *Environ. Microbiol.* **2009,** *11,* 1376–1385. doi:10.1111/j.1462-2920.2009.01864.x
15. Todd, J. D.; Curson, A. R. J.; Kirkwood, M.; Sullivan, M. J.; Green, R. T.; Johnston, A. W. B. *Environ. Microbiol.* **2011,** *13,* 427–438. doi:10.1111/j.1462-2920.2010.02348.x
16. Kettle, A.; Andreae, M. O. *J. Geophys. Res.* **2000,** *105,* 26793–26808. doi:10.1029/2000JD900252
17. Lovelock, J. E.; Maggs, R. J.; Rasmussen, R. A. *Nature* **1972,** *237,* 452–453. doi:10.1038/237452a0
18. Charlson, R. J.; Lovelock, J. E.; Andreae, M. O.; Warren, S. G. *Nature* **1987,** *326,* 655–661. doi:10.1038/326655a0
19. Vallina, S. M.; Simó, R. *Science* **2007,** *315,* 506–508. doi:10.1126/science.1133680
20. Dickschat, J. S.; Zell, C.; Brock, N. L. *ChemBioChem* **2010,** *11,* 417–425. doi:10.1002/cbic.200900668
21. Seyedsayamdost, M. R.; Case, R. J.; Kolter, R.; Clardy, J. *Nat. Chem.* **2011,** *3,* 331–335. doi:10.1038/nchem.1002
22. Seyedsayamdost, M. R.; Carr, G.; Kolter, R.; Clardy, J. *J. Am. Chem. Soc.* **2011,** *133,* 18343–18349. doi:10.1021/ja207172s
23. Schaefer, A. L.; Greenberg, E. P.; Oliver, C. M.; Oda, Y.; Huang, J. J.; Bittan-Banin, G.; Peres, C. M.; Schmidt, S.; Juhaszova, K.; Sufrin, J. R.; Harwood, C. S. *Nature* **2008,** *454,* 595–599. doi:10.1038/nature07088
24. Dickschat, J. S.; Wenzel, S. C.; Bode, H. B.; Müller, R.; Schulz, S. *ChemBioChem* **2004,** *5,* 778–787. doi:10.1002/cbic.200300813

25. Schulz, S.; Dickschat, J. S. *Nat. Prod. Rep.* **2007,** *24,* 814–842. doi:10.1039/b507392h
26. Joulain, D.; König, W. A. *The Atlas of Spectral Data of Sesquiterpene Hydrocarbons;* E. B.-Verlag: Hamburg, Germany, 1998.
27. Adams, R. P. *Identification of Essential Oil Components by Gas Chromatography/Mass Spectrometry;* Allured: Carol Stream, IL, 2007.
28. Hussain, S. A. M. T.; Ollis, W. D.; Smith, C.; Stoddart, J. F. *J. Chem. Soc., Perkin Trans. 1* **1975,** 1480–1492. doi:10.1039/P19750001480
29. Riclea, R.; Aigle, B.; Leblond, P.; Schoenian, I.; Spiteller, D.; Dickschat, J. S. *ChemBioChem* **2012**. doi:10.1002/cbic.201200260
30. Hilgraf, R.; Zimmermann, N.; Tröger, A.; Francke, W. *Beilstein J. Org. Chem.* **2012,** submitted for publication.
31. Guntrum, E.; Kuhn, W.; Spönlein, W.; Jäger, V. *Synthesis* **1986,** 921–925. doi:10.1055/s-1986-31823
32. Yoneda, E.; Zhang, S.-W.; Zhou, D.-Y.; Onitsuka, K.; Takahashi, S. *J. Org. Chem.* **2003,** *68,* 8571–8576. doi:10.1021/jo0350615
33. Tamaru, Y.; Mizutani, M.; Furukawa, Y.; Kawamura, S.; Yoshida, Z.; Yanagi, K.; Minobe, M. *J. Am. Chem. Soc.* **1984,** *106,* 1079–1085. doi:10.1021/ja00316a044
34. Chiarello, J.; Joullié, M. M. *Synth. Commun.* **1989,** *19,* 3379–3383. doi:10.1080/00397918908052744
35. Höller, U.; Wright, A. D.; Matthée, G. F.; König, G. M.; Draeger, S.; Aust, H.-J.; Schulz, B. *Mycol. Res.* **2000,** *104,* 1354–1365. doi:10.1017/S0953756200003117

License and Terms

Beilstein Journal of Organic Chemistry

Stereoselective synthesis of *trans*-fused iridoid lactones and their identification in the parasitoid wasp *Alloxysta victrix*, Part I: Dihydronepetalactones

Nicole Zimmermann, Robert Hilgraf, Lutz Lehmann, Daniel Ibarra and Wittko Francke*

Full Research Paper

Open Access

Address:
Department of Chemistry - Organic Chemistry, University of Hamburg, Martin-Luther-King-Platz 6, D-20146 Hamburg, Germany

Email:
Wittko Francke* - francke@chemie.uni-hamburg.de

* Corresponding author

Keywords:
Alloxysta victrix; identification; iridoid; stereoselective synthesis; *trans*-fused dihydronepetalactone

Beilstein J. Org. Chem. **2012,** *8,* 1246–1255.
doi:10.3762/bjoc.8.140

Received: 16 March 2012
Accepted: 20 July 2012
Published: 07 August 2012

This article is part of the Thematic Series "Biosynthesis and function of secondary metabolites". Part II [1] describes the synthesis of enantiomerically pure *trans*-fused iridomyrmecins by this approach.

Guest Editor: J. S. Dickschat

Abstract

Starting from the enantiomers of limonene, all eight stereoisomers of *trans*-fused dihydronepetalactones were synthesized. Key compounds were pure stereoisomers of 1-acetoxymethyl-2-methyl-5-(2-hydroxy-1-methylethyl)-1-cyclopentene. The stereogenic center of limonene was retained at position 4a of the target compounds and used to stereoselectively control the introduction of the other chiral centers during the synthesis. Basically, this approach could also be used for the synthesis of enantiomerically pure *trans*-fused iridomyrmecins. Using synthetic reference samples, the combination of enantioselective gas chromatography and mass spectrometry revealed that volatiles released by the endohyperparasitoid wasp *Alloxysta victrix* contain the enantiomerically pure *trans*-fused (4*R*,4a*R*,7*R*,7a*S*)-dihydronepetalactone as a minor component, showing an unusual (*R*)-configured stereogenic center at position 7.

Introduction

The endohyperparasitoid wasp *Alloxysta victrix* is part of the tetratrophic system of oat plants (*Avena sativa*), grain aphids (*Sitobion avenae*), primary parasitoids (*Aphidius uzbekistanicus*) and hyperparasitoids (*Alloxysta victrix*). Chemical communication by volatile signals is considered to play a major role in interactions between these trophic levels, and some semiochemicals of the lower trophic levels such as oat plant and grain aphid have been identified [2-4]. However, there is nearly no information about the intra- and interspecific signaling pathways between primary parasitoids and hyperparasitoids. In order to gain further information about the chemical structures and the biological significance of corresponding signals, we

examined the volatile components of pentane extracts from dissected heads as well as headspace volatiles of *Alloxysta victrix* by coupled gas chromatography/mass spectrometry (GC/MS). Figure 1 shows one major component and several trace components which could be identified as 6-methyl-5-hepten-2-one (**1**), neral (**2**), geranial (**3**), actinidine (**4**), and geranylacetone (**5**). Bioassays revealed the main compound **1** to be repellent to the aphid-parasitoid, *Aphidius*, by warning the primary parasitoid of the presence of the hyperparasitoid [5]. The prenyl-homologue of **1**, geranylacetone (**5**), seems to be a component of the sex pheromone of *Alloxysta victrix* [6]. In addition, GC/MS of cephalic secretions of both sexes showed a minor component **X**, the mass spectrum of which suggested it to be a *trans*-fused dihydronepetalactone. Since no synthetic reference compounds were available, we had to synthesize all eight *trans*-fused dihydronepetalactones to unambiguously identify the natural product **X**. The realization of this task is the subject of the present paper.

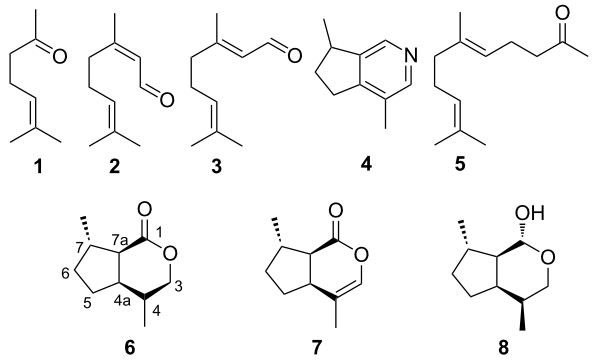

Figure 1: Terpenoids **1**–**5** present in *Alloxysta victrix* and *cis*-fused bicyclic iridoids known from other insects (**6**–**8**).

Results and Discussion

Apart from a couple of known acyclic terpenoids (Figure 1), analysis by gas chromatography coupled with mass spectrometry (GC/MS) revealed the presence of an unknown minor component **X** in both sexes of *Alloxysta victrix*. Chemical ionization analysis (GC/CIMS) showed the molecular mass of the compound to be $M^+ = 168$, while high resolution mass spectrometry (GC/HRMS) proved its atomic composition to be $C_{10}H_{16}O_2$, suggesting an oxygenated monoterpene as the target structure. The fragmentation pattern, exhibited in the 70 eV EI-mass spectrum (Figure 2), showed some similarities to that of the known *cis*-fused dihydronepetalactone (**6**) [7], however, differences in relative abundances of fragment ions pointed to a *trans*-fused dihydronepetalactone as the target structure [8]. In the mass spectrum of the *cis*-fused compound *m*/*z* 67 and *m*/*z* 95 were of similarly low intensity (30%), while in that of the unknown natural product **X** the two fragments were highly abundant (80%). The most striking differences in the spectra were pronounced signals for the molecular ion $M^+ = 168$ and $M^+ - 15$ (70% and 40%, respectively) for the *cis*-fused dihydronepetalactone whilst in the spectrum of **X** the two signals were of only low abundance (Figure 2).

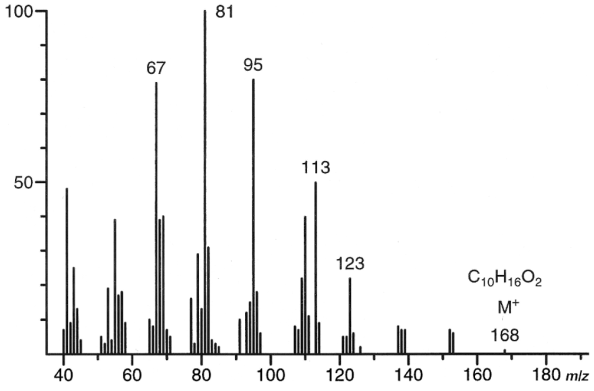

Figure 2: 70 eV EI-mass spectrum of the iridoid **X**, a component of the volatile secretions of the parasitoid wasp *Alloxysta victrix*.

Dihydronepetalactones are derivatives of nepetalactone (**7**) which was first isolated by Mc Elvain in 1941 from the essential oil of catmint, *Nepeta cataria* (Figure 1) [9]. Relative configurations of *cis*-fused nepetalactones and some related derivatives have been investigated [10,11]. Nepetalactone and *cis*- as well as *trans*-fused dihydronepetalactones have been isolated from the leaves and galls of the plant *Actinidia polygama* [8]. In addition, dihydronepetalactones are components of the defensive secretions of some ant species [12], while nepetalactone and the corresponding lactol showing (1*R*)-configuration have been identified as pheromones of aphids [13,14]. (1*R*,4*S*,4a*R*,7*S*,7a*R*)-Dihydronepetalactol (**8**) was characterized as a semiochemical for lacewings [15].

The dihydronepetalactone skeleton shows four contiguous stereogenic centers, giving rise to eight *trans*-fused stereoisomers **a**–**d** and the corresponding enantiomers **a'**–**d'** (Figure 3).

Whilst several stereoselective syntheses of the relatively widespread and well known *cis*-fused nepetalactone and its dihydro derivatives have been carried out [16-19], only very few approaches specifically aiming at the synthesis of *trans*-fused iridoid lactones have been published. Starting from (*S*)-pulegone (**9**) or its enantiomer, Wolinsky [20,21] described a route to this group of iridoids that can be applied to synthesize pure stereoisomers of dihydronepetalactones as well as the structurally related iridomyrmecins, another class of iridoids. However, Wolinsky's method suffers from several major disadvantages such as high costs of (*S*)-pulegone and difficult separa-

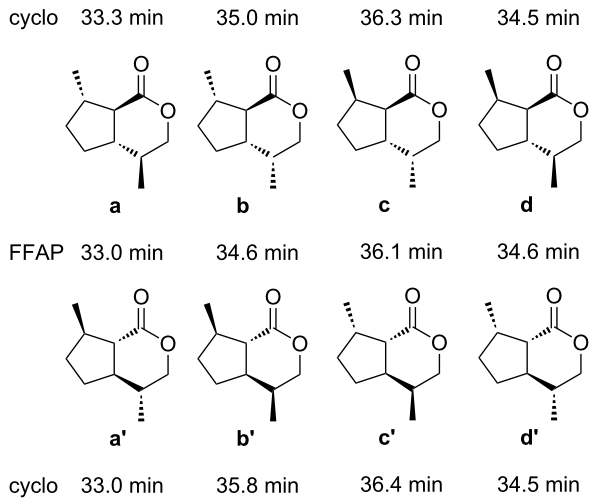

Figure 3: Structures and gas chromatographic retention times of *trans*-fused dihydronepetalactones on a conventional FFAP column (FFAP) and on an enantioselective cyclodextrin column (cyclo). For experimental details see Supporting Information File 1. The racemates **b**/**b'** and **d**/**d'**, which coeluted on FFAP, could be separated from each other on DB5 (data not shown).

tions of diastereomeric mixtures. Therefore, as an alternative, we present a novel stereoselective route to *trans*-fused dihydronepetalactones starting from pure, cheaply available enantiomers of limonene.

Route to *trans*-fused dihydronepetalactones **a** and **b** starting from (*S*)-pulegone

For comparison, the synthesis of **a** and **b** was carried out following Wolinsky's approach: (*S*)-Pulegone (**9**) was transformed to *trans*-pulegenic acid **10** via bromination, Favorskii rearrangement, and subsequent elimination (Scheme 1). Stereoselective addition of hydrochloric acid afforded the chloride **11**, and subsequent elimination of hydrochloric acid gave a mixture of the methyl esters **12** and **13** (methyl *trans*-pulegenate) [20-22] which could be separated by chromatography on silica gel. Hydroboration and lactonization of **12** furnished a mixture of the C4-epimers **a** and **b** that once again needed to be separated by chromatography on silica gel [23].

Analytical data of the first eluting component **a** were in accordance with those reported in the literature [24]. The same sequence starting from (*R*)-pulegone yielded a mixture of diastereomers **a'** and **b'**. The relative configuration of **a** at C4 was assigned according to NOESY experiments. Decisive NO-effects were found between the protons 4-H and 7a-H as well as between 7a-H and 7-CH_3 (Figure 4).

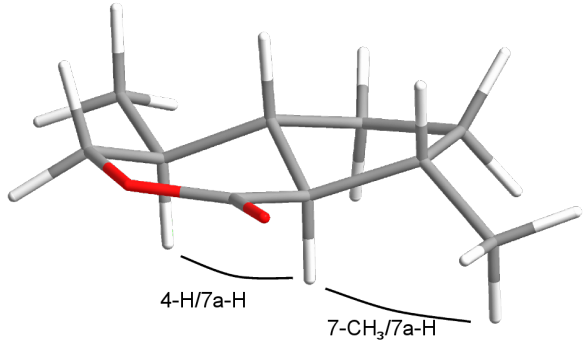

Figure 4: Configuration of the dihydronepetalactone **a**.

Basically, the sequence developed by Wolinsky could also provide access to the diastereomers **c** and **d** (and their enantiomers) if *trans*-pulegenic acid (**10**) would be replaced by *cis*-

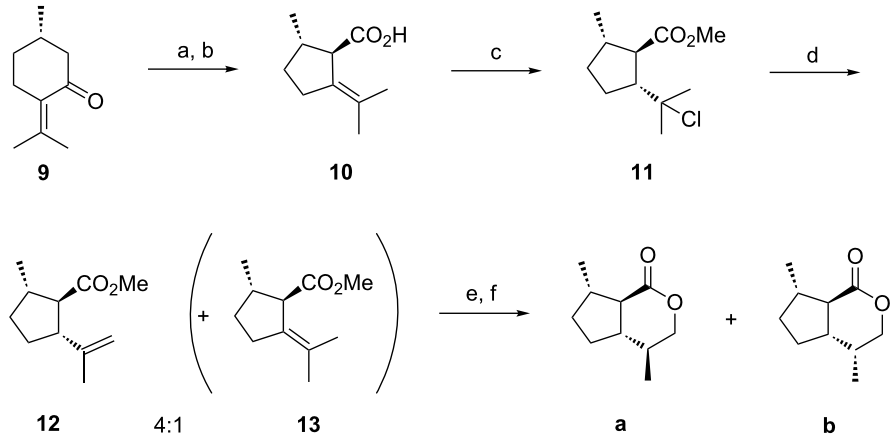

Scheme 1: Route from (*S*)-pulegone to the mixture of dihydronepetalactones **a** and **b**, consequently following Wolinsky's approach [23]. Reaction conditions: a) Br_2, HOAc, 0 °C; b) KOH, H_2O, reflux (15%, 2 steps); c) MeOH/HCl, rt, 96 h (82%); d) 2,6-lutidine, reflux, 72 h (75% of **12** + **13**); e) $BH_3{\cdot}SMe_2$, 0 °C, THF, NaOH, H_2O_2 (86% mixture of diastereomers); f) *p*-TsOH, toluene, reflux (17% of a + b).

pulegenic acid. A mixture of the latter and its *trans*-isomer (60:40) can be obtained by using a different base in the Favorskii-rearrangement step [22], again requiring a difficult chromatographic separation. Furthermore, this multistep route has several major disadvantages: The formation of mixtures of epimers entails to separations at several stages which have proven to be problematic. Moreover, several reaction steps afford unsatisfactory yields [23]. In addition, one of the main disadvantages is the fact that (*S*)-pulegone (*S*-**9**) is a highly expensive starting material for the synthesis of four of the eight *trans*-fused dihydronepetalactones. That excludes this route for the synthesis of larger amounts.

Route to stereochemically pure *trans*-fused dihydronepetalactones from (*R*)-limonene

Due to the shortcomings of the route described above, we designed an improved strategy towards *trans*-fused dihydronepetalactones. Starting from 1-formyl-2-methyl-5-(1-methylethenyl)-1-cyclopentene (**15**) as the key intermediate, the stereoselective synthesis of all eight stereoisomers could be achieved (Figure 5). The aldehyde **15** could be readily prepared from commercially available pure and cheap (*R*)-limonene (**14**) [25-27]. Non-selective hydroboration of the double bond in the side chain of **15** would yield a pair of diastereomers **16**/**16*** which would have to be separated. However, we expected that the chiral center at C5 would cause stereocontrol by forcing the reaction to proceed through the sterically least hindered transition state. We envisioned that stereoselective hydrogenation of the endocyclic double bond of the key intermediate **16** (and its diastereomer **16***) in either a "*syn*"- or "*anti*"-fashion could yield two pairs of diastereomeric hydroxy carboxylic acids **17**/**17*** or **18**/**18*** after some simple functional group transformations. These hydroxy acids would then yield the desired *trans*-fused dihydronepetalactones **a**–**d** during a final lactonization step.

Starting from cheap and pure (*S*)-limonene (**14'**), the corresponding *trans*-fused dihydronepetalactones **a'**–**d'** could be synthesized in the same way, showing our novel route to be a versatile alternative to Wolinsky's sequence [20,21]. In contrast to the latter, which fixed the stereogenic center of pulegone at position 7 of the final dihydronepetalactone, in our route the stereogenic center of limonene is retained at position 4a of the target compound and used for the stereoselective introduction of additional chiral centers.

Synthesis of the key intermediate **16**

The synthesis of the key intermediate **16** – which shows two differentiated primary alcohol functions – started from enantiomerically pure (*R*)-limonene (**14**, Scheme 2). Ozonolysis followed by reductive workup with dimethyl sulfide produced (3*R*)-3-(1-methylethenyl-6-oxoheptanal), which yielded the formyl cyclopentene **15** upon intramolecular aldol condensation [25-27]. Subsequently, the aldehyde **15** was reduced to

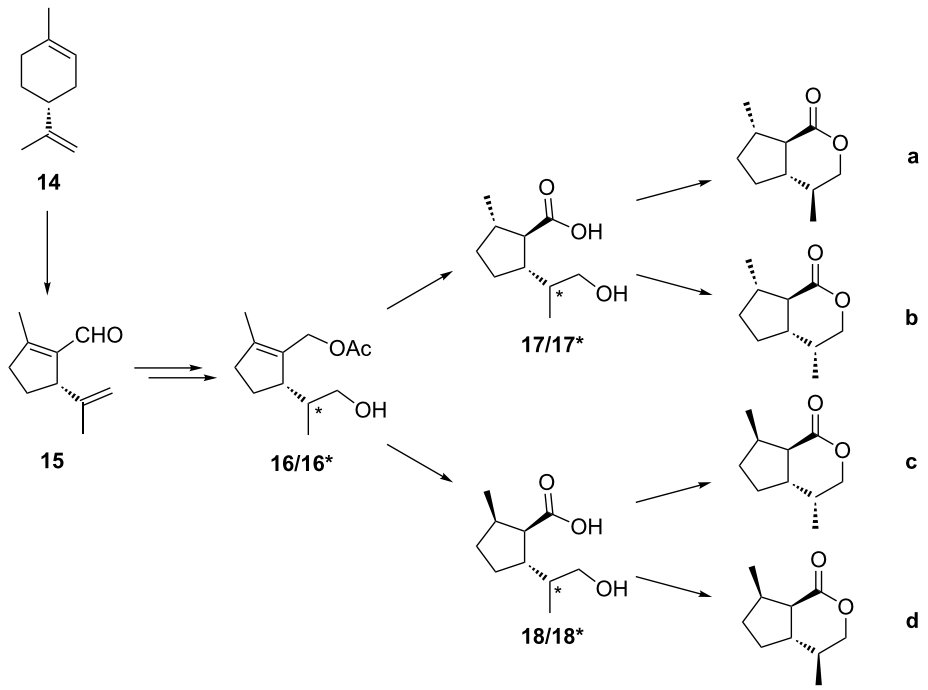

Figure 5: Route to stereochemically pure *trans*-fused dihydronepetalactones **a**–**d** from (*R*)-limonene.

the allylic alcohol **19** with $LiAlH_4$ and converted into the acetate **20** [28]. Hydroboration of **20** using disiamylborane proceeded with high stereoselectivity affording **16** as a single stereoisomer [17,28]. Similar results of highly stereoselective hydroborations of structurally related chiral cyclopentene derivatives have been reported [20,21].

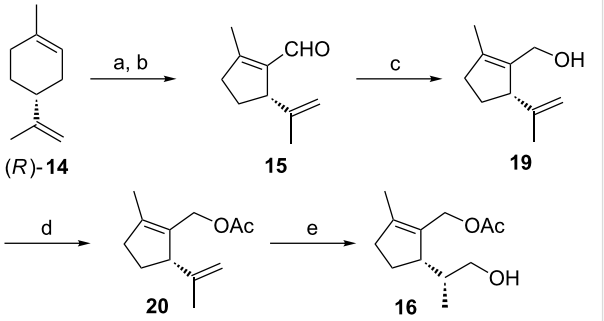

Scheme 2: Synthesis of the key compound **16**. Reaction conditions: a) O_3, MeOH, −50 °C (86%); b) AcOH, piperidine, C_6H_6, reflux (85%); c) $LiAlH_4$, Et_2O (82%); d) Ac_2O, pyridine, rt (91%); e) B_2H_6, 2-methyl-2-butene, 0 °C, THF, NaOH, H_2O_2 (66%).

Synthesis of *trans*,*trans*-dihydronepetalactone **b**

To install a *trans*,*trans*-configuration between the substituents at C5-C1 and C1-C2 of the cyclopentane backbone – which would later reflect the *trans,trans* relationship between substituents at C7-C7a and at C7a-C4a of the dihydronepetalactones **a** and **b** – a formal "*anti*"-addition of hydrogen to the cyclopentene **16** had to be carried out (Scheme 3). Usually, both homogeneous and heterogeneous catalytic hydrogenation reactions proceed via "*syn*"-addition of hydrogen to olefinic double bonds. Only subsequent isomerization processes may lead to a formal "*anti*"-addition. To obtain a suitable precursor, which, due to enolization of the hydrogenation product, might allow this formal "*anti*"-addition of hydrogen, the key intermediate **16** was transformed to the aldehyde **23**.

In the course of this short sequence, the free hydroxy group of **16** was protected as the TBDMS ether to yield **21** which afforded the mono-protected diol **22** after treatment with KOH in methanol. Subsequently, **22** was oxidized with pyridinium dichromate to give aldehyde **23**.

We expected that catalytic hydrogenation of the trisubstituted cylopentene **23** with a heterogeneous catalyst would preferentially take place from the sterically less hindered side of the molecule. This would lead to an all-*cis* configured hydrogenation product which would endure considerable steric strain. Due to the CH-acidity at the α-position of the formyl group, epimerization of the all-*trans* product **24** under acidic or basic conditions could be expected. Lange et al. reported the catalytic hydrogenation of a structurally close analogue, (5*R*)-1-formyl-2-methyl-5-isopropylcyclopent-1-ene, over Pd/C (10%) to give a 9:1 mixture of the all-*cis* versus the all-*trans* product [29]. In our case, the application of Lange's method to the aldehyde **23** led to the formation of a 3:1 mixture of the all-*cis* versus the all-*trans* epimer. Subsequent treatment with sodium methoxide in MeOH at rt for 20 h completely shifted the equilibrium to the thermodynamically more stable all-*trans* product **24**. Unfortunately, these results could not be reproduced on larger reaction scales (>5 mmol). After screening of a variety of other hydrogenation conditions, we found the hydrogenation of **23** with ammonium formate over palladium on carbon (10%) to be the method of choice [30]. Using this approach, the all-*trans* aldehyde **24** was almost exclusively formed. The presence of ammonium formate in the reaction mixture probably leads to an "in-situ" epimerization at C2 from the kinetically formed all-*cis*

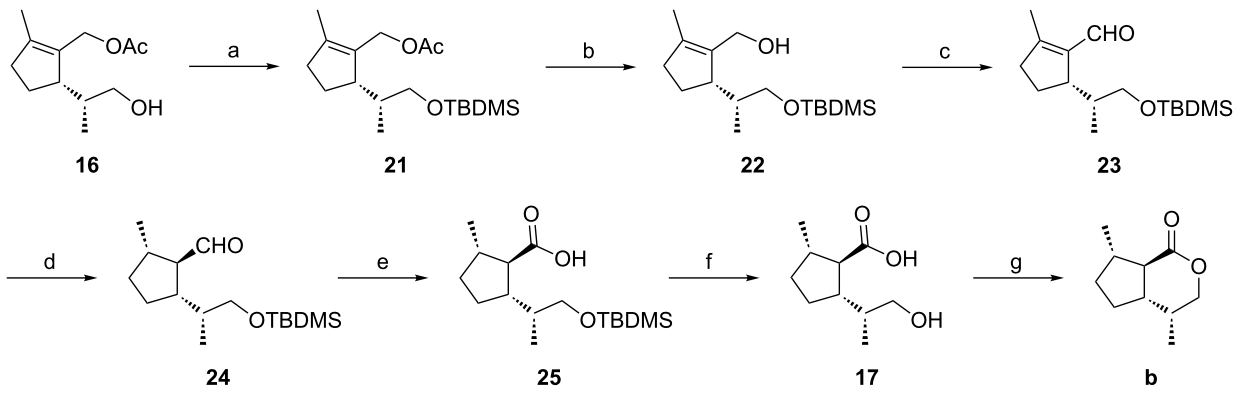

Scheme 3: Synthesis of *trans*,*trans*-substituted dihydronepetalactone **b**. Reaction conditions: a) TBDMSCl, imidazole, DMF, 0 °C (99%); b) KOH, MeOH, 0 °C (87%); c) PDC, MS, CH_2Cl_2, 0 °C to rt (61%); d) ammonium formate, Pd/C, MeOH, reflux (48%); e) $KMnO_4$, *t*-BuOH, pH 4.5, 0 °C (22%); f) TBAF, THF (100%); g) DCC, DMAP, CH_2Cl_2 (66%).

to the thermodynamically more stable all-*trans* product. Relative configurations of all substituents of compound **24** were confirmed by NOESY experiments (Figure 6). Strong NO-effects were found between the protons 5-CH_3 and 1-H, 1-H and 1'H (the proton at C1 of the side chain), 5-H and 2-H as well as between protons of 1-CHO and 2-H which is in line with a *trans,trans*-configuration (using the nomenclature described above).

Starting from **24**, the *trans*,*trans*-dihydronepetalactone **b** was synthesized in three subsequent steps (Scheme 3). First, oxidation of the aldehyde group with potassium permanganate in the presence of a phosphate buffer (pH 4.5) afforded the carboxylic acid **25** without epimerization at C1 [23,31]. Subsequent deprotection of the TBDMS ether with tetrabutylammonium fluoride (TBAF) yielded **17**, and lactonization with *N*,*N*-dicyclohexylcarbodiimide (DCC) and 4-dimethylaminopyridine (DMAP) in dichloromethane afforded the *trans*,*trans*-dihydronepetalactone **b**.

The relative configuration of the *trans*,*trans*-dihydronepetalactone **b** was confirmed by NOESY experiments. Decisive NO-effects could be observed between 4-CH_3 and 7a-H as well as between 4-CH_3 and 5-Ha, and furthermore, between 5-Ha and 7a-H as well as between 7a-H and 7-CH_3 (Figure 6). The enantiomer **b'** was synthesized via the same route starting from (*S*)-limonene. Analytical data of compound **b'** were identical to those which were obtained of **b** when Wolinky's route was followed (see above).

Synthesis of *cis*,*trans*-fused dihydronepetalactone **c**

For the synthesis of the *cis*,*trans* dihydronepetalactone **c**, a *cis*,*trans*-configuration between the substituents at C5-C1 and C1-C2 of the cyclopentane backbone needed to be established. With acetate **16** as the key intermediate, a stereoselective "*syn*"-addition of hydrogen from the same side as the (*R*)-configured side chain at C5 would provide the desired stereochemical outcome of the hydrogenation reaction (Scheme 4). We

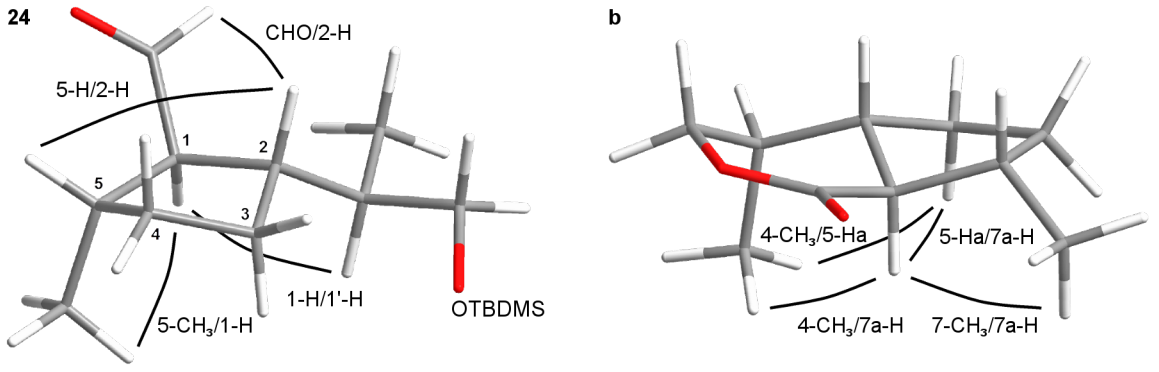

Figure 6: Configurations of compound **24** and the dihydronepetalactone **b**.

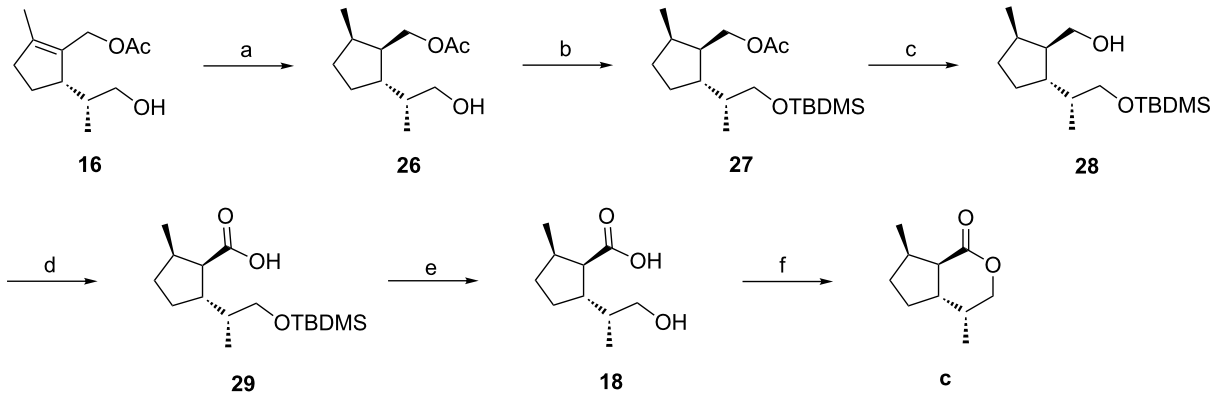

Scheme 4: Synthesis of *cis*,*trans*-substituted dihydronepetalactone **c**. Reaction conditions: a) Crabtree's catalyst [Ir(cod)PCy_3(py)]PF_6 (11 mol %), 1 bar H_2, CH_2Cl_2, rt (81%); b) TBDMSCl, imidazole, DMF, 0 °C (100%); c) KOH, MeOH, rt (93%); d) $RuCl_3 \cdot 3H_2O$ (2 mol %), $NaIO_4$, CCl_4, CH_3CN, phosphate buffer (pH 7), rt (81%); e) HF, CH_3CN, rt (100%); f) DCC, DMAP, CH_2Cl_2 (66%).

expected the free hydroxy group of **16** to coordinate to an appropriate homogenous hydrogenation catalyst, controlling the stereochemical course of the hydrogen transfer from the same side as the side chain at C5 through chelation. We chose Crabtree's iridium catalyst ([Ir(cod)PCy_3(py)]PF_6) which has been reported to furnish excellent facial selectivities during directed hydrogenations of cyclic olefins [32-34].

Hydrogenation of acetate **16** in the presence of 11 mol % of Crabtree's catalyst under 1 bar hydrogen pressure for 1.5 h yielded the desired product **26** as a single diastereomer. Alternative hydrogenation methods using optically active catalysts failed. In one case we investigated the hydrogenation of the endocylic double bond of the allylic alcohol **19** (Scheme 2) with one of Noyori's ruthenium BINAP catalysts ([Ru((*S*)-BINAP)]$(OAc)_2$) [35,36] but reduction occurred only at the side chain.

Relative configurations of all substituents of the acetate **26** were confirmed by NOESY experiments (Figure 7). Strong NO-effects were observed between the protons 5-CH_3 and 1'-H (protons of the acetoxymethyl group at C1), 5-CH_3 and 2-H, 1'-H and 2-H as well as 5-H and 1''-CH_3 (protons of the methyl group at C1 of the side chain) which is in line with a *cis,trans*-configuration (using the nomenclature described above).

Starting from **26**, the synthesis of the *cis,trans*-dihydronepetalactone **c** was completed in five subsequent steps (Scheme 4). First, the free hydroxy group of **26** was protected as the TBDMS ether to yield **27**. Then, the acetate group was removed with methanolic KOH to afford the alcohol **28**. Careful oxidation of the primary alcohol function [37,38] with ruthenium(III) chloride and sodium periodate in a biphasic mixture of carbon tetrachloride, acetonitrile, and phosphate buffer (pH 7) produced the carboxylic acid **29** without epimerization at C1. After removal of the TBDMS protecting group with HF in acetonitrile, the hydroxy acid **18** was lactonized in the presence of DCC and catalytic amounts of DMAP in dichloromethane at rt to afford *cis,trans*-dihydronepetalactone **c**. Its enantiomer **c'** was synthesized from enantiomerically pure (*S*)-limonene, following the same route. The relative configuration of **c** was confirmed by NOESY experiments (Figure 7). Decisive NO-effects could be observed between 4a-H and 7-CH_3 as well as between 4-CH_3 and 7a-H, and furthermore, between 4-CH_3 and 5-Ha as well as between 5-Ha and 7a-H.

Synthesis of a mixture of *trans*-fused dihydronepetalactones **c** and **d**

The stereogenic center at C1' of the acetate **26** keeps (*R*)-configuration which resulted from highly stereoselective hydroboration of the acetate **20** to yield the key intermediate **16** as shown above (Scheme 2). For the synthesis of the *cis,trans*-dihydronepetalactone **d**, this stereocenter needed to be isomerized to keep the (4*S*)-configuration in the final product (Scheme 5). To achieve the required inversion, the acetate **26** was oxidized to the aldehyde **30**, which could be epimerized using *p*-toluenesulfonic acid in benzene under reflux conditions to provide a 2:3 mixture of the desired aldehydes **30** and its epimer **30***. Subsequent steps were carried out with the mixture of diastereomers. Reaction of **30**/**30*** with sodium borohydride at −20 °C reduced the aldehyde function to yield a mixture of the diastereomers **26**/**26***. The following sequence, yielding a mixture of the dihydronepetalactones **c** and **d** was essentially the same as described above (Scheme 4).

Transformation of the free hydroxy group to the TBDMS ethers **27**/**27*** was followed by cleavage of the acetate moiety with methanolic KOH to give a mixture of the alcohols **28**/**28***. Oxi-

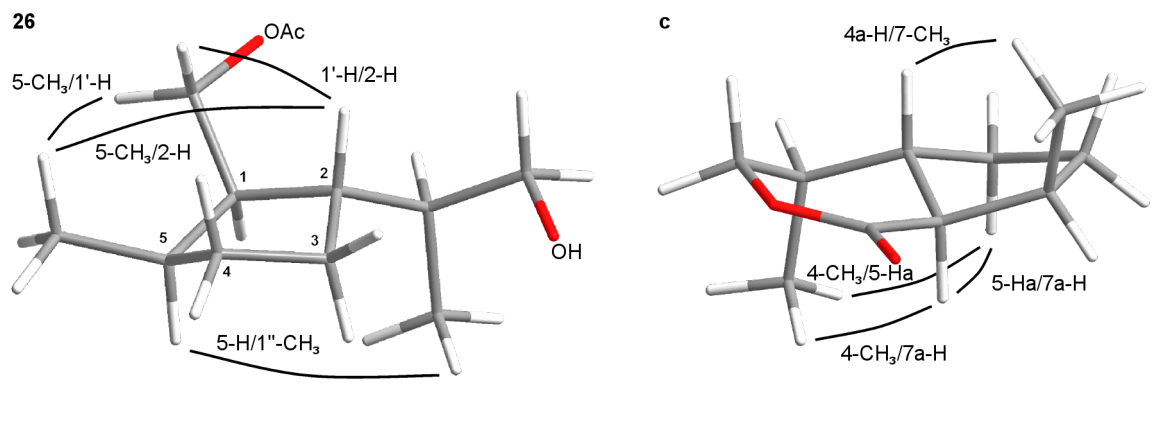

Figure 7: Configurations of compound **26** and the dihydronepetalactone **c**.

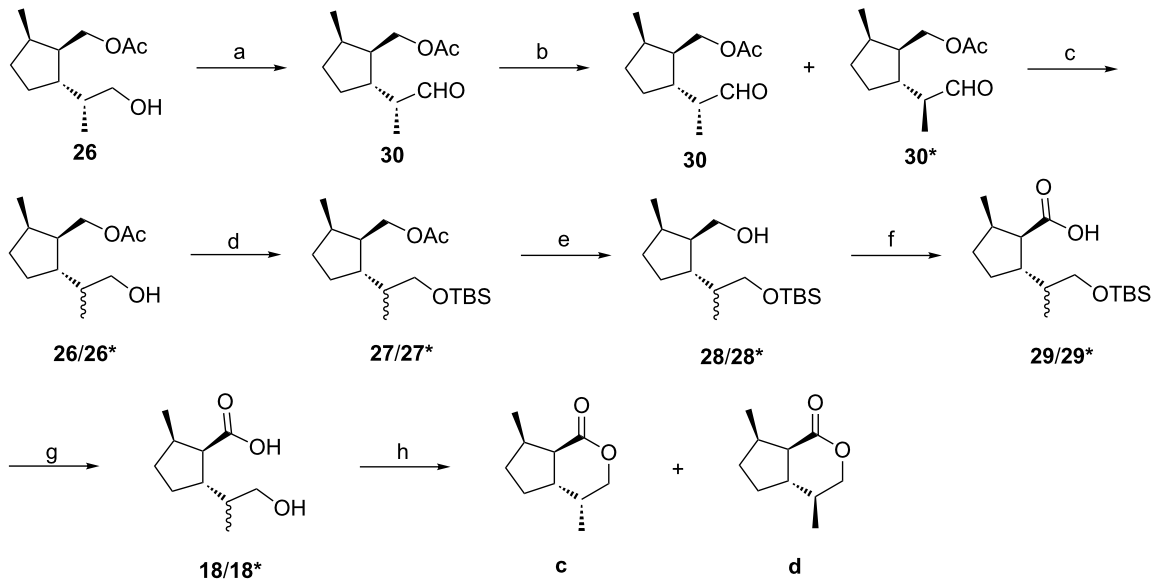

Scheme 5: Synthesis of a 2:3 mixture of dihydronepetalactones **c** and **d**. Reaction conditions: a) $(COCl)_2$, DMSO, CH_2Cl_2, −70 °C to 0 °C (71%); b) *p*-TsOH, benzene, reflux (96%); c) $NaBH_4$, MeOH, −20 °C; d) TBDMSCl, imidazole, DMF, 0 °C (78%) (over two steps); e) KOH, MeOH, rt (94%); f) $RuCl_3{\cdot}3H_2O$ (2 mol %), $NaIO_4$, CCl_4, CH_3CN, phosphate buffer (pH 7), rt (69%); g) HF, CH_3CN, rt (98%); h) DCC, DMAP, CH_2Cl_2 (62%).

dation of the primary alcohol function with ruthenium(III) chloride and sodium periodate in a biphasic mixture of carbon tetrachloride, acetonitrile and phosphate buffer (pH 7) afforded the carboxylic acids **29**/**29*** without epimerization at C1 [37,38]. After cleavage of the TBDMS ether with HF in acetonitrile, a mixture of dihydronepetalactones **c** and **d** was formed by lactonization of the hydroxy acids **18**/**18*** with DCC and DMAP in dichloromethane at rt. The C4 epimeric dihydronepetalactones **c** and **d** could be separated by column chromatography over silica. Starting from the enantiomer of **26**, a mixture of dihydronepetalactones **c'** and **d'** was synthesized by following the same reaction sequence.

Formal synthesis of a mixture of *trans*-fused dihydronepetalactones **a** and **b** from (*R*)-limonene

As outlined above, six of the eight possible stereoisomers of *trans*-fused dihydronepetalatones were synthesized from the enantiomers of limonene following a new route. Compound **a** and its enantiomer **a'** were prepared according to the procedure described by Wolinsky [20,21]. However, our new approach also includes a formal synthesis of **a** and **a'**. A mixture of **a** and **b** will be easily obtained from the protected hydroxy aldehyde **24** by the straight forward procedure outlined in Scheme 6.

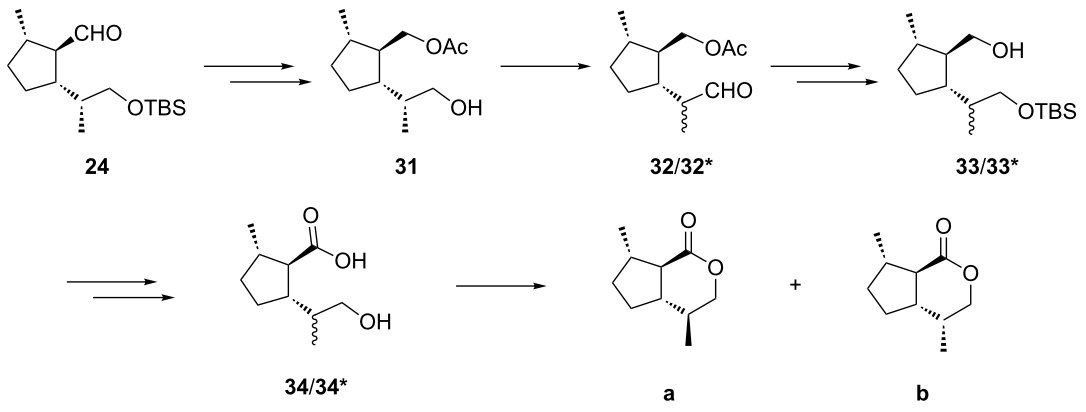

Scheme 6: Formal synthesis of a mixture of dihydronepetalactones **a** and **b** from (*R*)-limonene.

Reduction of the aldehyde function of **24** and acetylation of the resulting primary alcohol followed by cleavage of the silyl group will furnish the primary alcohol **31**, which upon oxidation will yield the corresponding aldehyde that can be epimerized to the diastereomers **32**/**32*** as shown above. Subsequent reduction of **32**/**32***, silylation of the resulting primary alcohols and saponification will produce a mixture of the diastereoisomers **33**/**33***. Oxidation of the primary alcohol moiety, followed by cleavage of the silyl group will yield the epimeric hydroxy acids **34**/**34*** which will form a mixture of the dihydronepetalactones **a** and **b** after lactonization. As shown above, this mixture can be separated upon column chromatography.

Conclusion

In summary, we synthesized all eight *trans*-fused stereoisomeric dihydronepetalactones. After having used the enantiomers of pulegone as educts in Wolinsky's route to (4*S*,4a*S*,7*S*,7a*R*)-dihydronepetalactone (**a**) and its enantiomer **a'** [23], we developed an improved and general way for the synthesis of all *trans*-fused dihydronepetalactones, starting from pure enantiomers of limonene. Our approach is also superior to that starting from optically active carvone that yields the starting material for the synthesis of *trans*-fused iridoid lactones only as a byproduct [15].

Identification of a *trans*-fused dihydronepetalactone in the parasitoid wasp *Alloxysta victrix*

Upon gas chromatography using FFAP as a polar achiral stationary phase, the stereoisomers **a** and **c** could be well separated while **b** and **d** coeluted. However, the latter pair could be resolved on a less polar DB5-capillary, where **b**/**b'** eluted after **d**/**d'** (data not shown). As a result, the relative configuration of each of the *trans*-fused dihydronepetalactones could be unambiguously assigned by GC/MS.

With the exception of (4*S*,4a*S*,7*R*,7a*R*)-dihydronepetalactone (**d**) and its enantiomer **d'**, the stereoisomers could well be distinguished by enantioselective gas chromatography using a 1:1-mixture of OV1701 and heptakis-(6-*O*-*tert*-butyldimethylsilyl-2,3-di-*O*-methyl)-β-cyclodextrin as an optically active stationary phase. Figure 3 shows the corresponding retention times of all eight stereoisomers that were obtained with the two used capillary column systems. Coupled GC/MS using FFAP as the stationary phase revealed the target natural iridoid lactone **X** to show the same mass spectrum and the same retention time as **a**/**a'**, the first eluting pair of the synthetic dihydronepetalactones (Figure 3). Enantioselective gas chromatography on a cyclodextrin column showed **X** to coelute with **a'** which was well separated from its enantiomer by an α-value of **a'**:**a** = 1.01 (Figure 3). Consequently, the structure of **X** was unambiguously assigned to be (4*R*,4a*R*,7*R*,7a*S*)-dihydronepetalactone. It should be noted that Meinwald et al. identified **a**/**a'** (absolute configuration not assigned) as a component of secretions of the abdominal defense glands of the rove beetle *Creophilus maxillosus* [39]. Interestingly, the structure of **a'** is relatively close to that of nepetalactone **7** and lactol **8**, the sex pheromone of the grain aphid *S. avenae* [13] which keeps the second level in the investigated tetratrophic system. Grant et al., found the *trans*-fused (1*R*,4a*S*,7*R*,7a*R*)-1-methoxy-4,7-dimethyl-1,4a,5,6,7,7a)-hexahydrocyclopenta[*c*]pyran, called (1*R*)-1-methoxymyodesert-3-ene, among the volatiles of the Ellangowan poison bush, which they transformed to the corresponding lactone **a'** [24]. Apart from this compound and very few others, the stereogenic center carrying the methyl group in the five-membered ring of iridoid lactones including insect semiochemicals [13-15] generally shows (*S*)-configuration. Only recently, two isomeric iridoid lactones showing (7*R*)-configuration have been identified from the *Drosophila* parasitoid *Leptopilina heterotoma* [40]. Compound **X** has been identified in the mandibular gland secretions of other *Alloxysta* species, too, [41]. However, its biological significance is not yet clear and will need further investigations.

The differentiation of the oxygen containing functional groups in the trisubstituted cyclopentene **16**, a key-compound in our synthetic approach, provides access to a large number of iridoids including nepetalactones but also iridomyrmecins and monocyclic compounds. Consequently, having reference compounds at hand, structures of hitherto unknown iridoids [42] may now be assigned. It may turn out that the chiral center carrying the methyl group in the five-membered ring of iridoids may much more often show (*R*)-configuration than it is known today.

Supporting Information

Supporting Information File 1

Experimental details and characterization data for synthesized compounds.
[http://www.beilstein-journals.org/bjoc/content/supplementary/1860-5397-8-140-S1.pdf]

Acknowledgements

The biological material was kindly provided by Prof. Dr. Urs Wyss, University of Kiel, Germany. Financial support by the German Science Foundation, Deutsche Forschungsgemeinschaft (DFG – Fr 12/1) is gratefully acknowledged.

References

1. Hilgraf, R.; Zimmermann, N.; Lehmann, L.; Tröger, A.; Francke, W. *Beilstein J. Org. Chem.* **2012,** *8,* 1256–1264. doi:10.3762/bjoc.8.141
2. Lilley, R.; Hardie, J.; Merritt, L. A.; Pickett, J. A.; Wadhams, L. J.; Woodcock, C. M. *Chemoecology* **1994,** *5,* 43–46. doi:10.1007/BF01259972
3. Dawson, G. W.; Pickett, J. A.; Smiley, D. W. M. *Bioorg. Med. Chem.* **1996,** *4,* 351–361. doi:10.1016/0968-0896(96)00012-0
4. Petersen, G.; Matthiesen, C.; Francke, W.; Wyss, U. *Eur. J. Entomol.* **2000,** *97,* 545–550.
5. Höller, C.; Micha, S. G.; Schulz, S.; Francke, W.; Pickett, J. A. *Experientia* **1994,** *50,* 182–185. doi:10.1007/BF01984961
6. Petersen, G.; Matthiesen, C.; Stolzenberg, N.; Zimmermann, N.; Hilgraf, R.; Lehmann, L.; Francke, W.; Wyss, U. *Mitt. Dtsch. Entomol. Ges.* **2001,** *13,* 51–55.
7. Regnier, F. E. In *Biochemical Application of Mass Spectrometry;* Waller, G. R., Ed.; Wiley & Sons: New York, 1972; pp 723–734.
8. Sakai, T.; Nakajima, K.; Sakan, T. *Bull. Chem. Soc. Jpn.* **1980,** *53,* 3683–3686. doi:10.1246/bcsj.53.3683
9. McElvain, S. M.; Bright, R. D.; Johnson, P. R. *J. Am. Chem. Soc.* **1941,** *63,* 1558–1563. doi:10.1021/ja01851a019
10. Bates, R. B.; Eisenbraun, E. J.; McElvain, S. M. *J. Am. Chem. Soc.* **1958,** *80,* 3420–3424. doi:10.1021/ja01546a054
11. Eisenbraun, E. J.; Browne, C. E.; Irvin-Willis, D. J.; McGurk, E. L.; Eliel, E. L.; Harris, D. L. *J. Org. Chem.* **1980,** *45,* 3811–3814. doi:10.1021/jo01307a016
12. Cavill, G. W. K.; Clark, D. V. *J. Insect Physiol.* **1967,** *13,* 131–135. doi:10.1016/0022-1910(67)90009-1
13. Pickett, J. A.; Wadhams, L. J.; Woodcock, C. M.; Hardie, J. *Annu. Rev. Entomol.* **1992,** *37,* 67–90. doi:10.1146/annurev.en.37.010192.000435
14. Goldansaz, S. H.; Dewhirst, S.; Birkett, M. A.; Hooper, A. M.; Smiley, D. W. M.; Pickett, J. A.; Wadhams, L.; McNeil, J. N. *J. Chem. Ecol.* **2004,** *30,* 819–834. doi:10.1023/B:JOEC.0000028434.19319.b4
15. Hooper, A. M.; Donald, B.; Woodcock, C. M.; Park, J. H.; Paul, R. L.; Boo, K. S.; Hardie, J.; Pickett, J. A. *J. Chem. Ecol.* **2002,** *28,* 849–864. doi:10.1023/A:1015201129331
16. Ficini, J.; d'Angelo, J. *Tetrahedron Lett.* **1976,** *17,* 687–690. doi:10.1016/S0040-4039(00)74597-7
17. Lee, E.; Yoon, C. H. *J. Chem. Soc., Chem. Commun.* **1994,** 479–481. doi:10.1039/C39940000479
18. Nangia, A.; Prasuna, G.; Rao, P. B. *Tetrahedron* **1997,** *53,* 14507–14545. doi:10.1016/S0040-4020(97)00748-5 And references cited therein.
19. Beckett, J. S.; Beckett, J. D.; Hofferberth, J. E. *Org. Lett.* **2010,** *12,* 1408–1411. doi:10.1021/ol100077z And references cited therein.
20. Wolinsky, J.; Gibson, T.; Chan, D.; Wolf, H. *Tetrahedron* **1965,** *21,* 1247–1261. doi:10.1016/0040-4020(65)80066-7
21. Wolinsky, J.; Eustace, E. J. *J. Org. Chem.* **1972,** *37,* 3376–3378. doi:10.1021/jo00986a051
22. Achmad, S. A.; Cavill, G. W. K. *Aust. J. Chem.* **1963,** *16,* 858–868. doi:10.1071/CH9630858
23. Ibarra-Wiltschek, D. Identifizierung und Synthese mono- und sesquiterpenoider Inhaltsstoffe aus Hymenopteren. Ph.D. Thesis, Universität Hamburg, Hamburg, Germany, 1995.
24. Grant, H. G.; O'Regan, P. J.; Park, R. J.; Sutherland, M. D. *Aust. J. Chem.* **1980,** *33,* 853–878. doi:10.1071/CH9800853
25. Auer, L.; Weymuth, C.; Scheffold, R. *Helv. Chim. Acta* **1993,** *76,* 810–818. doi:10.1002/hlca.19930760205
26. Naemura, K.; Hasegawa, T.; Miyabe, H.; Chikamatsu, H. *Bull. Chem. Soc. Jpn.* **1992,** *65,* 203–209. doi:10.1246/bcsj.65.203
27. Wolinsky, J.; Slabaugh, M. R.; Gibson, T. *J. Org. Chem.* **1964,** *29,* 3740–3742. doi:10.1021/jo01035a537
28. Wolinsky, J.; Nelson, D. *Tetrahedron* **1969,** *25,* 3767–3774. doi:10.1016/S0040-4020(01)82908-2
29. Lange, G. L.; Neidert, E. E.; Orrom, W. J.; Wallace, D. J. *Can. J. Chem.* **1978,** *56,* 1628–1633. doi:10.1139/v78-266
30. Rao, H. S. P.; Reddy, K. S. *Tetrahedron Lett.* **1994,** *35,* 171–174. doi:10.1016/0040-4039(94)88193-6
31. Abiko, A.; Roberts, J. C.; Takemasa, T.; Masamune, S. *Tetrahedron Lett.* **1986,** *27,* 4537–4540. doi:10.1016/S0040-4039(00)84997-7
32. Crabtree, R. H.; Davis, M. W. *Organometallics* **1983,** *2,* 681–682. doi:10.1021/om00077a019
33. Crabtree, R. H.; Davis, M. W. *J. Org. Chem.* **1986,** *51,* 2655–2661. doi:10.1021/jo00364a007
34. Brown, J. M. *Angew. Chem., Int. Ed. Engl.* **1987,** *26,* 190–203. doi:10.1002/anie.198701901
35. Ohta, T.; Miyake, T.; Seido, N.; Kumobayashi, H.; Takaya, H. *J. Org. Chem.* **1995,** *60,* 357–363. doi:10.1021/jo00107a014
36. Takaya, H.; Ohta, T.; Sayo, N.; Kumobayashi, H.; Akatagawa, S.; Inoue, S.; Kasahara, I.; Noyori, R. *J. Am. Chem. Soc.* **1987,** *109,* 1596–1597. doi:10.1021/ja00239a065
37. Carlsen, P. H. J.; Katsuki, T.; Martin, V. S.; Sharpless, K. B. *J. Org. Chem.* **1981,** *46,* 3936–3938. doi:10.1021/jo00332a045
38. Mori, K.; Ebata, T. *Tetrahedron* **1986,** *16,* 4413–4420. doi:10.1016/S0040-4020(01)87280-X
39. Jefson, M.; Meinwald, J.; Nowicki, S.; Hicks, K.; Eisner, T. *J. Chem. Ecol.* **1983,** *9,* 159–180. doi:10.1007/BF00987779
40. Stökl, J.; Hofferberth, J.; Pritschet, M.; Brummer, M.; Ruther, J. *J. Chem. Ecol.* **2012,** *38,* 331–339. doi:10.1007/s10886-012-0103-0
41. Hübner, G.; Völkl, W.; Francke, W.; Dettner, K. *Biochem. Syst. Ecol.* **2002,** *30,* 505–523. doi:10.1016/S0305-1978(01)00137-5
42. Huth, A.; Dettner, K. *J. Chem. Ecol.* **1990,** *16,* 2691–2711. doi:10.1007/BF00988079

License and Terms

Beilstein Journal of Organic Chemistry

Stereoselective synthesis of *trans*-fused iridoid lactones and their identification in the parasitoid wasp *Alloxysta victrix*, Part II: Iridomyrmecins

Robert Hilgraf, Nicole Zimmermann, Lutz Lehmann, Armin Tröger and Wittko Francke*

Full Research Paper

Open Access

Address:
Department of Chemistry - Organic Chemistry, University of Hamburg, Martin-Luther-King-Platz 6, D-20146 Hamburg, Germany

Email:
Wittko Francke* - francke@chemie.uni-hamburg.de

* Corresponding author

Keywords:
Alloxysta victrix; identification; iridoid; stereoselective synthesis; *trans*-fused iridomyrmecin

Beilstein J. Org. Chem. **2012,** *8,* 1256–1264.
doi:10.3762/bjoc.8.141

Received: 16 March 2012
Accepted: 20 July 2012
Published: 08 August 2012

This article is part of the Thematic Series "Biosynthesis and function of secondary metabolites". Part I [1] describes the synthesis of dihydronepetalactones by this approach.

Guest Editor: J. S. Dickschat

Abstract

Following our earlier approach to the synthesis of dihydronepetalactones, all eight stereoisomers of *trans*-fused iridomyrmecins were synthesized starting from the enantiomers of limonene. Combined gas chromatography and mass spectrometry including enantioselective gas chromatography revealed that volatiles released by the endohyperparasitoid wasp *Alloxysta victrix* contain (4*S*,4a*R*,7*S*,7a*R*)-iridomyrmecin of 95–97% ee and stereochemically pure (4*S*,4a*S*,7*R*,7a*S*)-iridomyrmecin as a minor component.

Introduction

In the course of our studies on volatile signals of the endohyperparasitoid wasp, *Alloxysta victrix*, we identified several acyclic terpenoids and the *trans*-fused (4*S*,4a*R*,7*R*,7a*S*)-dihydronepetalactone (**X**) as volatile components of cephalic secretions released by this species (Figure 1) [1,2]. However, gas chromatograms showed the presence of two additional major volatiles **Y** and **Z** which, according to their mass spectra, were suggested to be *trans*-fused iridomyrmecins [3,4]. Since no synthetic reference compounds were available, all eight *trans*-fused iridomyrmecins had to be prepared. To complete the synthesis of this suite, we started from optically active limonene following a strategy similar to our route leading to *trans*-fused dihydronepetalactones [1]. The realization of this task and the unambiguous structure assignment of the natural products **Y** and **Z** is subject of the present paper.

Results and Discussion

Upon coupled gas chromatography/mass spectrometry (GC/MS), two major components, **Y** and **Z**, of the volatile secretions of both sexes of *Alloxysta victrix* (although in much

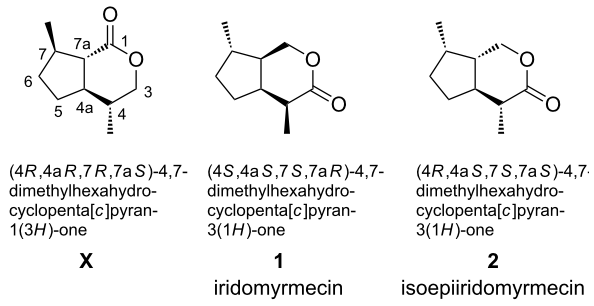

Figure 1: Structures of *cis*- and *trans*-fused iridoid lactones.

higher amounts in males) gave almost identical 70 eV EI-mass spectra (Figure 2); somewhat resembling that of the *trans*-fused dihydronepetalactone that we had already found in the insects [1]. Gas chromatography coupled with chemical ionization mass spectrometry (GC/CIMS) proved the molecular mass of the target compounds to be $[M]^+ = 168$, while high resolution mass spectrometry (GC/HRMS) showed their atomic composition to be $C_{10}H_{16}O_2$, confirming the compounds to be isomers of dihydronepetalactone. Though the fragmentation pattern showed some similarities to that of the *cis*-fused iridomyrmecin (**1**), a comparison with mass spectral data published for the *trans*-fused isoepiiridomyrmecin (**2**) suggested that the substances **Y** and **Z** are *trans*-fused iridomyrmecins. While the plotted mass spectrum of **1** showed *m*/*z* 95 as the base peak and similar abundances of about 55% for *m*/*z* 67, *m*/*z* 81 and *m*/*z* 109 [3], the data of **2** refer to *m*/*z* 81 as the base peak and *m*/*z* 95 and *m*/*z* 109 to reach 48% and 33%, respectively [4]; this is more close to the spectra of **Y** and **Z** (Figure 2).

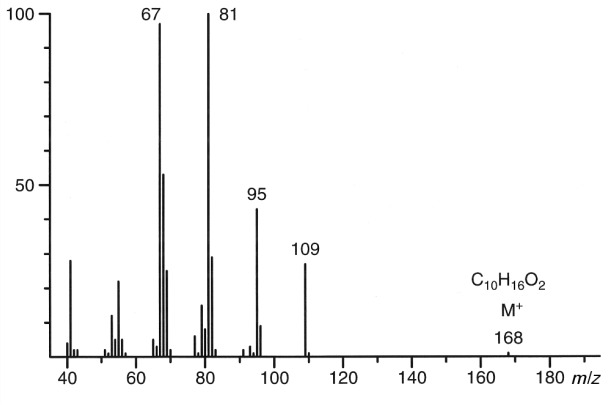

Figure 2: 70 eV EI-mass spectrum of compounds **Y** and **Z** of *Alloxysta victrix*.

Iridomyrmecin (**1**) was first isolated from ants (Figure 1) [5] and along with some other volatile iridoids it has since been reported to be a potent insecticide and antibiotic from several natural sources [6]. Due to their challenging molecular structures and their interesting physiological properties, iridomyrmecins are attractive targets in stereoselective synthesis.

Similar to dihydronepetalactones, the iridomyrmecin skeleton shows four contiguous stereogenic centers giving rise to four *trans*-fused stereoisomers **A**–**D** and four corresponding enantiomers **A'**–**D'** (Figure 3, **D'** is identical to **2** in Figure 1). The presence of the four chiral centers complicates a stereoselective synthesis despite the small size of the molecule. Several methods have been published for the preparation of optically active *cis*-fused bicyclic iridoid lactones [7-10], whereas only a few syntheses of *trans*-fused ring systems have been reported [11]. Starting from enantiomerically pure (*R*)-pulegone, mixtures of (7*R*)-configured diastereomers **A'** and **B'** as well as **C** and **D** have been synthesized by Wolinsky [12]. The set of stereochemically pure (7*S*)-configured, *trans*-fused iridomyrmecins **A**, **B**, **C'**, and **D'** has been prepared by Trave [13]. Though Wolinky's route may generally be used for the synthesis of all eight stereoisomers of *trans*-fused iridomyrmecins, it suffers from several major disadvantages such as high costs of (*S*)-pulegone and difficult separations of diastereomeric mixtures.

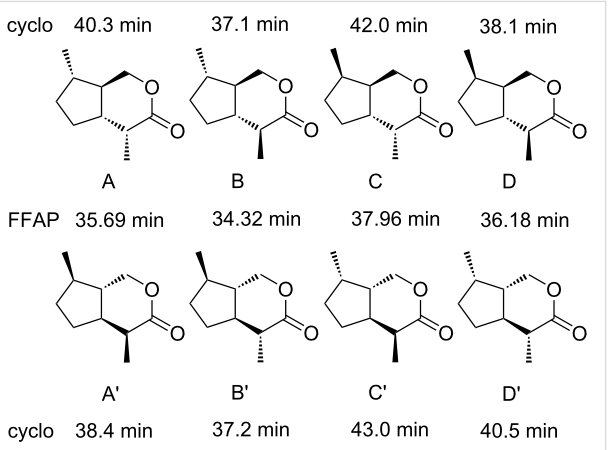

Figure 3: Chemical structures of all eight stereoisomers of *trans*-fused iridomyrmecins and their gas chromatographic retention times (min) on FFAP and on a cyclodextrin column (cyclo). For experimental details see Supporting Information File 1.

Starting from the cheaply available pure enantiomers of limonene, we had reported a novel stereoselective route towards *trans*-fused dihydronepatalactones [1] which we now extended to the synthesis of all eight stereoisomers of *trans*-fused iridomyrmecins. Subsequently, the volatile components **Y** and **Z** – present in *Alloxysta victrix* – were confirmed to be *trans*-fused iridomyrmecins, and their absolute configurations could be determined by comparison of their analytical data with those of all eight synthetic stereoisomers.

Synthesis of *trans*-fused iridomyrmecins

Our approach to the eight *trans*-fused iridomyrmecins starting from the enantiomers of limonene followed our general route for the synthesis of *trans*-fused dihydronepetalactones (Figure 4) [1].

Starting from pure (*R*)-limonene (**3**), the key intermediate **4** was prepared as described previously [1] and was used for both the synthesis of *trans,trans* and *cis,trans* (these designations refer to the relative configurations between the methyl group at C-7 and the substitution pattern at C-7a and C-4a, respectively) configured iridomyrmecins. Key steps were two stereoselective hydrogenations: A transfer hydrogenation for a formal "*anti*" delivery of hydrogen [14,15], as represented in **5**, and the use of Crabtree's catalyst in a directed hydrogenation for a "*syn*" addition of hydrogen as represented in **6** [16-18]. Subsequent to the hydrogenation step, the synthesis of *trans*-fused iridomyrmecins could be completed after some standard functional group modifications. The synthesis of the corresponding enantiomers followed the same way, starting from (*S*)-limonene (**3'**).

Synthesis of *trans*-fused iridomyrmecins **A** and **B**

The aldehyde **8**, derived from (*R*)-limonene (**3**), served as the key intermediate for the synthesis of the *trans*-fused iridomyrmecins **A** and **B** (Scheme 1). As shown in the stereo-

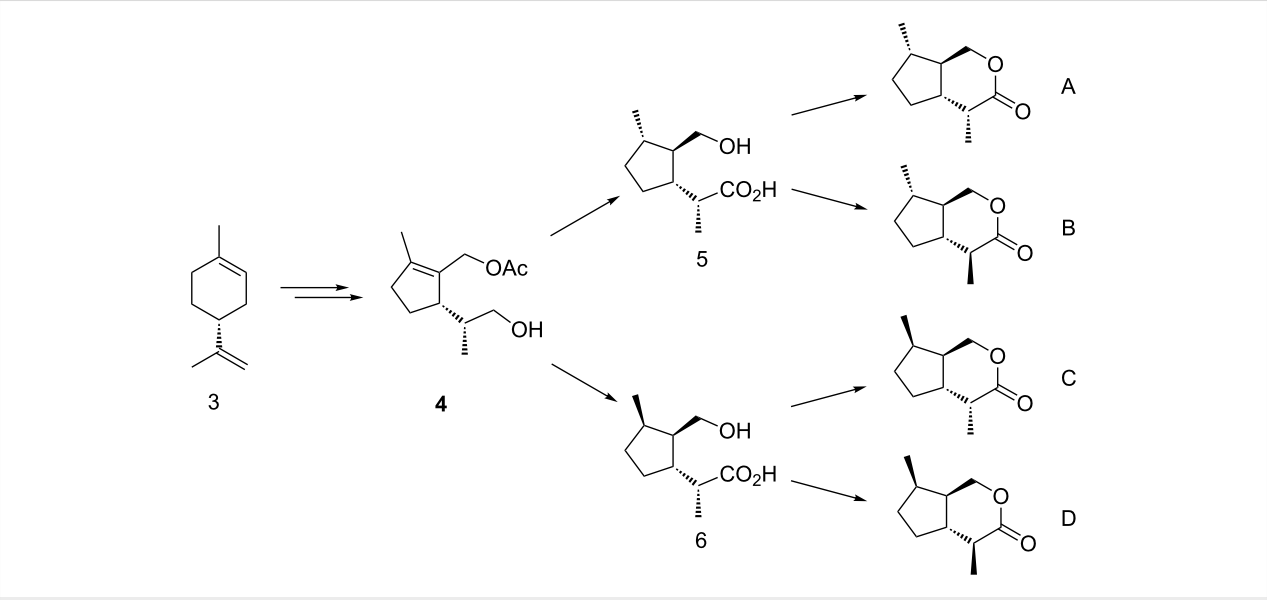

Figure 4: Strategy for the stereoselective synthesis of *trans*-fused iridomyrmecins **A**–**D** from (*R*)-limonene.

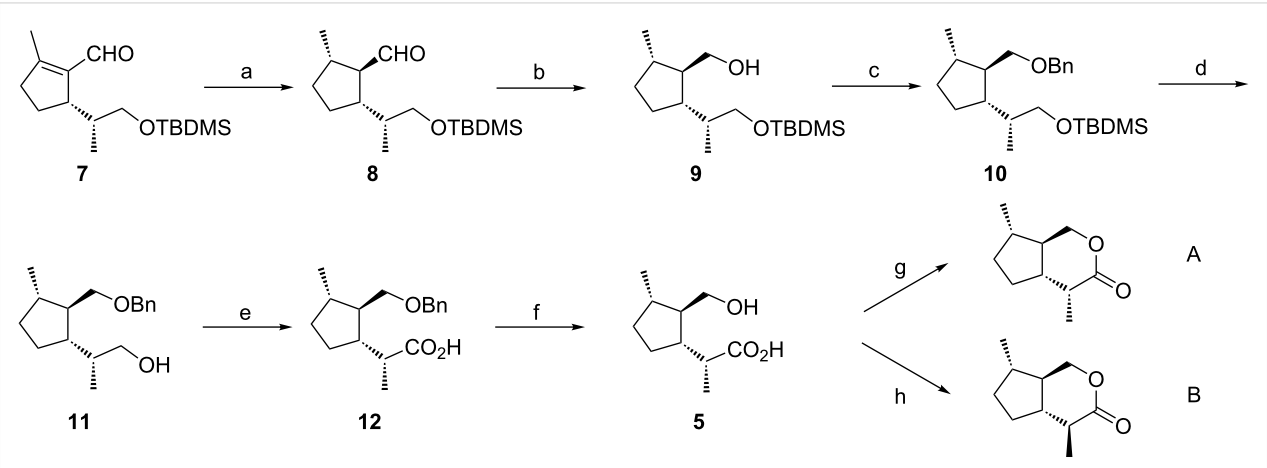

Scheme 1: Synthesis of the *trans*-fused iridomyrmecins **A** and **B**. Reaction conditions and yields: a) ammonium formate, Pd/C, MeOH, reflux (48%); b) $NaBH_4$, MeOH, H_2O, rt (79%); c) NaH, BnBr, THF, reflux (96%); d) HF, CH_3CN, rt (71%); e) CrO_3, H_2SO_4, acetone, rt (99%); f) Pd/C, 40 bar H_2, THF, rt (100%); g) DCC, DMAP, CH_2Cl_2, rt (66%); h) *p*-TsOH, benzene, reflux (56%).

selective synthesis of *trans*-fused dihydronepetalactones [1], this key intermediate could be obtained via a highly diastereoselective transfer hydrogenation of the known [19] trisubstituted cyclopentene **7** with ammonium formate over palladium [1,14,15]. Starting from the aldehyde **8**, the relative configuration of which had been confirmed by NOE experiments [1], the synthesis of **A** and **B** was completed in six additional steps.

First, the aldehyde **8** was reduced with sodium borohydride, and the resulting alcohol **9** was protected as the benzyl ether to form **10**. Deprotection of the TBDMS ether was carried out with HF in acetonitrile to yield the mono-protected diol **11**. Using Jones reagent, the free hydroxy group of **11** was oxidized to the carboxylic acid **12**, and the benzyl ether was cleaved upon catalytic hydrogenation over Pd/C to produce the hydroxy acid **5**. The latter served as the immediate precursor for the formation of either of the two diastereomeric iridomyrmecins **A** and **B**: Careful cyclization using dicyclohexylcarbodiimide (DCC) and 4-dimethylaminopyridine (DMAP) in dichloromethane at rt afforded iridomyrmecin **A**. In contrast, treatment of **5** with catalytic amounts of *p*-toluenesulfonic acid in benzene under reflux conditions for 12 h resulted in a complete epimerization at the CH-acidic C-4 position, exclusively yielding the thermodynamically more stable iridomyrmecin **B**. All reaction steps were also carried out starting from enantiomerically pure (*S*)-limonene affording *trans*-fused iridomyrmecins **A'** and **B'**. Relative configurations of iridomyrmecins **A**, **A'** and **B**, **B'** were confirmed by NOESY experiments. In **A** (Figure 5, A) decisive NOEs could be observed between 1-Hb and 4a-H as well as between 1-Hb and 7-H which showed 4a-H and 7-H to be located at the same side of the molecule. In addition, NOEs between 4-CH_3 and 7a-H as well as between 7-CH_3 and 7a-H proved the two methyl groups to be located at the same side of the molecule. In contrast, as shown in Figure 5, **B'**, NOEs between 4-H and 7a-H as well between 7-CH_3 and 7a-H, prove that in **B'** the two methyl groups are situated at opposite sides of the molecule.

Synthesis of *trans*-fused iridomyrmecins **C** and **D**

As shown in our previous paper on the synthesis of *trans*-fused dihydronepetalactones, the double bond of the acetate **4** could be hydrogenated with high stereocontrol to the diastereomerically pure acetate **13** [1] by using Crabtree's catalyst [16-18]. The synthesis of the iridomyrmecins **C** and **D** was completed in three additional steps (Scheme 2). The oxidation with Jones reagent yielded **14**, and subsequent saponification of the acetate group with methanolic KOH afforded the hydroxy acid **6**. Similar to the approach described above, careful lactonization with DCC and DMAP gave iridomyrmecin **C**, whereas treatment with *p*-toluenesulfonic acid in benzene under reflux conditions led to complete epimerization at C-4 and afforded iridomyrmecin **D**. All reaction steps were also carried out starting from enantiomerically pure (*S*)-limonene (**3'**) and afforded iridomyrmecins **C'** and **D'**.

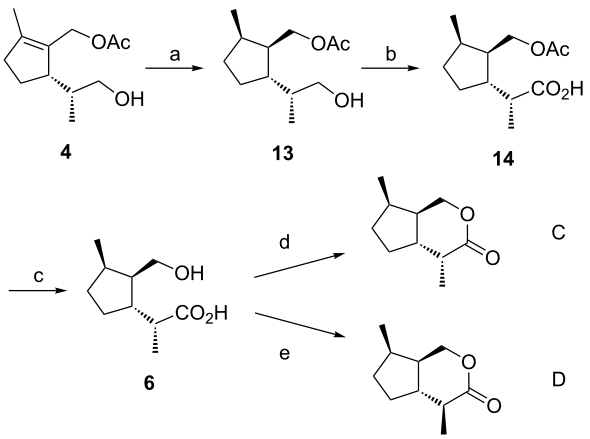

Scheme 2: Synthesis of the *trans*-fused iridomyrmecins **C** and **D**. Reaction conditions and yields: a) Crabtree's catalyst [Ir(cod)PCy_3(py)]PF_6 (10 mol %), 1 bar H_2, CH_2Cl_2, rt (81%); b) CrO_3, H_2SO_4, acetone, rt (86%); c) KOH, MeOH, rt (97%); d) DCC, DMAP, CH_2Cl_2, rt (41%); e) *p*-TsOH, benzene, reflux (59%).

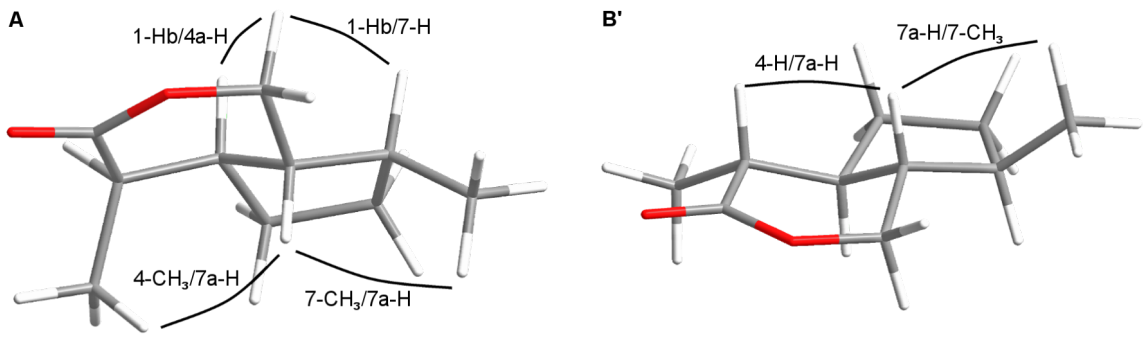

Figure 5: Configurations of the *trans*-fused iridomyrmecins **A** and **B'**.

Relative configurations of the iridomyrmecins **C**, **C'** and **D**, **D'** were confirmed by NOESY experiments. In **C** (Figure 6, **C**) decisive NOEs between 1-Hb and 4a-H as well as between 1-Hb and 7-CH_3 proved 4a-H and 7-CH_3 to be located at the same side of the molecule. The NOE between 4-CH_3 and 7a-H showed them to be geometrically close and the two methyl groups to be in opposite positions. In contrast, as shown in Figure 6, **D'** NOEs between 4a-H and 4-CH_3 as well as between 4a-H and 1-Hb and furthermore between 1-Hb and 7-CH_3 proved the methyl groups in **D'** to be at the same side of the molecule. This is confirmed by a NOE between 4-H and 7a-H.

In summary, we have completed the first enantioselective synthesis of all eight stereoisomers of *trans*-fused iridomyrmecins, starting from either of the cheaply available enantiomers of limonene. The acetate **4** is the decisive intermediate, and key reaction steps are two stereoselective hydrogenations: A transfer hydrogenation for a formal "*anti*" delivery of hydrogen and the use of Crabtree's catalyst in a directed hydrogenation for a "*syn*"-addition of hydrogen. Starting from pure enantiomers of limonene [1] these novel synthetic routes provided iridomyrmecins **A**, **A'** and **B**, **B'** in 2–3% yield over 15 steps as well as iridomyrmecins **C**, **C'** and **D**, **D'** in 10–15% yield over 9 steps.

All eight stereoisomers of *trans*-fused iridomyrmecins could be separated by gas chromatography using a capillary column coated with FFAP as an achiral polar stationary phase and a second capillary coated with a 1:1 mixture of OV1701 and heptakis(6-*O*-*tert*-butyldimethylsilyl-2,3-di-*O*-methyl)-β-cyclodextrin as an enantioselective stationary phase. Figure 3 shows the structures and retention times of all eight stereoisomers of *trans*-fused iridomyrmecins on both capillary column systems. Despite the small differences in retention times between **B** and **B'** on the cyclodextrin column, the enantiomers could be well distinguished under the experimental conditions.

Structure assignment of volatile components **Y** and **Z** in the parasitoid wasp *Alloxysta victrix*

Comparison of mass spectra and GC retention times of synthetic iridomyrmecins with corresponding data of the volatile substances **Y** and **Z** – which are present in pentane extracts of heads of *Alloxysta victrix* – allowed their unambiguous identification as *trans*-fused iridomyrmecins.

Coupled GC/MS analysis using FFAP as the stationary phase revealed the natural iridoid lactones **Y** and **Z** to show the same mass spectra and retention times as the two early eluting racemates of the synthetic iridomyrmecins, i.e., **B**/**B'** and **A**/**A'**, respectively (Figure 3). Enantioselective gas chromatography on heptakis(6-*O*-*tert*-butyldimethylsilyl-2,3-di-*O*-methyl)-β-cyclodextrin showed that **A** and **A'** were well separated with an α-value of **A**:**A'** = 1.05 (Figure 3). Consequently, the structure of **Z** could be easily determined to be **A'**, namely (4*S*,4a*S*,7*R*,7a*S*)-iridomyrmecin. Under the same experimental conditions, **B** and **B'** were only poorly resolved, however, heptaiks(2,6-di-*O*-methyl-3-*O*-pentyl)-β-cyclodextrin produced a good α-value of **B'**:**B** = 1.015 [20]. As a result, **Y** was unambiguously identified to be (4*S*,4a*R*,7*S*,7a*R*)-iridomyrmecin. A careful inspection of the analytical data obtained with the cyclodextrin column revealed the presence of small amounts of (4*R*,4a*S*,7*R*,7a*S*)-iridomyrmecin **B'** in the natural extract, showing the ee of natural **B** to be ca. 95–97%. Figure 7 shows a typical gas chromatogram (obtained with FFAP as the stationary phase) of an extract of heads of male *A. victrix*. Identified structures are assigned.

Structural relations between the *Alloxysta*-compounds and other insect iridoids

The iridoid lactones which are present in the cephalic secretions of *Alloxysta victrix* show an unusual *trans*-fusion. Among the compounds showing this structure, only the lactone **X** [1]

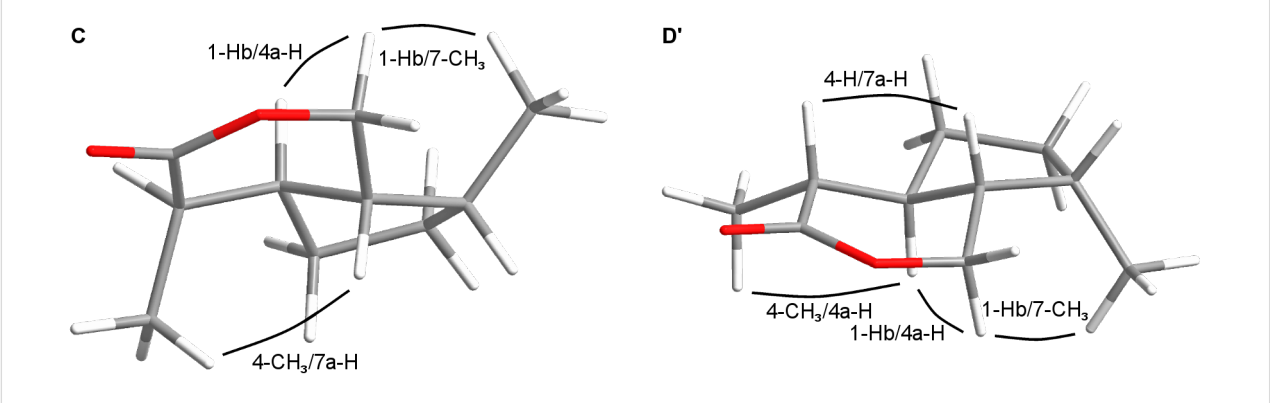

Figure 6: Configurations of the *trans*-fused iridomyrmecins **C** and **D'**.

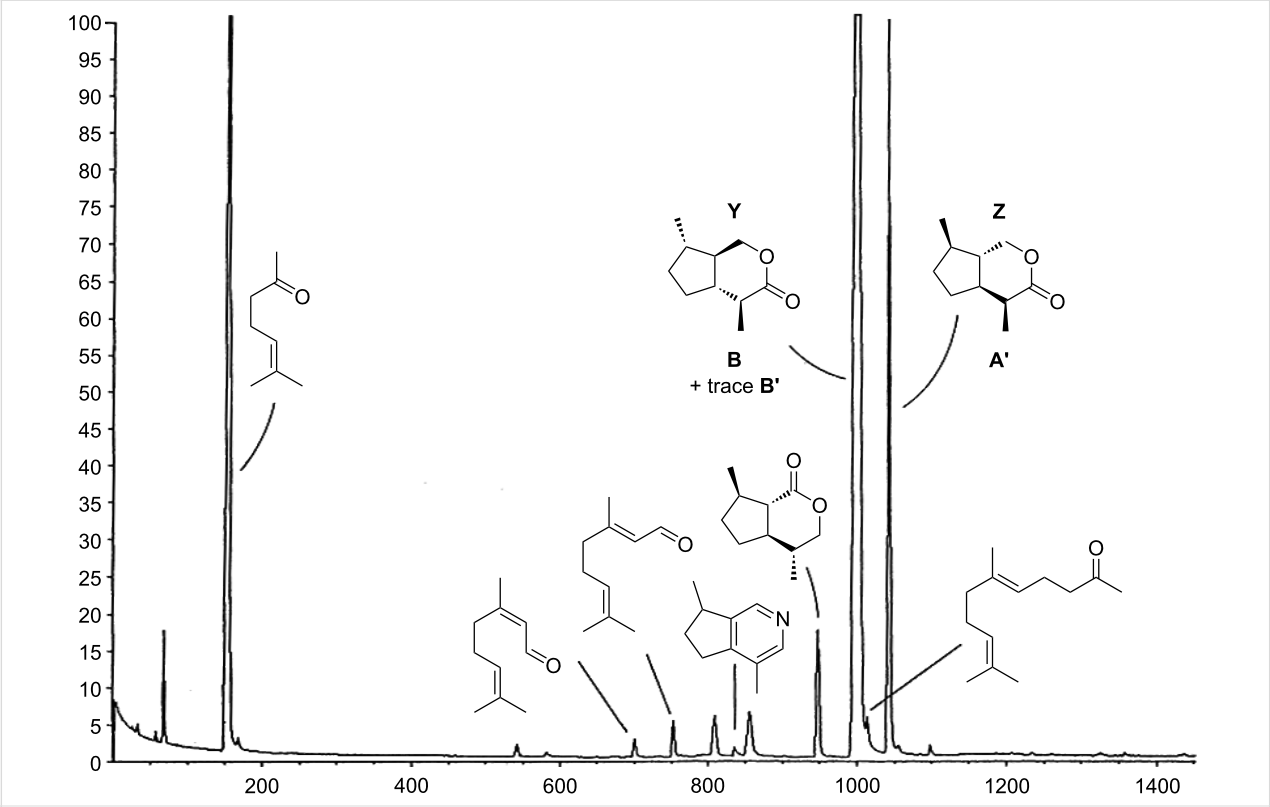

Figure 7: Volatile terpenoids in the cephalic secretion of *Alloxysta victrix*. For the identification of compounds other than **Y** and **Z** see [1].

(Figure 1) and a compound with the same relative configuration [21] have been described from insects so far. In contrast to that, the *cis*-fused nepetalactone **15** and diastereomers thereof are typical components of many species of the plant genus *Nepeta* [22,23]. Along with the corresponding hemiacetal **16**, which shows (1*R*)-configuration, **15** is also a most important sex pheromone of aphids [24] (Figure 8). Nevertheless, iridoids are usually associated with defense chemistry. Whilst configurations at the stereogenic centers of **15** and related iridoid lactones in insects appear to be stereotypic, several monocyclic iridoids show further stereochemical variation. Lactol **16** and iridodial (**17**) have first been identified as defense compounds of ants [25]. More recently, **17** – which shows (*R*)-configuration at C1 of the side-chain – was found to be a male-produced aggregation pheromone of lacewings [26,27].

The *cis*-fused iridomyrmecin (**1**) and dolichodial (**18**) are constituents of the anal gland secretion of the Argentine ant *Iridomyrmex humilis* [28]. More recently, (1*S*,2*R*,3*S*)-dolichodial (**18**) has been identified as an electrophysiologically active volatile released from the rosy apple aphid *Dysaphis plantaginea* oviparae and has been discussed apart from **15** and **16** as a possible third component of the aphid sex pheromone [29]. Actually, **18** was first identified in the defensive secretions of dolichoderine ants [25]. The same substance

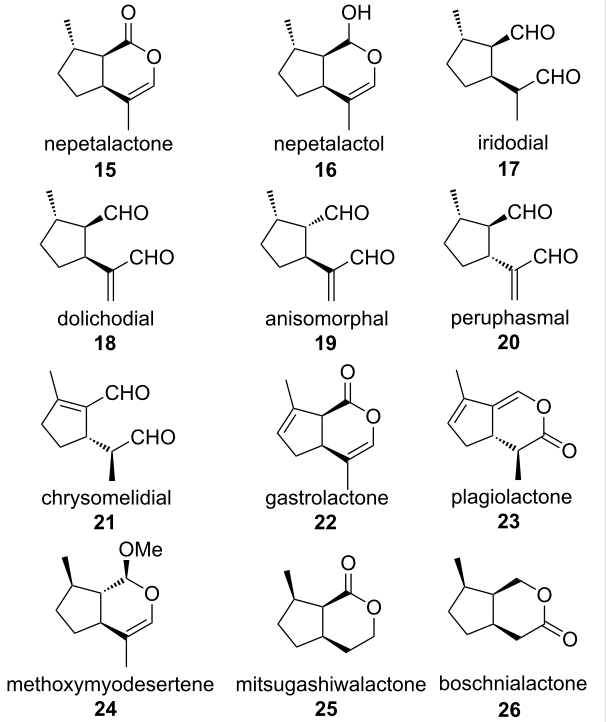

Figure 8: Structures of iridoids from insects and plants. Absolute configurations of **19** and **20** are "educated guesses".

(or its enantiomer) has been found as a defensive compound of *Nematine larvae* [30] and in adults and larvae of the thrips *Calloccithrips fuscipennis* [31]. A stereoisomer of dolichodial – anisomorphal (**19**) – is a component of the defensive secretion of the walking stick *Anisomorpha buprestoides* [32], whilst a third stereoisomer – peruphasmal (**20**) – has been identified in another walking stick, *Peruphasma schultei* [33,34]. Recent investigations show that the qualitative and quantitative composition of cyclopentanoid iridoids in the defensive secretion of *A. buprestoides* may vary with age and population. The secretion may contain all three isomers **18**, **19** and **20** which the insect can produce from glucose [35]. The absolute configurations of **19** and **20** are still unknown. It should be mentioned that along with other iridoids **18** and **19** are also components of the essential oil of some plant species [36]. A related cyclopentene derivative is chrysomelidial (**21**), a relatively widespread defense compound in larvae of phytophagous leaf beetles *Chrysomelidae* [37,38], which has been found in other insects, too. In the defensive secretion of oribatid mites it keeps the depicted (5*S*,8*S*)-configuration [39]. In some species, chrysomelidial is accompanied by the dehydronepetalactone **22** (gastrolactone) [40] or the didehydroiridomyrmecin **23** (plagiolactone) [37]. To the best of our knowledge, the two iridomyrmecins **Y** and **Z** are new natural products, representing the first *trans*-fused iridoid lactones of this type.

Whilst the *trans*-fused nature of the new iridoid lactones is very unusual, their stereochemical pattern (Figure 7) is even more puzzling: The configurational arrangements of the substituents in **X** and **Y** are strictly opposite, whereas the relations between **X** and **Z** are relatively close, showing inversion at C-4 only. Strangely, **Z** is not the expected C-4-epimer of **Y**, but the C-4-epimer of its enantiomer.

Apart from very few exceptions such as methoxymyodesertene (**24**) [41], the 4-*nor*-nepetalactone mitsugashiwalactone (**25**) [42] and its "*nor*-iridomyrmecin-complement" boschnialactone (**26**), [43] which all are plant volatiles, the methyl group in the typical five-membered ring of iridoids keeps its (*S*)-configuration (see also Figure 8), which is just in contrast to **X** and **Z** [44]. However, recently, two stereoisomers of iridomyrmecin showing (7*R*)-configuration have been reported to be components of the defense chemistry of the *Drosophila* parasitoid *Leptopilina heterotoma* [45].

Remarks on the biosynthesis of iridoids

Today it is generally accepted that the biosynthesis of iridoids starts from the acyclic geraniol (**27**). In a series of careful, elegant experiments it was shown that **27** is oxidized to 8-hydroxygeraniol (**28**) which is further transformed to 8-oxogeranial (**29**) [46-48] (Figure 9).

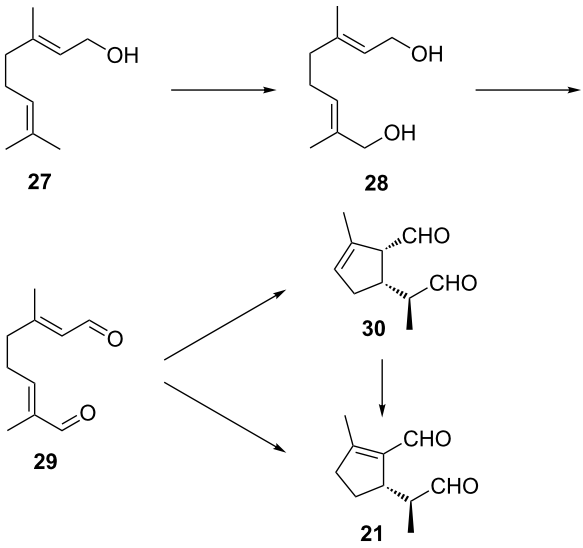

Figure 9: Biosynthetic ways to iridoids from geraniol.

During these investigations the stereochemistry of the subsequent cyclization to iridoids was found to be different in larvae of herbivorous leaf beetles and in carnivorous rove beetles. In *Phaedon cochleariae* (Chrysomelidae), cyclization of **29** directly affords chrysomelidial (**21**). In contrast, in *Phylonthus* sp. (Staphylinidae) the first step is the formation of plagiodial (**30**), which was first identified from larvae of several leaf beetle species [49,50]. Subsequently, **30** may rearrange to the thermodynamically more stable, conjugated **21**. Despite these results, there are still a lot of open questions concerning the biosynthesis of iridoids. Recently, it could be shown that leaf beetles may produce iridoid monoterpenes de novo [33] but they are also able to sequester glycosidically bound terpene precursors from their food plants [51-53] which is highly interesting with regards to the evolution of insect-plant relationships and insect defense chemistry. At present, nothing is known about the formation of "saturated" iridoids such as iridodial (**17**) or the iridoid lactones in *Alloxysta*. The strange stereochemical relations between these compounds may well be the result of different mechanisms in the enzymatic hydrogenation steps.

Conclusion

The new iridoid lactones have been found in the mandibular gland secretions of several alloxystine wasps [54] and their activity in intraspecific and interspecific communication has been discussed [55]. According to first bioassays, the new iridoids seem to play a multifunctional role in the tritrophic system of the aphid *Sitobion avenae*, its parasite, the wasp *Aphidius uzbekistanicus*, and the hyperparasitoide *Alloxysta victrix* as they obviously sedate *Sitobion* and repell *Aphidius*.

However, additional bioassays will be needed to better understand the biological significance of the newly identified iridoid lactones. As our way from limonene to iridoids provides relatively easy access to a large variety of iridoid lactones and monocyclic iridoids, behavior experiments using synthetic compounds may shed some more light on the complex relationships between host aphids, primary parasitoids such as *Aphidius* spp., and aphid hyperparasitoids such as *Alloxysta* spp. [56].

Supporting Information

Supporting Information File 1

Experimental details and characterization data for synthesized compounds.
[http://www.beilstein-journals.org/bjoc/content/supplementary/1860-5397-8-141-S1.pdf]

Acknowledgements

The biological material used in this investigation was kindly provided by Prof. Dr. Urs Wyss, University of Kiel, Germany. Financial support by the German Science Foundation, Deutsche Forschungsgemeinschaft (DFG – Fr 12/1), is gratefully acknowledged.

References

1. Zimmermann, N.; Hilgraf, R.; Lehmann, L.; Ibarra, D.; Francke, W. *Beilstein J. Org. Chem.* **2012,** *8,* 1246–1255. doi:10.3762/bjoc.8.140
2. Petersen, G.; Matthiesen, C.; Francke, W.; Wyss, U. *Eur. J. Entomol.* **2000,** *97,* 545–550.
3. Regnier, F. E. In *Biochemical Application of Mass Spectrometry;* Waller, G. R., Ed.; Wiley & Sons: New York, 1972; pp 723–734.
4. Sakai, T.; Nakajima, K.; Sakan, T. *Bull. Chem. Soc. Jpn.* **1980,** *53,* 3683–3686. doi:10.1246/bcsj.53.3683
5. Pavan, M. *Ric. Sci.* **1950,** *20,* 1853–1855.
6. Roth, L. M.; Eisner, T. *Annu. Rev. Entomol.* **1962,** *7,* 107–136. doi:10.1146/annurev.en.07.010162.000543
7. Thomas, A. F.; Bessière, Y. The Synthesis of Monoterpenes, 1980–1986. In *The Total Synthesis of Natural Products;* ApSimon, J. W., Ed.; Wiley-Interscience: New York, 1988; Vol. 7, pp 275–454.
(and references cited therein).
8. Nangia, A.; Prasuna, G.; Bheema Rao, B. *Tetrahedron* **1997,** *53,* 14507–14545. doi:10.1016/S0040-4020(97)00748-5
(and literature cited therein).
9. Ernst, M.; Helmchen, G. *Synthesis* **2002,** 1953–1955.
10. Beckett, J. S.; Beckett, J. D.; Hofferberth, J. E. *Org. Lett.* **2010,** *12,* 1408–1411. doi:10.1021/ol100077z
(and references cited therein).
11. Sisido, K.; Inomata, K.; Kageyqama, T.; Utimoto, K. *J. Org. Chem.* **1968,** *33,* 3149–3155. doi:10.1021/jo01272a027
12. Wolinsky, J.; Gibson, T.; Chan, D.; Wolf, H. *Tetrahedron* **1965,** *21,* 1247–1261. doi:10.1016/0040-4020(65)80066-7
13. Trave, R.; Marchesini, A.; Garanti, L. *Gazz. Chim. Ital.* **1970,** *100,* 1061–1075.
14. Lange, G. L.; Neidert, E. E.; Orrom, W. J.; Wallace, D. J. *Can. J. Chem.* **1978,** *56,* 1628–1633. doi:10.1139/v78-266
15. Rao, H. S. P.; Reddy, K. S. *Tetrahedron Lett.* **1994,** *35,* 171–174. doi:10.1016/0040-4039(94)88193-6
16. Crabtree, R. H.; Davis, M. W. *Organometallics* **1983,** *2,* 681–892. doi:10.1021/om00077a019
17. Crabtree, R. H.; Davis, M. W. *J. Org. Chem.* **1986,** *51,* 2655–2661. doi:10.1021/jo00364a007
18. Brown, J. M. *Angew. Chem., Int. Ed. Engl.* **1987,** *26,* 190–203. doi:10.1002/anie.198701901
19. Wolinsky, J.; Slabaugh, M. R.; Gibson, T. *J. Org. Chem.* **1964,** *29,* 3740–3742. doi:10.1021/jo01035a537
20. Ibarra-Wiltschek, D. Identifizierung und Synthese mono- und sesquiterpenoider Inhaltsstoffe aus Hymenopteren. Ph.D. Thesis, Universität Hamburg, Germany, 1995.
21. Jefson, M.; Meinwald, J.; Nowicki, S.; Hicks, K.; Eisner, T. *J. Chem. Ecol.* **1983,** *9,* 159–180. doi:10.1007/BF00987779
22. Meinwald, J. *J. Am. Chem. Soc.* **1954,** *76,* 4571–4573. doi:10.1021/ja01647a018
23. Regnier, F. E.; Waller, G. R.; Eisenbraun, E. J. *Phytochemistry* **1967,** *6,* 1281–1289. doi:10.1016/S0031-9422(00)86090-2
24. Dawson, G. W.; Griffiths, D. C.; Merritt, L. A.; Mudd, A.; Pickett, J. A.; Wadhams, L. J.; Woodcock, C. M. *J. Chem. Ecol.* **1990,** *16,* 3019–3030. doi:10.1007/BF00979609
25. Cavill, G. W. K.; Hinterberger, H. *Aust. J. Chem.* **1961,** *14,* 143–149. doi:10.1071/CH9610143
26. Hooper, A. M.; Donato, B.; Woodcock, C. M.; Park, J. H.; Paul, R. L.; Boo, K. S.; Hardie, J.; Pickett, J. A. *J. Chem. Ecol.* **2002,** *28,* 849–864. doi:10.1023/A:1015201129331
27. Zhang, Q.-H.; Sheng, M.; Chen, G.; Aldrich, J. R.; Chamhan, K. R. *Naturwissenschaften* **2006,** *93,* 461–465. doi:10.1007/s00114-006-0132-z
28. Cavill, G. W. K.; Houghton, E.; McDonald, F. J.; Williams, P. J. *Insect Biochem.* **1976,** *6,* 483–490. doi:10.1016/0020-1790(76)90072-X
29. Dewhirst, S. Y.; Birkett, M. A.; Fitzgerald, J. D.; Stewart-Jones, A.; Wadhams, L. J.; Woodcock, C. M.; Hardie, J.; Pickett, J. A. *J. Chem. Ecol.* **2008,** *34,* 1575–1583. doi:10.1007/s10886-008-9561-9
30. Boevé, J.-L.; Braekman, J. C.; Daloze, D.; Honart, M.; Pasteels, J. M. *Experientia* **1984,** *40,* 546–547. doi:10.1007/BF01982322
31. Tschuch, G.; Lindemann, P.; Moritz, G. *J. Chem. Ecol.* **2008,** *34,* 742–747. doi:10.1007/s10886-008-9494-3
32. Meinwald, J.; Chadha, M. S.; Hurst, J. J.; Eisner, T. *Tetrahedron Lett.* **1962,** *3,* 29–33. doi:10.1016/S0040-4039(00)62038-5
33. Dossey, A. T.; Walse, S. S.; Rocca, J. R.; Edison, A. S. *ACS Chem. Biol.* **2006,** *1,* 511–514. doi:10.1021/cb600318u
34. Zhang, F.; Dossey, A. T.; Zachariah, C.; Edison, A. S.; Brüschweiler, R. *Anal. Chem.* **2007,** *79,* 7748–7752. doi:10.1021/ac0711586
35. Dossey, A. T.; Walse, S. S.; Edison, A. S. *J. Chem. Ecol.* **2008,** *34,* 584–590. doi:10.1007/s10886-008-9457-8
36. Pagnoni, U. G.; Pinetti, A.; Trave, R.; Garanti, L. *Aust. J. Chem.* **1976,** *29,* 1375–1381. doi:10.1071/CH9761375
37. Meinwald, J.; Jones, T. H.; Eisner, T.; Hicks, K. *Proc. Natl. Acad. Sci. U. S. A.* **1977,** *74,* 2189–2193. doi:10.1073/pnas.74.6.2189
38. Blum, M. S.; Wallace, J. B.; Duffield, R. M.; Brand, J. M.; Fales, H. M.; Sokoloski, E. A. *J. Chem. Ecol.* **1978,** *4,* 47–53. doi:10.1007/BF00988259
39. Shimizu, N.; Yakumaru, Z.; Sakata, T.; Shimano, S.; Kuwahara, Y. *J. Chem. Ecol.* **2012,** *38,* 29–35. doi:10.1007/s10886-012-0064-3

40. Jones, T. H.; Blum, M. S. *Tetrahedron Lett.* **1981,** *22,* 4373–4376. doi:10.1016/S0040-4039(01)82960-9
41. Grant, H. G.; O'Regan, P. J.; Park, R. J.; Sutherland, M. D. *Aust. J. Chem.* **1980,** *33,* 853–878. doi:10.1071/CH9800853
42. Sakan, T.; Murai, F.; Isoe, S.; Hyeon, S. B.; Hayashi, S. *J. Chem. Soc. Jpn., Pure Chem. Sect.* **1969,** *90,* 507–511.
43. Sakan, T.; Murai, F.; Hayashi, Y.; Honda, Y.; Shono, T.; Nakajima, M.; Kato, M. *Tetrahedron* **1967,** *23,* 4635–4652. doi:10.1016/S0040-4020(01)92562-1
44. Sampaio-Santos, M. I.; Kaplan, M. A. C. *J. Braz. Chem. Soc.* **2001,** *12,* 144–153. doi:10.1590/S0103-50532001000200004
45. Stökl, J.; Hofferberth, J.; Pritschet, M.; Brummer, M.; Ruther, J. *J. Chem. Ecol.* **2012,** *38,* 331–339. doi:10.1007/s10886-012-0103-0
46. Lorenz, M.; Boland, W.; Dettner, K. *Angew. Chem., Int. Ed. Engl.* **1993,** *32,* 912–914. doi:10.1002/anie.199309121
47. Veith, M.; Lorenz, M.; Boland, W.; Simon, H.; Dettner, K. *Tetrahedron* **1994,** *50,* 6859–6874. doi:10.1016/S0040-4020(01)81338-7
48. Weibel, D. B.; Oldham, N. J.; Feld, B.; Glombitza, G.; Dettner, K.; Boland, W. *Insect Biochem. Mol. Biol.* **2001,** *31,* 583–591. doi:10.1016/S0965-1748(00)00163-6
49. Sugawara, F.; Matsuda, K.; Kobayashi, A.; Yamashita, K. *J. Chem. Ecol.* **1979,** *5,* 929–939. doi:10.1007/BF00990215
50. Pasteels, J. M.; Braekman, J. C.; Daloze, D.; Ottinger, R. *Tetrahedron* **1982,** *38,* 1891–1897. doi:10.1016/0040-4020(82)80038-0
51. Daloze, D.; Pasteels, J. M. *J. Chem. Ecol.* **1994,** *20,* 2089–2097. doi:10.1007/BF02066245
52. Feld, B. K.; Pasteels, J. M.; Boland, W. *Chemoecology* **2001,** *11,* 191–198. doi:10.1007/PL00001851
53. Kunert, M.; Søe, A.; Bartram, S.; Discher, S.; Tolzin-Banasch, K.; Nie, L.; David, A.; Pasteels, J.; Boland, W. *Insect Biochem. Mol. Biol.* **2008,** *38,* 895–904. doi:10.1016/j.ibmb.2008.06.005
54. Hübner, G.; Völkl, W.; Francke, W.; Dettner, K. *Biochem. Syst. Ecol.* **2002,** *30,* 505–523. doi:10.1016/S0305-1978(01)00137-5
55. Petersen, G.; Matthiesen, C.; Stolzenberg, N.; Zimmermann, N.; Hilgraf, R.; Lehmann, L.; Francke, W.; Wyss, U. *Mitt. Dtsch. Entomol. Ges.* **2001,** *13,* 51–55.
56. Grasswitz, T. R.; Reese, B. D. *BioControl* **1998,** *43,* 261–271. doi:10.1023/A:1009987609371

License and Terms